Carbon TerraVault III
Class VI Permit Application
Narrative Report

Submitted to:
U.S. Environmental Protection Agency Region 9
San Francisco, CA

Prepared by:

27200 Tourney Road, Suite 200
Santa Clarita, CA 91355
(888) 848-4754

Table of Contents

1.0 Project Background and Contact Information 1
2.0 Site Characterization 3
2.1 Regional Geology, Hydrogeology, and Local Structural Geology 3
2.1.1 Geologic History 3
2.1.2 Site Geology Overview 4
2.1.3 Geological Sequence 8
2.2 Maps and Cross Sections of the AoR 10
2.2.1 Data 10
2.2.Site Stratigraphy 14
2.2.3 Map of the Area of Review 17
2.3 Faults and Fractures 19
2.3.1 Overview 19
2.4 Injection and Confining Zone Details 22
2.4.1 Mineralogy 22
2.4.2 Porosity and Permeability 23
2.4.3 Injection Zone and Confining Zone Capillary Pressure 29
2.4.4 Depth and Thickness 29
2.4.5 Structure Maps 30
2.4.6 Isopach Maps 30
2.5 Geomechanical and Petrophysical Information 31
2.5.1 Caprock Ductility 31
2.5.2 Stress Field 33
2.6 Seismic History 36
2.7 Hydrologic and Hydrogeologic Information 40
2.7.1 Hydrologic Information 41
2.7.2 Base of Fresh Water and Base of USDWs 42
2.7.3 Formations with USDWs 44
2.7.4 Geologic Cross Sections Illustrating Formations with USDWs 46
2.7.5 Principal Aquifers 48
2.7.6 Potentiometric Maps 49
2.7.7 Water Supply Wells 53
2.8 Geochemistry 54
2.8.1 Formation Geochemistry 54

2.8.2 Fluid Geochemistry 54
2.8.3 Fluid-Rock Reactions 56
2.9 Other Information (Including Surface Air and/or Soil Gas Data, if Applicable) 56
2.10 Site Suitability 57
3.0 AoR and Corrective Action 58
4.0 Financial Responsibility 59
5.0 Injection and Monitoring Well Construction 59
5.1 Proposed Stimulation Program 60
5.2 Construction Procedures 60
5.2.1 Casing and Cementing 62
6.0 Pre-Operational Logging and Testing 65
7.0 Well Operation 65
7.1 Operational Procedures 65
7.2 Proposed Carbon Dioxide Stream 65
8.0 Testing and Monitoring 67
9.0 Injection Well Plugging 67
10.0 Post-Injection Site Care (PISC) and Site Closure 68
11.0 Emergency and Remedial Response 68
12.0 Injection Depth Waiver and Aquifer Exemption Expansion 68
13.0 Reference 69

ATTACHMENT A: CLASS VI PERMIT APPLICATION NARRATIVE
40 CFR 146.82(a)

Carbon TerraVault III

1.0 Project Background and Contact Information

Carbon TerraVault Holdings LLC (CTV), a wholly owned subsidiary of California Resources Corporation (CRC), proposes to construct and operate six CO_2 geologic sequestration wells at CTV III located in San Joaquin County, California. This application was prepared in accordance with the U.S. Environmental Protection Agency's (EPA's) Class VI, in Title 40 of the Code of Federal Regulations (40 CFR 146.81) under the Safe Drinking Water Act (SDWA). CTV is not requesting an injection depth waiver or aquifer exemption expansion.

CTV will obtain the required authorizations from applicable local and state agencies, including the associated environmental review process under the California Environmental Quality Act. Appendix A1 outlines potential local, state and federal permits and authorizations. Federal act considerations and additional consultation, which includes the Endangered Species Act, the National Historic Preservation Act and consultations with Tribes in the area of review, are presented in the Federal Acts and Consultation attachment.

CTV forecasts the potential CO_2 stored in the Mokelumne River Formation at an average rate of 2.5 million tonnes annually for 28 years. CO_2 will be sourced from a blue hydrogen and ammonia plant (up to 377,000 tonnes per annum) that will be located in proximity to the storage site, direct air capture and other CO_2 sources in the project area.

The Carbon TerraVault III (CTV III) storage site is located in the Sacramento Valley, 15 miles southeast of the Rio Vista Field near Stockton, California (**Figure 2.1-1**) within the southern Sacramento Basin. The project will consist of six injectors, surface facilities, and monitoring wells. This supporting documentation applies to the six injection wells.

CTV will actively communicate project details and submitted regulatory documents to County and State agencies:

1. Geologic Energy Management Division (CalGEM)
   District Deputy
   Mark Ghann-Amoah: (661) 322-4031

2. CA Assembly District 13
   Assemblyman Carlos Villapudua
   31 East Channel Street – Suite 306
   Stockton, CA 95202
   (209) 948-7479

3. San Joaquin County
   District 3 Supervisor –Tom Patti
   (209) 468-3113
   tpatti@sjgov.org

4. San Joaquin County Community Development
   Director – David Kwong
   1810 East Hazelton Avenue
   Stockton, CA 95205
   (209) 468-3121

5. San Joaquin Council of Governments
   Executive Director – Diane Nguyen
   555 East Weber Avenue
   Stockton, CA 95202
   (209) 235-0600

6. Region 9 Environmental Protection Agency
   75 Hawthorne Street
   San Francisco, CA 94105
   (415) 947-8000

2.0 Site Characterization

2.1 Regional Geology, Hydrogeology, and Local Structural Geology [40 CFR 146.82(a)(3)(vi)]

2.1.1 Geologic History

The CTV III storage site is located 15 miles southeast of major gas field Rio Vista. Two smaller gas fields lie closer to the project area: McDonald Island to the north and the Union Island Gas Field to the east. The McDonald Island Gas Field was discovered first in June 1936 and the Union Island Gas Field was later discovered in 1972, both by Union Oil Company of California. The McDonald Island Field produced 184 BCFG from the Mokelumne River Formation (Downey 2010). Although located in a region of prolific gas production, Victoria Island only contains a few exploration type wells and no hydrocarbon accumulations have been discovered in the project area (**Figure 2.1-1**). The Mokelumne River Formation is the target reservoir.

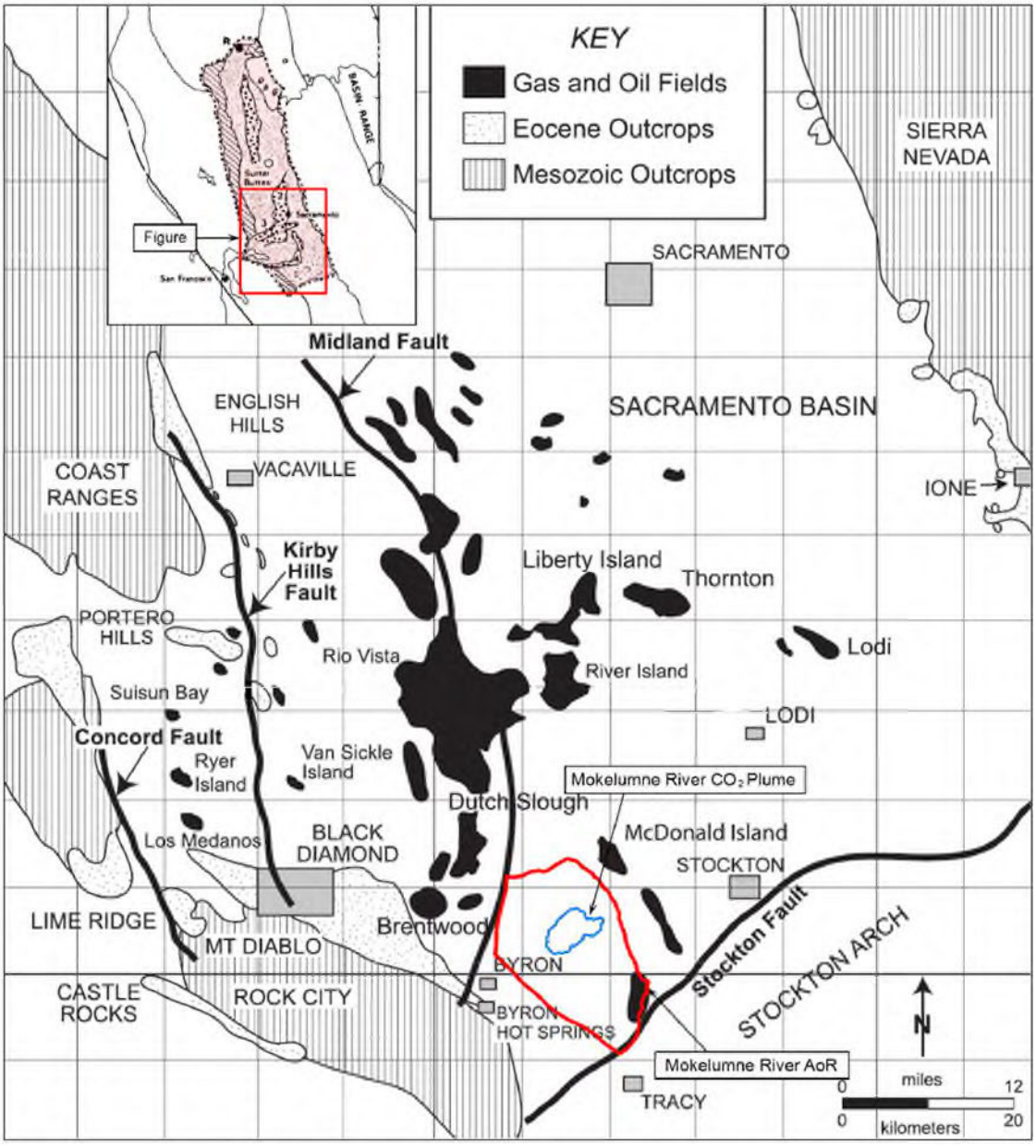

Figure 2.1-1. Location map of the project area with the proposed injection AoR (red) in relation to the Sacramento Basin. CO_2 plume boundary shown in blue.

2.1.2 Site Geology Overview

The CTV III project area lies within the Sacramento Basin in northern California (**Figure 2.1-2**). The Sacramento Basin is the northern, asymmetric sub-basin of the larger, Great Valley Forearc. This portion of the basin, that contains a steep western flank and a broad, shallow eastern flank, spans approximately 240 miles in length and 60 miles wide (Magoon 1995).

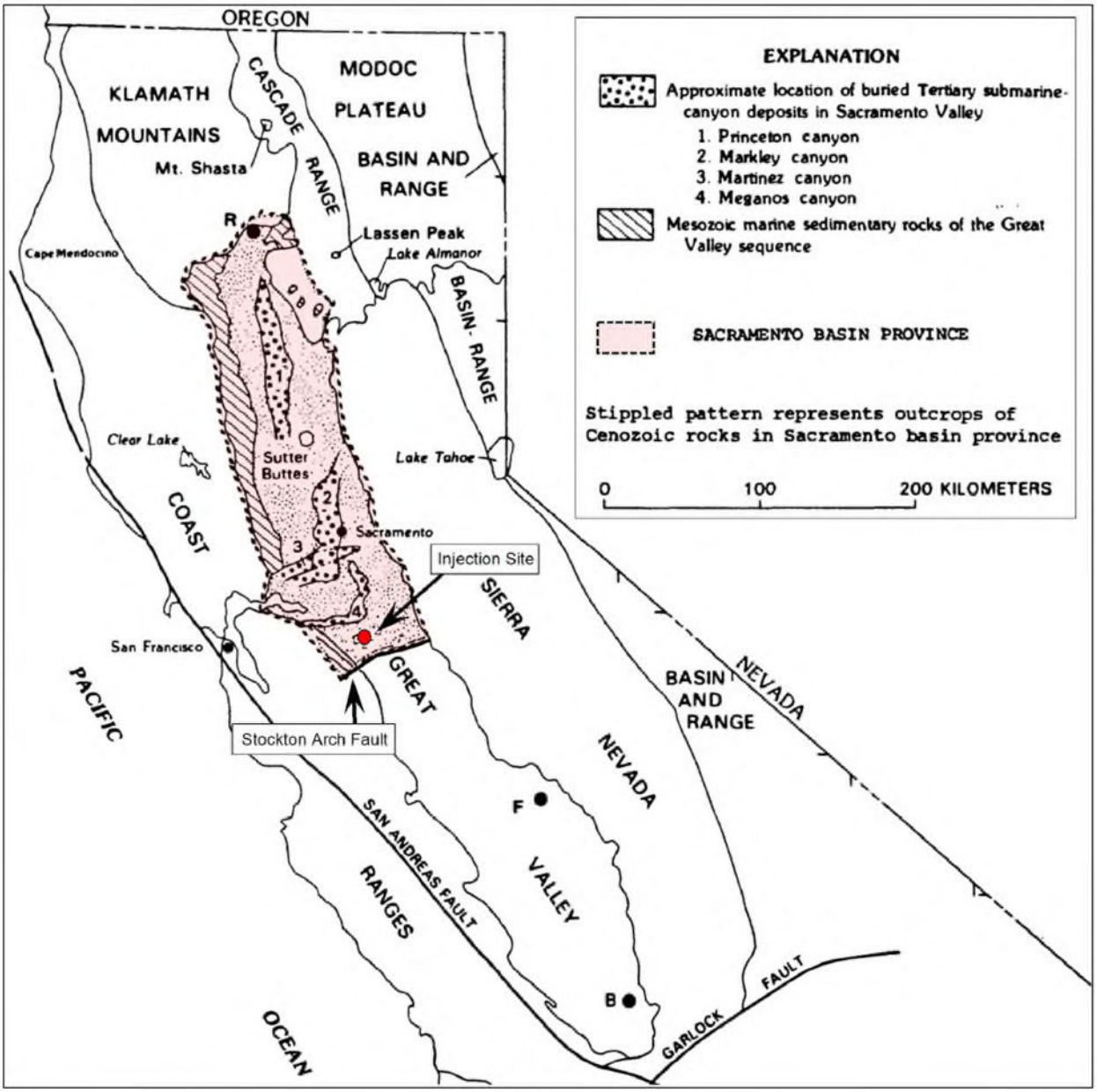

Figure 2.1-2. Location map of California modified from (Beyer, 1988) & (Sullivan, 2012). The Sacramento Basin regional study area is outlined by a dashed black line. B – Bakersfield; F – Fresno; R – Redding.

2.1.2.1 Basin Structure

The Great Valley was developed during mid to late Mesozoic time. The advent of this development occurred under convergent-margin conditions via eastward, Farallon Plate subduction, of oceanic crust beneath the western edge of North America (Beyer 1988). The convergent, continental margin, that characterized central California during the Late Jurassic through Oligocene time, was later replaced by a

transform-margin tectonic system. This occurred as a result of the northward migration of the Mendocino Triple Junction (from Baja California to its present location off the coast of Oregon), located along California's coast (**Figure 2.1-3**). Following this migrational event was the progressive cessation of both subduction and arc volcanism as the progradation of a transform fault system moved in as the primary tectonic environment (Graham 1984). The major current day fault, the San Andreas, intersects most of the Franciscan subduction complex, which consists of the exterior region of the extinct convergent-margin system (Graham 1984).

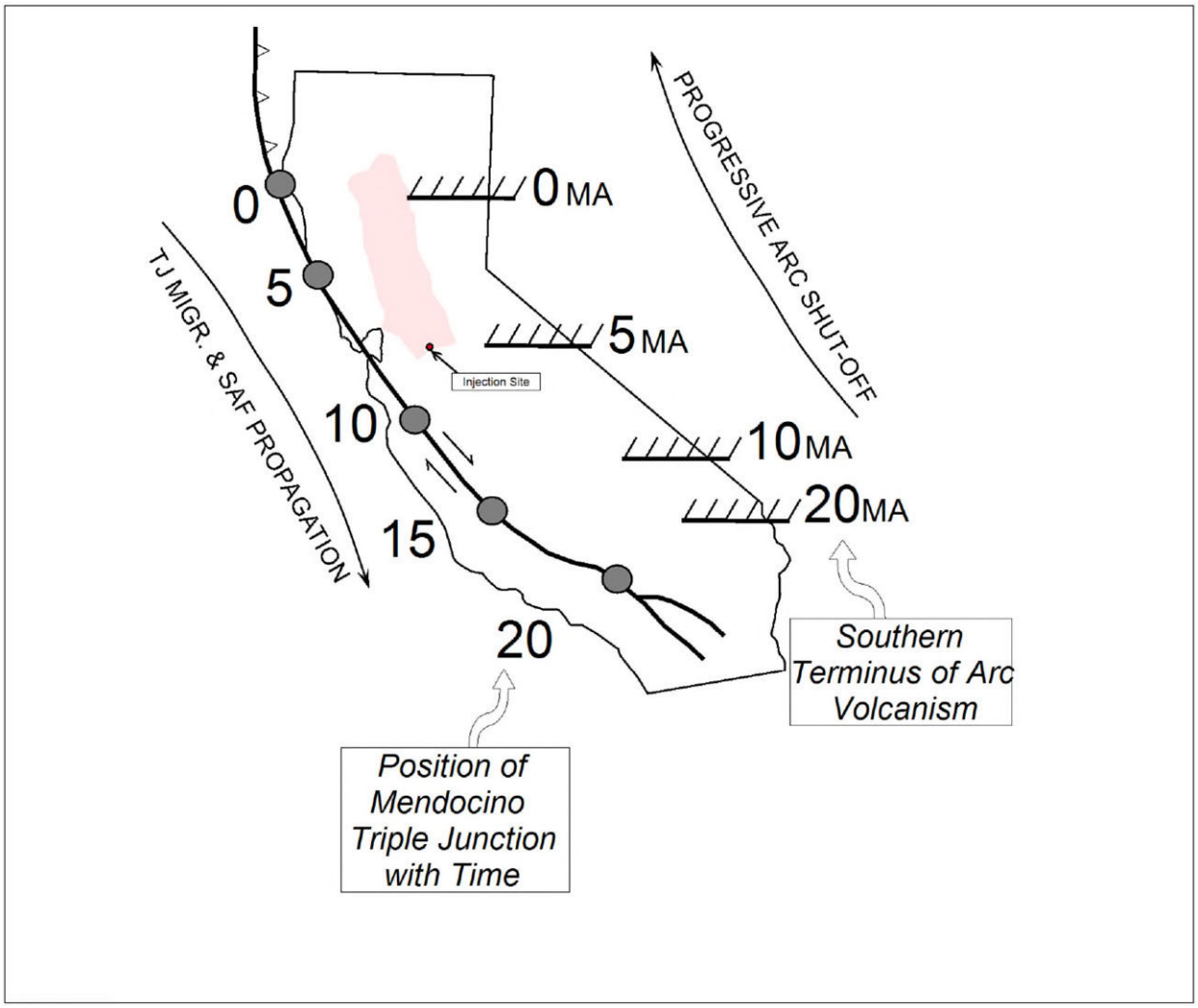

Figure 2.1-3. Migrational position of the Mendocino triple junction (Connection point of the Gorda, North American and Pacific plates) on the west and migrational position of Sierran arc volcanism in the east (Graham, 1984). The figure indicates space-time relations of major continental-margin tectonic events in California during Miocene.

2.1.2.2 Basin Stratigraphy

The structural trough that developed subsequent to these tectonic events, that became named the Great Valley, became a depocenter for eroded sediment and thereby currently contains a thick infilled sequence of sedimentary rocks. These sedimentary formations range in age from Jurassic to Holocene. The first deposits occurred as an ancient seaway and through time were built up by the erosion of the surrounding structures. The basin is constrained on the west by the Coast Range Thrust, on the north by the Klamath

Mountains, on the east by the Cascade Range and Sierra Nevada and the south by the Stockton Arch Fault (**Figure 2.1-2**). To the west the Coastal Range boundary was created by uplifted rocks of the Franciscan Assemblage (**Figure 2.1-4**). The Sierra Nevadas, that make up the eastern boundary, are a result of a chain of ancient volcanos.

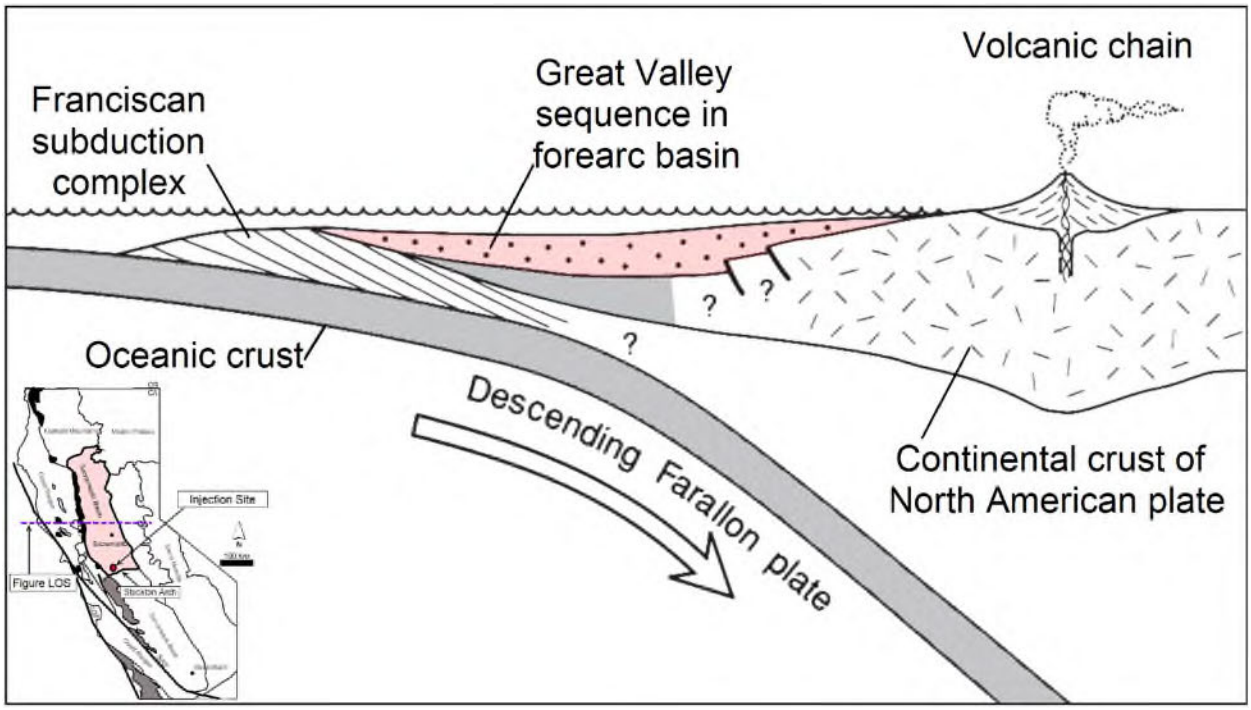

Figure 2.1-4. Schematic W-E cross-section of California, highlighting the Sacramento Basin, as a continental margin during late Mesozoic. The oceanic Farallon plate was forced below the west coast of the North American continental plate.

Basin development is broken out into evolutionary stages at the end of each time-period of the arc-trench system, from Jurassic to Neogene, in **Figure 2.1-5**. As previously stated, sediment infill began as an ancient seaway and was later sourced from the erosion of the surrounding structures. Sedimentary infill consists of Cretaceous-Paleogene fluvial, deltaic, shelf and slope sediments. Due to the southward tilt of the basin sedimentation thickens towards the southern end near the Stockton Arch fault which lies approximately 5 miles southeast of the CTV III Area of Review (AoR), shown in red on **Figure 2.1-1**, creating sequestration quality sandstones. The smaller blue boundary signifies the CO_2 plume extent 100 yrs. after the cessation of injection. The larger red boundary is the AoR of the project which was determined based on the pressure front developed during the project by the methodology described in Attachment B.

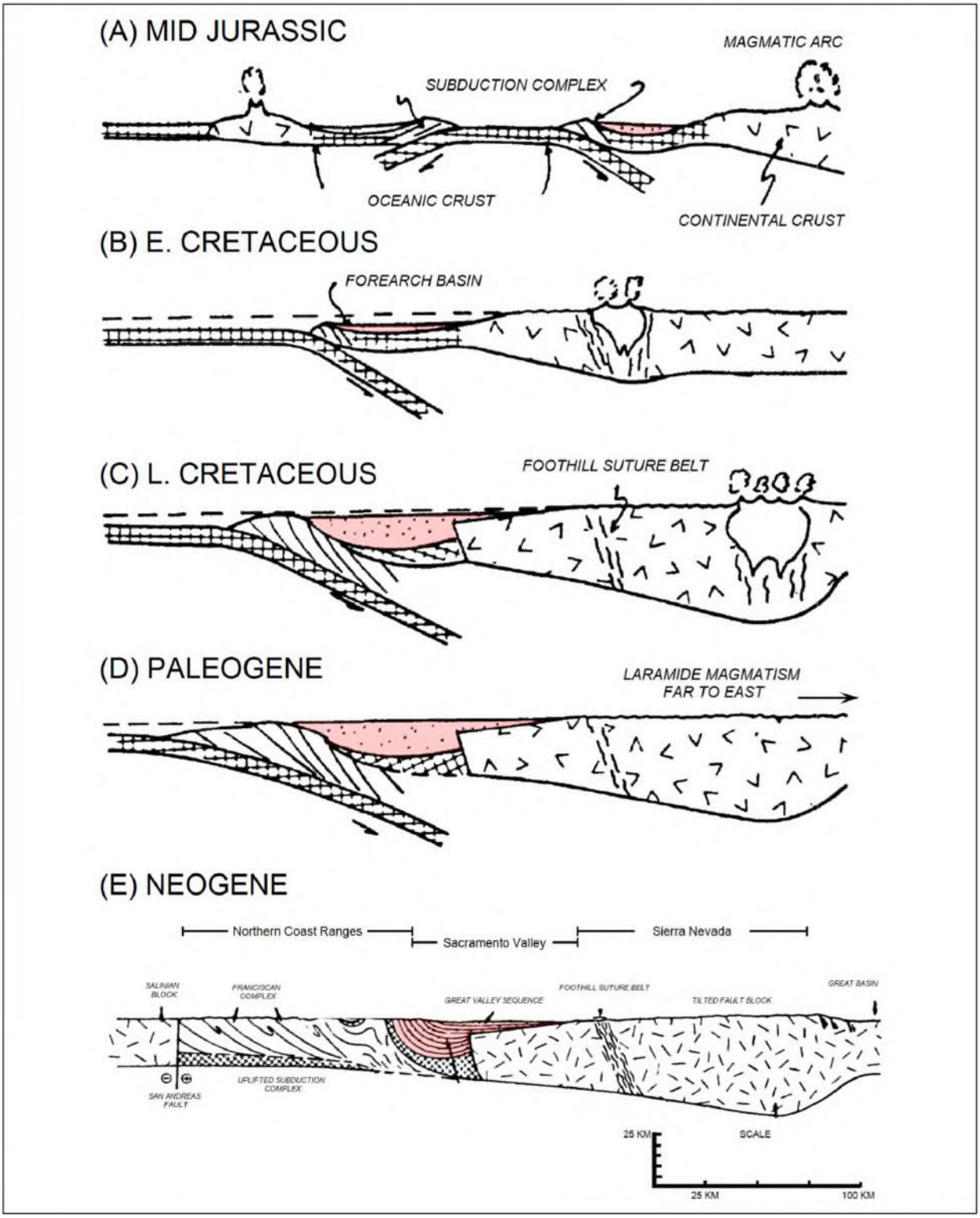

Figure 2.1-5. Evolutionary stages showing the history of the arc-trench system of California from Jurassic (A) to Neogene (E) (modified from Beyer, 1988).

In the southern Sacramento Basin the Mokelumne River Formation is a thick-bedded sandstone that creates the principal reservoir facies in the CTV III area. This area is a minor structural trap with a slight dip of about 2.8 degrees to the west leaving the area mostly flat.

2.1.2.3. Submarine Canyons

Falling sea levels and tectonics caused the Paleogene Markley, Martinez and Meganos submarine canyons to form throughout the Sacramento Basin (**Figure 2.1-2**)**.** The erosional events caused by these canyons played a large part in the current distribution and continuity of Upper Cretaceous and early Tertiary formations within the basin (Downey 2010). The Late Paleocene/Early Eocene Meganos canyon lies on the western edge of the AoR. Trending in a northeast-southwest direction and cutting deeply into the Mokelumne River Formation sediments this erosional event spans approximately 25-30 miles from southern Sacramento County through northwestern San Joaquin County, and then westward into Contra Costa County. This event caused erosional troughs that were later filled in with fine-grained submarine fan deposits and transgressive deep-water shale due to renewed rising sea levels. This infilled sequence can be seen outcropping on the flanks of Mount Diablo where it has a minimum thickness of 2,200 ft. and serves as the primary trapping mechanism for the Brentwood Oil Field (Downey 2010).

2.1.3 Geological Sequence

Figure 2.1-6 is a schematic representing the local stratigraphy CTV III, highlighting the area east of the Midland Fault and west of the Stockton Arch fault. The injection zone is shown in red as the Mokelumne River Formation. The six chosen injection wells will inject CO_2 into the Cretaceous aged Mokelumne River Formation, east of the Meganos Canyon. The average injection depth is approximately -6975 TVDSS.

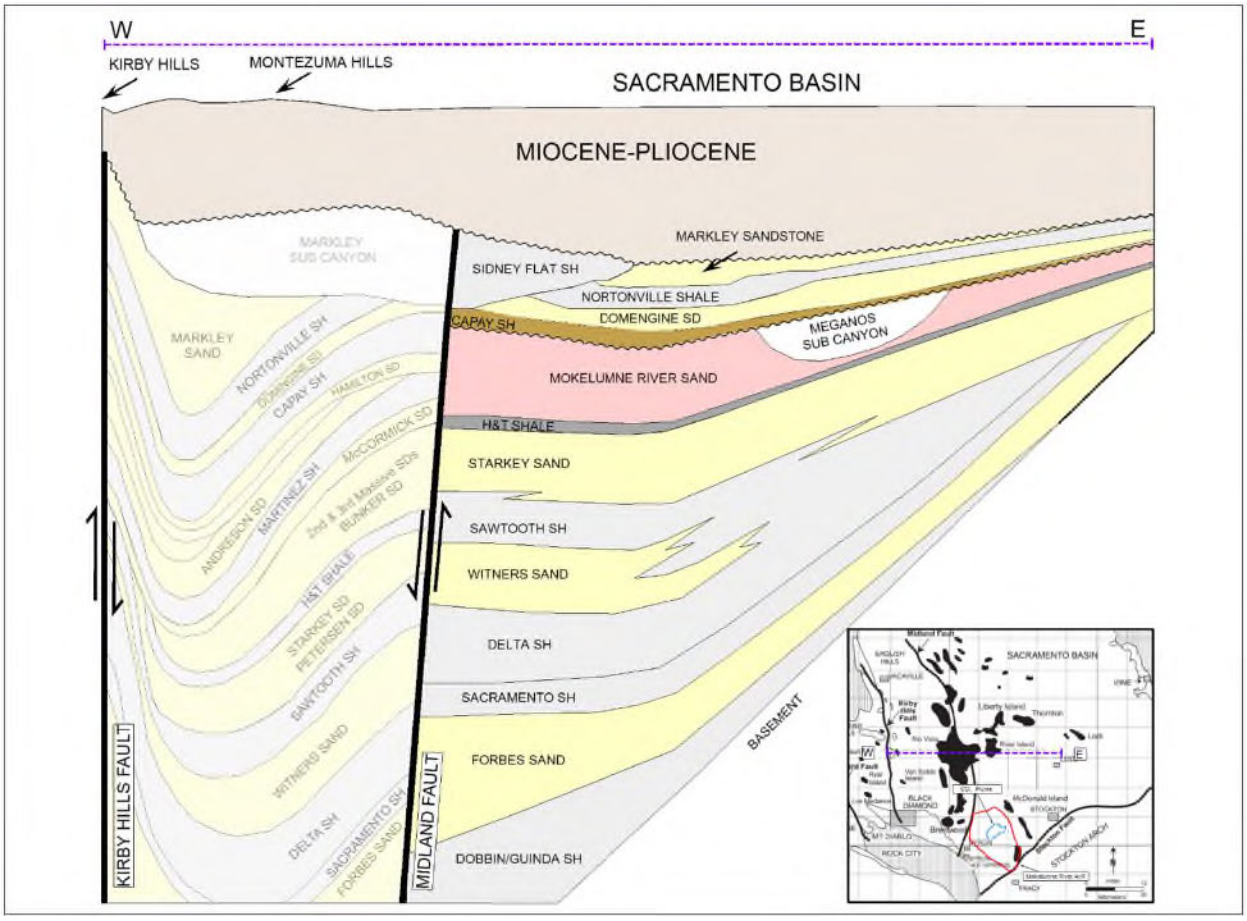

Figure 2.1-6. Schematic west to east cross section in the Sacramento basin.

Following its deposition, the Mokelumne River Formation was buried under the Capay Shale which carries throughout most of its distribution. This formation serves as the upper confining zone for the Mokelumne River reservoir due to its low permeability, thickness, and regional continuity that spans beyond the AoR (**Figure 2.1-7**). Above the Capay Shale is the Domengine Sandstone and Nortonville Shale.

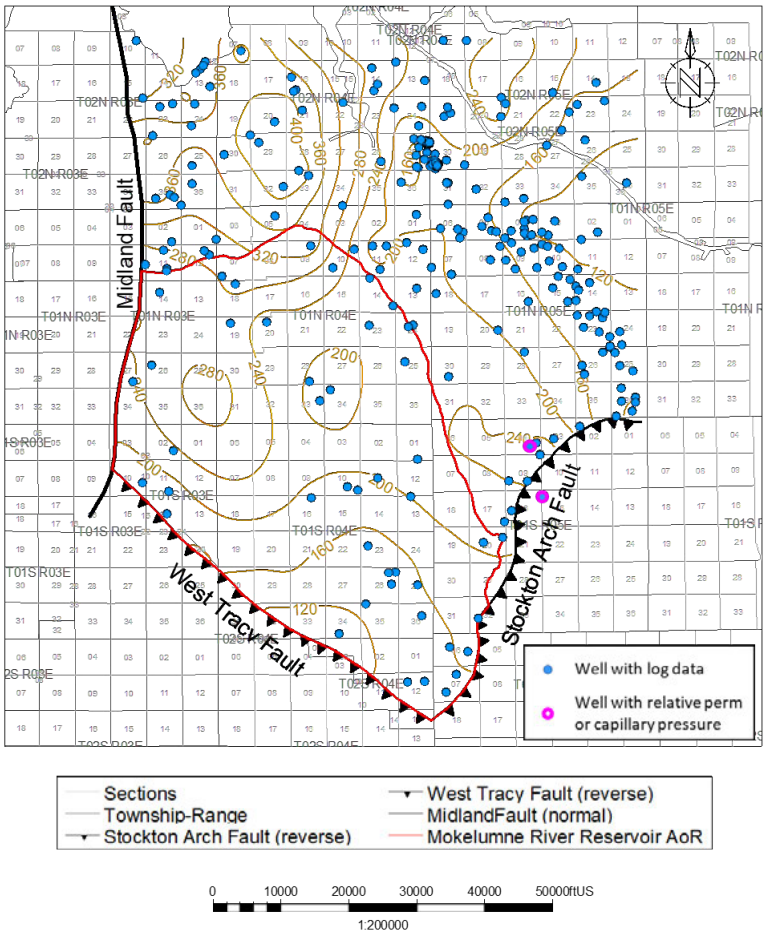

Figure 2.1-7. Capay Shale isopach map for the greater Victoria Island area. Wells shown as blue dots on the map penetrate the Capay Shale and have open-hole logs. Wells with relative permeability or capillary pressure data are shown as magenta circles.

2.2 Maps and Cross Sections of the AoR [40 CFR 146.82(a)(2), 146.82(a)(3)(i)]

2.2.1 Data

To date, 46 wells have been drilled to various depths within the project AoR. Along with an extensive database of wells in this field, seismic coverage, core and reservoir performance data such as production and pressure give an adequate description of the reservoir (**Figure 2.2-1**).

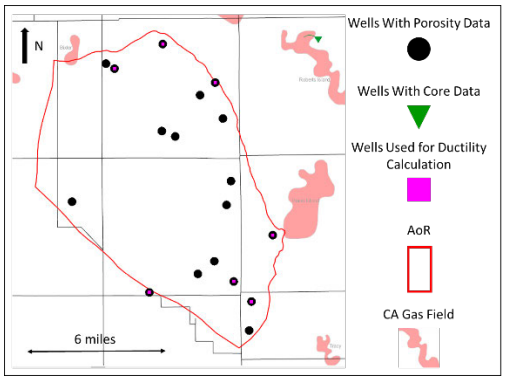

Figure 2.2-1. Wells drilled in the project area with porosity data are shown in black, wells with core are shown in green and wells used for ductility calculation are shown in pink.

Well data are used in conjunction with three-dimensional (3D) and two-dimensional (2D) seismic to define the structure and stratigraphy of the injection zone and confining layers (**Figure 2.2-2**)**. Figure 2.2-3** shows outlines of the seismic data used and the area of the structural framework that was built from these seismic surveys. The 3D data in this area were merged using industry standard pre-stack time migration in 2013, allowing for a seamless interpretation across the seismic datasets. The 2D data used for this model were tied to this 3D merge in both phase and time to create a standardized datum for mapping purposes. The following layers were mapped across the 2D and 3D data:

- A shallow marker to aid in controlling the structure of the velocity field
- The approximate base of the Valley Springs Formation which is unconformable with the Eocene strata below
- Domengine
- Mokelumne River
- H&T Shale
- Winters
- Forbes

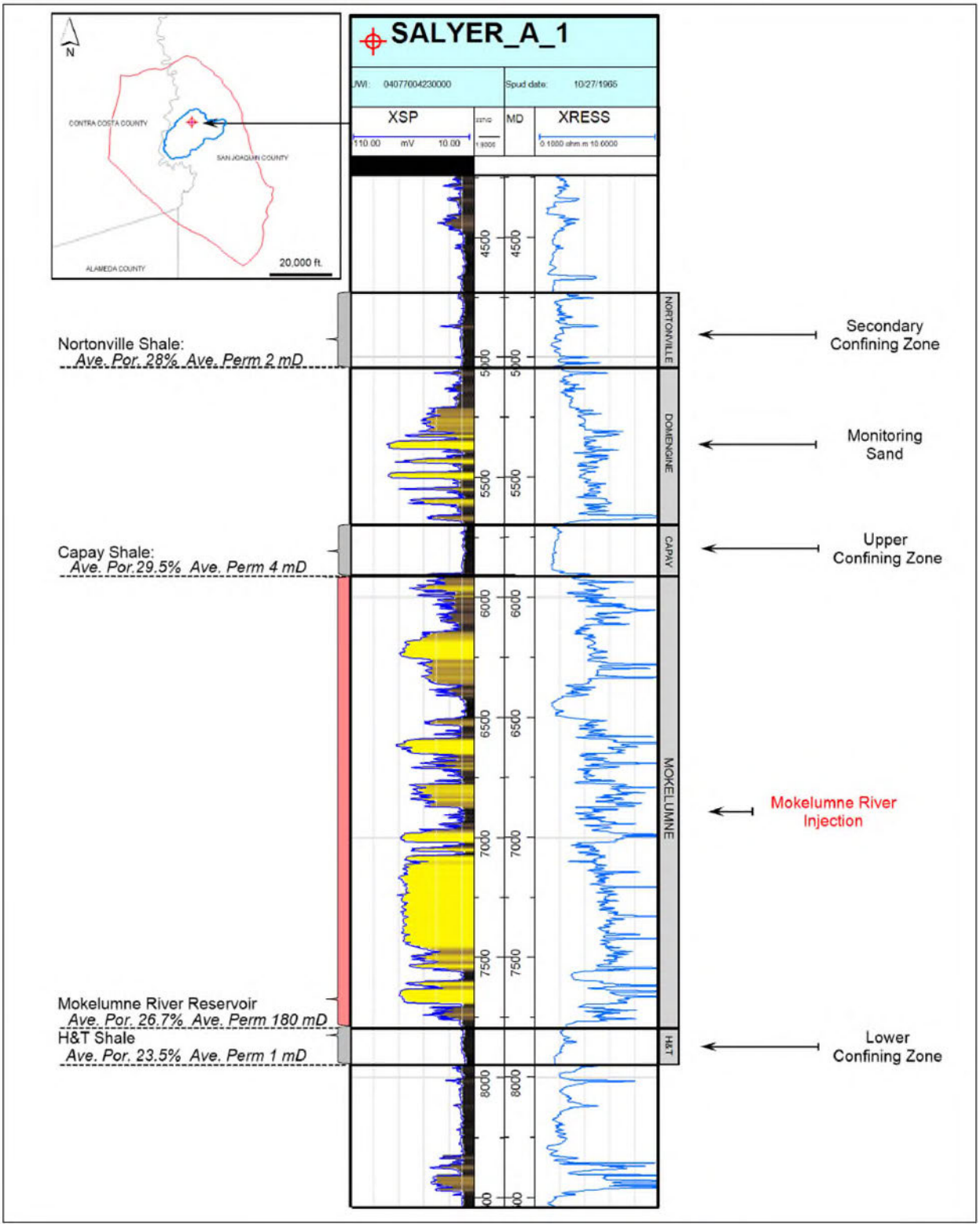

Figure 2.2-2. Type well taken from within the CO_2 boundary showing confining and injection zone average rock properties.

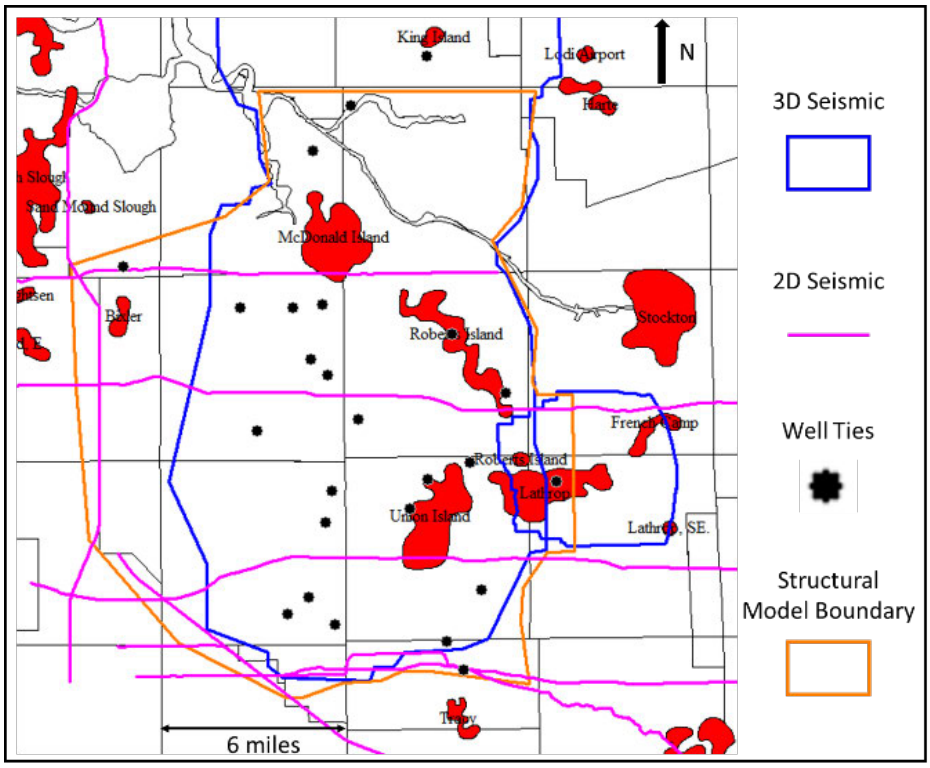

Figure 2.2-3. Summary map and area of seismic data used to build structural model. The 3D surveys were acquired in 1998 and reprocessed in 2013. The 2D seismic were acquired between 1980 and 1985. California gas fields are shown for reference

The top of the Cretaceous Forbes Formation was used as the base of this structural model due to the depth and imaging of Basement not being sufficient to create a reliable and accurate surface. Interpretation of these layers began with a series of well ties at well locations shown in **Figure 2.2-3**. These well ties create an accurate relationship between wells which are in depth and the seismic which is in time. The layers listed above were then mapped in time and gridded on a 550 by 550 foot cell basis. Alongside this mapping was the interpretation of any faulting in the area which is discussed further in the Faults and Fracture section of this document.

The gridded time maps and a sub-set of the highest quality well ties and associated velocity data are then used to create a 3D velocity model. This model is guided between well control by the time horizons and is iterated to create an accurate and smooth function. The velocity model is used to convert both the gridded time horizons and interpreted faults into the depth domain. The result is a series of depth grids of the layers listed above which are then used in the next step of this process.

The depth horizons are the basis of a framework which uses conformance relationships to create a series of depth grids that are controlled by formation well tops picked on well logs. The grids are used as structural control between these well tops to incorporate the detailed mapping of the seismic data. These grids incorporate the thickness of zones from well control and the formation strike, dip, and any fault offset from the seismic interpretation. The framework is set up to create the following depth grids for input in to the geologic and plume growth models:

- Nortonville Shale
- Domengine

- Domengine Top Sand
- Capay Shale
- Mokelumne River Formation
- H&T Shale
- Winters
- Delta Shale
- Delta Shale Base

2.2.Site Stratigraphy

Major stratigraphic intervals within the field, from oldest to youngest, include the H&T Shale (L. Cretaceous), Mokelumne River Formation (L. Cretaceous-E. Paleocene), Capay Shale (E. Eocene), Domengine Sandstone (L. Eocene), and Nortonville Shale (L. Eocene) (**Figure 2.2-4**). Of these formations the regional upper seal rock that partitions the reservoir consists of the Capay Shale. Also shown in **Figure 2.2-4** is the basin-wide unconformity separating overlying Paleocene and younger beds from Cretaceous rocks. This unconformity resides above the Mokelumne River Formation at the base of the Capay shale, creating a seal between reservoir and USDW. During Paleogene time, marine and deltaic deposits continued in the basin until the activity of the Stockton Arch began to separate Sacramento Basin from the San Joaquin basin in late Paleogene time (Downey 2010).

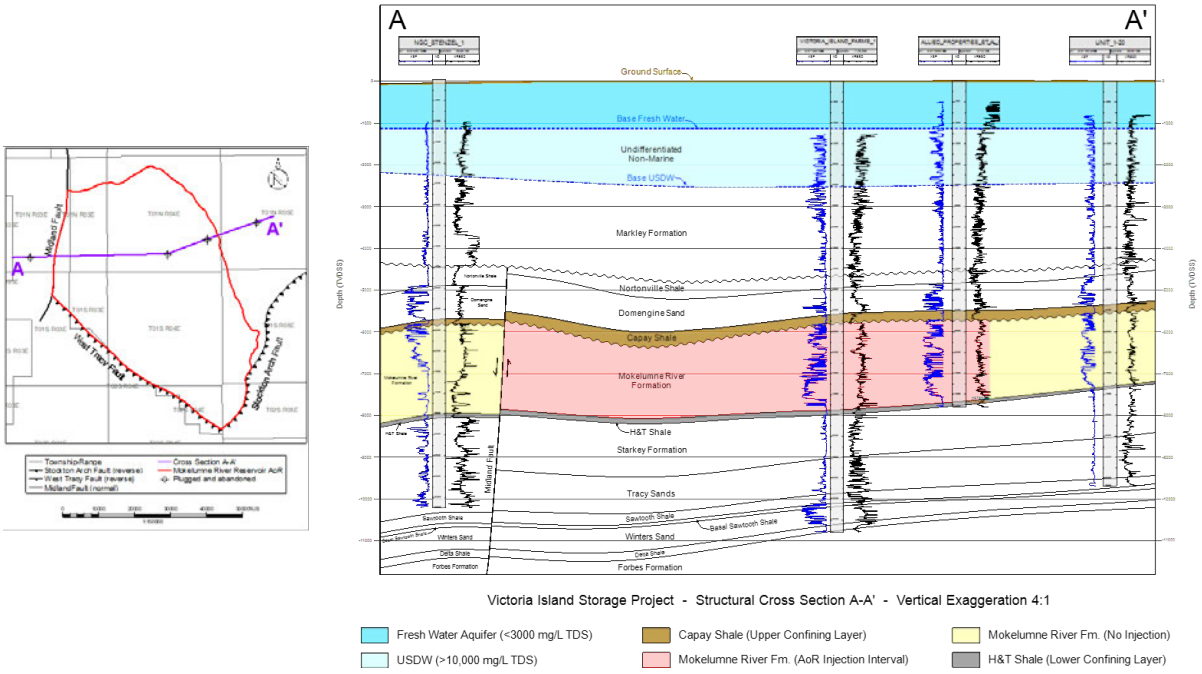

Figure 2.2-4. Cross section showing stratigraphy and lateral continuity of major formations across the AoR.

2.2.2.1 H&T Shale

The H&T Shale acts as a conformable contact to the Mokelumne River Formation and a lower confining zone. Moving southwest, the H&T thickens and contains a facies change with the upper marine shale as the Starkey section progressively adds, creating a thicker shale (Downey 2010).

2.2.2.2 Mokelumne River Formation

The Mokelumne River Formation sandstones are great reservoir quality sands whose trap types include fault truncations, stratigraphic traps and unconformity traps sealed by intervening shales as well as overlying Meganos submarine canyon mudstone infill (Downey 2006). Deposited as a fluvial-deltaic sequence, this sandstone was sourced by the Sierra Nevada terrain to the east and prograded west-southwestward into the forearch basin. This formation truncates to the north by the post-Cretaceous angular unconformity until it pinches out in southern Yolo and Sutter counties (Downey 2006). These large sands can be locally eroded or completely absent due to the downcutting by the Meganos submarine canyons, which are located along the west side of the AoR. In the northwestern portion of Sacramento county the sandstone is as shallow as 2,000 feet and deepens to over 10,500 feet moving to south-central Solano County. Thickness in this area ranges from hundreds of feet thick, separated by thin shales, to 2,500 feet thick (Downey 2010). Within the AoR, thickness ranges from 316 to 1,336 feet and varies in depth from 5,044 to 7,395 TVD (**Figure 2.2-5**).

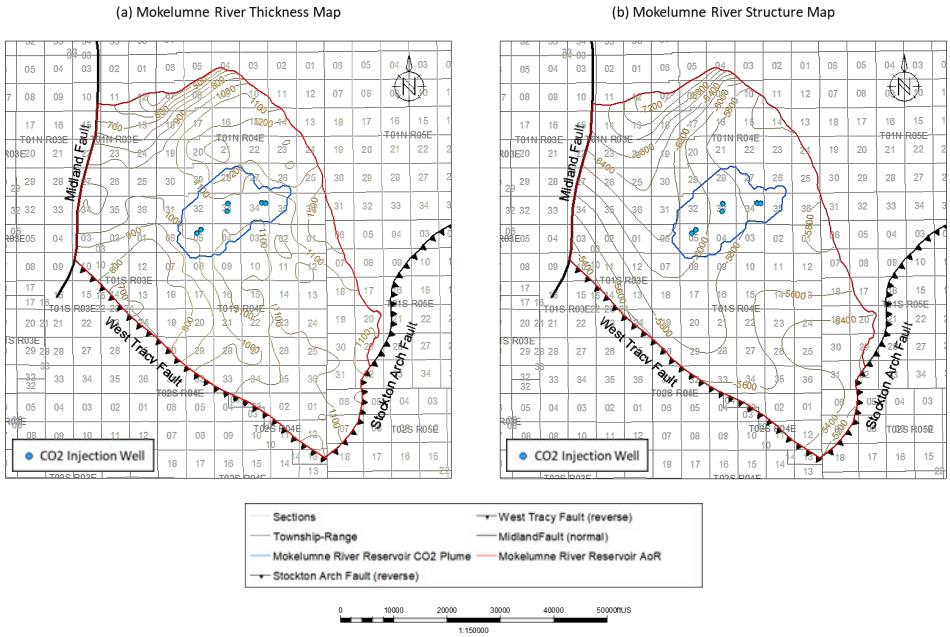

Figure 2.2-5. (a) Mokelumne River Formation thickness map. (b) Mokelumne River Formation structure map.

Six injectors were chosen to inject into the Mokelumne River sandstone. Injectors for this project are shown in **Figure 2.2-6**.

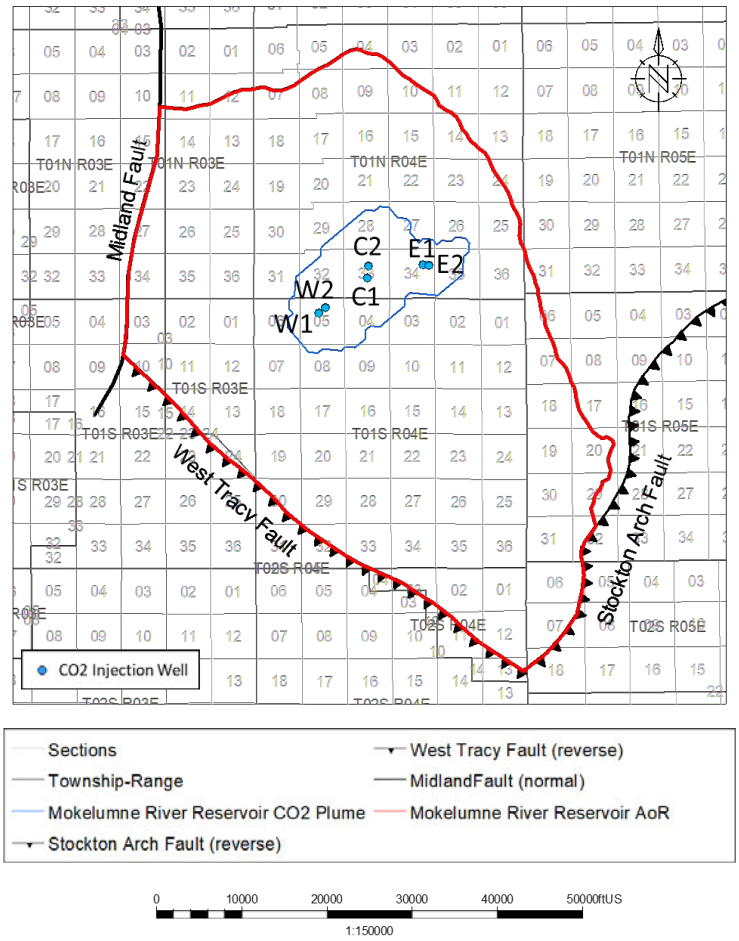

Figure 2.2-6. Injection well location map for the project area. The three groups of injection wells (W1 & W2, C1 & C2, E1 & E2) are approximately 7,000 ft. apart.

2.2.2.3 Capay Shale (Upper Confining Zone)

The Capay Shale provides upper confinement to the Mokelumne River Formation as it spans across the basin as a major regional flooding surface. This Eocene aged formation was deposited as a transgressive surface blanketing the shelf with shales. East of the Midland fault zone, the Martinez Shale has been stripped by erosion, and the Mokelumne River Formation is unconformable overlain by the Capay Shale. Due to its low permeability, this formation acts as a seal to the Mokelumne River Formation injection zone and is a vertical barrier to any CO_2, from reaching the USDW, if any migration were to occur.

2.2.2.4 Domengine Sandstone (Monitoring Zone)

The Domengine Formation is approximately 800-1,200 feet thick on the north flank of Mt. Diablo (Nilsen 1975). Prograding across the Capay Shelf in early-middle Eocene, this formation is characterized by interbedded sandstones, shales and coals. This sand ranges from medium to coarse grain silty mudstone and fine sandstone and onlaps the Capay Shale. It is separated from the Capay by a regional unconformity which progressively truncates older units until the Domengine rests on Cretaceous rocks, moving west. The Domengine consists of an upper and lower portion. The lower member is made up of fluvial and estuarine sandstones. Regionally the lower member is separated from the upper member by an extensive

surface of transgression and change in depositional style. This formation acts as a monitoring zone for injection into the Mokelumne River Formation.

2.2.2.5 Nortonville Shale (Secondary Confining Zone)

Above the Domengine Sandstone is the Nortonville Shale which is separated by a widespread surface of transgression and acts as a secondary confining zone to the Mokelumne River Formation. The Nortonville Shale is a mudstone member of the Kreyenhagen Formation. It is approximately 500 ft. on the north flank of Mt. Diablo and is considered the upper portion of the Domengine Sandstone (Nilsen 1975). Overlying the Domengine Sandstone, this shale acts as a seal throughout most of the southern Sacramento and northern San Joaquin Basins.

2.2.2.6 Marine Strata (Markley to Valley Springs)

The upper Paleogene and Neogene sequence begin with the Valley Springs Formation which represents fluvial deposits that blanket the entire southern Sacramento Basin. The unconformity at the base of the Valley Springs marks a widespread Oligocene regression and separates the more deformed Mesozoic and lower Paleogene strata below from the less deformed uppermost Paleogene and Neogene strata above. The Markley Formation contains approximately 3,000 - 10,000 milligrams per liter (mg/l) total dissolved solids (TDS) water and is the lower most USDW in the AoR (**Figure 2.2-4**). The USDWs are discussed in Section 2.7 of this document.

2.2.3 Map of the Area of Review

As required by 40 CFR 146.82(a)(2), **Figure 2.2-7** shows surface bodies of water, surface features, transportation infrastructure, political boundaries, and cities. Major water bodies in the area are Discovery Bay, Clifton Court Forebay, Victoria Canals, Grant Line Canal, and the Indian Slough. The AoR is in San Joaquin, Contra Costa, and Alameda Counties. This figure does not show the surface trace of known and suspected faults because there are no known surface faults in the AoR. There are also no known mines or quarries in the AoR. **Figure 2.2-8** indicates the locations of State- or EPA-approved subsurface cleanup sites. This cleanup site information was obtained from the State Water Resources Control Board's GeoTracker database, which contains records for sites that impact, or have the potential to impact, groundwater quality. Water wells within and adjacent to the AoR are discussed in Section 2.7.7 of this document.

Figure 2.2-7. Surface Features and the AoR

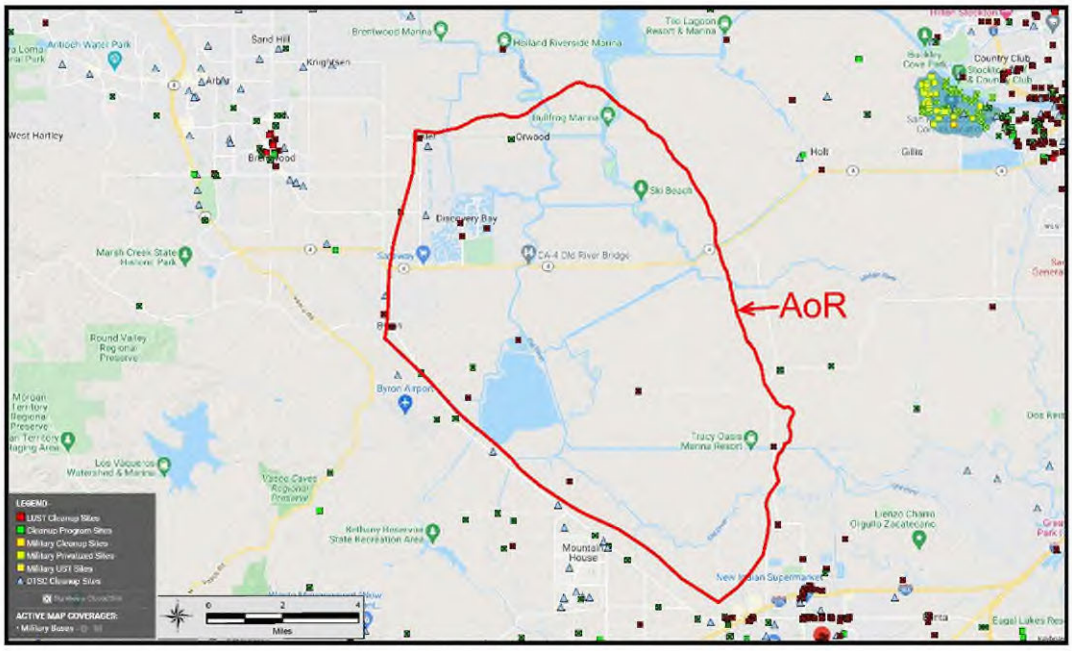

Figure 2.2-8. State or EPA Subsurface Cleanup Sites

2.3 Faults and Fractures [40 CFR 146.82(a)(3)(ii)]

2.3.1 Overview

A combination of 3D and 2D seismic, along with well control, were used to define faulting within the area (**Figure 2.2-3**). The AoR is bound on the east, south, and west sides by faulting, with the boundaries to the north and north-east open (**Figure 2.3-1**). There is one normal fault within the CO_2 plume boundary that transects the injection zone.

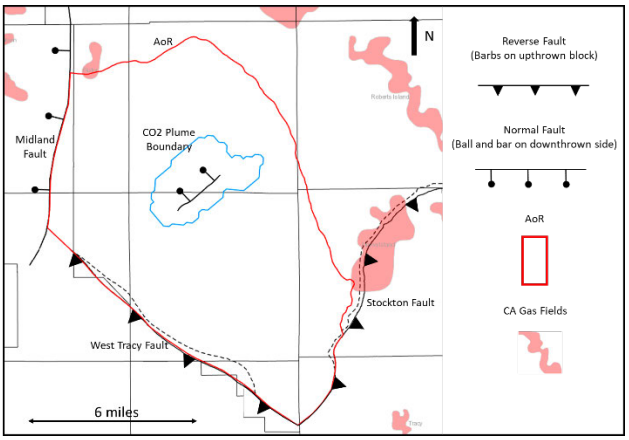

Figure 2.3-1. Faults interpreted from seismic, well, and published data that intersect the AoR.

Firstly, the normal fault within the CO_2 boundary is covered by 3D seismic data and is interpreted as having 100 ft. of offset in the uppermost Mokelumne River Formation. In the nearby Victoria Islands Farms 1 (04077206780000) well the thickness of the upper confining zone Capay Shale is approximately 220 ft. Our geologic model shows an average Capay Shale thickness within the CO_2 plume boundary to be 210 ft. The offset on the fault is not large enough to completely offset the Capay Shale against another formation. As discussed in the Injection and Confining Zone Details section, mineralogy data will be collected for the Capay Shale, but based on data from the H&T Shale we expect the Capay to be clay rich and therefore continue to provide a vertical seal to the Mokelumne River Formation within the fault zone. The Domengine sands above the Capay Shale will be monitored as part of the monitoring and testing plan. **Figure 2.3-2** shows a schematic cross-section across this fault based upon the seismic interpretation.

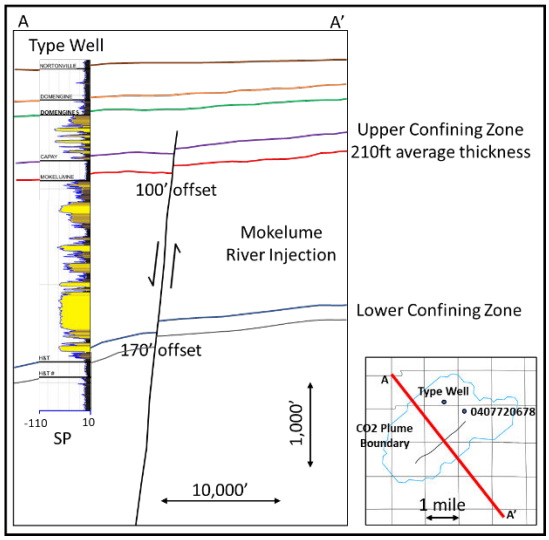

Figure 2.3-2: Schematic cross-section across the normal fault within the CO_2 plume boundary. Properties of the Capay Shale will be confirmed in pre-operational testing and this fault will be monitored during injection in the Domengine sands above.

The AoR is bound to the west by the Midland Fault. The Midland Fault is a west-side-down normal fault that strikes northwest and dips towards the west. This fault was active in the late Cretaceous-Eocene time (Unruh et al. 2009). This movement created the Rio Vista sub-basin that has become a developed natural gas field approximately 12-15 miles north of the CTV III area. At Rio Vista, there is gas production on either side of the Midland Fault with the Midland acting as a seal for trapped hydrocarbons in structural closures. On the eastern side of the Midland Fault at Rio Vista, natural gas has been trapped in three-way closures against the fault at two levels within the Mokelumne River Formation. These Mokelumne River Formation sands include the Midland sand which had an initial pressure gradient of approximately 0.46 psi/ft and the M-5 sand around 0.44 psi/ft, both at 4,500ft or greater. The deeper Winters Formation produces from both sides of the Midland Fault at Rio Vista with pressure gradients ranging from 0.49-0.53 psi/ft. Due to the sealing nature of the fault to the north, it is considered a closed and sealing boundary in our model. Unruh et al. (2009) interpret that the southern end of the Midland fault was later reactivated as a reverse fault in the late Cenozoic modern transpressional tectonic setting. The trace of the fault was created using the work of Downey and Clinkenbeard (2010) and confirmed on 2D seismic data licensed by CRC/CTV.

The eastern portion of the AoR abuts with a portion of the Stockton Fault. The trace and offset of this fault are well defined by the 3D seismic data and well control in the nearby Union Island Gas Field. This thrust fault is associated with Post-Eocene/Pre-Miocene movement and production from the Union Island Gas Field is from a fault-related trap in the footwall. The sealing nature of this fault is demonstrated from this gas trap and the associated pressure draw down from 5,040 psi at field discovery (~0.52 psi/ft) down to current pressure of 1,200 psi (~0.12 psi/ft) in the Winters Formation. The trace of the Stockton Fault interpreted from the 3D seismic data agrees with the Fault Activity Map from the California Geologic Survey (https://maps.conservation.ca.gov/cgs/fam/).

At the southern end of the AoR is the West Tracy Thrust Fault. This fault is drawn through a mix of 3D and 2D seismic data and is interpreted to connect to the Midland and Stockton Faults through the review of published work. Unruh and Hitchcock (2015) reviewed additional 2D seismic data along with other ancillary data and concluded that the West Tracy Fault was probably active between the Eocene and Miocene with later reactivation during late Cenozoic transpression. This blind reverse fault has steeply dipping strata in the south-west hanging wall and may have ruptured the surface near Byron, CA. Their interpretation also connects the West Tracy Fault to the Midland fault at its western junction. Their work was a more detailed description following that of Unruh and Krug (2007). In both publications the eastern end of the West Tracy Fault is somewhat connected to the Vernalis Fault that runs east-west to the east of the project area. Our analysis suggests the West Tracy Fault is better connected to the trace of the Stockton Fault given the strike of the faults in the region. This would agree with the fault trace drawn by Downey and Clinkenbeard (2010). There are no established hydrocarbon fields along the West Tracy Fault that demonstrate fault seal. Due to the sealing nature of the other sub-regional faults in the area, including the Vernalis Fault to the east that seals hydrocarbons at the Vernalis Gas Field, we consider the West Tracy Fault to be sealing. Other evidence for this includes the offset and steeply dipping strata on the south-west side of the fault, with our interpretation of licensed 2D data indicating offsets ranging from 700ft to 1,000ft at the top Mokelumne River Formation across the West Tracy Fault.

None of the three bounding faults for the AoR come in contact with the CO_2 Plume Boundary and therefore only the pressure front is considered. Our modeling has the Mokelumne River Formation under-pressured across the AoR relative to hydrostatic. This will be confirmed in pre-operational testing. In this case, the pressure increase associated with CO_2 injection is seen to increase pressure of the Mokelumne River Formation back to pressures that are documented at other locations along these fault traces within the AoR boundary. **Figure 2.3-3** shows the locations of three pseudo wells where pressures are extracted from the model to calculate the pressures that will be seen across the injection life of this project. Central locations relative to the fault trace within the AoR are chosen. **Table 2.3-1** shows the average initial, maximum (14 years after initial injection), and 100 years post injection pressure at these locations. An average pressure increase is also provided, and these numbers are averages across the Mokelumne River Formation. Given that other formations around these faults, including equivalent Mokelumne River units, have held back hydrocarbons at similar as well as higher pressures above hydrostatic, we believe this to be a safe standard for fault stability. The natural seismic history of this area is discussed in the Seismic History section of this document and Attachment C of this application details the seismicity monitoring plan for this injection site.

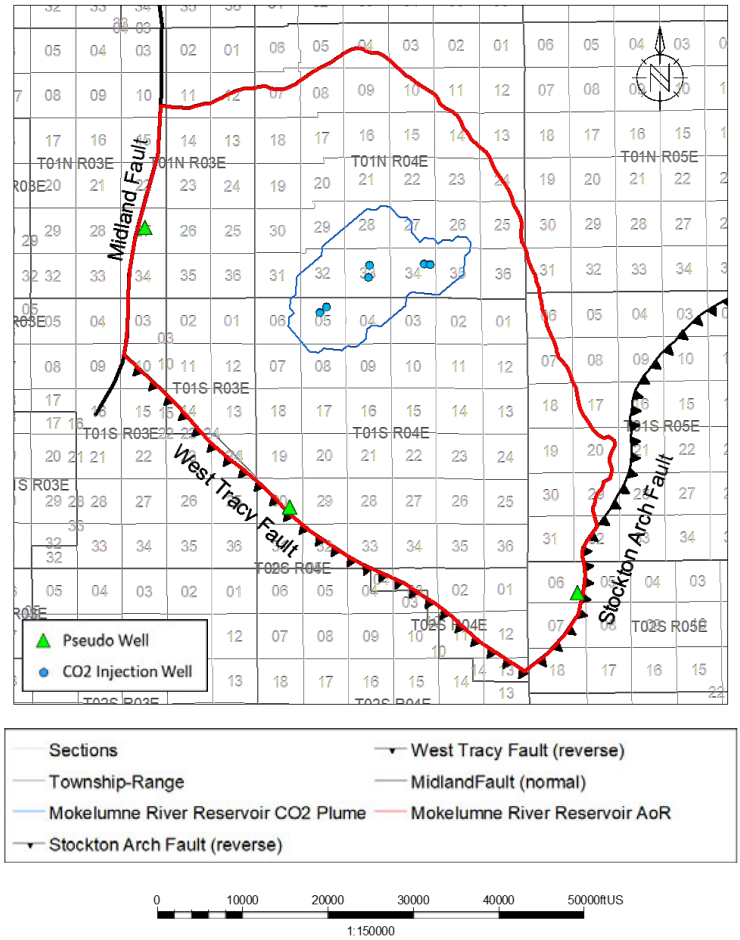

Figure 2.3-3: Green triangles show pseudo well locations at central areas along the three bounding faults relative to the AoR. Pressure data were extracted from the plume model to capture the expected pressure values at each location. Average of these results are presented in **Table 2.3-1**.

Table 2.3-1: Summary of results of pressures extracted from modeling at the pseudo well locations shown in **Figure 2.3-3**. Maximum pressure is 14 years after initial injection starts. Pressure averages shown in both absolute and gradient formats for the Mokelumne River Formation.

Well Location	Depth Range (TVD)	Initial Pressure Average	Max Pressure Average	100 years Post Inj Pressure Average	Delta Average
Midland Fault	6299'-7899'	2915 PSI / 0.415 psi/ft	3120 PSI / 0.444 psi/ft	2916 PSI / 0.415 psi/ft	205 PSI
West Tracy Fault	5729'-7019'	2637 PSI / 0.413 psi/ft	2822 PSI / 0.442 psi/ft	2637 PSI / 0.413 psi/ft	185 PSI
Stockton Arch Fault	5351'-6831'	2498 PSI / 0.412 psi/ft	2653 PSI / 0.438 psi/ft	2498 PSI / 0.412 psi/ft	155 PSI

2.4 Injection and Confining Zone Details [40 CFR 146.82(a)(3)(iii)]

2.4.1 Mineralogy

No quantitative mineralogy information exists within the AoR boundary. Mineralogy data will be acquired across all the zones of interest as part of pre-operational testing. Several wells outside the AoR have mineralogy over the respective formations of interest, and that data is presented below.

2.4.1.1 Mokelumne River Formation

The Speckman_Decarli_1 well outside the AoR has x-ray diffraction (XRD) data for the Mokelumne River Formation (see **Figure 2.4-1** for well locations). Reservoir sand from four samples within this well averages 33% quartz, 42% plagioclase and potassium feldspar, and 24% total clay (see **Table 2.4-1**). The primary clay minerals are kaolinite and mixed layer illite/smectite. Calcite & dolomite were not detected in any of the samples.

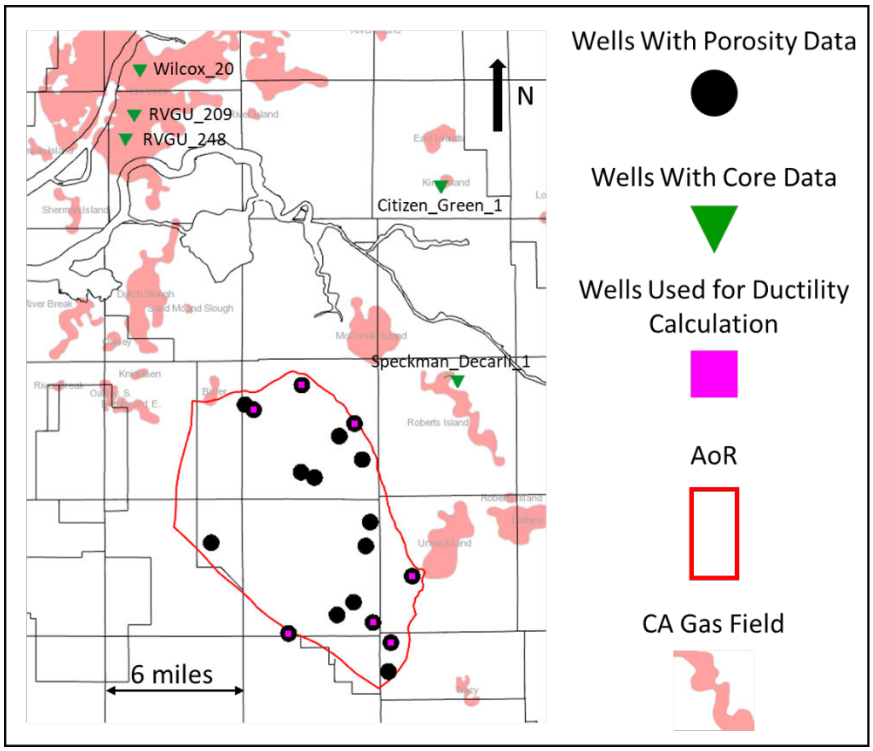

Figure 2.4-1. Map showing location of wells with mineralogy data relative to the AoR.

Table 2.4-1: Formation mineralogy from x-ray diffraction and Fourier transform infrared spectroscopy (FTIR) in four wells.

Well	Zone	Depth (ft)	Quartz	Plagioclase	K-Feldspar	Calcite	Dolomite	Glauconite	Pyrite	Kaolinite	Chlorite	Illite & Mica	Smectite	MXL I/S	Total Clay
Wilcox_20	Capay	4622.0	42.2	18.7	10.7	0.0	0.0		0.6	9.4	3.4	4.5		10.5	27.8
Wilcox_20	Capay	4905.0	34.9	20.7	10.2	0.7	0.0		1.1	15.2	5.8	5.8		5.5	32.3
RVGU_209	Capay	4442.5	26.0	25.0	17.0	1.0	0.0			5.0	3.0			23.0	31.0
RVGU_209	Capay	4480.5	26.0	23.0	20.0	0.0	0.0			0.0	6.0			25.0	31.0
RVGU_209	Capay	4476.5	30.0	23.0	18.0	0.0	0.0			5.0	9.0			15.0	29.0
RVGU_209	Capay	4454.5	30.0	29.0	15.0	0.0	0.0			2.0	6.0			18.0	26.0
RVGU_209	Capay	4498.5	34.0	26.0	19.0	0.0	0.0			1.0	2.0			18.0	21.0
RVGU_209	Capay	4500.5	28.0	19.0	19.0	0.0	0.0			0.0	12.0			22.0	34.0
RVGU_248	Capay	4425.5	35.0	25.0	15.0					5.0	5.0	5.0	10.0		25.0
Speckman_Decarli_1	Mokelumne	6987.0	35.0	18.0	17.0	0.0	0.0	3.0	0.0	10.0	4.0			13.0	27.0
Speckman_Decarli_1	Mokelumne	6989.0	26.0	21.0	15.0	0.0	0.0	0.0	0.0	12.0	8.0			18.0	38.0
Speckman_Decarli_1	Mokelumne	6991.0	39.0	25.0	19.0	0.0	0.0	1.0	0.0	3.0	2.0			11.0	16.0
Speckman_Decarli_1	Mokelumne	7000.0	28.0	26.0	17.0	0.0	0.0	2.0	0.0	10.0	4.0			13.0	27.0
Speckman_Decarli_1	Mokelumne	7002.0	20.0	17.0	14.0	0.0	0.0	0.0	0.0	19.0	8.0			22.0	49.0
Speckman_Decarli_1	Mokelumne	7006.0	28.0	30.0	15.0	0.0	0.0	2.0	0.0	8.0	6.0			11.0	25.0
Speckman_Decarli_1	H&T Shale	8828.0	23.0	21.0	9.0	3.0	0.0	0.0	1.0	12.0	5.0			26.0	43.0
Speckman_Decarli_1	H&T Shale	8830.0	30.0	17.0	11.0	0.0	0.0	0.0	4.0	3.4	14.4	6.1	14.1		38.0
Speckman_Decarli_1	H&T Shale	8909.0	20.0	20.0	13.0	0.0	0.0	2.0	2.0	5.0	3.0			35.0	43.0
Speckman_Decarli_1	H&T Shale	8937.0	20.0	12.0	8.0	0.0	0.0	0.0	2.0	14.0	6.0			38.0	58.0
Speckman_Decarli_1	H&T Shale	8939.0	24.0	18.0	11.0	1.0	0.0	0.0	3.0	3.0	15.5	7.7	16.8		43.0
Speckman_Decarli_1	H&T Shale	8940.0	23.0	29.0	12.0	0.0	0.0	0.0	0.0	4.0	5.0			27.0	36.0
Speckman_Decarli_1	H&T Shale	8942.0	23.0	15.0	10.0	0.0	0.0	0.0	2.0	12.0	5.0			33.0	50.0
Speckman_Decarli_1	H&T Shale	9439.0	20.0	14.0	9.0	0.0	0.0	0.0	1.0	0.0	5.0			51.0	56.0
Speckman_Decarli_1	H&T Shale	9441.0	21.0	19.0	12.0	2.0	0.0	0.0	3.0	0.0	0.0			43.0	43.0

2.4.1.2 Capay Shale

Mineralogy data is available for the Capay Shale from three wells in the Rio Vista Field (RVGU_209, RVGU_248, and Wilcox_20). The RVGU_209 has FTIR, while the other two wells have XRD data. Nine samples show an average of 29% total clay, with mixed layer illite/smectite being the dominant species, with kaolinite and chlorite still prevalent. They also contain 32% quartz, 39% plagioclase and potassium feldspar, minimal pyrite, and less than 1% calcite & dolomite.

2.4.1.3 H&T Shale

Mineralogy data is available for the H&T Shale from the Speckman_Decarli_1 well. Nine samples show an average of 46% total clay, with mixed layer illite/smectite being the dominant species, with kaolinite and chlorite still prevalent. They also contain 23% quartz, 29% plagioclase and potassium feldspar, 2% pyrite, and 1% calcite & dolomite.

2.4.2 Porosity and Permeability

2.4.2.1 Mokelumne River Formation

Wireline log data was acquired with measurements that include but are not limited to spontaneous potential, natural gamma ray, borehole caliper, compressional sonic, resistivity as well as neutron porosity and bulk density.

Formation porosity is determined one of two ways: from bulk density using 2.65 g/cc matrix density as calibrated from core grain density and core porosity data, or from compressional sonic using 55.5 µsec/ft matrix slowness and the Raymer-Hunt equation.

Volume of clay is determined by spontaneous potential and is calibrated to core data.
Log-derived permeability is determined by applying a core-based transform that utilizes capillary pressure porosity and permeability along with clay values from x-ray diffraction or Fourier transform infrared spectroscopy. Core data from two wells with 13 data points was used to develop a permeability transform. An example of the transform from core data is illustrated in **Figure 2.4-2** below.

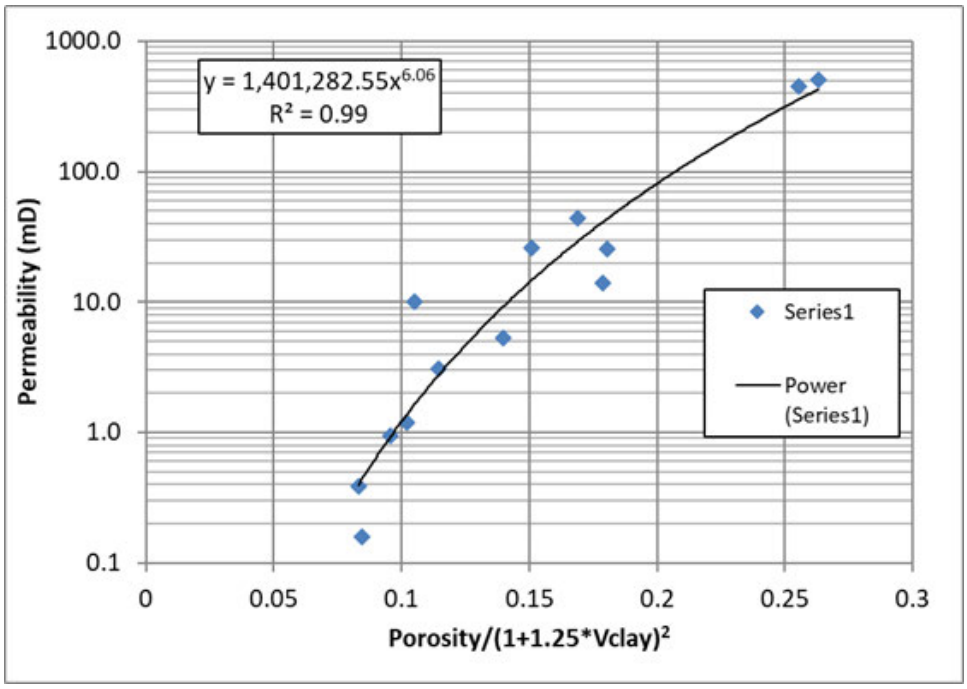

Figure 2.4-2. Permeability transform for Sacramento basin zones.

Comparison of the permeability transform to log generated permeability (Timur-Coates method) from a nuclear magnetic resonance (NMR) log in the Citizen_Green_1 well in King Island Gas Field is almost 1:1 and matches rotary sidewall core permeability over the Capay-Mokelumne River Formation interval (**Figure 2.4-3**). See **Figure 2.4-1** for location of Citizen_Green_1 well.

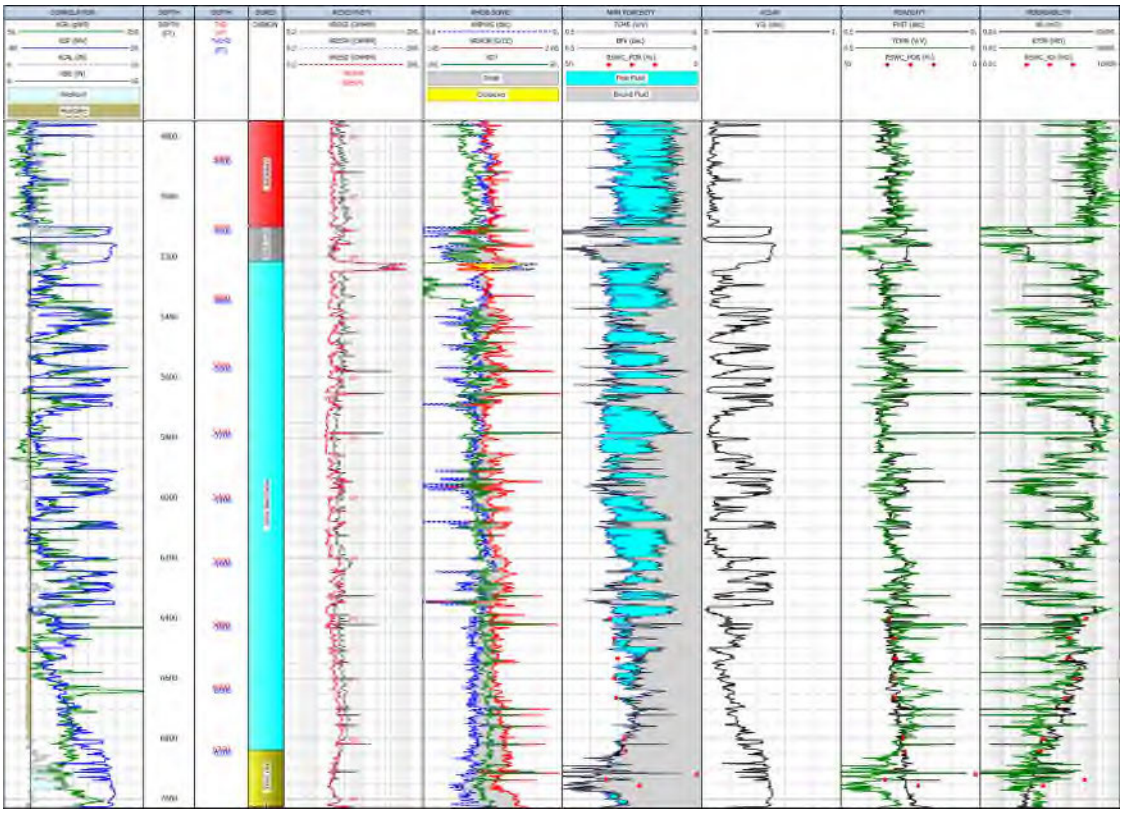

Figure 2.4-3. Example log from the Citizen_Green_1 well in King Island Gas Field. The last track shows a comparison of the permeability calculated from the transform (black) shown in **Figure 2.4-2** to permeability calculated from an NMR log (green) and rotary sidewall core permeability (red dots). Track 1: Correlation and caliper logs. Track 2: Measured depth. Track 3: Vertical depth and vertical subsea depth. Track 4: Zones. Track 5: Resistivity. Track 6: Compressional sonic, density, and neutron logs. Track 7: NMR total porosity and bound fluid. Track 8: Volume of clay. Track 9: Porosity calculated from sonic and NMR total porosity (green). Track 10: Permeability calculated using transform and NMR Timur-Coates permeability.

In the well Ohlendorf_Unit_1_1, for the Mokelumne River Formation, the porosity ranges from 1.5% - 34% with a mean of 26.5% (**Figure 2.4-4**). The permeability ranges from 0.003 mD - 697 mD with a log mean of 68 mD (**Figure 2.4-5**).

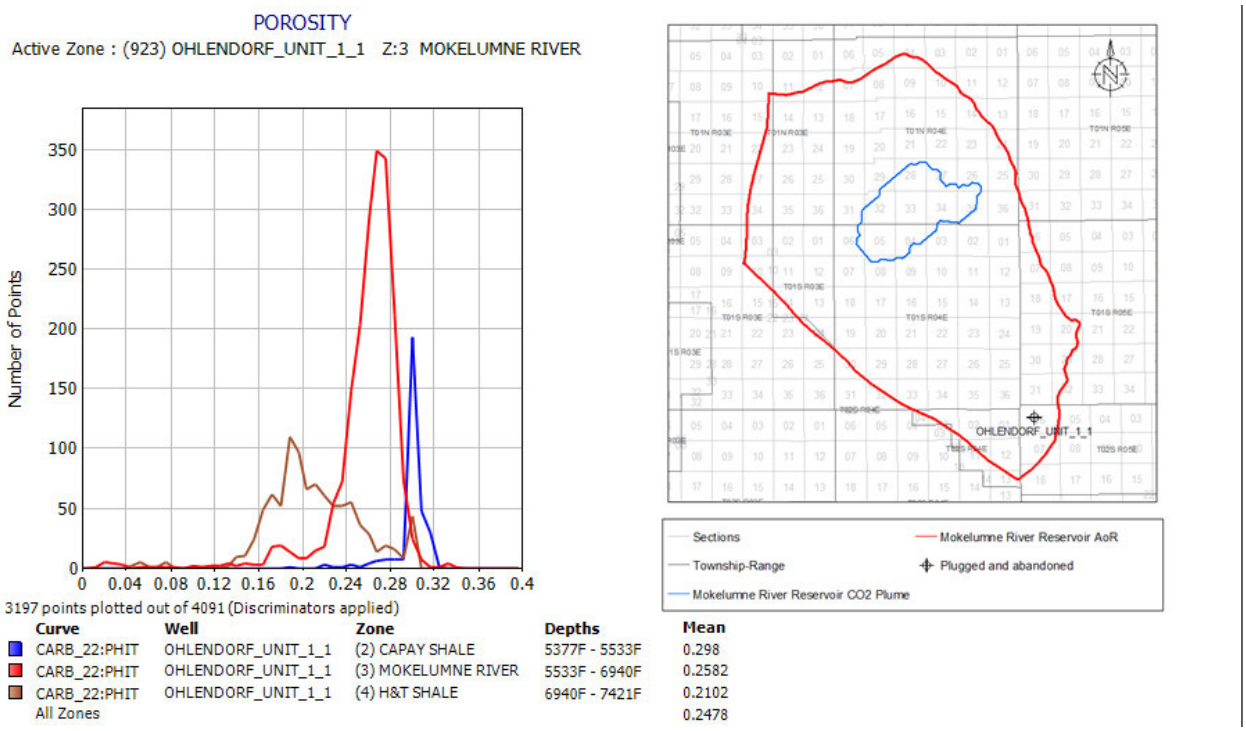

Figure 2.4-4. Porosity histogram for well Ohlendorf_Unit_1_1. In the histogram, blue represents the Capay Shale, red the Mokelumne River Formation, and brown the H&T Shale. For the two shale intervals, only data with VCL>0.25 is shown, and for the Mokelumne River Formation only data with VCL<=0.25 is shown.

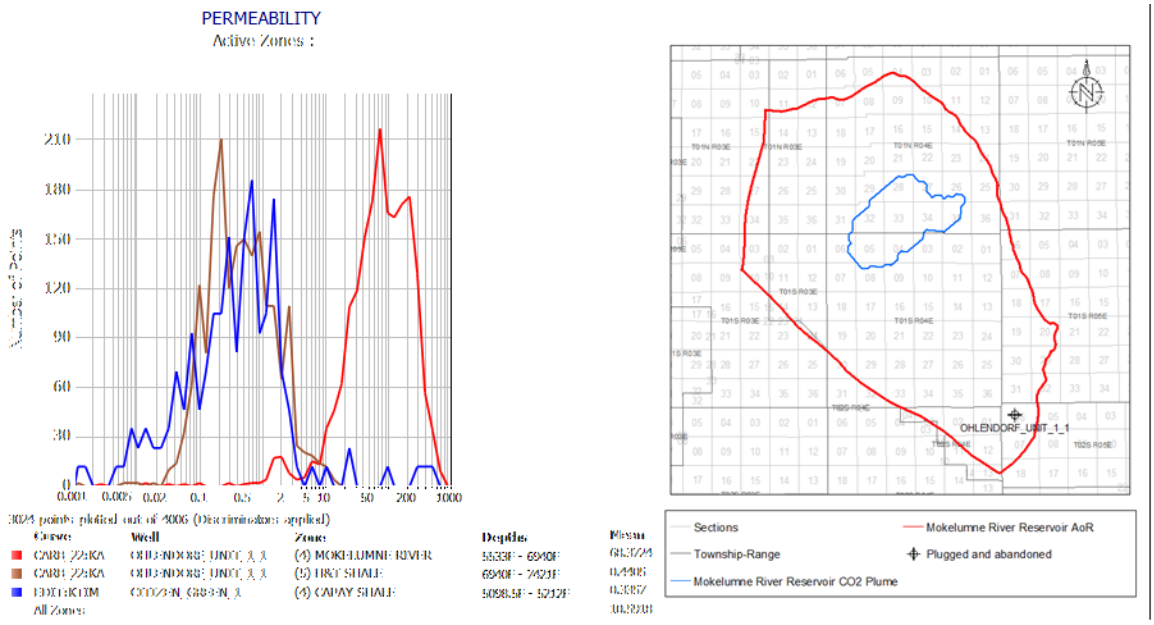

Figure 2.4-5. Permeability histogram for wells Ohlendorf_Unit_1_1 and Citizen_Green_1. In the histogram, blue represents the Capay Shale, red the Mokelumne River Formation, and brown the H&T Shale. For the two shale intervals, only data with VCL>0.25 is shown, and for the Mokelumne River Formation only data with VCL<=0.25 is shown.

A log plot for the Ohlendorf_Unit_1_1 is included in **Figure 2.4-6**.

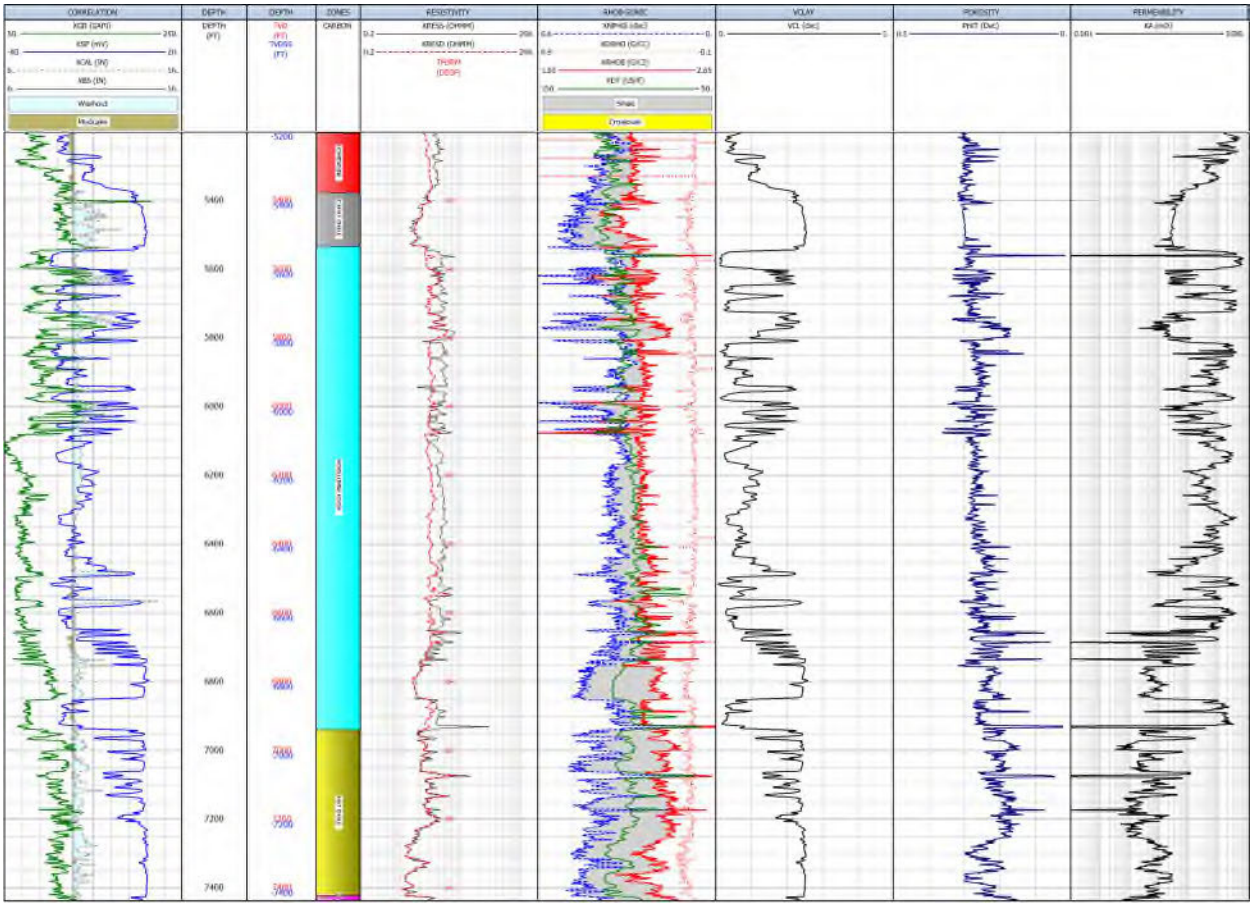

Figure 2.4-6. Log plot for well Ohlendorf_Unit_1_1, showing the log curves used as inputs into calculations of clay volume, porosity and permeability, and their outputs. Track 1: Correlation and caliper logs. Track 2: Measured depth. Track 3: Vertical depth and vertical subsea depth. Track 4: Zones. Track 5: Resistivity. Track 6: Compressional sonic, neutron, and density logs. Track 7: Volume of clay. Track 8: Porosity calculated from log curves. Track 9: Permeability calculated using transform. See **Figure 2.4-7** for well location.

The average porosity for the Mokelumne River Formation is 27.0%, based on 18 wells with porosity logs and 30487 individual logging data points. See **Figure 2.4-7** for location of wells used for porosity and permeability averaging.

The geometric average permeability for the Mokelumne River Formation is 75.4 mD, based on 18 wells with porosity logs and 30073 individual logging data points.

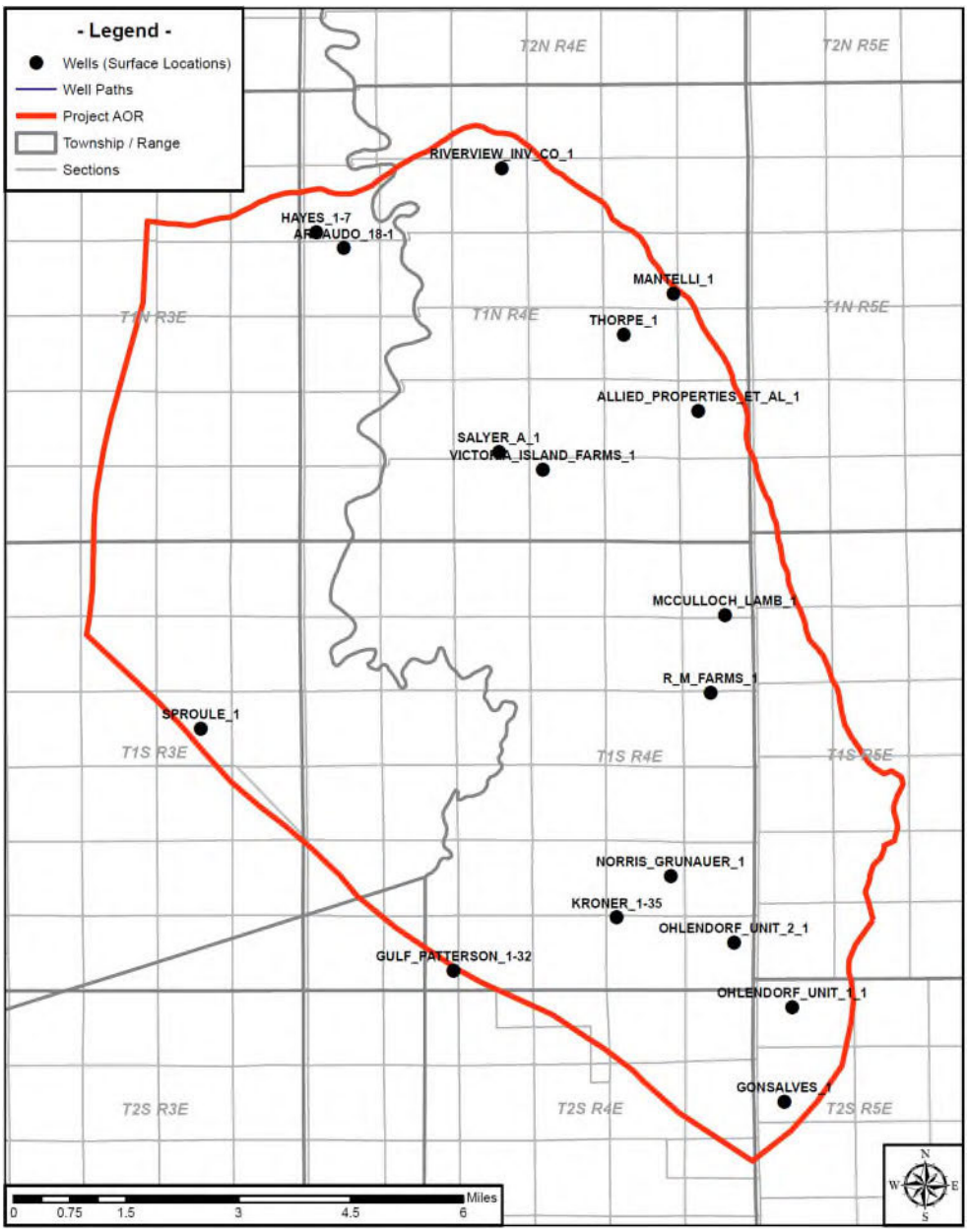

Figure 2.4-7. Map of wells with porosity and permeability data.

2.4.2.2 Capay Shale

The average porosity of the upper confining zone (Capay Shale) is 29.3%, based on 17 wells with porosity logs and 10044 individual logging data points.

The geometric average permeability of the upper confining zone (Capay Shale) is 0.34 mD, based on the Citizen_Green_1 well NMR permeability from the Timur-Coates method (see **Figure 2.4-1** for well location).

2.4.2.3 H&T Shale

The average porosity of the lower confining zone (H&T Shale) is 21.4%, based on 16 wells with porosity logs and 31279 individual logging data points.

The geometric average permeability of the lower confining zone (H&T Shale) is 0.49 mD, based on 16 wells with porosity logs and 30853 individual logging data points.

2.4.3 Injection Zone and Confining Zone Capillary Pressure

Capillary pressure is the difference across the interface of two immiscible fluids. Capillary entry pressure is the minimum pressure required for an injected phase to overcome capillary and interfacial forces and enter the pore space containing the wetting phase.

No capillary pressure data was available for the Capay Shale. This data will be acquired as part of pre-operational testing.

No capillary pressure data was available for the Mokelumne River Formation (Injection zone) in the project area. For computational modeling purposes, capillary pressure data obtained in the similar geologic age and setting Winters Formation in the nearby Union Island Gas field was used. Site and zone specific Capillary pressure data will be obtained as part of pre-operational testing. **Figure 2.4-8** shows the capillary pressure data used for the computational modeling.

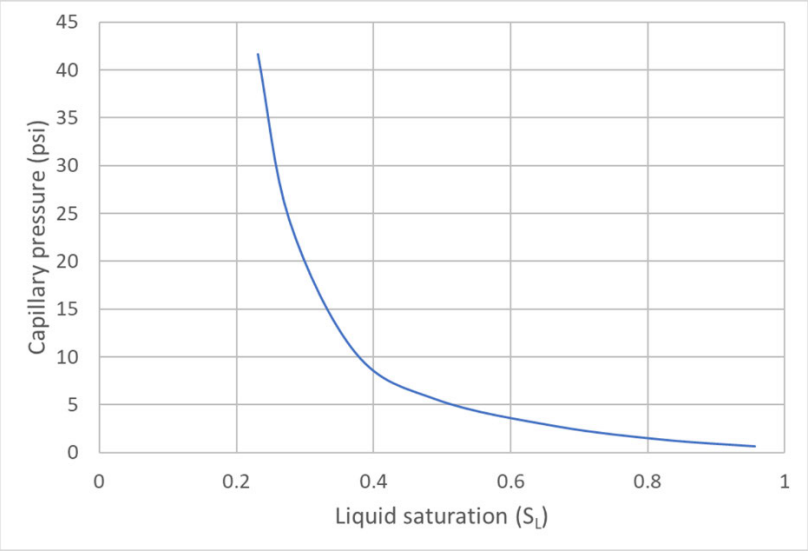

Figure 2.4-8. Injection zone Capillary pressure used for Computational modeling.

2.4.4 Depth and Thickness

Depths and thickness of the Mokelumne River Formation reservoir and Capay confining zone (**Table 2.4-2**) are determined by structural and isopach maps (**Figure 2.4-9**) based on well data (wireline logs). Variability of the thickness and depth measurements is due to:

1. Structural variability within the Mokelumne River and Capay Formations are caused by the Meganos submarine canyon erosional event.
2. The Capay Shale remains consistent throughout the AoR both structurally and stratigraphically.
3. Thickness variability within the Mokelumne River Formation is due to the Meganos submarine canyon erosion.

Table 2.4-2: Capay Shale and Mokelumne River Formation gross thickness and depth within the AoR.

Zone	Property	Low	High	Mean
Upper Confining Zone	Thickness (feet)	100	360	207
Capay Shale	Depth (feet TVD)	4,954	6,164	5,582
Reservoir	Thickness (feet)	316	1,336	1,024
Mokelumne River Formation	Depth (feet TVD)	5,044	10,281	7,395

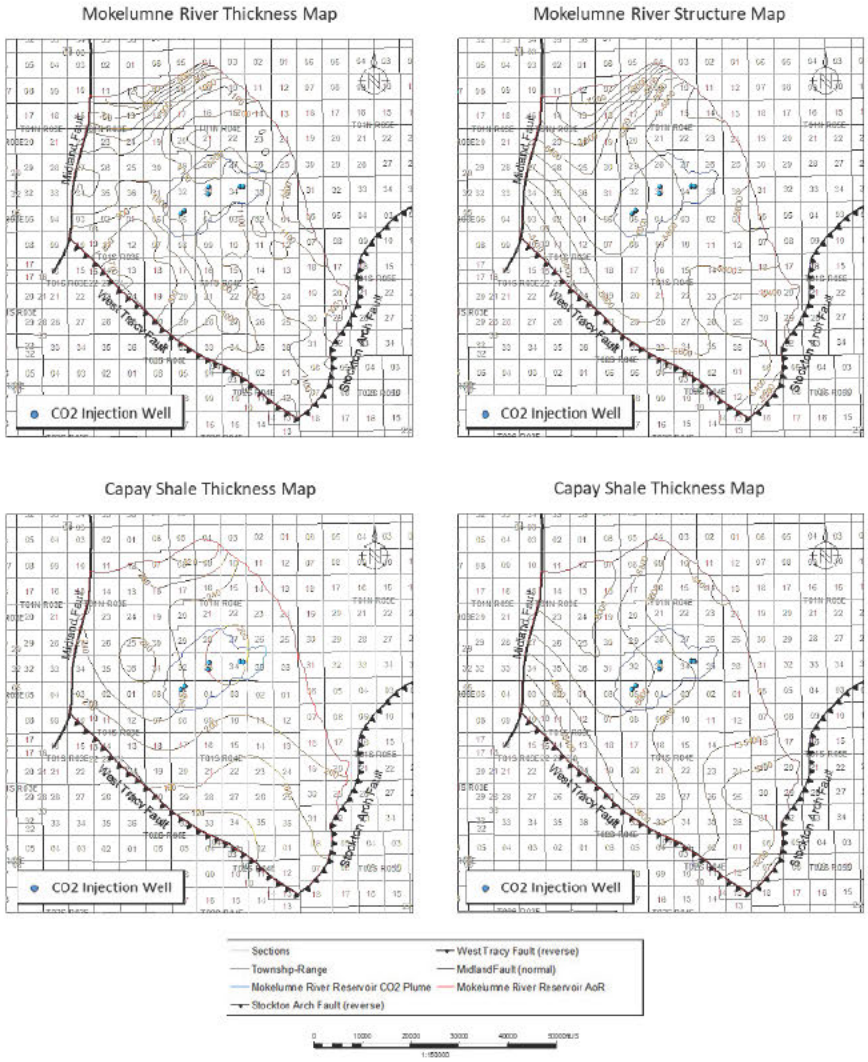

Figure 2.4-9. Thickness and structure maps for the Mokelumne River and Capay Shale Formations within the AoR.

2.4.5 Structure Maps

Structure maps are provided in order to indicate a depth to reservoir adequate for supercritical-state injection.

2.4.6 Isopach Maps

Spontaneous potential (SP) logs from surrounding gas wells were used to identify sandstones. Negative millivolt deflections on these logs, relative to a baseline response in the enclosing shales, define the

sandstones. These logs were baseline shifted to 0mV. Due to the log vintage variability, there is an effect on quality which creates a degree of subjectivity within the gross sand, however this will not have a material impact on the maps.
Variability in the thickness and depth of either the Capay Shale or the Mokelumne River Formation sandstone will not impact confinement. CTV will utilize thickness and depth shown when determining operating parameters and assessing project geomechanics.

2.5 Geomechanical and Petrophysical Information [40 CFR 146.82(a)(3)(iv)]

2.5.1 Caprock Ductility

Ductility and the unconfined compressive strength (UCS) of shale are two properties used to describe geomechanical behavior. Ductility refers to how much a rock can be distorted before it fractures, while the UCS is a reference to the resistance of a rock to distortion or fracture. Ductility generally decreases as compressive strength increases.

Ductility and rock strength calculations were performed based on the methodology and equations from Ingram & Urai, 1999 and Ingram et. al., 1997. Brittleness is determined by comparing the log derived unconfined compressive strength (*UCS*) vs. an empirically derived UCS for a normally consolidated rock (UCS_{NC}).

$$\log UCS = -6.36 + 2.45 \log\left(0.86V_p - 1172\right) \quad (1)$$

$$\sigma' = OB_{pres} - P_p \quad (2)$$

$$UCS_{NC} = 0.5\sigma' \quad (3)$$

$$BRI = \frac{UCS}{UCS_{NC}} \quad (4)$$

Units for the UCS equation are *UCS* in MPa and V_p (compressional velocity) in m/s. OB_{pres} is overburden pressure, P_p is pore pressure, σ' is effective overburden stress, and *BRI* is brittleness index.

If the value of BRI is less than 2, empirical observation shows that the risk of embrittlement is lessened, and the confining zone is sufficiently ductile to accommodate large amounts of strain without undergoing brittle failure. However, if BRI is greater than 2, the "risk of development of an open fracture network cutting the whole seal depends on more factors than local seal strength and therefore the BRI criterion is likely to be conservative, so that a seal classified as brittle may still retain hydrocarbons" (Ingram & Urai, 1999).

2.5.1.1 Capay Shale

Within the AoR, six wells had compressional sonic and bulk density data over the Capay Shale to calculate ductility, comprising 3,769 individual logging data points, see pink squares in **Figure 2.4-1**. 15 wells had compressional sonic data over the Capay Shale to calculate UCS, comprising 9413 individual logging data

points, see black circles in **Figure 2.4-1**. The average ductility of the confining zone based on the mean value is 1.50. The average rock strength of the confining zone, as determined by the log derived UCS equation above, is 2,091 psi.

An example calculation for the well Ohlendorf_Unit_1_1 is shown below (**Figure 2.5-1**). UCS_CCS_VP is the UCS based on the compressional velocity, UCS_NC is the UCS for a normally consolidated rock, and BRI is the calculated brittleness using this method. Brittleness less than two (representing ductile rock) is shaded red.

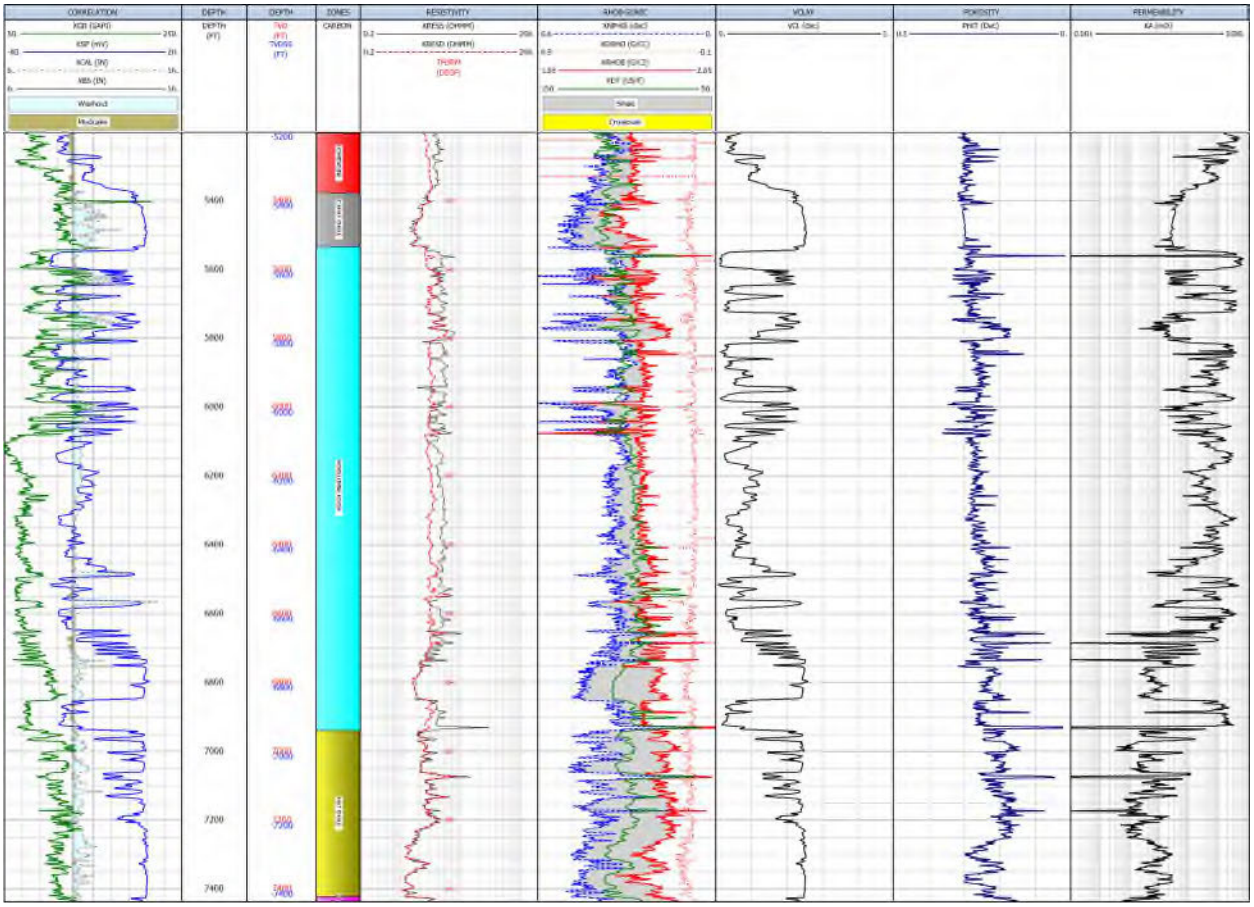

Figure 2.5-1. Unconfined compressive strength and ductility calculations for well Ohlendorf_Unit_1_1. The Capay Shale ductility is less than two, as is the shallower Nortonville Shale. Track 1: Correlation logs. Track 2: Measured depth. Track 3: Vertical depth and vertical subsea depth. Track 4: Zones. Track 5: Resistivity. Track 6: Density and neutron logs. Track 7: Density and compressional sonic logs. Track 8: Volume of clay. Track 9: Porosity calculated from sonic and density. Track 10: Water saturation. Track 11: Permeability. Track 12: Caliper. Track 13: Overburden pressure and hydrostatic pore pressure. Track 14: UCS and UCS_NC. Track 15: Brittleness. See **Figure 2.4-4** for well location.

Within the Capay Shale, the brittleness calculation drops to a value less than two. Additionally, the Nortonville Shale above the Capay Shale has a brittleness value less than two. As a result of the Capay Shale ductility, there are no fractures that will act as conduits for fluid migration from the Mokelumne River Formation.

2.5.2 Stress Field

The stress of a rock can be expressed as three principal stresses. Formation fracturing will occur when the pore pressure exceeds the least of the stresses. in this circumstance, fractures will propagate in the direction perpendicular to the least principal stress (**Figure 2.5-2**).

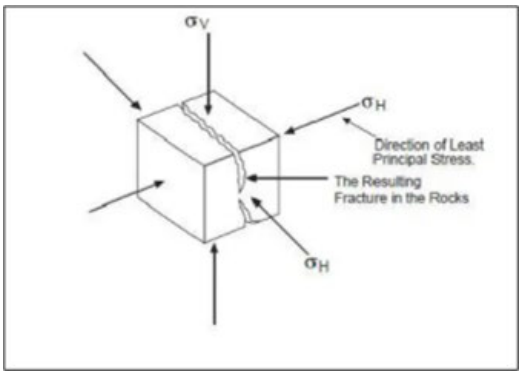

Figure 2.5-2: Stress diagram showing the three principal stresses and the fracturing that will occur perpendicular to the minimum principal stress.

Stress orientations in the Sacramento basin have been studied using both earthquake focal mechanisms and borehole breakouts (Snee and Zoback, 2020, Mount and Suppe, 1992). The azimuth of maximum principal horizontal stress (S_{Hmax}) was estimated at N40ºE ± 10º by Mount and Suppe, 1992. Data from the World Stress Map 2016 release (Heidbach et al., 2016) shows an average S_{Hmax} azimuth of N37.4ºE once several far field earthquakes with radically different S_{Hmax} orientations are removed (**Figure 2.5-3**), which is consistent with Mount and Suppe, 1992. The earthquakes in the area indicate a strike-slip/reverse faulting regime.

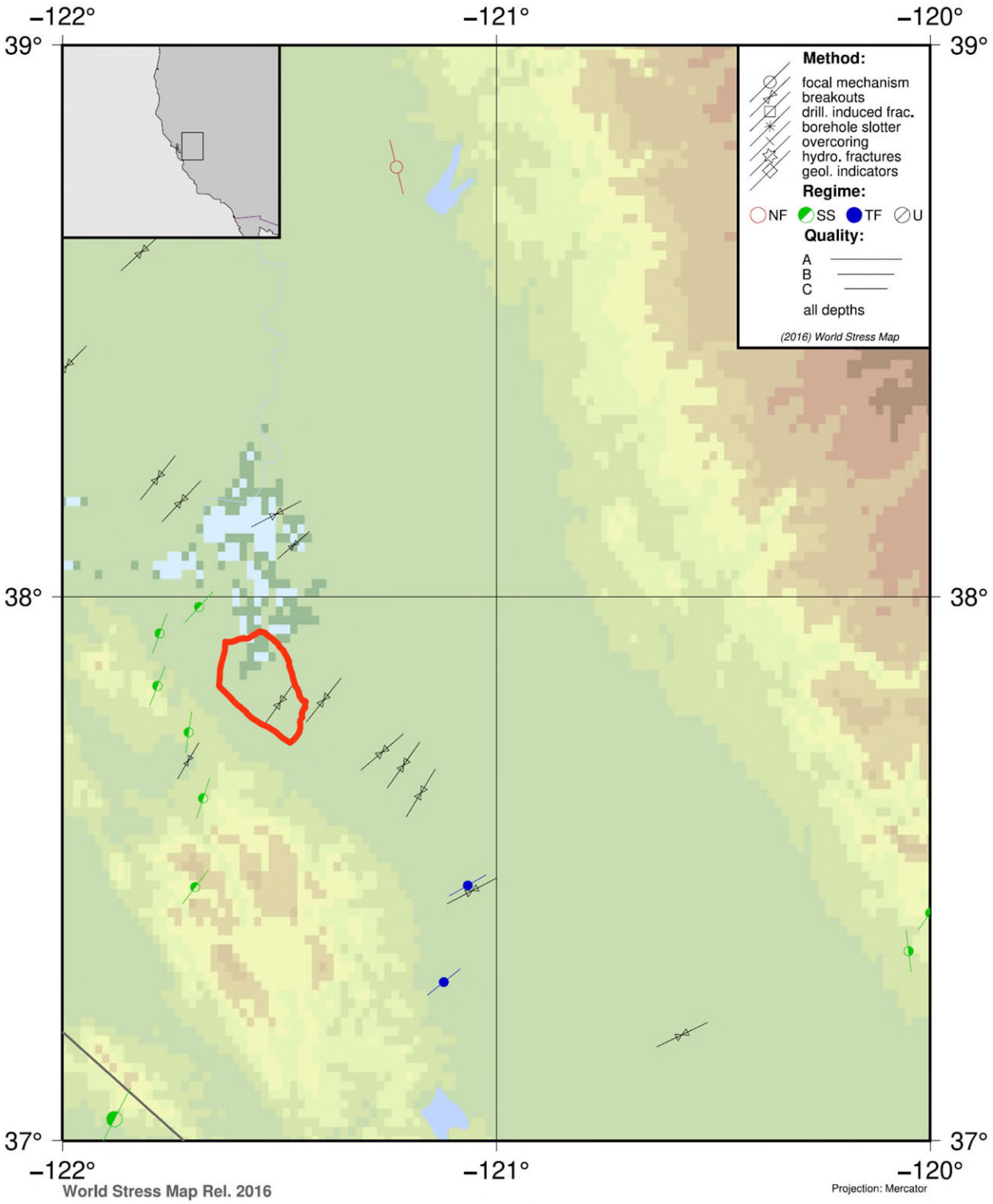

Figure 2.5-3: World Stress Map output showing S_{Hmax} azimuth indicators and earthquake faulting styles in the Sacramento Basin (Heidbach et al., 2016). In red is the outline of the Mokelumne River Formation AoR. The background coloring represents topography.

In the project AoR there is no site specific Mokelumne River Formation fracture pressure or fracture gradient. A Mokelumne River Formation step rate test will be conducted as per the pre-operational testing plan. However, several wells in the Union Island Gas Field have formation integrity tests (FIT) for the Mokelumne River Formation and H&T shale. Two wells recorded minimum fracture gradients of 0.75-0.76 psi/ft based on FIT in the Mokelumne River Formation (Galli_1 and Yamada_Line_Well_1, see **Figure 2.5-4** for well locations). For the computational simulation modeling and well performance modeling, a frac gradient of 0.76 psi/ft was assumed for now.

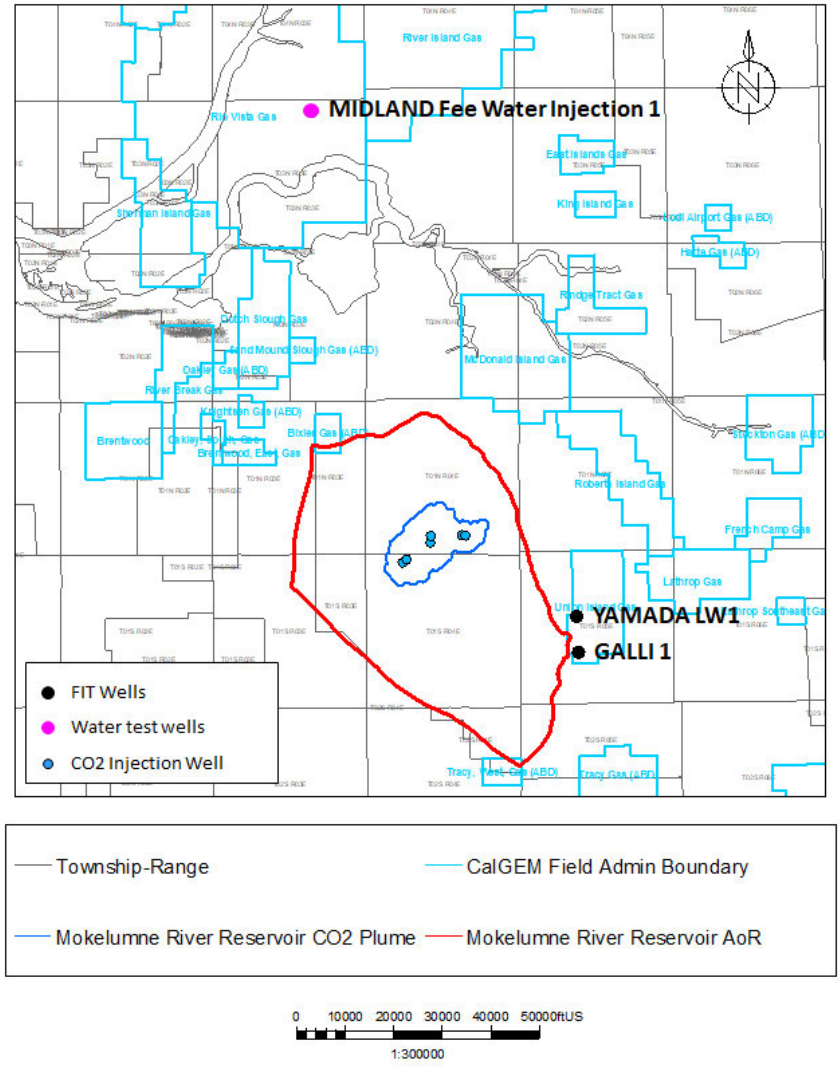

Figure 2.5-4. Map showing the location of wells with water tests and formation integrity tests (FIT).

In the project AoR there is no site specific Capay Shale fracture pressure or fracture gradient. A Capay Shale step rate test will be conducted as per the pre-operational testing plan. In the interim, CTV is making the assumption that the Capay Shale will have a similar fracture gradient as the Mokelumne River Formation.

The overburden stress gradient in the reservoir and confining zone is 0.91 psi/ft. No data currently exists for the pore pressure of the confining zone. This will be determined as part of the preoperational testing plan.

2.6 Seismic History [40 CFR 146.82(a)(3)(v)]

As discussed in prior sections, 3D seismic, along with two-dimensional seismic and well data, were used to create depth surfaces for the major faults within the AoR. The traces of these faults agree with published work, with one example being the Fault Activity Map created by the California Geologic Survey (CGS) shown in **Figure 2.6-1**. The CGS categorize the Midland Fault as a Quarternary Fault of undifferentiated age, and the Stockton Fault as Pre-Quaternary. The CGS does not display a trace for the West Tracy Fault, likely due to the limited public information available to document its presence. As discussed in Unruh and Hitchcock (2015), seismic reflection data from the hydrocarbon industry is needed to map this fault. Further discussion on the timing on each of the faults is provided in the Faults and Fractures section of this document.

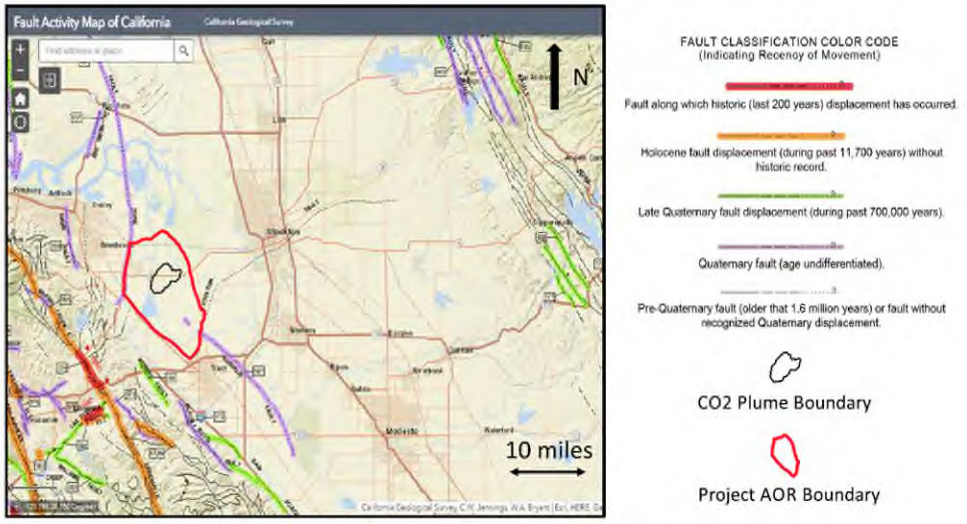

Figure 2.6-1. Fault Activity Map from the California Geologic Survey. Fault traces shown agree with the interpretation of CRC/CTV. The Stockton Arch Fault is considered Pre-Quaternary associated with Post-Eocene/Pre-Miocene movement. The Midland Fault was active in the late Cretaceous-Eocene time, however the southern end of the Midland fault has been interpreted as reactivated as a reverse fault in the late Cenozoic transpressional tectonic setting.

The United States Geologic Survey (USGS) provides an earthquake catalog tool (https://earthquake.usgs.gov/earthquakes/search/) which can be used to search for recent seismicity that could be associated with faults in the area for movement. A search was made for earthquakes in the greater vicinity of the project area from 1850 to modern day with events of a magnitude greater than three. **Figure 2.6-2** shows the results of this search. **Table 2.6-1** summarizes some of the data taken from them. Events were cut down to include those only in the vicinity of the faults mapped for this project and events associated with the Marsh Creek Fault system to the west are removed from the data table.

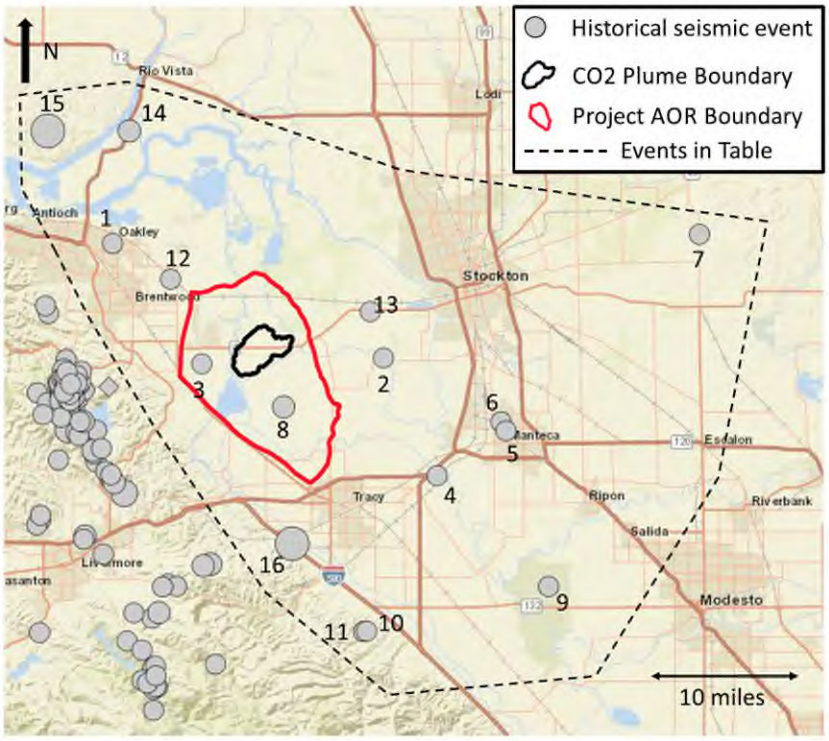

Figure 2.6-2. Historical earthquakes from the USGS catalog tool for the greater area. Data from these events are compiled in **Table 2.6-1** in chronological order associated with events 1 through 16 on the map. Events are sized by magnitude and those to the west are removed due to their association with a different fault trend.

Table 2.6-1: Data from USGS earthquake catalog for faults in the region of CTV III.

Number	Date	Latitude	Longitude	Depth (km)	Magnitude	Last Updated	Location
1	6/22/2018	37.99	-121.72	10.4	3.2	7/9/2021	1km SW of Oakley, CA
2	10/15/2010	37.88	-121.39	14.6	3.1	1/23/2017	9 km WSW of Taft Mosswood, California
3	9/29/2002	37.87	-121.61	4.3	3.4	2/12/2020	2 km ENE of Byron, California
4	2/10/1992	37.77	-121.32	14.6	3.1	2/9/2016	8km SSW of Lathrop, California
5	2/4/1991	37.81	-121.24	7.7	3.1	12/18/2016	2 km NW of Manteca, California
6	2/3/1991	37.82	-121.24	9.4	3.1	12/18/2016	2 km E of Lathrop, California
7	1/27/1980	38.00	-121.00	6.0	3.3	4/2/2016	8km ESE of Linden, CA
8	8/6/1979	37.83	-121.51	6.0	4.3	4/1/2016	6km NNE of Mountain House, CA
9	2/2/1979	37.66	-121.19	18.0	3.5	4/1/2016	10km WSW of Salida, CA
10	10/6/1976	37.61	-121.41	2.9	3.3	12/15/2016	13 km S of Tracy, California
11	9/5/1976	37.61	-121.41	6.5	3.5	12/15/2016	13 km S of Tracy, California
12	6/9/1975	37.96	-121.65	15.0	3.1	12/15/2016	2 km SE of Knightsen, California
13	2/2/1944	37.93	-121.40	6.0	3.8	1/28/2016	7km SW of Country Club, CA
14	2/14/1909	38.10	-121.70		4.5	6/4/2018	7 km S of Rio Vista, California
15	05/19/1889	38.10	-121.80		6.0	2/16/2021	North of Antioch, California
16	07/15/1866	37.70	-121.50		6.0	1/30/2021	Southwest of Stockton, California

Figure 2.6-3. combines the events from the USGS catalog with the mapped faults within the AoR including the West Tracy Fault. Events 16, 10 and 11 were likely associated with the Black Butte – Midway Fault system to the south-west of the project area. Events 4 and 9 are substantially deeper than the sedimentary section and coincide with the trace of the Vernalis Fault, both faults are shown on the CGS Fault Activity

Map (**Figure 2.6-1**)**.** Events 5 and 6 have no clear relationship to any mapped fault system, were one day apart, and relatively deep (both greater than 7.5km as estimated by the USGS catalog). Event 1, to the west of the AoR occurring in 2018, is close to the Davis Fault on the west side of Brentwood. There are no mapped faults nearby event 15, significantly away from the AoR.

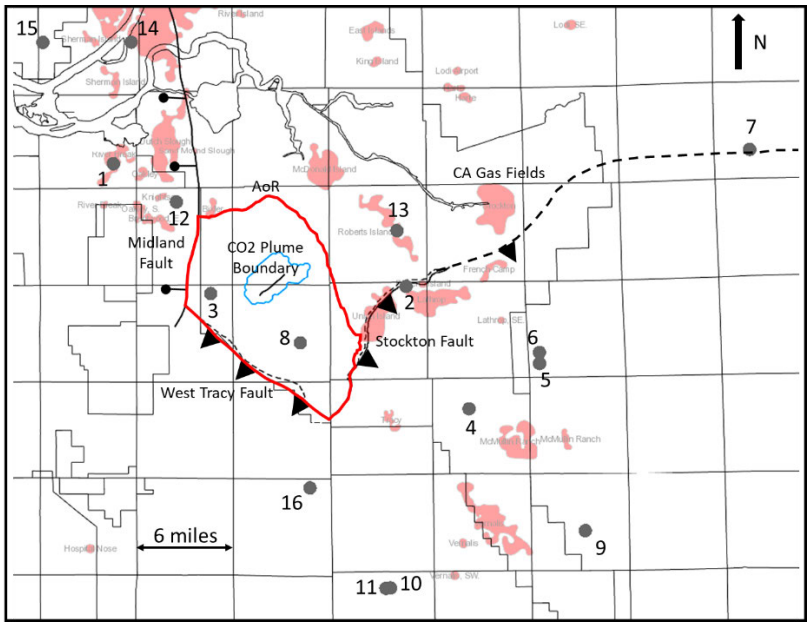

Figure 2.6-3. Summary map of event locations from the USGS catalog relative to the mapped faults in the AoR of CTV III. California Gas Fields are also shown for reference.

Event 8 appears to be isolated from the fault zones at a depth of 6km. Reviewing the 3D seismic data in that area there may be a structural feature at the level of seismic basement, but it is not well imaged. The event does not continue into the shallower sediments that are thousands of feet deeper than the proposed injection zone. Similar can be said for event 13, another deep (6km) event that is outside of the AoR.

For the Stockton Fault, event numbers 2 and 7 are clearly related to the fault trace. Event 7 was a significant distance from the AoR and event 2 was significantly deeper (14.55km) than the proposed injection zone. Finally, events 3, 12, and 14 are in the closest proximity to the Midland Fault. Event 14 appears to align with the Rio Vista Fault, a mapped fault by the CGS that may be a splay of the Midland Fault and to the north of the CTV III AoR. Event 12 is interpreted to be at a significant depth (14.95km) away from the injection zone and far beneath the sedimentary section of the basin. Event 3 is likely the most concerning, this earthquake happened in 2002, at the approximate seismic basement level which is interpreted to be around 16,000 ft (4.88km). The average depth of prior seismic events in the region based on these data (**Table 2.6-1**) is approximately 9.3km, far deeper than the proposed injection zone and sedimentary section.

Given the history of seismicity in the region, minimizing pressure on the mapped faults is a key part of CTV III. Our modeling shows the Mokelumne River Formation to be under-pressured across the AoR, which will be confirmed in pre-operational testing. The Faults and Fractures section of this document provides further information on the expected pressures seen at these faults and discusses the gradients relative to other geologic zones along them. As stated previously, given that other formations around these faults

have held back hydrocarbons at pressures above hydrostatic, we believe this to be a safe standard for fault stability.

Lund-Snee and Zoback (2020) published updated maps for crustal stress estimates across North America. **Figure 2.6-4** shows a modified image from that work highlighting the CTV III area. This work agrees with previous estimates of maximum horizontal stress in the region of approximately N40°E in a strike-slip to reverse stress regime (Mount and Suppe, 1992) and is consistent with World Stress map data for the area (Heidbach et al, 2016). Attachment C of this application discusses the seismicity monitoring plan for this injection site.

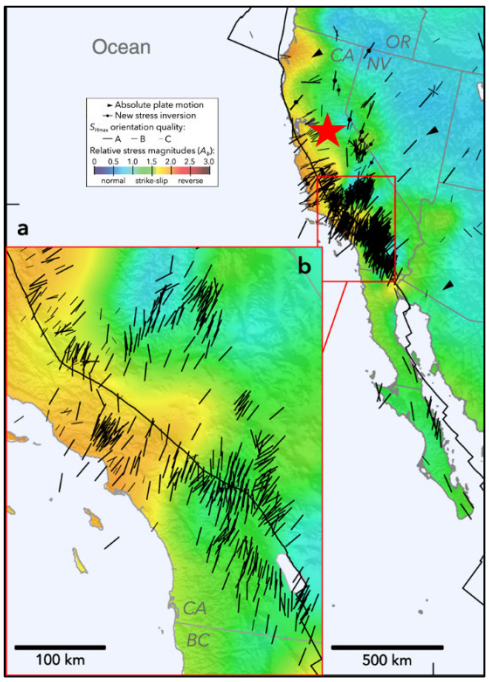

Figure 2.6-4. Image modified from Lund-Snee and Zoback (2020) showing relative stress magnitudes across California. Red star indicates the CTV III site area.

2.6.2 Seismic Hazard Mitigation

CTV III is in an area of historical seismicity, but no events have impacted surrounding oil and gas reservoirs and infrastructure, such as at the nearby Union Island Gas Field. This document defines the confining zone, beginning with the Capay Shale, that separate the Mokelumne River Formation injection interval from USDW.

The following is a summary of CTVs seismic hazard mitigation for CTV III:

The project has a geologic system capable of receiving and containing the volumes of CO_2 proposed to be injected

- Extensive historical operations in the area across multiple geologic formations, including Mokelumne River Formation at Rio Vista, provide valuable experience to understand operating conditions such as injection volumes and reservoir containment. The strategy to limit the injected CO_2 to keep the maximum pressures seen at faults to at or below levels they

have been exposed to from other and equivalent zones, will mitigate the potential for induced seismic events and endangerment of the USDW
- There are no faults or fractures identified in the AoR that will impact the confinement of CO_2 injectate. The bounding faults of the AoR are not reached by the CO_2 plume and the small normal fault within the plume does not breach confining zones

Will be operated and monitored in a manner that will limit risk of endangerment to USDWs, including risks associated with induced seismic events

- Injection pressure will be lower than the fracture gradient of the sequestration reservoir with a safety factor (90% of the fracture gradient)
- Injection and monitoring well pressure monitoring will ensure that pressures are beneath the fracture pressure of the sequestration reservoir and confining zone. Injection pressure will be lower than the fracture gradients of the sequestration reservoir and confining zone with a safety factor (90% of the fracture gradients)
- A seismic monitoring program will be designed to detect events lower than seismic events that can be felt. This will ensure that operations can be modified with early warning events, before a felt seismic event

Will be operated and monitored in a way that in the unlikely event of an induced event, risks will be quickly addressed and mitigated

- Via monitoring and surveillance practices (pressure and seismic monitoring program) CTV personnel will be notified of events that are considered an early warning sign. Early warning signs will be addressed to ensure that more significant events do not occur
- CTV will establish a central control center to ensure that personnel have access to the continuous data being acquired during operations

Minimizing potential for induced seismicity and separating any events from natural to induced

- Pressure will be monitored in each injector and sequestration monitoring well to ensure that pressure does not exceed the fracture pressure of the reservoir or confining zone
- Seismic monitoring program will be installed pre-injection for a period to monitor for any baseline seismicity that is not being resolved by current monitoring programs
- Average depth of prior seismic hazard in the region based on reviewed historical seismicity has been approximately 9.3km. Significantly deeper than the proposed injection zone

2.7 Hydrologic and Hydrogeologic Information [40 CFR 146.82(a)(3)(vi), 146.82(a)(5)]

The California Department of Water Resources has defined 515 groundwater basins and subbasins with the state. The AoR is primarily within the Tracy Subbasin (Subbasin No. 5-22.15), which lies in the northwestern portion of the San Joaquin Valley Groundwater Basin. **Figure 2.7-1** shows the AoR, Tracy Subbasin, and the surrounding areas. The Subbasin encompasses an area of about 238,429 acres (370 square miles) in San Joaquin and Alameda counties (DWR 2006).

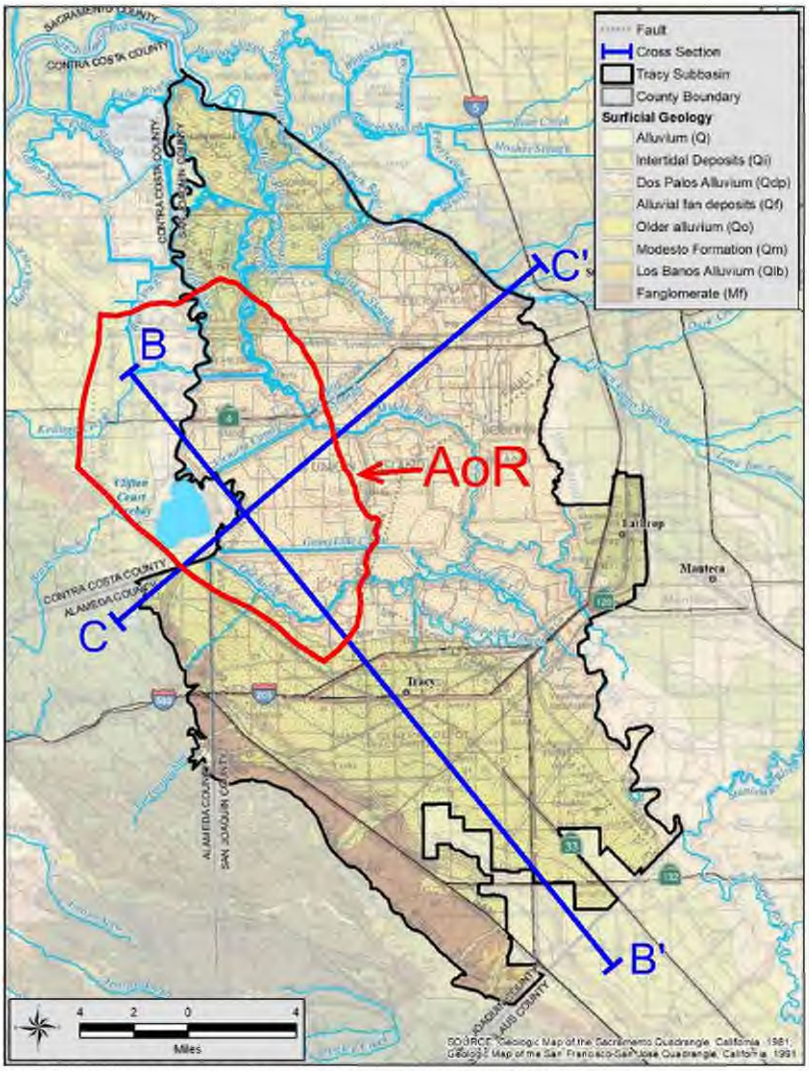

Modified from: GEI Consultants, Inc.; Tracy Subbasin Groundwater Sustainability Plan. November 1, 2021

Figure 2.7-1 Tracy Subbasin, Surface Geology, and Cross Section Index Map

2.7.1 Hydrologic Information

Major surface water bodies within the Tracy Subbasin consist of the San Joaquin, Old, and Middle rivers. **Figure 2.7-1** shows the location of these surface water bodies. The San Joaquin River makes up almost the entire eastern boundary of the Subbasin and it feeds water into the SWP Clifton Court Forebay, which is located just west of the Subbasin.

Two major pump stations pump water out of the Old River from the Clifton Court Forebay into two large canals: the California Aqueduct and the Delta-Mendota Canal. These large canals traverse the southwestern portion of the Subbasin, and transport water from the Delta to other agricultural and urban water suppliers in the San Joaquin Valley and southern California. In addition to the major natural waterways there is a large network of irrigation canals, which convey surface water to agricultural properties.

2.7.2 Base of Fresh Water and Base of USDWs

The owner or operator of a proposed Class VI injection well must define the general vertical and lateral limits of all USDWs and their positions relative to the injection zone and confining zones. The intent of this information is to demonstrate the relationship between the proposed injection formation and any USDWs, and it will support an understanding of the water resources near the proposed injection wells. A USDW is defined as an aquifer or its portion which supplies any public water system; or which contains a sufficient quantity of ground water to supply a public water system; and currently supplies drinking water for human consumption; or contains fewer than 10,000 mg/l total dissolved solids; and which is not an exempted aquifer.

2.7.2.1 Base of Fresh Water

The base of fresh water (BFW) helps define the aquifers that are used for public water supply. Local water agencies in the Tracy Subbasin have participated in various studies to comply with the 2014 Sustainable Groundwater Management Act (SGMA). Luhdorff & Scalmanini (2016) performed a study that focused on the geologic history of freshwater sediments from which groundwater is extracted for beneficial uses as defined and regulated under SGMA.

Few groundwater wells exist in the Tracy Subbasin because surface water is the source for irrigation use within delta islands. Groundwater usage is limited to eastern Contra Costa County and the Tracy area to the south. In most of western San Joaquin County in the Delta the fresh groundwater aquifers are limited to relatively shallow depths of 500 to 700 feet bgs in the Contra Costa County area, and to 1,600 feet bgs in the Tracy area (Luhdorff & Scalmanini, 2016).

Luhdorff & Scalmanini (1999) performed a study of over 500 well logs in eastern Contra Costa County groundwater for five water agencies. The focus of this study was the uppermost 500 feet, where most water wells were completed. Subsequently Luhdorff & Scalmanini (2016) used logs also examined for the nature of geologic units at greater depths to better define the BFW. The top of the geophysical logs tended to be at 800 feet or greater depths. These logs generally show fine-grained geologic units with few sand beds. The depth to base of fresh water was difficult to discern in available geophysical logs because of the lack of sand beds. The elevation of the base of freshwater aquifers determined from logs were plotted on a base map (see **Figure 2.7-2**). Contour lines of one hundred feet were drawn, but are variable based on well control.

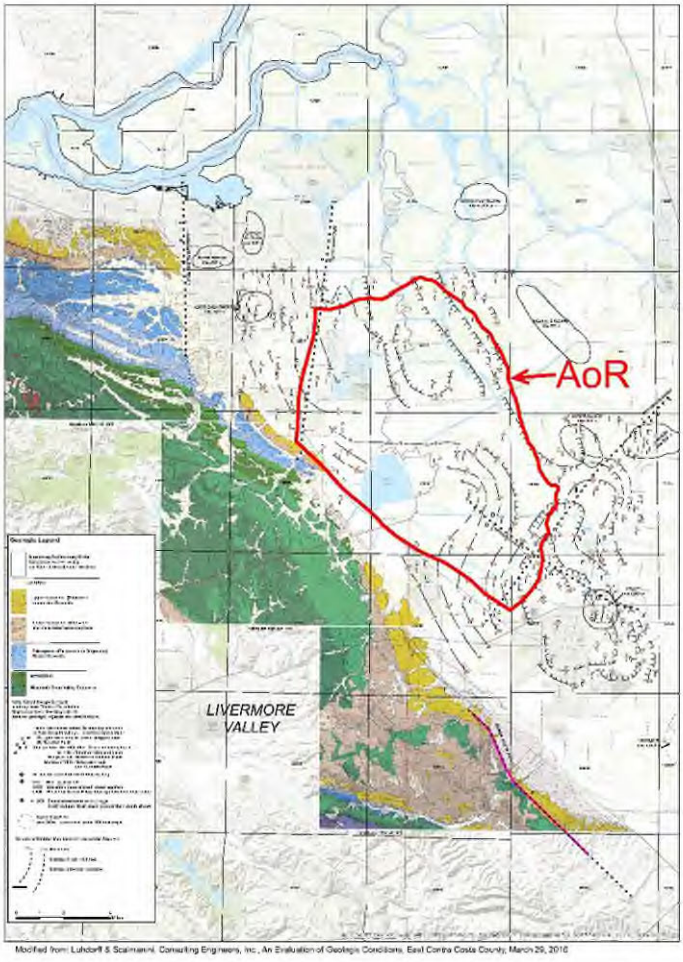

Figure 2.7-2 Geologic Map and Base of Fresh Water

2.7.2.2 Calculation of Base of Fresh Water and USDW

CRC has used geophysical logs to investigate the USDWs and the base of the USDWs. The calculation of salinity from logs used by CRC is a four-step process:

(1) converting measured density or sonic to formation porosity

The equation to convert measured density to porosity is:

$$POR = \frac{(Rhom - RHOB)}{(Rhom - Rhof)} \quad (5)$$

Parameter definitions for the equation are:

POR is formation porosity

Rhom is formation matrix density grams per cubic centimeters (g/cc); 2.65 g/cc is used for sandstones

RHOB is calibrated bulk density taken from well log measurements (g/cc)

Rhof is fluid density (g/cc); 1.00 g/cc is used for water-filled porosity

The equation to convert measured sonic slowness to porosity is:

$$POR = -1\left(\frac{\Delta tma}{2\Delta tf} - 1\right) - \sqrt{\left(\frac{\Delta tma}{2\Delta tf} - 1\right)^2 + \frac{\Delta tma}{\Delta tlog} - 1} \quad (6)$$

Parameter definitions for the equation are:

POR is formation porosity

Δtma is formation matrix slowness (µs/ft); 55.5 µs/ft is used for sandstones

Δtf is fluid slowness (µs/ft); 189 µs/ft is used for water-filled porosity

Δtlog is formation compressional slowness from well log measurements (µs/ft)

(2) calculation of apparent water resistivity using the Archie equation,

The Archie equation calculates apparent water resistivity. The equation is:

$$Rwah = \frac{POR^m R_t}{a} \quad (7)$$

Parameter definitions for the equation are:

Rwah is apparent water resistivity (ohmm)

POR is formation porosity

m is the cementation factor; 2 is the standard value

R_t is deep reading resistivity taken from well log measurements (ohmm)

a is the archie constant; 1 is the standard value

(3) correcting apparent water resistivity to a standard temperature

Apparent water resistivity is corrected from formation temperature to a surface temperature standard of 75 degrees Fahrenheit:

$$Rwahc = Rwah\frac{TEMP+6.77}{75+6.77} \quad (8)$$

Parameter definitions for the equation are:

Rwahc is apparent water resistivity (ohmm), corrected to surface temperature

TEMP is down hole temperature based on temperature gradient (DegF)

(4) converting temperature corrected apparent water resistivity to salinity.

The following formula was used (Davis 1988):

$$SAL\_a\_EPA = \frac{5500}{Rwahc} \quad (9)$$

Parameter definitions for the equation are:

SALa_EPA is salinity from corrected Rwahc (ppm)

The base of fresh water and the USDW are shown on the geologic Cross Section A-A' (**Figure 2.2-4**) The base of fresh water and based of the lowermost USDW is at a measure depth of approximately 1100 ft and 2500 ft respectively.

2.7.3 Formations with USDWs

Formations with USDWs, from youngest to oldest, include Alluvium, Flood Basin and Intertidal deposits, Alluvial Fan Deposits, Older Alluvium, Modesto Formation, Los Banos Alluvium, Tulare Formation, and Fanglomerates. These formations, except for the Tulare Formation, are shown on **Figure 2.7-1**. The Tulare Formation is not exposed at ground surface. The cumulative thickness of these formations increases from about 330 feet near the Coast Range foothills to about 2,000 feet just north of Tracy. Information regarding the water-bearing units and groundwater conditions were taken from several sources (Hotchkiss and Balding 1971, Bertoldi et al. 1991, Davis G.H. et al. 1959) and sorted to agree with more recent geologic map compilation (Wagner et al. 1991).

2.7.3.1 Alluvium

The Alluvium (Q) includes sediments deposited in the channels of active streams as well as overbank deposits and terraces of those streams. They consist of unconsolidated silt, sand, and gravel. Sand and gravel zones in the younger alluvium are highly permeable and yield significant quantities of water to wells. The thickness of the younger alluvium in the Tracy Subbasin is less than 100 feet (DWR 2006).

2.7.3.2 Flood Basin and Intertidal Deposits

The Flood Basin Deposits (Dos Palos Alluvium [Qdp]) and Intertidal Deposits (Qi) are in the Delta portions of the Subbasin. These sediments consist of peaty mud, clay, silt, sand and organic materials. Stream-channel deposits of coarse sand and gravel are also included in this unit. The flood basin deposits have low permeability and generally yield low quantities of water to wells due to their fine-grained nature. Flood basin deposits generally contain poor quality groundwater with occasional zones of fresh water. The maximum thickness of the unit is about 1,400 feet (DWR 2006).

2.7.3.3 Alluvial Fan Deposits

Along the southern margin of the Subbasin, in the Non-Delta uplands areas of the Subbasin are fan deposits (Qf) from the Coast Ranges. These deposits consist of loosely to moderately compacted sand, silt, and gravel deposited in alluvial fans during the Pliocene and Pleistocene ages. The fan deposits likely interfinger with the Flood Basin Deposits. The thickness of these fans is about 150 feet (DWR 2006).

2.7.3.4 Modesto Formation

The Modesto Formation (Qm) is located along the east side of the San Joaquin River and is slightly older that the Alluvial Fan Deposits. The formation consists of granitic sands over stratified silts and sands. Near the southern margin of the Tracy Subbasin, there are small occurrences of Los Banos Alluvium (Qlb) and Older Alluvium (Qo) that are of similar age as the Modesto Formation (GEI 2021).

2.7.3.5 Tulare Formation

The Tulare Formation is Pleistocene in age and consists of semi consolidated, poorly sorted, discontinuous deposits of clay, silt, sand and gravel. The Tulare Formation is not exposed at ground surface in the Tracy Subbasin. The Tulare Formation sand and gravel deposits are moderately permeable, and most of the larger agricultural, municipal, and industrial supply wells extract water from this formation. Wells completed in the Tulare Formation can produce up to 3,000 gallons per minute (gpm). The thickness of the Tulare Formation is about 1,400 feet (GEI 2021).

Within the Tulare Formation is the Corcoran Clay, one of the largest lakebed deposits in the San Joaquin Valley. The clay is about 60 to 100 feet thick**. Figure 2.7-3** shows the lateral extent and structure of the Corcoran Clay. Near the southern edge of the Subbasin the Corcoran Clay is apparently absent. The extent of the Corcoran Clay is not fully characterized to the west and north (Page 1986) due to the lack of deep wells. Geologic sections indicate that the clay likely continues to the west, into the East Contra Costa Subbasin (GEI 2007).

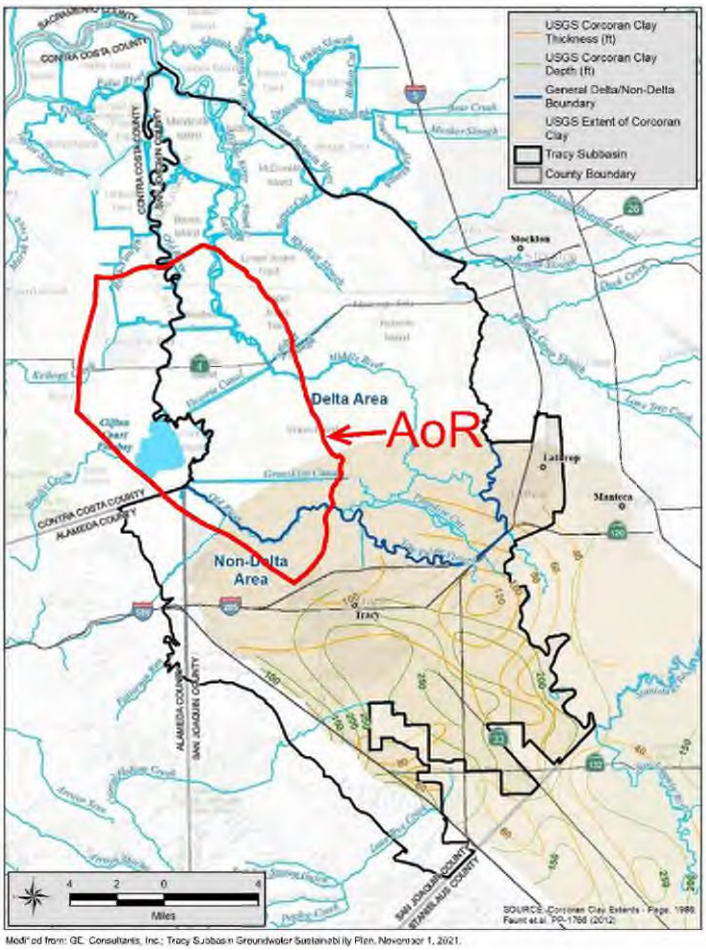

Modified from: GE Consultants, Inc.; Tracy Subbasin Groundwater Sustainability Plan, November 1, 2021.

Figure 2.7-3 Estimated Corcoran Clay Thickness and Extent

2.7.3.6 Undifferentiated Non-marine Sediments

The upper Paleogene and Neogene sequence begin with the Valley Springs Formation which represents fluvial deposits that blanket the entire southern Sacramento Basin. The unconformity at the base of the Valley Springs marks a widespread Oligocene regression and separates the more deformed Mesozoic and lower Paleogene strata below from the less deformed uppermost Paleogene and Neogene strata above. The undifferentiated non-marine sediments contain approximately 3,000 - 10,000 milligrams per liter (mg/l) TDS water and is the lowermost USDW in the AoR (**Figure 2.2-3**).

2.7.4 Geologic Cross Sections Illustrating Formations with USDWs

Geologic sections, as shown on **Figures 2.7-1**, span the length of the Subbasin to illustrate the relationship of the geologic units. The geologic sections were originally prepared for the Tracy Subbasin Groundwater Management Plan (GEI 2007) and were modified for the Tracy Subbasin GSP ((GEI 2021)) to reflect additional information obtained since 2007. Lithologic information from well logs was normalized and digitized to generally conform with the Unified Soil Classification System. Lithology and well screens from groundwater monitoring wells constructed since the sections were created were also added to the geologic sections. The soil profiles show the subsurface relationships and location of the formations and coarse-grained sediments that comprise the principal aquifers. The cross sections show the sediment

types, the approximate base of freshwater, and the estimated contact between the Tulare Formation sediments and younger formations. The cross sections also illustrate the location and extent of the Corcoran Clay (GEI 2021).

Geologic Cross Section B-B' (**Figure 2.7-4)** runs northwest-southeast through the non-Delta and Delta portions of the Tracy Subbasin. The Subbasin generally has low permeability clays and silts (shown in brown color) near surface and permeable sediments (sands and gravels shown in light blue) scattered throughout the profile. Continuous layers of sand and gravels, other than one at the top of the Corcoran Clay have not been identified. The lack of continuous layers of sand and gravels is likely due to the nature of the river channels, and flood deposits associated with these types of sediments. The Corcoran Clay (or its equivalent) seems to extend to the west and into the East Contra Costa Subbasin. In the southern non-Delta portion of the Subbasin, fine-grained sediments are more prevalent. Based upon groundwater levels and water quality information, the shallow aquifer is likely unconfined and separated from the deeper confined aquifer (GEI 2021).

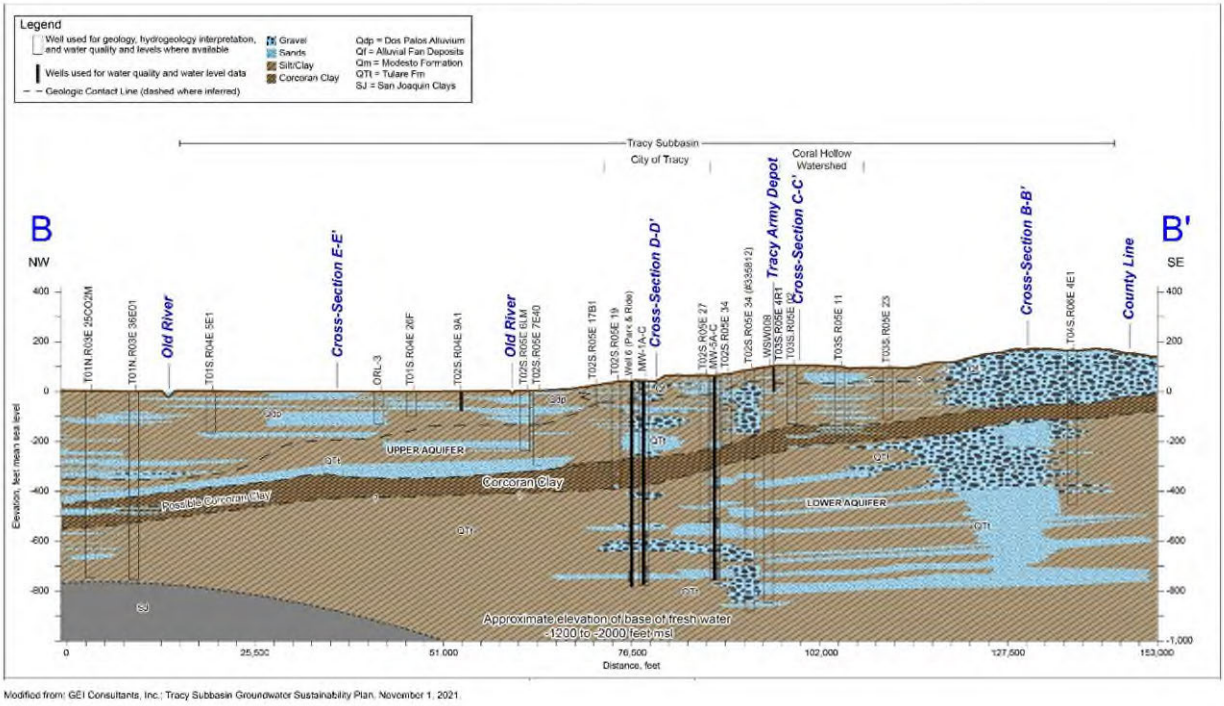

Modified from: GEI Consultants, Inc.; Tracy Subbasin Groundwater Sustainability Plan, November 1, 2021

Figure 2.7-4 Geologic Cross Section B-B'

Geologic Cross Section C-C' (**Figure 2.7-5**) runs a northeast-southwest orientation across the Delta area. This geologic section illustrates the types of sediments, the estimated base of freshwater, the possible location of the Corcoran Clay (or its equivalent). Where the clay location is uncertain, no wells were present that penetrated deep enough to confirm its presence or absence. The base of fresh water varies throughout the Subbasin and is shown on the sections. It is as shallow as -400 feet mean sea level (msl) to as much as -2,000 feet msl (GEI 2021).

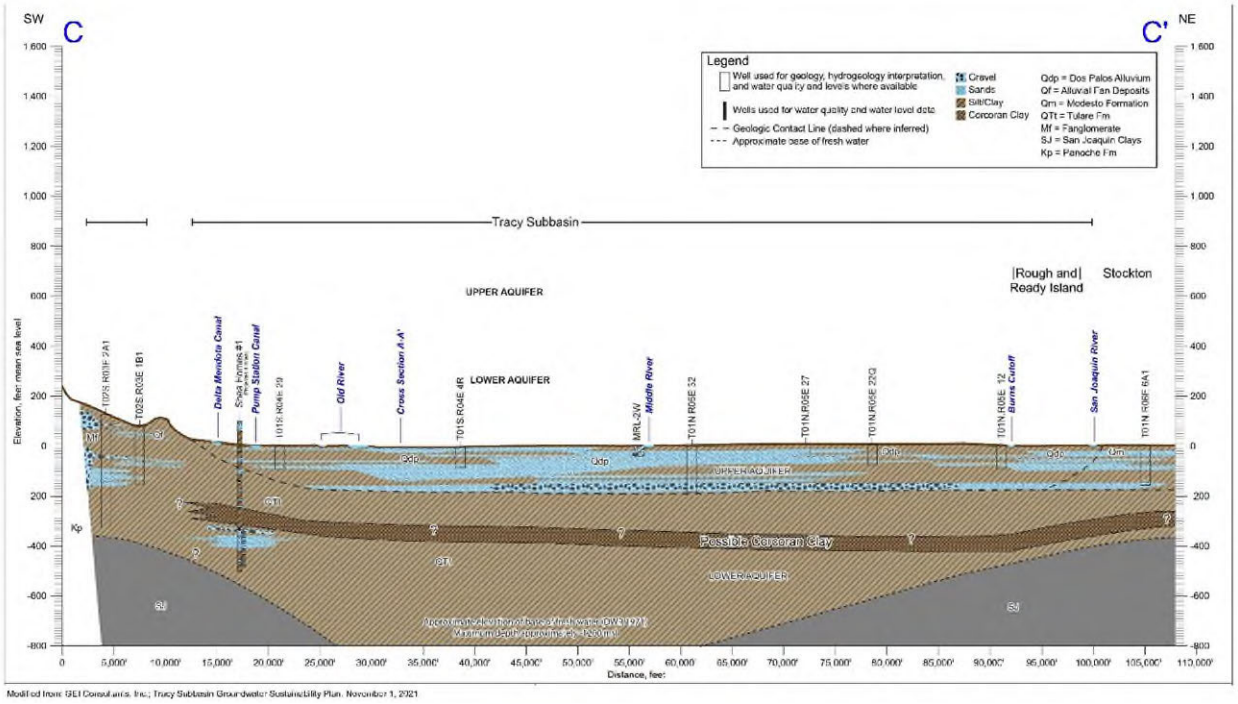

Figure 2.7-5 Geologic Cross Section C-C'

2.7.5 Principal Aquifers

The Tracy Subbasin has two principal aquifers that are separated by the Corcoran Clay. Where the clay is absent, which is the condition within most of the Delta area, only the Upper Aquifer is present. The Upper and Lower Aquifers combine where the Corcoran Clay is absent, near the southwestern portion of the subbasin adjacent to the foothills. In this area, the aquifers would be unconfined and are the Upper Aquifer. The Upper and Lower Aquifers also merge north of the Old River in the northern part of the Subbasin (GEI 2021).

2.7.5.1 Upper Aquifer

The Upper Aquifer is used by domestic, community water systems, and for agriculture. The Upper aquifer also supports native vegetation where groundwater levels are less than 30 feet bgs (GEI 2021). The Upper Aquifer is an unconfined to semi-confined aquifer. It is present above the Corcoran Clay and where the clay is absent. The Upper aquifer exists in the Alluvial Fan Deposits, Intertidal Deposits, Modesto Formation, Flood Basin Deposits, the upper portions of the Tulare Formation.

There are multiple coarse-grained sediment layers that make up the unconfined aquifer, however the water levels are generally similar. Generally, the aquifer confinement tends increase with depth becoming semi-confined conditions. There is also typically a downward gradient in the aquifers (Hotchkiss and Balding 1971) in the non-Delta areas; the gradient ranges from a few feet bgs to as much as 70 feet bgs. The groundwater levels in the Upper Aquifer are usually 10 to 30 feet higher than in the Lower Aquifer. The groundwater levels In the Delta are typically at sea level and artesian flowing wells are common in the center of the islands (Hydrofocus 2015).

The hydraulic characteristics of the unconfined aquifer are highly variable. The USGS estimated horizontal hydraulic conductivity values for organic sediments ranging from 0.0098 ft/d to 133.86 ft/d (Hydrofocus 2015). Wells in the unconfined aquifer produce 6 to 5,300 gpm. The transmissivity of the unconfined aquifers, ranges between 600 to greater than 2,300 gallons per day per foot (gpd/ft). The storativity is about 0.05 (GEI 2021).

Water quality in the Upper Aquifer is mostly transitional, with no single predominate anion. Most water are characterized as sulfate bicarbonate and chloride bicarbonate type (Hotchkiss and Balding 1971). The TDS of these transitional water ranges between 400 to 4,200 mg/L. Nitrate is generally high in the Upper aquifer in the non-Delta portions of the Subbasin. Nitrate is generally low in the Delta portions of the Subbasin (GEI 2021).

2.7.5.2 Lower Aquifer

The Lower Aquifer is typically used by community water systems (City of Tracy) and agriculture. The Lower Aquifer is mainly comprised of the lower portions of the Tulare Formation below the Corcoran Clay and extends to the base of fresh water. The clay is present in the southern third of the Subbasin; the clay's extent to the west and north is uncertain and has been estimated to have a vertical permeability ranging from 0.01 to 0.007 feet per day (Burow et al. 2004).

The groundwater levels are generally deeper than water levels in the Upper Aquifer (Hotchkiss and Balding 1971). Groundwater levels in the confined aquifer are about -25 to -75 feet msl. The groundwater levels are normally 60 to 200 feet above the top of the Corcoran Clay.

Wells in the Lower Aquifer produce about 700 to 2,500 gpm. The transmissivity typically ranges from 12,000 to 37,000 gpd/ft, but can be 120,000 gpd/ft. The storage coefficient or storativity has been measured to be 0.0001 (Padre 2004).

Water quality in the Lower Aquifer in the western portions are chloride type water but mostly transitional type of sulfate chloride near the valley margins and sulfate bicarbonate and bicarbonate sulfate near the San Joaquin River (Hotchkiss and Balding 1971). In general, the TDS ranges between 400 and 1,600 mg/L. Nitrate is typically low in the Lower Aquifer. Wells completed below the Corcoran Clay sometimes have elevated levels sulfate and total dissolved solids above the drinking water MCLs. Only at one deep location, east of Tracy, are chloride levels elevated (GEI 2021).

2.7.6 Potentiometric Maps

The Tracy Subbasin GSP (GEI 2021) used groundwater level measurements in over 226 wells, which have been reported to DWR's CASGEM or Water Data Library systems. To evaluate groundwater levels, the GSP only used wells with known total depths and construction details so that the wells were assigned to a principal aquifer. To supplement data from these wells, additional monitoring wells were located that were being used for other regulatory programs.

2.7.6.1 Upper Aquifer

Groundwater elevations in the Delta area are typically below sea level because the ground surface in the islands have subsided to below sea level; the drains within the island keep groundwater levels bgs to allow for farming. **Figure 2.7-6** shows a schematic profile for groundwater surfaces that are expected at the islands. Although each island has distinct groundwater elevations, there are similar hydraulics on all islands. Groundwater elevations are higher near the island edges (adjacent to waterways) and deepen equivalent with the deepest land surface and drain. Groundwater elevations in the islands are managed by the elevations of the drains and canals. There is very little, if any, pumping of wells for agriculture. Since

drains and canals control the groundwater elevations, groundwater contours are not developed/monitored for the Delta islands (GEI 2021).

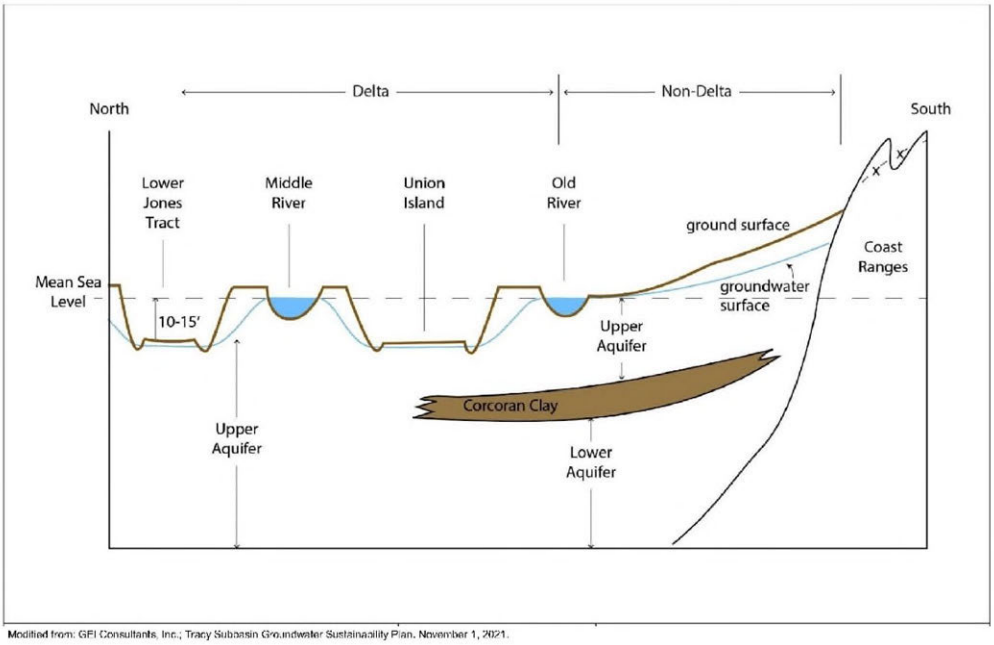

Figure 2.7-6 Principal Aquifer Schematic Profile

In the non-Delta areas west of the San Joaquin River, groundwater contours for the Upper Aquifer indicate groundwater elevations are highest near the Coast Ranges and decrease toward the Delta. Flow directions indicate that recharge areas are present along the foothills and that groundwater discharges into the Old River and/or Tom Paine Slough (**Figure 2.7-7**). Groundwater gradients in the non-Delta portions of the Subbasin are the steepest, at approximately 0.008 ft/ft. East of the San Joaquin River, near Lathrop, the river recharges the Upper Aquifer and flows towards a pumping depression near Stockton. Groundwater contours at the southeastern edge of the Subbasin are perpendicular to the Stanislaus-San Joaquin County line, suggesting that there is no flow in the Upper Aquifer between the subbasins, other than the areas of the Delta Mendota Subbasin north of the County line, where water apparently flows into and out of both subbasins.

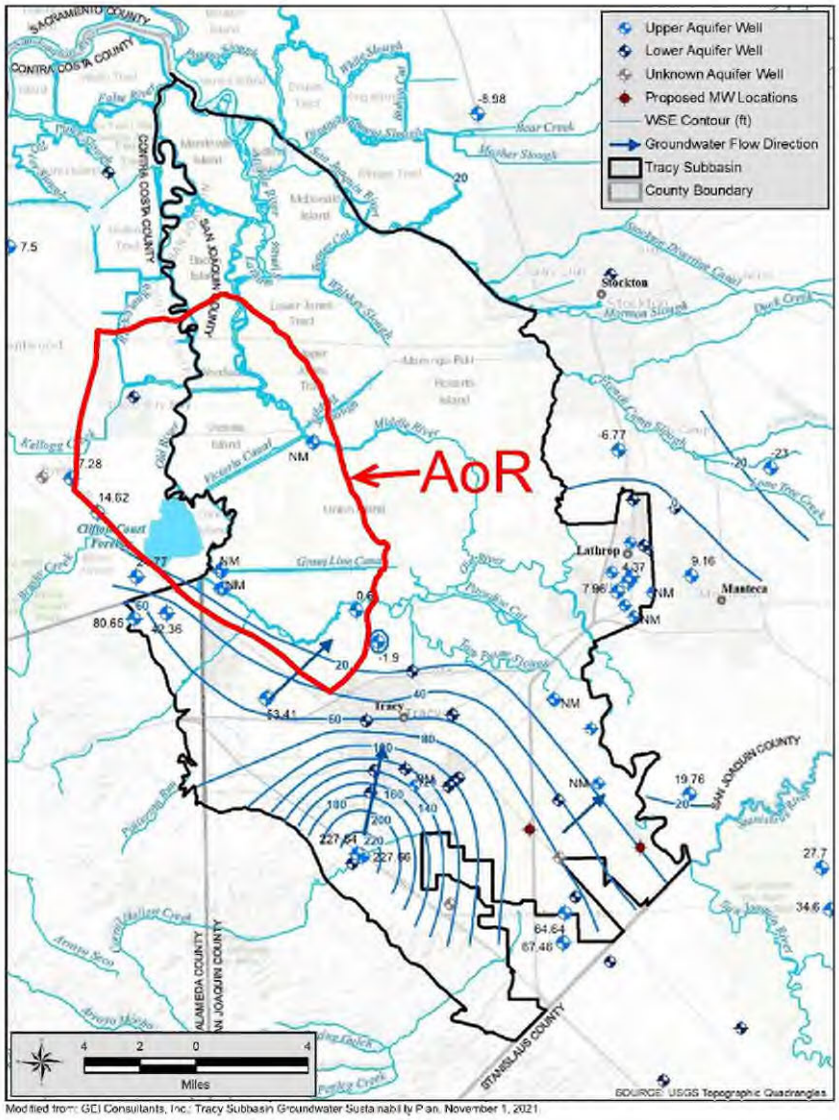

Figure 2.7-7 Upper Aquifer Groundwater Elevations Fall 2019

2.7.6.2 Lower Aquifer

The Corcoran Clay extends throughout the non-Delta areas and only slightly into the Delta area, at Union Island. Groundwater contours for the Lower Aquifer were developed using data from the CASGEM monitoring wells that are constructed below the Corcoran Clay and supplemented by data from municipal wells (**Figure 2.7-8**). Groundwater monitoring well data were used from the adjacent Delta Mendota Subbasin (GEI 2021).

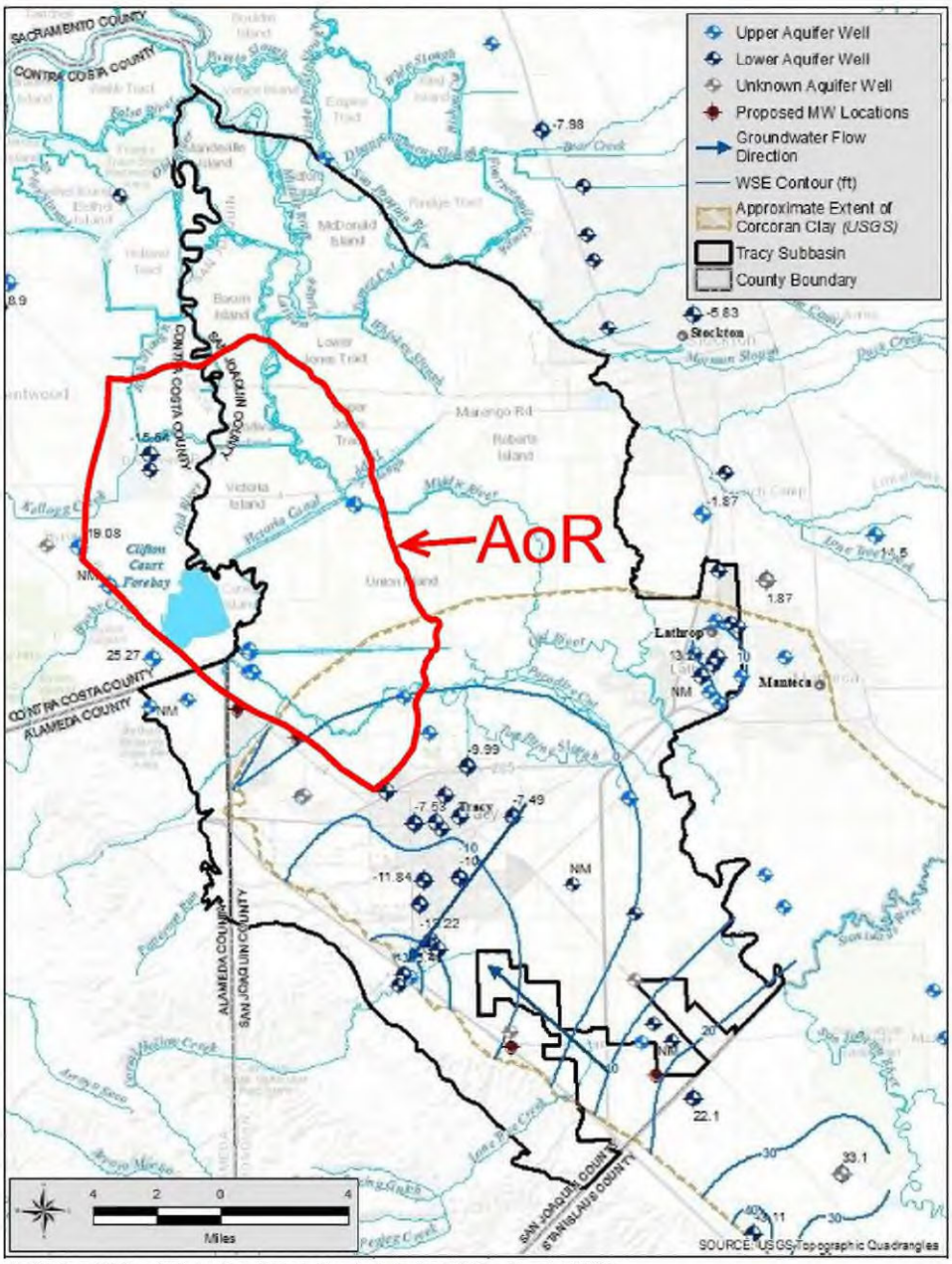

Modified from: GEI Consultants, Inc.; Tracy Subbasin Groundwater Sustainability Plan, November 1, 2021.

Figure 2.7-8 Lower Aquifer Groundwater Elevations Spring 2019

Groundwater elevation contours in the Lower Aquifer imply groundwater is entering the subbasin from the south (Delta Mendota Subbasin) and from the east (Eastern San Joaquin Subbasin). Pumping in the vicinity of the City of Tracy has apparently modified this overall regional flow, resulting in a pumping depression towards the City of Tracy. The groundwater levels are expected to be at sea level near the northern edge of the Corcoran Clay extent (GEI 2021).

The groundwater gradient in Fall 2019 from the Delta Mendota and the Eastern San Joaquin subbasins is estimated to be 0.0009 foot/foot into the Tracy Subbasin. Due to the pumping depression, the gradient

increases around the City of Tracy. The gradient near the western edge of the subbasin cannot be determined to the lack of monitoring wells constructed below the Corcoran Clay (GEI 2021).

2.7.7 Water Supply Wells

The California State Water Resources Control Board Groundwater Ambient Monitoring Assessment Program (GAMA), and the Department of Water Resources (DWR) public databases were searched to identify any water supply wells within a one-mile radius of the AOR. A total of 155 water supply wells were identified within one mile of the AoR. A map of well locations and table of information are found in **Figure 2.7-9** Water Well Location Map and the attached **Table 2.7-1** Water Well Information, respectively.

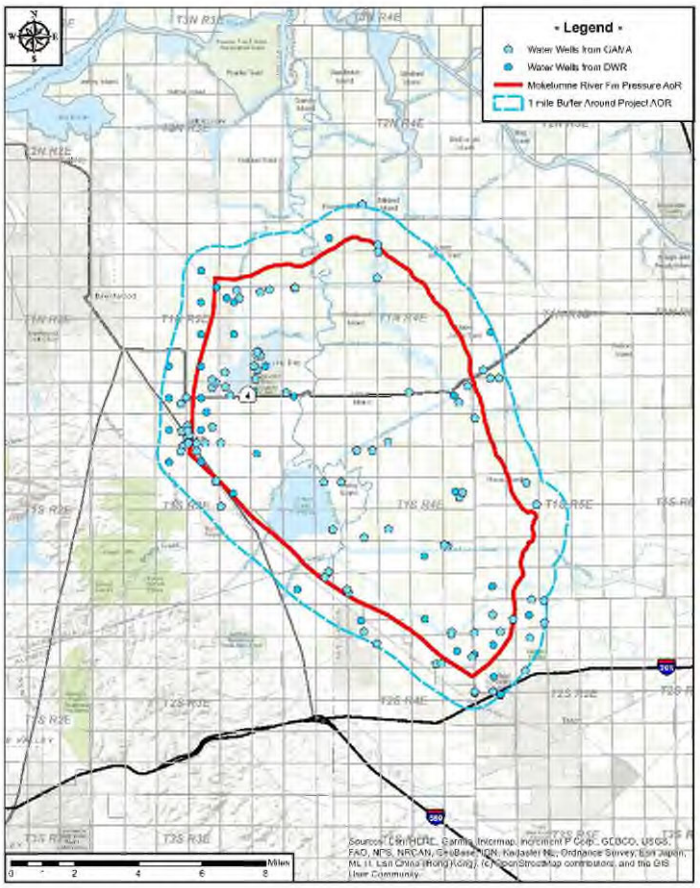

Figure 2.7-9 Water Well Location Map

Groundwater in the Subbasin is used for municipal, industrial, irrigation, domestic, stock watering, frost protection, and other purposes. The number of water wells is based on well logs filed and contained within public records may not reflect the actual number of active wells because many of the wells contained in files may have been destroyed and others may not have been recorded.

There are many more wells in the non-Delta areas, south of the Old River, than in the Delta area of the Subbasin. The depths of wells are generally deeper in the non-Delta portion of the Subbasin as compared to the Delta portion of the Subbasin. Typically, the domestic wells are constructed to shallower depths than the production wells. The municipal wells are generally constructed deeper than either the domestic

or production wells (GEI 2021). The known water well depths and other information are included in the attached **Table 2.7-1.** Some well depths are unknown, but all water supply wells completion intervals are expected to be much shallower than the injection zone.

2.8 Geochemistry [40 CFR 146.82(a)(6)]

2.8.1 Formation Geochemistry

2.8.1.1 Mokelumne River Formation
As noted in the mineralogy section (section 2.4.1).

2.8.1.2 Capay Shale
As noted in the mineralogy section (section 2.4.1).

2.8.1.3 H&T Shale
As noted in the mineralogy section (section 2.4.1).

2.8.2 Fluid Geochemistry

The Mokelumne River Formation contains only saline water within the AoR. No water samples from the Mokelumne River Formation exist within the AoR, so a sample from Rio Vista Gas Field has been used. The well Midland_Fee_Water_Injection_1 was sampled in 1980 (see **Figure 2.5-4** for well location). The measurement of total dissolved solids (TDS) for the sample is 13,889.4 mg/L. The complete water chemistry is shown in **Figure 2.8-1**.

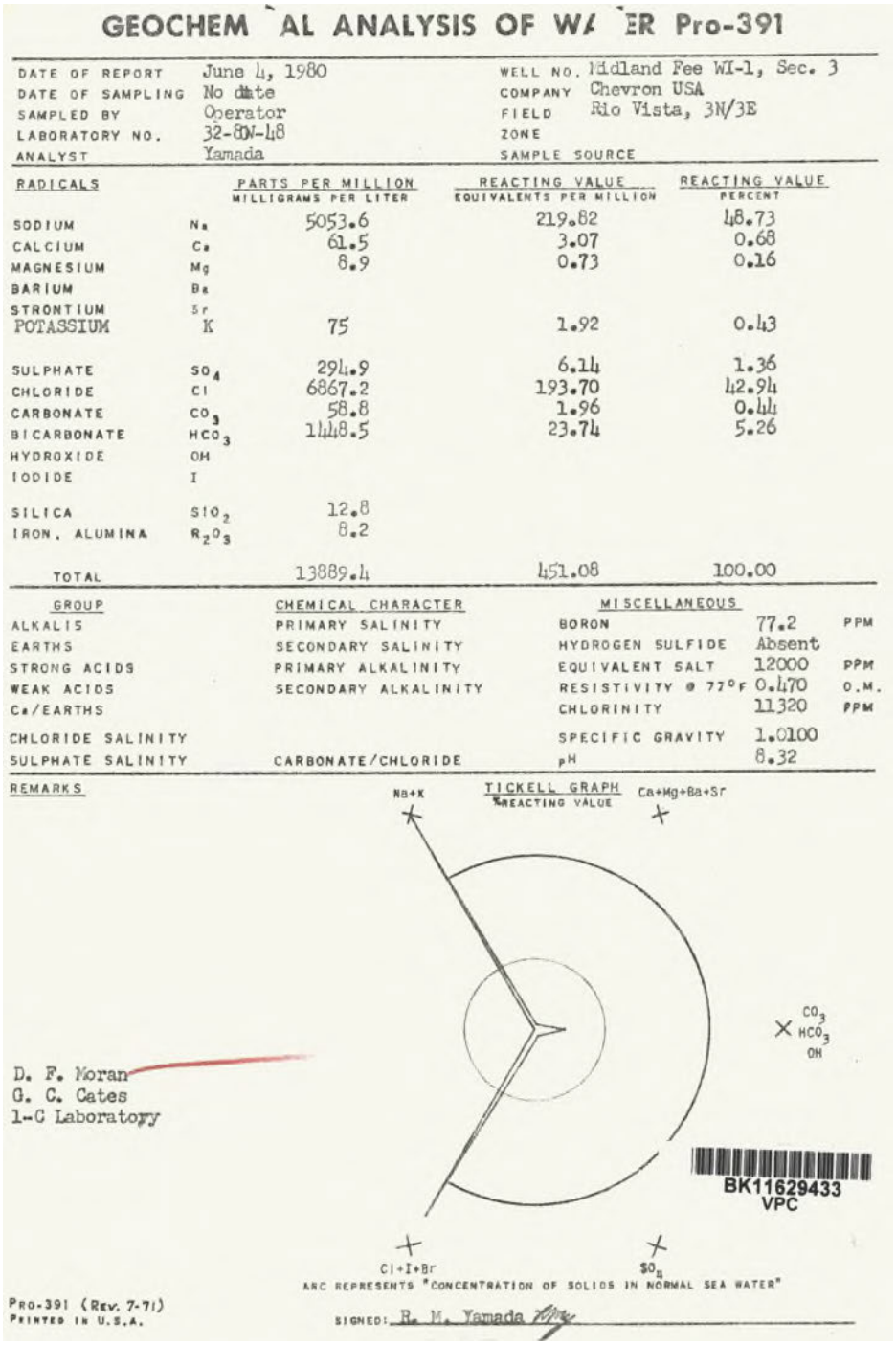

GEOCHEMICAL ANALYSIS OF WATER Pro-391

DATE OF REPORT	June 4, 1980	WELL NO.	Midland Fee WI-1, Sec. 3
DATE OF SAMPLING	No date	COMPANY	Chevron USA
SAMPLED BY	Operator	FIELD	Rio Vista, 3N/3E
LABORATORY NO.	32-8N-4E	ZONE	
ANALYST	Yamada	SAMPLE SOURCE	

RADICALS		PARTS PER MILLION MILLIGRAMS PER LITER	REACTING VALUE EQUIVALENTS PER MILLION	REACTING VALUE PERCENT
SODIUM	Na	5053.6	219.82	48.73
CALCIUM	Ca	61.5	3.07	0.68
MAGNESIUM	Mg	8.9	0.73	0.16
BARIUM	Ba			
STRONTIUM	Sr			
POTASSIUM	K	75	1.92	0.43
SULPHATE	SO_4	294.9	6.14	1.36
CHLORIDE	Cl	6867.2	193.70	42.94
CARBONATE	CO_3	58.8	1.96	0.44
BICARBONATE	HCO_3	1448.5	23.74	5.26
HYDROXIDE	OH			
IODIDE	I			
SILICA	SiO_2	12.8		
IRON, ALUMINA	R_2O_3	8.2		
TOTAL		13889.4	451.08	100.00

GROUP	CHEMICAL CHARACTER	MISCELLANEOUS		
ALKALIS	PRIMARY SALINITY	BORON	77.2	PPM
EARTHS	SECONDARY SALINITY	HYDROGEN SULFIDE	Absent	
STRONG ACIDS	PRIMARY ALKALINITY	EQUIVALENT SALT	12000	PPM
WEAK ACIDS	SECONDARY ALKALINITY	RESISTIVITY @ 77°F	0.470	O.M.
Ca/EARTHS		CHLORINITY	11320	PPM
CHLORIDE SALINITY		SPECIFIC GRAVITY	1.0100	
SULPHATE SALINITY	CARBONATE/CHLORIDE	pH	8.32	

REMARKS

D. F. Moran
G. C. Cates
1-C Laboratory

TICKELL GRAPH
%REACTING VALUE

ARC REPRESENTS "CONCENTRATION OF SOLIDS IN NORMAL SEA WATER"

PRO-391 (REV. 7-71)
PRINTED IN U.S.A.

SIGNED: R. M. Yamada

Figure 2.8-1: Water geochemistry for the Midland_Fee_Water_Injection_1 well.

Salinity calculations were also performed on logs from wells within the AoR, and these showed TDS in the Mokelumne River Formation being approximately 14,000 – 16,000 ppm. A conservative TDS of 15,500 ppm was used for the computational model. Formation fluid properties at reservoir conditions are shown in Table 2.8-1.

No gas is present within the Mokelumne River Formation within the boundaries of the AoR, so no hydrocarbon analysis is available.

Table 2.8-1: Injection zone formation fluid properties at reservoir conditions

Formation Fluid Property	Estimated Value/Range
Density, g/cm^3	1.01
Viscosity, cp	1.26
TDS, ppm	~14,000-16,000

2.8.3 Fluid-Rock Reactions

2.8.3.1 Mokelumne River Formation

Mineralogy and formation fluid interactions have been assessed for the Mokelumne River Formation. The following applies to potential reactions associated with the CO_2 injectate:

1. The Mokelumne River Formation has a negligible quantity of carbonate minerals and is instead dominated by quartz and feldspar. These minerals are stable in the presence of CO_2 and carbonic acid and any dissolution or changes that occur will be on grain surfaces.

2. The water within the Mokelumne River Formation contains minimal calcium and magnesium cations, which would be expected to react with the CO_2 to form calcium bearing minerals in the pore space.

2.8.3.2 Capay Shale

There is no fluid geochemistry analysis for the Capay Shale. The shale will only provide fluid for analysis if stimulated. However, given the low permeability of the rock and the low carbonate content, the Capay Shale is not expected to be impacted by the CO_2 injectate.

2.8.3.2 H&T Shale

There is no fluid geochemistry analysis for the H&T Shale. The shale will only provide fluid for analysis if stimulated. However, given the low permeability of the rock and the low carbonate content, the H&T Shale is not expected to be impacted by the CO_2 injectate.

2.8.3.3 Geochemical Modeling

Geochemical modeling for the injectate streams, detailed in Section 7.2 of this document, were conducted using the USGS geochemical modeling software PHREEQC (ph-REdox-Equilibrium) to understand the potential interactions of the injectates with the Injection zone and Upper-Confining zone formation mineralogy and fluids. The model was set up using the formation fluid data referenced in Section 2.8.2, and the Injection zone and Upper Confining zone mineralogy data referenced in Section 2.4.1 of the Narrative.

Geochemical modeling indicates that for either composition, minimal amounts of minerals will dissolve and precipitate, with expected net change in molar mass of 1.5-2%, and as such the formation and formation fluids are compatible with the proposed injectates.

Details of the modeling methodology and results can be found in the attached appendix – "CTV III Geochemical Modeling".

CTV will review and confirm the geochemical modeling results at pre-operational testing based on injectate sampling to ensure that they are consistent with the model inputs.

2.9 Other Information (Including Surface Air and/or Soil Gas Data, if Applicable)

No additional information to add.

2.10 Site Suitability [40 CFR 146.83]

Sufficient data from both wells and seismic demonstrate the integrity through lateral continuity of the reservoir as well as the confining zone. Regional mapping completed by West Coast Regional Carbon Sequestration Partnership (WESTCARB), California Geological Surgery (CGS), and the National Energy and Technology Lab (NETL) support our local stratigraphy, both indicating lateral continuity and regional thickness across the AoR (Downey 2010). This study covers formations with sequestration and seal potential from southern Sutter County down to the Stockton Arch Fault San Joaquin County, encompassing an area far beyond the AoR presented in Attachment B.

The vertical confinement and laterally continuous reservoir, described in Attachment A, will compensate for the CO_2 due to it being located within an open system. The Capay Shale is a continuous shale, described in section Attachment A, and will guide the lateral dispersion of CO_2 across the AoR (**Figure 2.10-1**). Surrounding oil and gas fields in the area demonstrate adequate seal capacity in the upper confining zone and surrounding faults. Corrosion resistant alloy (CRA) will be used for completion of the injection and monitoring wells, inhibiting any reaction between CO_2 and wellbores.

Thickness maps and petrophysics demonstrate confinement based on the upper confining zones laterally continuity, low permeability and thickness. A minor fault does extend within the CO_2 plume however thickness maps support an adequate seal across this offset. Pressures along bounding faults will be estimated using computational modeling and in-zone monitoring wells, to mitigate the possibility of fault re-activation.

Due to the regional continuity and low permeability of the upper confining zone (Capay Shale), no secondary confinement is necessary, however another shale barrier does exist above the Domengine Formation monitoring sand. This creates another impermeable zone of confinement separating the injection zone from the USDW.

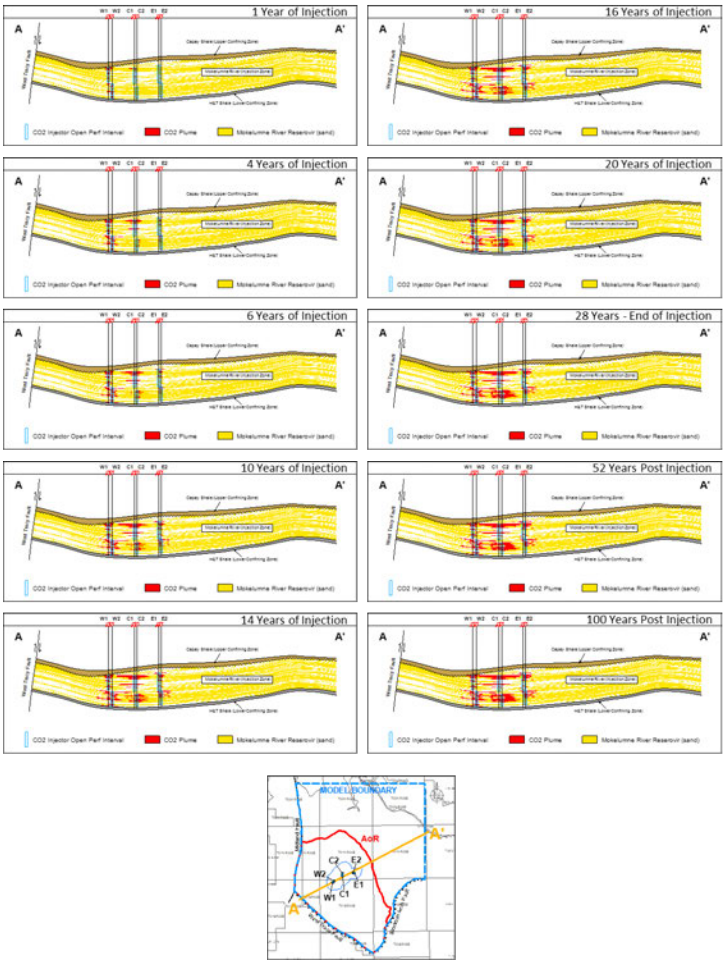

Figure 2.10-1. Proximity of CO_2 to the West Tracy Fault, lateral dispersion of CO_2 throughout time and confinement under the overlying Capay Shale through time.

CTV's estimates storage for the project area is up to 70.7 MMT of CO_2. This was arrived through computational modeling.

3.0 AoR and Corrective Action

CTV's AoR and Corrective Action plan pursuant to 40 CFR 146.82(a)(4), 40 CFR 146.82(a)(13) and 146.84(b), and 40 CFR 146.84(c) describes the process, software, and results to establish the AoR, and the wells that require corrective action.

AoR and Corrective Action GSDT Submissions
GSDT Module: AoR and Corrective Action ***Tab(s):*** All applicable tabs Please use the checkbox(es) to verify the following information was submitted to the GSDT: ☒ Tabulation of all wells within AoR that penetrate confining zone ***[40 CFR 146.82(a)(4)]***

☒ AoR and Corrective Action Plan *[40 CFR 146.82(a)(13) and 146.84(b)]*
☒ Computational modeling details ***[40 CFR 146.84(c)]***

4.0 Financial Responsibility

CTV's Financial Responsibility demonstration pursuant to 140 CFR 146.82(a)(14) and 40 CFR 146.85 is met with a line of credit for Injection Well Plugging and Post-Injection Site Care and Site Closure and insurance to cover Emergency and Remedial Responses.

Financial Responsibility GSDT Submissions
GSDT Module: Financial Responsibility Demonstration ***Tab(s):*** Cost Estimate tab and all applicable financial instrument tabs Please use the checkbox(es) to verify the following information was submitted to the GSDT: ☐ Demonstration of financial responsibility ***[40 CFR 146.82(a)(14) and 146.85]***

5.0 Injection and Monitoring Well Construction

CTV plans to drill six new injectors for the CTV III storage project. New injection wells C1, C2, E1, E2, W1, and W2 are planned and designed specifically for CO_2 sequestration purposes. These wells will target selective intervals within the injection zone to optimize plume development and injection conformance. Additionally, three new monitoring wells are required to support the storage project. M1 and M2 will be injection zone monitoring wells, and D1 will be an above-zone monitoring well. Two USDW monitoring wells, US1 and US2, will also be constructed prior to injection. Figure 1 shows the location of the new wells.

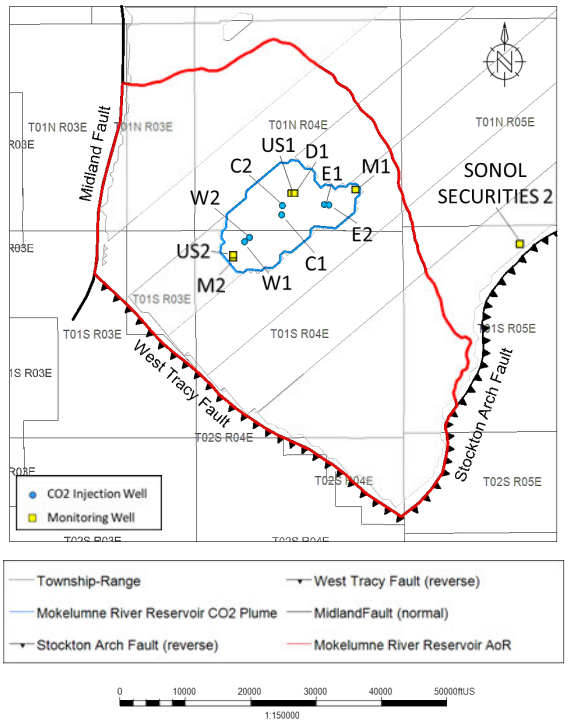

Figure 5.1: Map showing the location of injection wells and monitoring wells.

All planned new wells will be constructed with components that are compatible with the injectate and formation fluids encountered such that corrosion rates and cumulative corrosion over the duration of the project are acceptable. The proposed well materials will be confirmed based on actual CO_2 composition such that material strength is sufficient to withstand all loads encountered throughout the life of the well with an acceptable safety factor incorporated into the design. Casing points will be verified by trained geologists using real-time drilling data such as LWD and mud logs to ensure non-endangerment of USDW. Due to the depth of the base of USDW, an intermediate casing string will be utilized to isolate the USDW. Cementing design, additives, and placement procedures will be sufficient to ensure isolation of the injection zone and protection of USDW using cementing materials that are compatible with injectate, formation fluids, and subsurface pressure and temperature conditions.

Appendix C-1: Injection and Monitoring Well Schematics provides casing diagram figures for all injection and monitoring wells with construction specifications and anticipated completion details in graphical and/or tabular format.

Injection wells will have wellhead equipment sufficient to shut off injection at surface. The project does not anticipate risk factors that warrant downhole shut-off devices, such as high temperature, high pressure, presence of hydrogen sulfide, proximity to populated areas, or high likelihood of damage to the wellhead.

5.1 Proposed Stimulation Program [40 CFR 146.82(a)(9)]

There are no proposed stimulation programs currently.

5.2 Construction Procedures [40 CFR 146.82(a)(12)]

Injection and monitoring wells will be drilled during pre-operational testing, and no abnormal drilling and completion challenges are anticipated. The drilling histories of nearby wells provide key information to drilling professionals and identify the expected conditions to be encountered. The wells will be constructed with objectives to achieve target CO_2 injection rates, to prevent migration of fluids out of the

injection zone, to protect the shallow formations, and to allow for monitoring, as described by the following:

- Well designs will be sufficient to withstand all anticipated load cases including safety factors.
- Multiple cemented casing strings will protect shallow USDW-bearing zones from contacting injection fluid.
- All casing strings will be cemented in place with volume sufficient to place cement to surface using industry-proven recommended practices for slurry design and placement
- Cement bond logging (CBL) will be used to verify presence of cement in the production casing annulus through and above the confining layer.
- Mechanical integrity testing (MIT) will be performed on the tubing and the tubing/casing annulus.
- Upper completion design enables monitoring devices to be installed downhole, cased hole logs to be acquired and MIT to be conducted.
- All wellhead equipment and downhole tubulars will be designed to accommodate the dimensions necessary for deployment of monitoring equipment such as wireline-conveyed logging tools and sampling devices.
- Realtime surface monitoring equipment with remote connectivity to a centralized facility and alarms provides continual awareness to potential anomalous injection conditions
- Annular fluid (packer fluid) density and additives to mitigate corrosion provide additional protection against mechanical or chemical failure of production casing and upper completion equipment

Well materials utilized will be compatible with the CO_2 injectate and will limit corrosion.

- Wellhead – stainless steel or other corrosion resistant alloy
- Casing – 13Cr L-80 or other corrosion resistant alloy in specified sections of production string (ie. flow-wetted casing)
- Cement – Portland cement has been used extensively in enhanced oil recovery (EOR) injectors. Data acquired from existing wells supports that the materials are compatible with CO_2 where good cement bond between formation and casing exists.
- Tubing – 13Cr L-80 or other corrosion resistant alloy
- Packer – corrosion resistant alloy and hardened elastomer

Well materials follow the following standards:

- API Spec 5CT / ISO 11960 – Specification for Casing and Tubing
- API Spec 5CRA / ISO 13680 – Specification for Corrosion-Resistant Alloy Seamless Tubes for use as Casing, Tubing, and Coupling Stock
- API Spec 10A / ISO 10426-1 – Cements and Materials for Cementing
- API Spec 11D1 / ISO 14310 – Downhole Equipment – Packers and Bridge Plugs
- API Spec 6A / ISO 10423 – Specification for Wellhead and Tree Equipment

As required by §146.86(b)(1), casing and tubing material sizes, thicknesses, and grades were selected by evaluating the proposed well design internal pressures, external pressures, and axial loads that the well will be expected to withstand throughout construction and operations. Temperature effects under static or dynamic conditions, based on load scenario, have been incorporated into the modelling results. The design results indicate the materials selected have strengths sufficient to withstand all worst-case load scenarios and include industry-standard safety factors.

CTV will confirm that the properties of the CO2 stream are consistent with design assumptions based on pre-op injectate sampling.

5.2.1 Casing and Cementing

Well-specific casing diagrams including casing specifications are presented in Appendix C-1: Injection and Monitoring Well Schematics to meet the requirements of 40 CFR 146.86(b)(1)(iv). These specifications allow for the safe operation at bottomhole injection conditions not to exceed the maximum injection pressures specified in the Operational Procedures Appendix.

The injection zone pressure is neither significantly depleted or over pressured, and the temperature is approximately 151 degrees Fahrenheit. These conditions are not extreme, and standard cementing and casing best practices are sufficient to ensure successful placement and isolation. Industry standard practices and procedures for designing and placing primary cement in the casing annuli will be utilized to ensure mechanical integrity of cement and casing. Staged cementing is not an anticipated requirement.

Surface casing will be designed to protect the base of fresh water at a depth of around 400' TVD. Casing is planned to be set at 600'. Class G portland cement – an API grade cement – meets API standard specifications for this application. Accelerator additives will be used to speed up the thickening time of the cement, lost circulation additive may be used as macro plugging material, and extender additives may be used to protect shallow formations by reducing the weight of cement.

The intermediate casing will be set at a depth sufficient to cover the USDW. The depth to the base of USDW is expected to be encountered at approximately 2541' TVD. Casing will be set or below 2550' TVD to ensure protection of the USDW. Class G portland cement will be circulated to surface with retarding additives (depending on pump time) to decrease the speed of cement hydration as well as friction reducer additives to improve upon the flow properties of the cement slurry. Anti-foam additives, fluid loss additives, lost circulation material, dispersants, and extenders may also be considered based on industry best practices for slurry design to ensure effective placement of cement.

The long casing string will be set 120' into the lower confining layer. A combination of Class G portland lead slurry and Class G portland tail slurry with CO_2 resistant additives will be used to cement the long string. The tail slurry will be circulated from TD into the confining layer. The lead slurry will provide isolation of the long string casing in and above the confining layer to surface. Anti-foam additives, fluid loss additives, lost circulation material, dispersants, and extenders may also be considered based on industry best practices for slurry design to ensure effective placement of cement, along with considering the addition of silica flour for strength retrogression.

Operational parameters acquired throughout the pressure pumping operation will be used to compare modeled versus actual pressure and rate. The presence of circulated cement at surface will also be a primary indicator of effective cement placement. Cement evaluation logging will be conducted to confirm cement placement and isolation.

5.2.2 Tubing and Packer

The information in the tables provided in Appendix C-1: Injection and Monitoring Well Schematics is representative of completion equipment that will be used and meets the requirements at 40 CFR 146.86(c). Tubing and packer selection and specifications will be determined during pre-operational

testing and will be sufficient to withstand all load scenarios considering internal pressure, external pressure, axial loading, and temperature effects.

5.2.3 Annular Fluid

4% KCl completion fluid treated with corrosion inhibitor and biocide will be circulated in the tubing/casing annulus at the time of tubing installation. The corrosion inhibitor and biocide additives will be compatible with the wellbore environment and bottomhole temperatures to prevent internal corrosion of the 7" casing and external corrosion of the tubing.

5.2.4 Injectate and Formation Fluid Properties

CTV is planning to construct a carbon capture and sequestration "hub" project (*i.e.*, a project that collects carbon dioxide (CO_2) from multiple sources over time and injects the CO_2 stream(s) via a Class VI UIC permitted injection well(s)). Therefore, CTV is currently considering multiple sources of anthropogenic CO_2 for the project. The potential sources include capture from existing and potential future industrial sources, as well as Direct Air Capture (DAC). Minor constituents associated with the CO_2 stream may include, for example, water content (<25 lb/mmscf), oxygen, H_2S, and SO_x compounds. The CO_2 stream will be sampled at the transfer point from the source and analyzed according to the analytical methods described in the "CTV III – QASP" (Table 4) document and the "Attachment C: Testing and Monitoring plan" (Table 1) document.

The anticipated injection temperature at the wellhead is 90 – 130° F.

The Injectate 1 and Injectate 2 compositions and properties are detailed in Section 7.2 of the Attachment-A Narrative document.

No corrosion is expected in the absence of free phase water provided that the entrained water is kept in solution with the CO_2. This is ensured by the <25 lb/mmscf injectate specification limit, and this specification will be a condition of custody transfer at the capture facility. For transport through pipelines, which typically use standard alloy pipeline materials, this specification is critical to the mechanical integrity of the pipeline network, and out of specification product will be immediately rejected. Therefore, all product transported through pipeline to the injection wellhead is expected to be dry phase CO_2 with no free phase water present.

Injectate water solubility will vary with depth and time as temperature and pressures change. The water specification is conservative to ensure water solubility across super-critical operating ranges. CRA tubing will be used in the injection wells to mitigate any potential corrosion impact should free-phase water from the reservoir become present in the wellbore, such as during shut-in events when formation liquids, if present, could backflow into the wellbore. CTV may further optimize the maximum water content specification prior to injection based on technical analysis.

Geochemical analysis and properties of the connate formation water has been provided in Section 2.8 of the Attachment-A Narrative document. Water geochemistry representative of the project area does not indicate corrosiveness to standard cement and casing materials. A formation water analysis will be obtained during pre-operational testing and reviewed to ensure compatibility with well construction materials.

5.2.5 Alarms and Shut-Off Devices

As described in the Testing and Monitoring Plan, injection wells will be configured with real-time injection rate, injection pressure, and annular pressure monitoring and alarms. The Operating Procedures plan details the maximum injection rate and pressure thresholds for alarms and shut-off devices.

A surface shut-off valve will be installed on the wellhead and configured with automation and communication to the Central Control Facility (CCF). The valve will be utilized by the CCF operator remotely to respond to an emergency by shutting in the well. The valve will be configured to automatically shut-in the well if tubing or annular alarm thresholds are exceeded.

The project does not anticipate risk factors that warrant downhole shut-off devices, such as high temperature, high pressure, presence of hydrogen sulfide, proximity to populated areas, or high likelihood of damage to the wellhead.

6.0 Pre-Operational Logging and Testing

CTV has attached a pre-operational logging and testing plan pursuant to 40 CFR 146.82(a)(8) and 40 CFR 146.87.

Pre-Operational Logging and Testing GSDT Submissions
GSDT Module: Pre-Operational Testing ***Tab(s):*** Welcome tab Please use the checkbox(es) to verify the following information was submitted to the GSDT: ☒ Proposed pre-operational testing program ***[40 CFR 146.82(a)(8) and 146.87]***

7.0 Well Operation

7.1 Operational Procedures [40 CFR 146.82(a)(10)]

CTV has provided detailed operational procedures for each injection well. These procedures and parameters are provided for all injectors in the Appendix – Operational Procedures document attached with this application.

7.2 Proposed Carbon Dioxide Stream [40 CFR 146.82(a)(7)(iii) and (iv)]

CTV is planning to construct a carbon capture and sequestration "hub" project (*i.e.*, a project that collects carbon dioxide (CO_2) from multiple sources over time and injects the CO_2 stream(s) via a Class VI UIC permitted injection well(s)). Therefore, CTV is currently considering multiple sources of anthropogenic CO_2 for the project. CO_2 will be sourced from a blue hydrogen and ammonia plant (up to 377,000 tonnes per annum) that will be located in proximity to the storage site, direct air capture and other CO_2 sources in the project area. CTV would expect the CO_2 stream will be sampled at the transfer point from the source and analyzed according to the analytical methods described in the "CTV III – QASP" (Table 4) document and the "Attachment C – CTV III Testing and Monitoring plan" (Table 1) document. Should the injectate not meet the minimum requirements, it will be rejected.

The anticipated injection temperature at the wellhead is 90 – 130° F.

For the purposes of Geochemical modeling, CO2 Plume modeling, AoR determination, and Well design, two major types of Injectate compositions were considered based on the source.

- Injectate 1: is a potential injectate stream composition from a Direct Air Capture (DAC) or a Pre-Combustion source (such as a blue hydrogen facility) or a Post-Combustion source (such as a Natural Gas fired power plant or Steam Generator). The primary impurity in the injectate is Nitrogen.
- Injectate 2: is a potential injectate stream composition from a Biofuel Capture source (such as a Biodiesel Plant that produces Biodiesel from a biologic source feedstock) or from an Oil & Gas refinery. The primary impurity in the injectate is light end Hydrocarbons (Methane and Ethane).

The compositions for these two injectates are shown in Table 7.1, and are based on engineering design studies and literature.

Table 7.1 : Injectate compositions

Component	Injectate 1	Injectate 2
	Mass%	**Mass%**
CO2	99.213%	99.884%
H2	0.051%	0.006%
N2	0.643%	0.001%
H2O	0.021%	0.000%
CO	0.029%	0.001%
Ar	0.031%	0.000%
O2	0.004%	0.000%
SO2+SO3	0.003%	0.000%
H2S	0.001%	0.014%
CH4	0.004%	0.039%
NOx	0.002%	0.000%
NH3	0.000%	0.000%
C2H6	0.000%	0.053%
Ethylene	0.000%	0.002%
Total	**100.00%**	**100.00%**

For geochemical and plume modeling scenarios, these injectate compositions were simplified to a 4-component system, shown in Table 7.2 and then normalized for use in the modeling. The 4 component simplified compositions cover 99.9% by mass of Injectate 1 & 2 and cover particular impurities of concern (H2S and SO2). The estimated properties of the injectates at downhole conditions are specified in Table 7.3

Table 7.2: Simplified 4 component composition for Injectate 1 and Injectate 2

Injectate 1	
Component	**mass%**
CO2	99.213%
N2	0.643%
SO2+SO3	0.003%
H2S	0.001%

Injectate 2	
Component	**mass%**
CO2	99.884%
CH4	0.039%
C2H6	0.053%
H2S	0.014%

Table 7.3. Injectate properties range over project life at downhole conditions for Injectate 1 and Injectate 2

Injectate property at downhole conditions	Injectate 1	Injectate 2
Viscosity, cp	0.054	0.056
Density, lb/ft^3	41.39	42.56
Compressibility factor, Z	0.464	0.453

No corrosion is expected in the absence of free phase water provided that the entrained water is kept in solution with the CO_2. This is ensured by the <25 lb/mmscf injectate specification limit, and this specification will be a condition of custody transfer at the capture facility. For transport through pipelines, which typically use standard alloy pipeline materials, this specification is critical to the mechanical integrity of the pipeline network, and out of specification product will be immediately rejected. Therefore, all product transported through pipeline to the injection wellhead is expected to be dry phase CO_2 with no free phase water present.

Injectate water solubility will vary with depth and time as temperature and pressures change. The water specification is conservative to ensure water solubility across super-critical operating ranges. CRA tubing will be used in the injection wells to mitigate any potential corrosion impact should free-phase water from the reservoir become present in the wellbore, such as during shut-in events when formation liquids, if present, could backflow into the wellbore. CTV may further optimize the maximum water content specification prior to injection based on technical analysis.

8.0 Testing and Monitoring

CTV's Testing and Monitoring plan pursuant to 40 CFR 146.82 (a) (15) and 40 CFR 146.90 describes the strategies for testing and monitoring to ensure protection of the USDW, injection well mechanical integrity, and plume monitoring.

Testing and Monitoring GSDT Submissions
GSDT Module: Project Plan Submissions ***Tab(s):*** Testing and Monitoring tab Please use the checkbox(es) to verify the following information was submitted to the GSDT: ☒ Testing and Monitoring Plan [40 CFR 146.82(a)(15) and 146.90]

9.0 Injection Well Plugging

CTV's Injection Well Plugging Plan pursuant to 40 CFR 146.92 describes the process, materials and methodology for injection well plugging.

Injection Well Plugging GSDT Submissions
GSDT Module: Project Plan Submissions ***Tab(s):*** Injection Well Plugging tab Please use the checkbox(es) to verify the following information was submitted to the GSDT: ☒ Injection Well Plugging Plan [40 CFR 146.82(a)(16) and 146.92(b)]

10.0 Post-Injection Site Care (PISC) and Site Closure

CTV has developed a Post-Injection Site Care and Site Closure plan pursuant to 40 CFR 146.93 (a) to define post-injection testing and monitoring.

At this time CTV is not proposing an alternative PISC timeframe.

PISC and Site Closure GSDT Submissions
GSDT Module: Project Plan Submissions ***Tab(s):*** PISC and Site Closure tab Please use the checkbox(es) to verify the following information was submitted to the GSDT: ☒ PISC and Site Closure Plan [40 CFR 146.82(a)(17) and 146.93(a)]
GSDT Module: Alternative PISC Timeframe Demonstration ***Tab(s):*** All tabs (only if an alternative PISC timeframe is requested) Please use the checkbox(es) to verify the following information was submitted to the GSDT: ☐ Alternative PISC timeframe demonstration ***[40 CFR 146.82(a)(18) and 146.93(c)]***

11.0 Emergency and Remedial Response

CTV's Emergency and Remedial Response plan pursuant to 40 CFR 164.94 describes the process and response to emergencies to ensure USDW protection.

Emergency and Remedial Response GSDT Submissions
GSDT Module: Project Plan Submissions ***Tab(s):*** Emergency and Remedial Response tab Please use the checkbox(es) to verify the following information was submitted to the GSDT: ☐ Emergency and Remedial Response Plan *[40 CFR 146.82(a)(19) and 146.94(a)]*

12.0 Injection Depth Waiver and Aquifer Exemption Expansion

No depth waiver or Aquifer Exemption expansion is being requested as part of this application

Injection Depth Waiver and Aquifer Exemption Expansion GSDT Submissions
GSDT Module: Injection Depth Waivers and Aquifer Exemption Expansions ***Tab(s):*** All applicable tabs Please use the checkbox(es) to verify the following information was submitted to the GSDT: ☐ Injection Depth Waiver supplemental report ***[40 CFR 146.82(d) and 146.95(a)]*** ☐ Aquifer exemption expansion request and data ***[40 CFR 146.4(d) and 144.7(d)]***

13.0 Reference

Bartow. 1985. Maps showing Tertiary stratigraphy and structure of the Northern San Joaquin Valley, California. United States Geological Survey (USGS).

Berkstresser, C.F. Jr. 1973. Base of Fresh Ground-Water -- Approximately 3,000 micromhos -- in the Sacramento Valley and Sacramento-San Joaquin Delta, California. U.S. Geological Survey Water-Resource Inv. 40-73. 1973

Bertoldi, G., Johnston, R., & Evenson, K. 1991. Groundwater in the Central Valley, California - A Summary Report. USGS Professional Paper 1401-A. https://doi.org/10.3133/pp1401A.

Beyer, L.A. Summary of Geology and Petroleum Plays Used to Assess Undiscovered Recoverable Petroleum Resources of Sacramento Basin Province, California. United States Department of the Interior Geological Survey, 1988.

Burow, Karen R., Jennifer L. Shelton, Joseph A. Hevesi, and Gary S. Weissmann. 2004. Hydrologic Characterization of the Modesto Area, San Joaquin Valley, California. Preliminary Draft. U.S. Geological Survey. Water-Resources Investigation Report. Prepared in cooperation with Modesto Irrigation District. Sacramento, California.

California Department of Water Resources (DWR). 1995. Sacramento Delta San Joaquin Atlas.

California Department of Water Resources (DWR). 2006. California's Groundwater, Bulletin 118. San Joaquin Valley Groundwater Basin Tracy Subbasin. Last updated November 2021.

Davis G.H., J.H. Green, S.H. Olmstead, and D.W. Brown 1959. Davis, G. H., J.H. Green, S.H. Olmstead, and D.W. Brown. 1959. Ground water conditions and storage capacity in the San Joaquin Valley, California. U.S. Geological Survey Water Supply Paper No. 1469, 287 p.

Davis, K.E., 1988. *Survey of Methods to Determine Total Dissolved Solids Concentrations*. U.S. Environmental Protection Agency Underground Injection Control Program. Prepared by Ken E. Davis Associates under subcontract to Engineering Enterprises, INC. EPA LOE Contract No. 68-03-3416, Work Assignment No. 1-0-13, Keda Project No. 30-956.

Downey, C., and Clinkenbeard, J. 2010. Preliminary Geologic Assessment of the Carbon Sequestration Potential of the Upper Cretaceous Mokelumne River, Starkey, and Winters Formations – Southern Sacramento Basin, California. California Geological Survey.

Downey, C., and Clinkenbeard, J. 2006. An overview of geologic carbon sequestration potential in California, California Energy Commission, PIER Energy-Related Environmental Research Program.

GEI Consultants, Inc. (GEI) 2007. Tracy Regional Groundwater Management Plan.

GEI Consultants, Inc. (GEI) 2021. Tracy Subbasin Groundwater Sustainability Plan. November 1, 2021.

Graham, S.A., McCloy, C., Hitzman, M., Ward, R., Turner, R. 1984. Basin Evolution During Chance from Convergent to Transform Continental Margin in Central California. The American Association of Petroleum Geologists Bulletin V.68 No. 3.

Hotchkiss, W. R., and G.O. Balding. 1971. Geology, hydrology, and water quality of the Tracy-Dos Palos area, San Joaquin Valley, California. U.S. Geological Survey. Open-File Report. Hotchkiss and Balding. 1971.

Heidbach, O., M. Rajabi, X. Cui, K. Fuchs, B. Müller, J. Reinecker, K. Reiter, M. Tingay, F. Wenzel, F. Xie, M. O. Ziegler, M.-L. Zoback, and M. D. Zoback (2018): The World Stress Map database release 2016: Crustal stress pattern across scales. Tectonophysics, 744, 484-498, doi:10.1016/j.tecto.2018.07.007

Heidbach, Oliver; Rajabi, Mojtaba; Reiter, Karsten; Ziegler, Moritz; WSM Team (2016): World Stress Map Database Release 2016. GFZ Data Services, doi:10.5880/WSM.2016.001

Hydrofocus, 2015. San Joaquin County and Delta Quality Coalition Groundwater Quality Assessment Report, April 27, 2015.

Ingram G. M., Urai J. L., Naylor M. A. 1997. in Hydrocarbon Seals: Importance for Exploration and Production, Sealing processes and top seal assessment, Norwegian Petroleum Society (NPF) Special Publication, eds Moller-Pedersen P., Koestler A. G. 7, pp 165–175.

Ingram, Gary and Urai, Janos. 1999. Top-seal leakage through faults and fractures: the role of mudrock properties. Geological Society, London, Special Publications. 158. 125-135. 10.1144/GSL.SP.1999.158.01.10.

Johnson, D.S. 1990. Depositional environment of the Upper Cretaceous Mokelumne River Formation, Sacramento Basin. California. American Assoc. of Petroleum Geologists Bulletin 74: 5 1990: 686 p.

Leong, J.K., and J.R. Tenzer. 1994. Production Optimization of a Mature Gas Field. Paper presented at the SPE Western Regional Meeting, Long Beach, California.

Lund Snee, J-E, and Zoback, M. 2020. Multiscale variations of the crustal stress field throughout North America", Nature Communications 11, 1951.

Magoon, L.B., and Valin, Z.C. 1995. Sacramento Basin Province (009). United States Department of the Interior Geological Survey, National assessment of United States oil and gas resources-results, methodology, and supporting data.

Mount, Van and Suppe, John. 1992. Present-day stress orientations adjacent to active strike-slip faults - California and Sumatra. Journal of Geophysical Research. 971. 11995-12013. 10.1029/92JB00130.

Nilsen, T. H., and Clarke, Jr. S.H. 1975. Sedimentation and Tectonics in the Early Tertiary Continental Borderland of Central California. Geological Survey Professional Paper 925,.

O'Geen A, Saal M, Dahlke H, Doll D, Elkins R, Fulton A, Fogg G, Harter T, Hopmans J, Ingels C, Niederholzer F, Sandoval Solis S, Verdegaal P, Walkinshaw M. 2015. Soil suitability index identifies potential areas for groundwater banking on agricultural lands.

Padre and Associates, Inc. 2004. personnel communication with Mike Burke regarding aquifer testing at City of Tracy Well 8.

Page, R.W. 1986. Geology of the Fresh Ground-Water Basin of the Central Valley, California, with Texture Maps and Sections. USGS Professional Paper 1401-C.

Sullivan, Ray and Sullivan, Morgan. 2012. Sequence Stratigraphy and Incised Valley Architecture of the Domengine Formation, Black Diamond Mines Regional Preserve and the Southern Sacramento Basin, California, U.S.A. Journal of Sedimentary Research.

Towell, T. 1992. Public Health and Safety- Seismic and Geological Hazards July

U.S. Environmental Protection Agency Underground Injection Control Program. 1988. Survey of Methods to Determine Total Dissolved Solids Concentrations. Prepared by Ken E. Davis Associates under subcontract to Engineering Enterprises, INC. EPA LOE Contract No. 68-03-3416, Work Assignment No. 1-0-13, Keda Project No. 30-956.

Unruh, J.R., and Hitchcock, C.S., 2009. Characterization of Potential Seismic Sources in the Sacramento-San Joaquin Delta, California. U.S. Geological Survey National Earthquake Hazards Reduction Program.

Williamson, C.R., and Hill, D.R. 1981. Submarine-Fan Deposition of the Upper Cretaceous Winters Sandstone, Union Island Gas Field, Sacramento Valley, California.: The Society of Economic Paleontologists and Mineralogists (SEPM) Deep-Water Clastic Sediments (CW2).

Wagner, D.L., Bortugno, E.J., and Mc Junkin, R.D. 1991. Geologic Map of the San Francisco – San Jose Quadrangle. California Geological Survey, Regional Geologic Map No. 5A, 1:250,000 scale.

IEAGHG, 2011. Effects of impurities on geological storage of CO2. International Energy Agency Greenhouse Gas programme

B. Wetenhall et al. / International Journal of Greenhouse Gas Control 30 (2014) 197–211

NARRATIVE REPORT - FIGURES

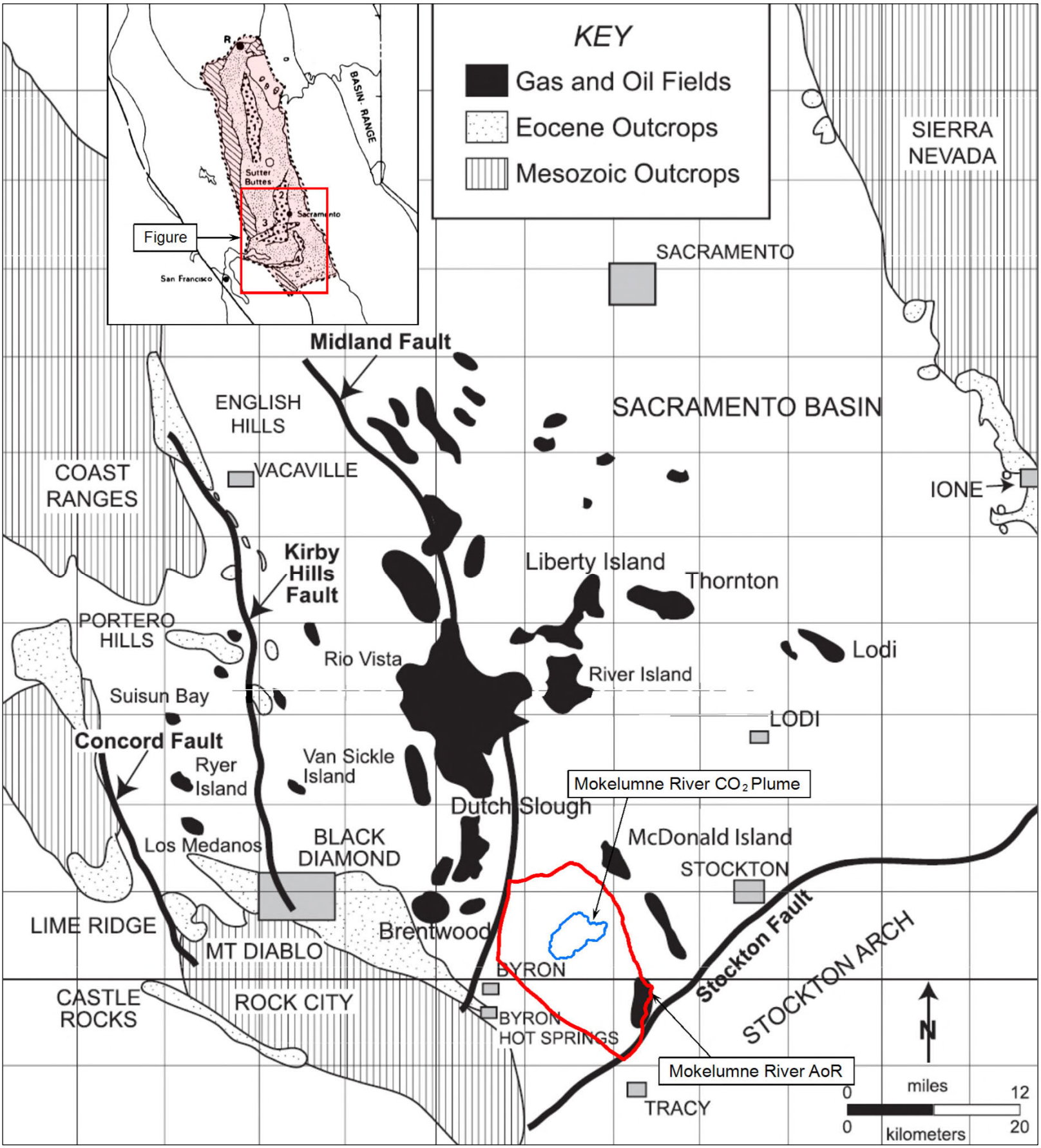

Figure 2.1-1. Location map of the proposed injection AoR (red) in relation to the Sacramento Basin. CO_2 plume boundary shown in blue.

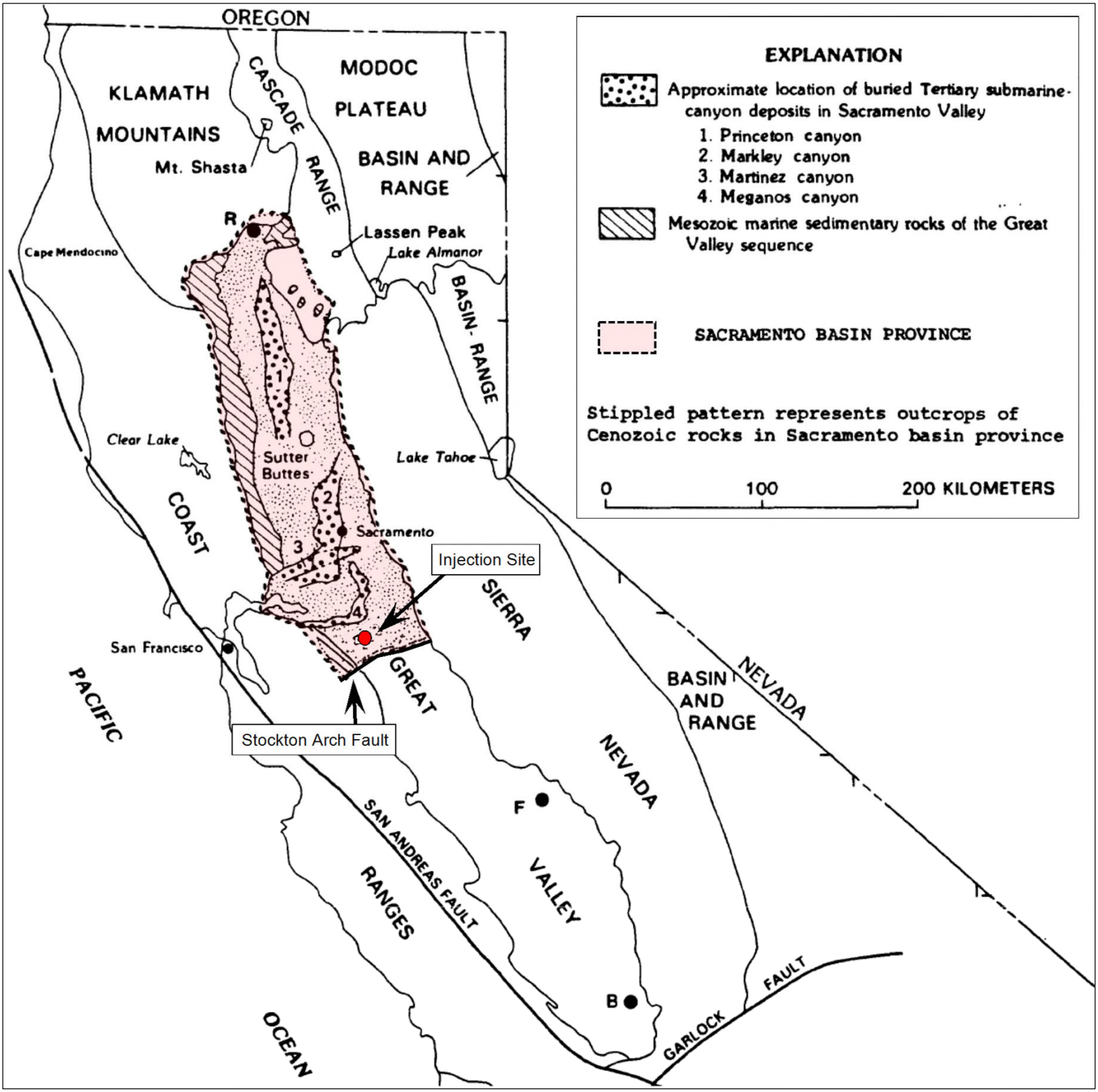

Figure 2.1-2. Location map of California modified from (Beyer, 1988) & (Sullivan, 2012). The Sacramento Basin regional study area is outlined by a dashed black line. B – Bakersfield; F – Fresno; R – Redding.

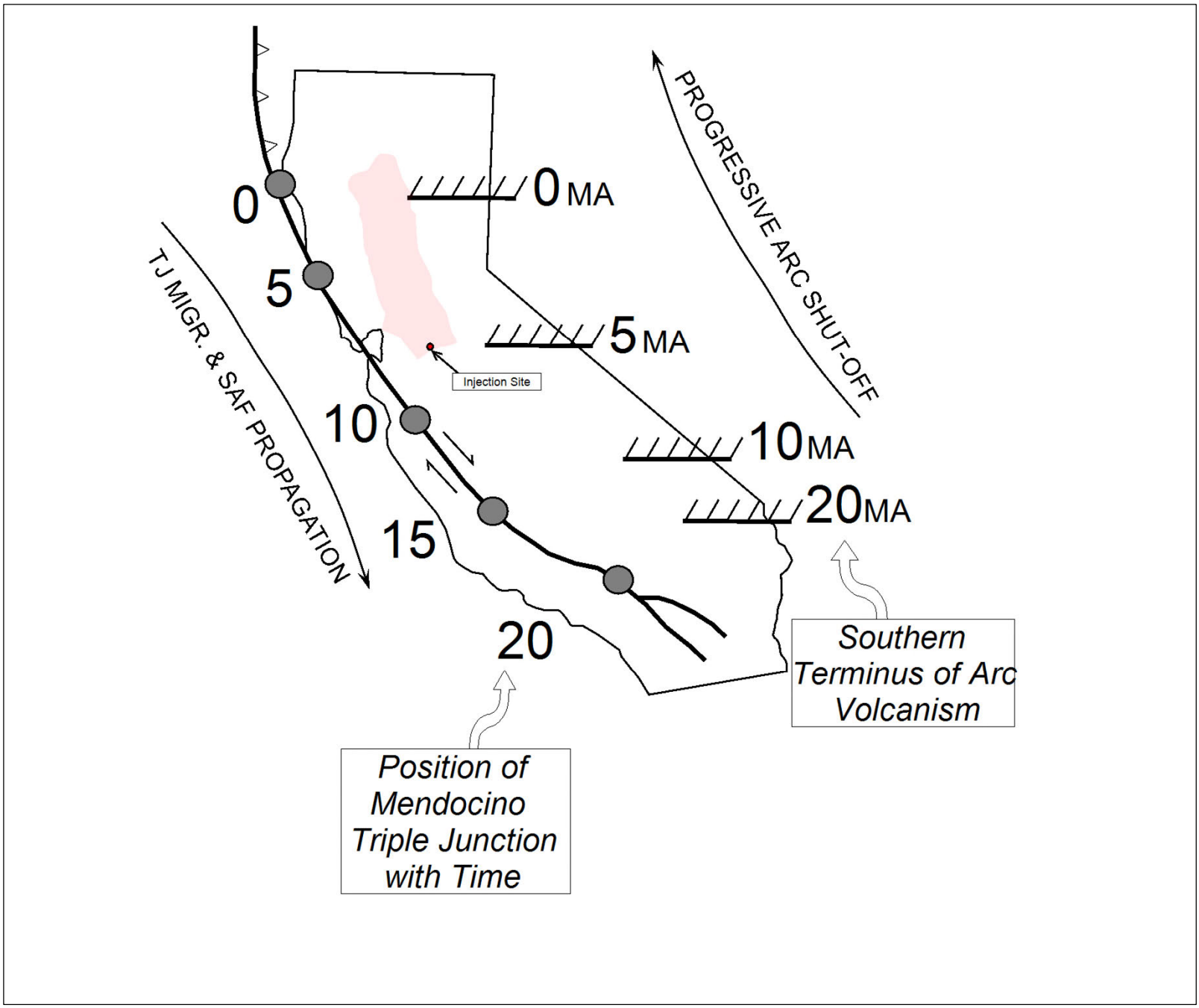

Figure 2.1-3. Migrational position of the Mendocino triple junction (Connection point of the Gorda, North American and Pacific plates) on the west and migrational position of Sierran arc volcanism in the east (Graham, 1984). Figure indicates space-time relations of major continental-margin tectonic events in California during Miocene.

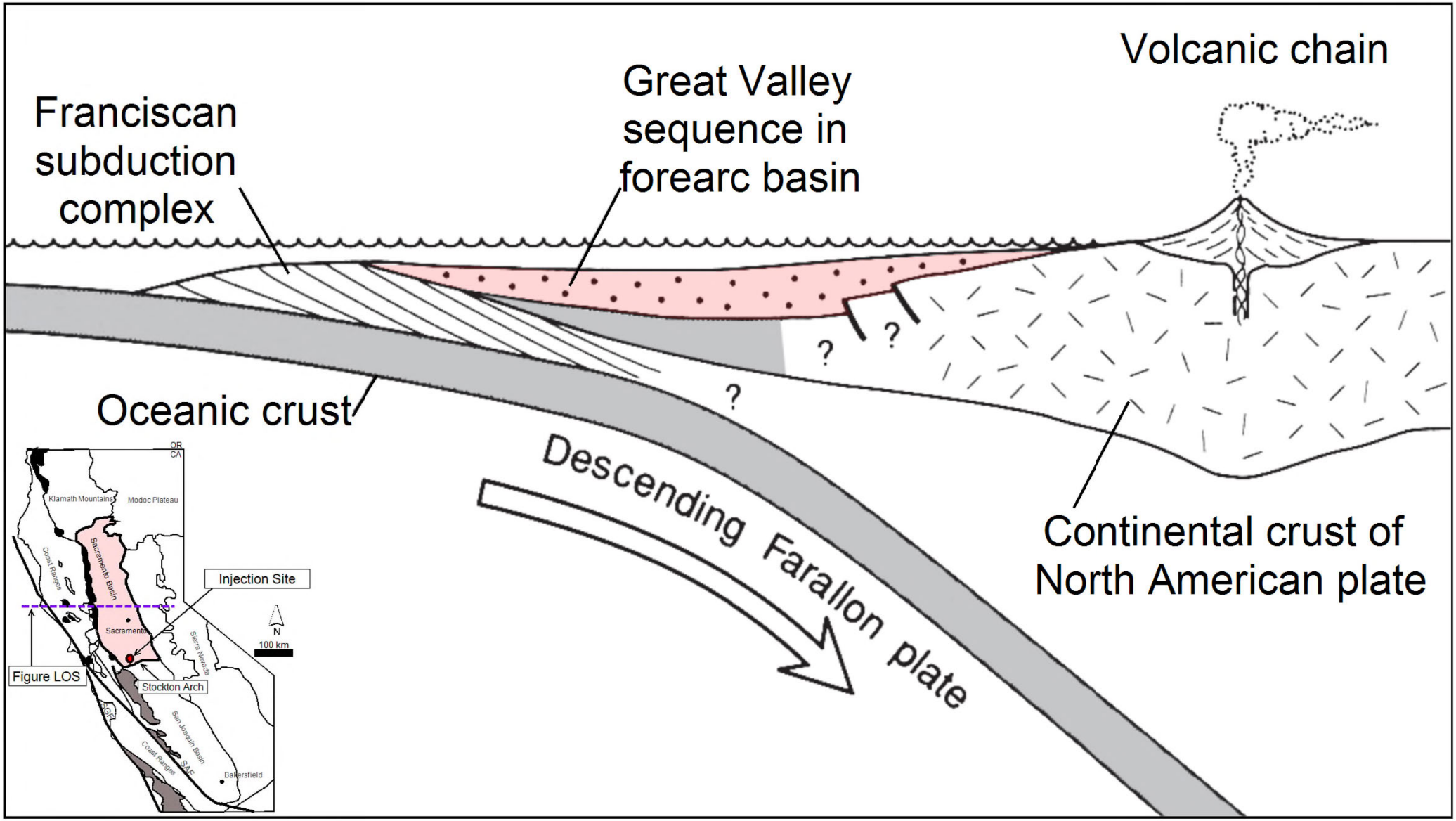

Figure 2.1-4. Schematic W-E cross-section of California, highlighting the Sacramento Basin, as a continental margin during late Mesozoic. The oceanic Farallon plate was forced below the west coast of the North American continental plate.

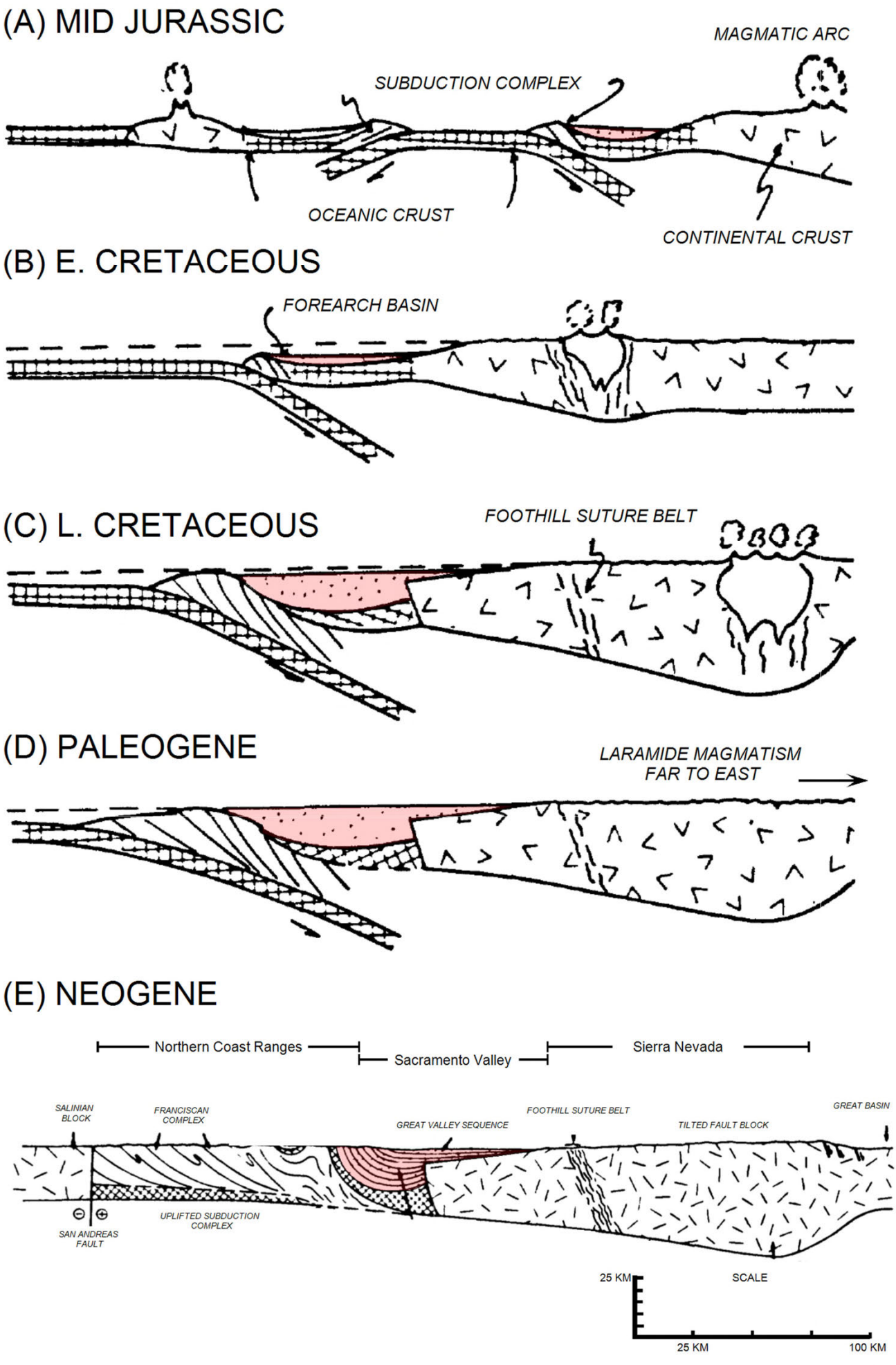

Figure 2.1-5. Evolutionary stages showing the history of the arc-trench system of California from Jurassic (A) to Neogene (E) (modified from Beyer, 1988).

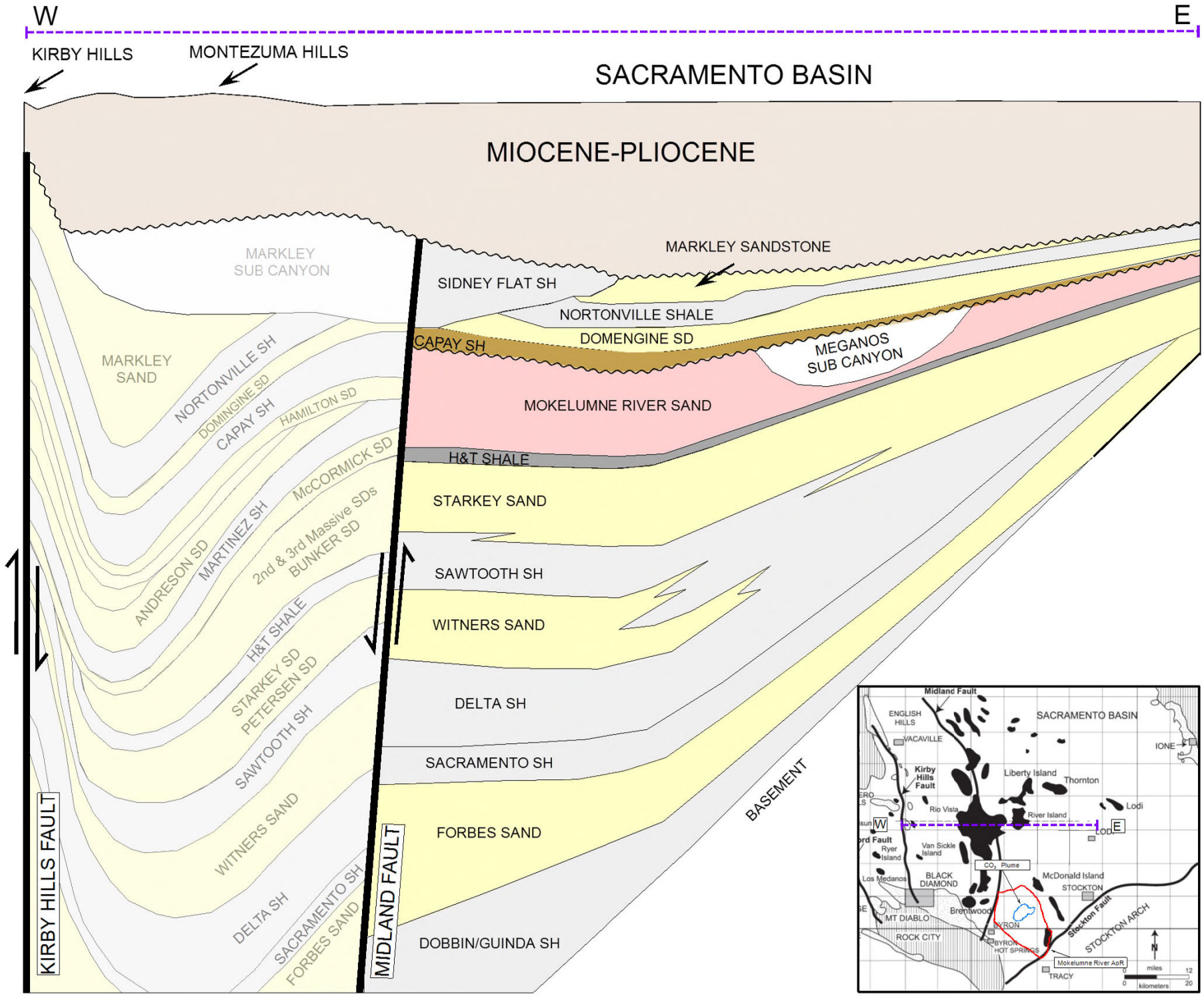

Figure 2.1-6. Schematic west to east cross section in the Sacramento basin.

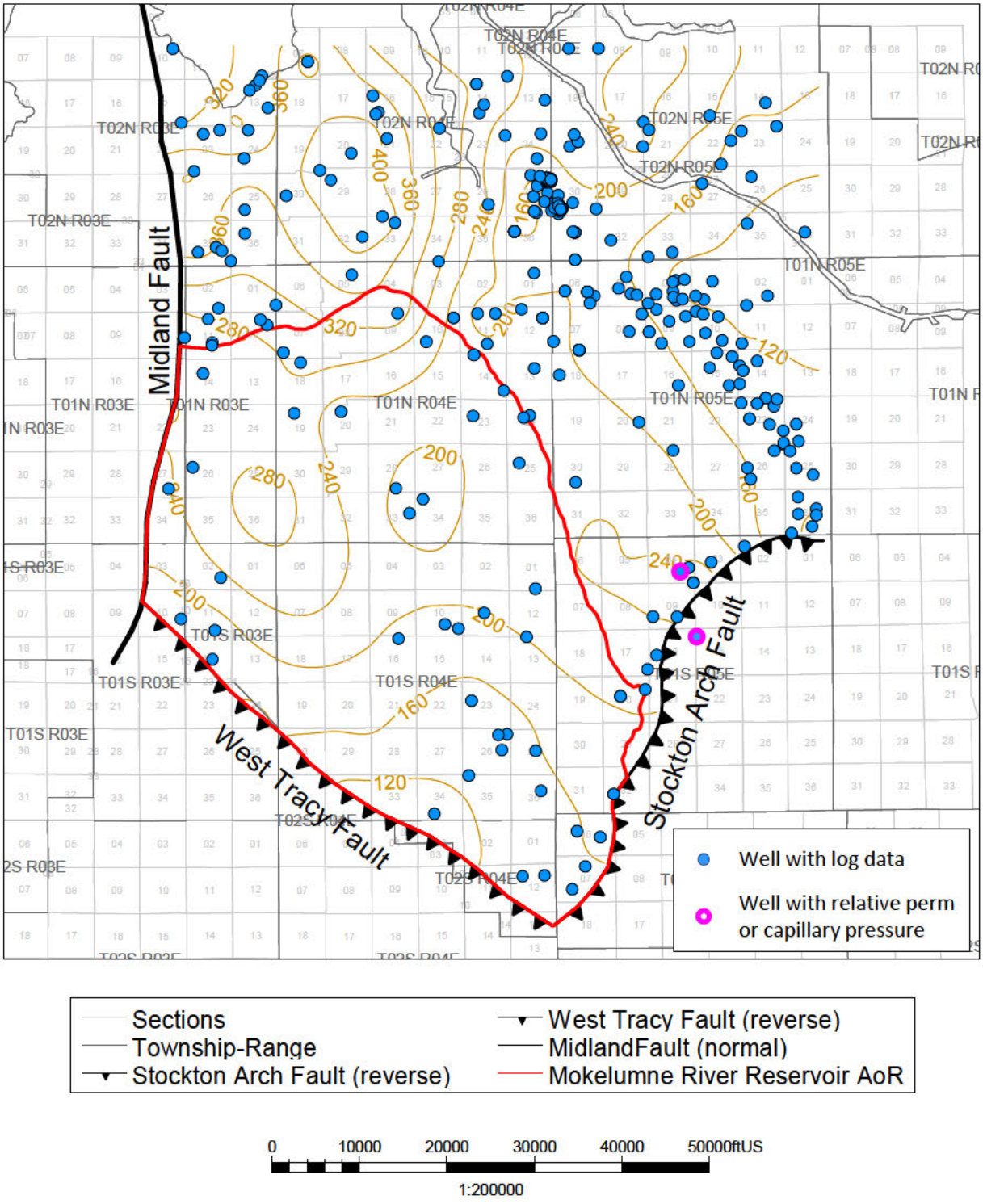

FIGURE 2.1-7. Capay Shale isopach map for the greater Victoria Island area. Wells shown as blue dots on the map penetrate the Capay Shale and have open-hole logs. Wells with relative permeability or capillary pressure data are shown as magenta circles.

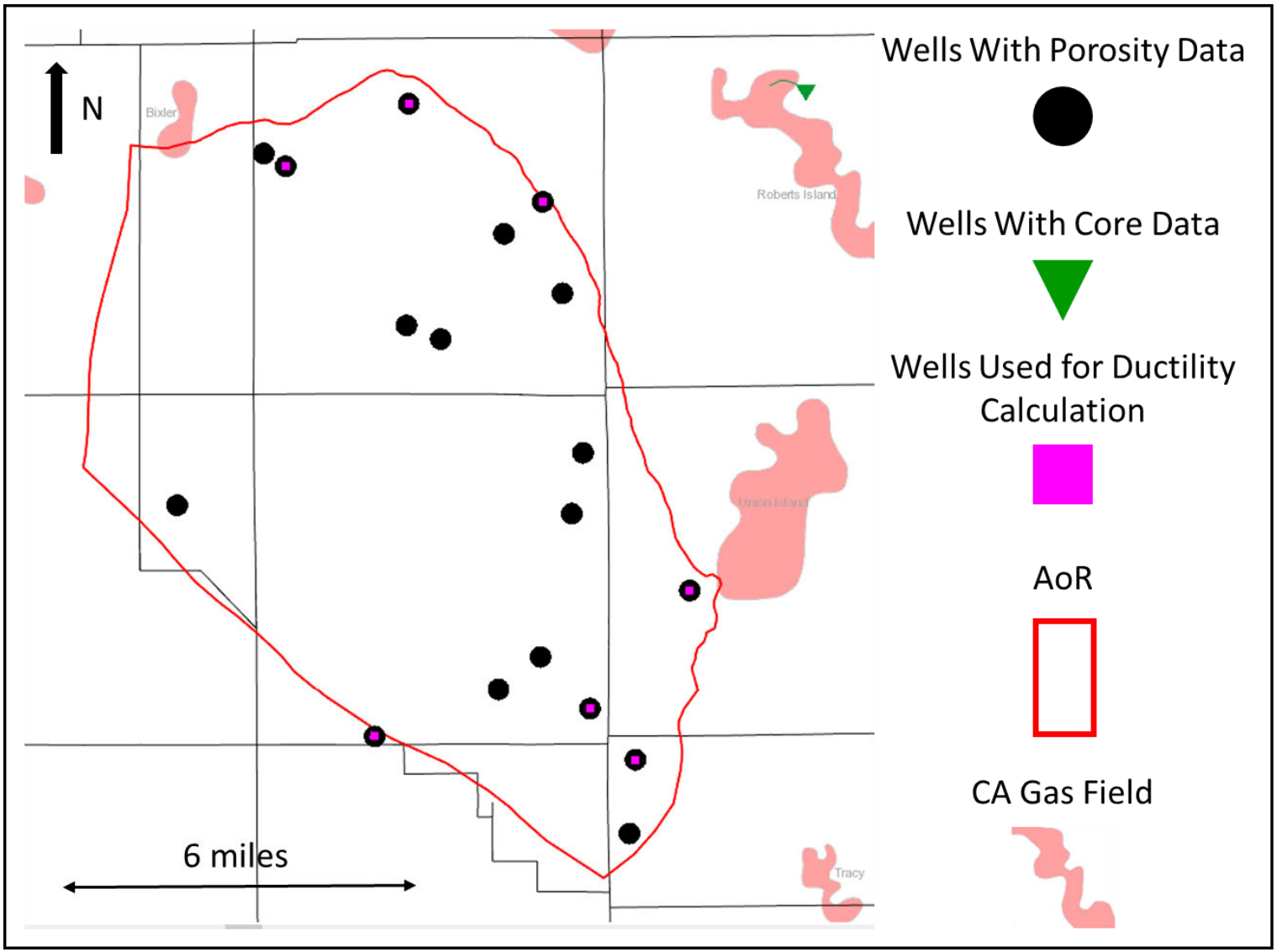

Figure 2.2-1. Wells drilled in the project area with porosity data are shown in black, wells with core are shown in green and wells used for ductility calculation are shown in pink.

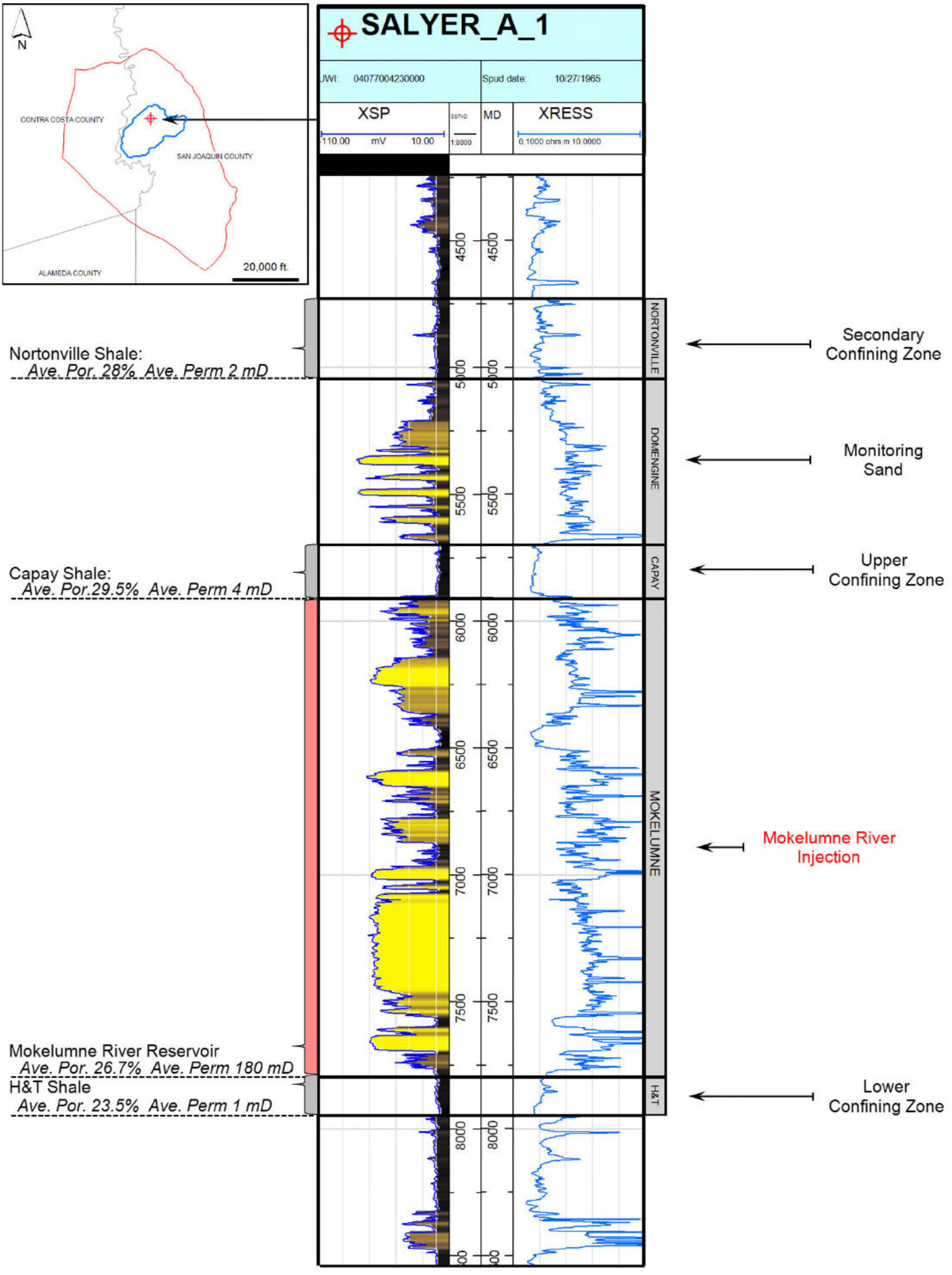

Figure 2.2-2. Type well taken from within the CO_2 boundary showing average rock properties used in the model for confining and injection zones.

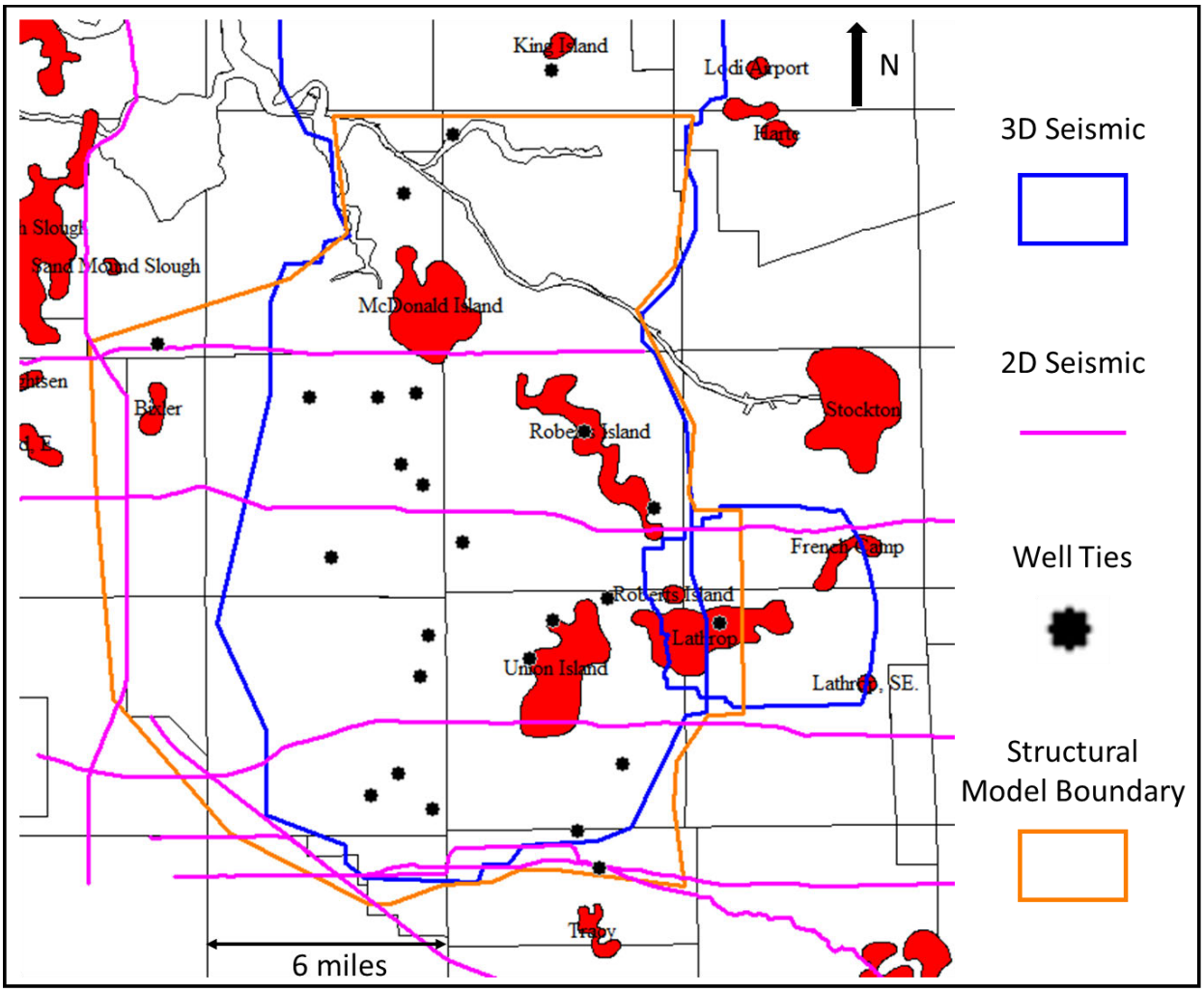

Figure 2.2-3. Summary map and area of seismic data used to build structural model. The 3D surveys were acquired in 1998 and reprocessed in 2013. The 2D seismic were acquired between 1980 and 1985. California gas fields are shown for reference.

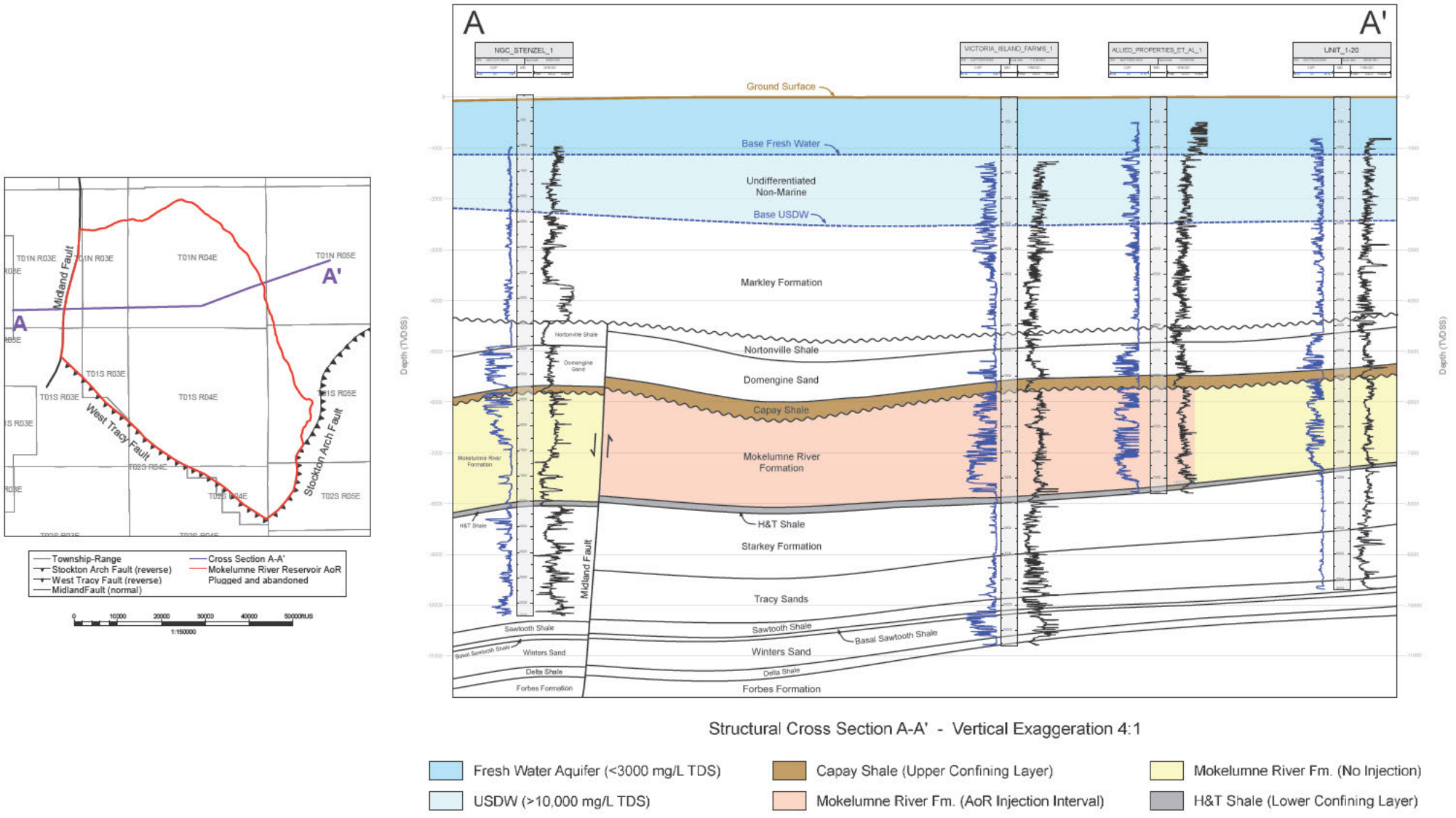

Figure 2.2-4. Cross section showing stratigraphy and lateral continuity of major formations across the AoR.

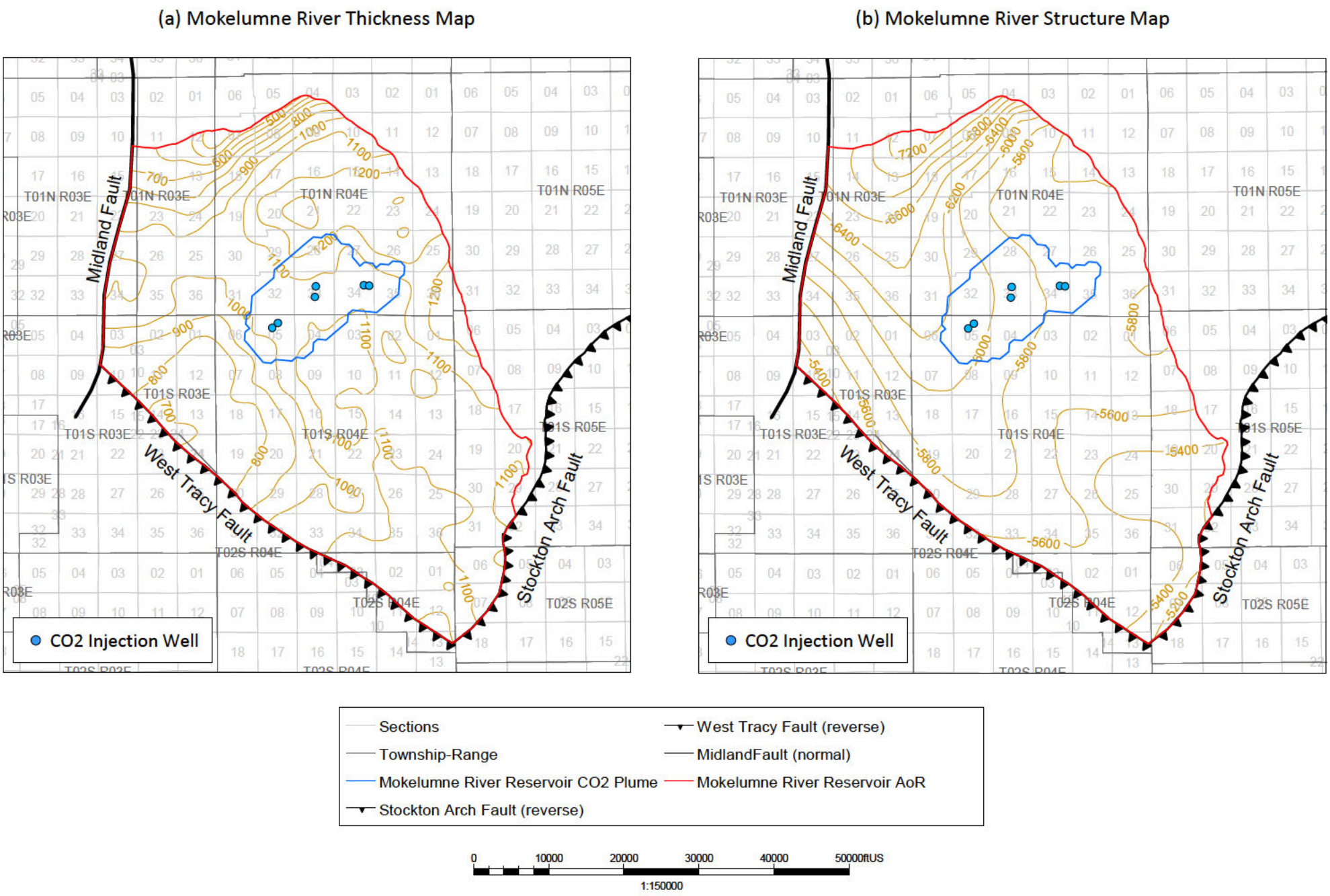

Figure 2.2-5. (a) Mokelumne River thickness map. (b) Mokelumne River structure map.

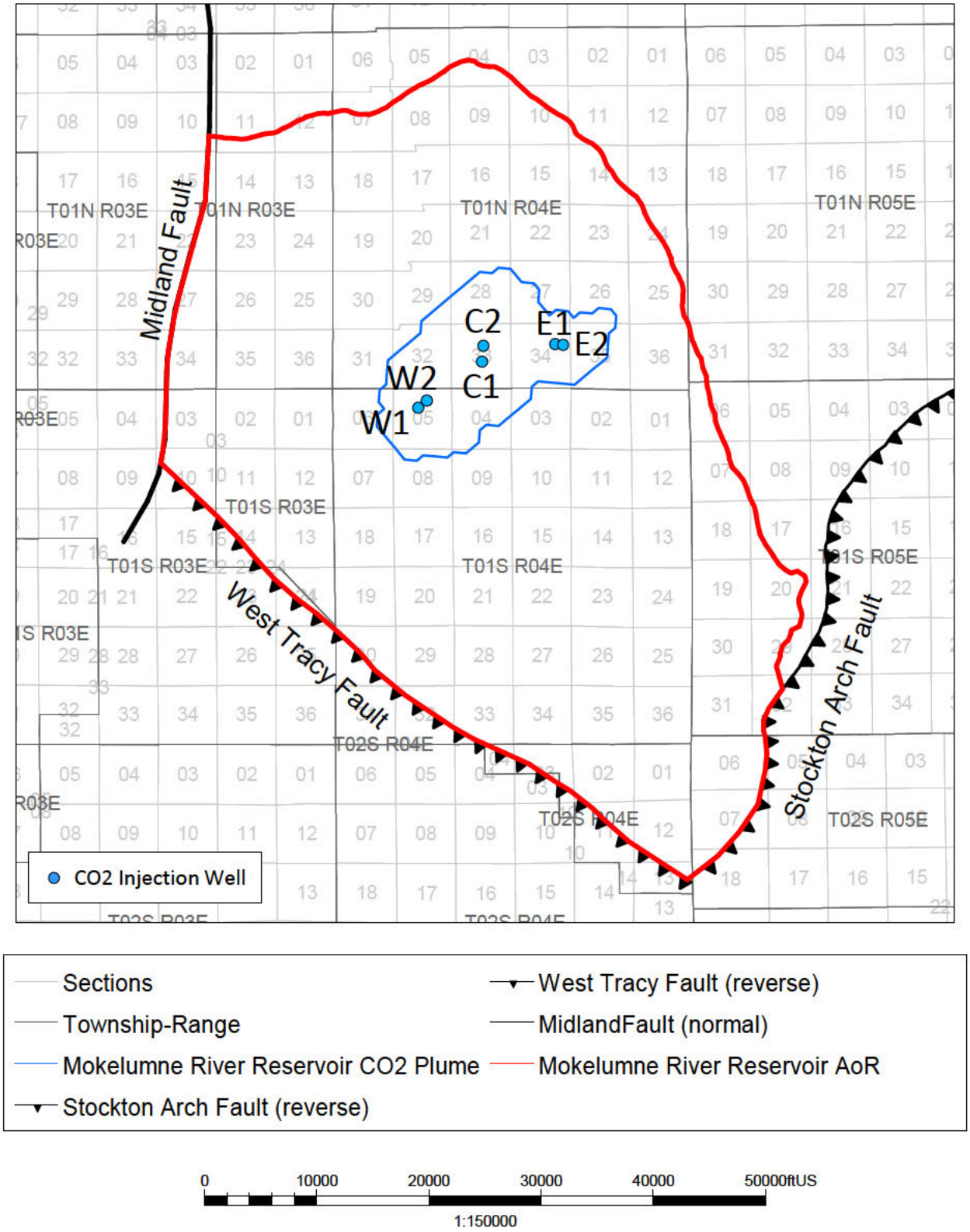

Figure 2.2-6. Injection well location map for the project area. The three groups of injection wells (W1 & W2, C1 & C2, E1 & E2) are approximately 7,000 ft. apart.

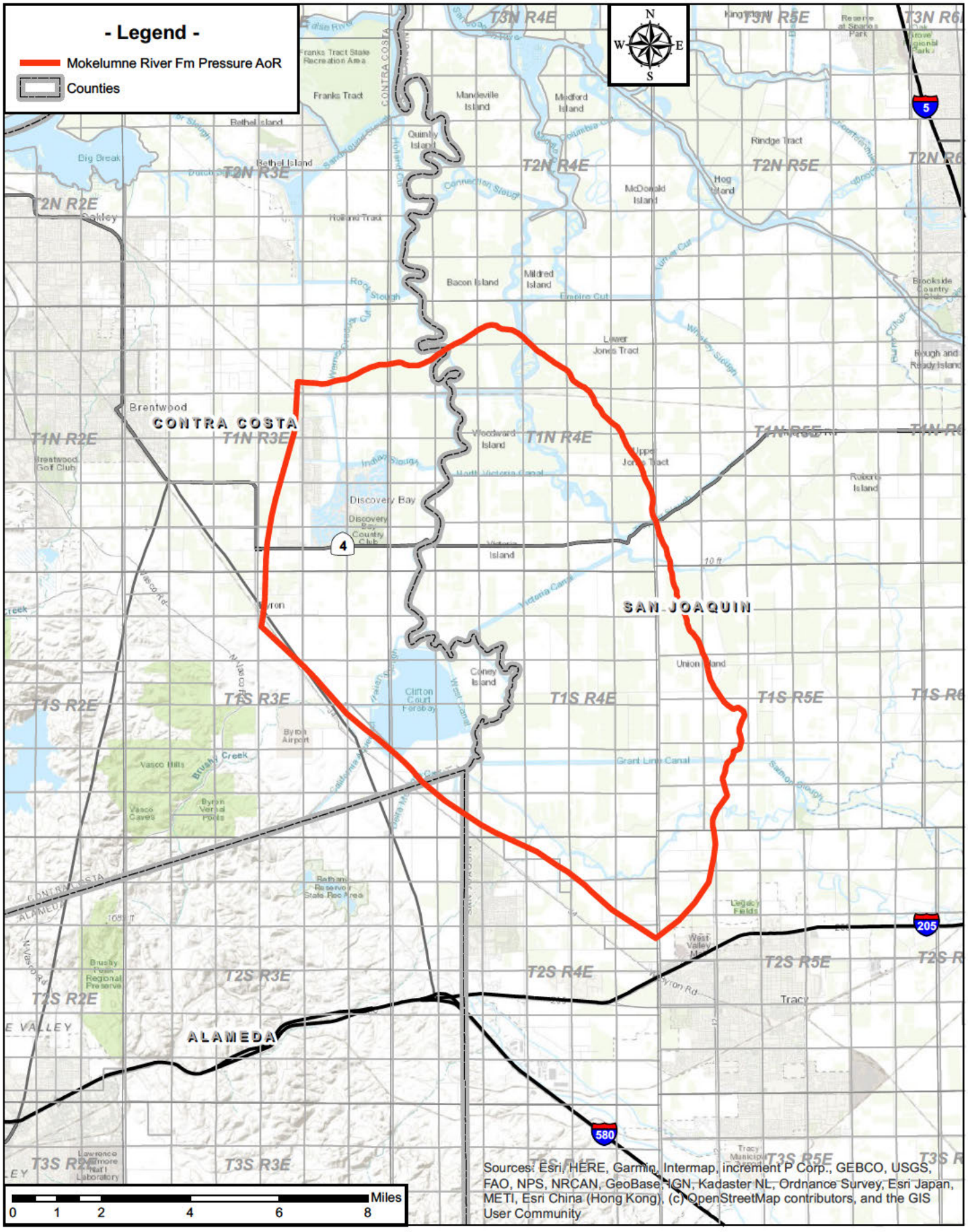

Figure 2.2-7 Surface Features and the AoR

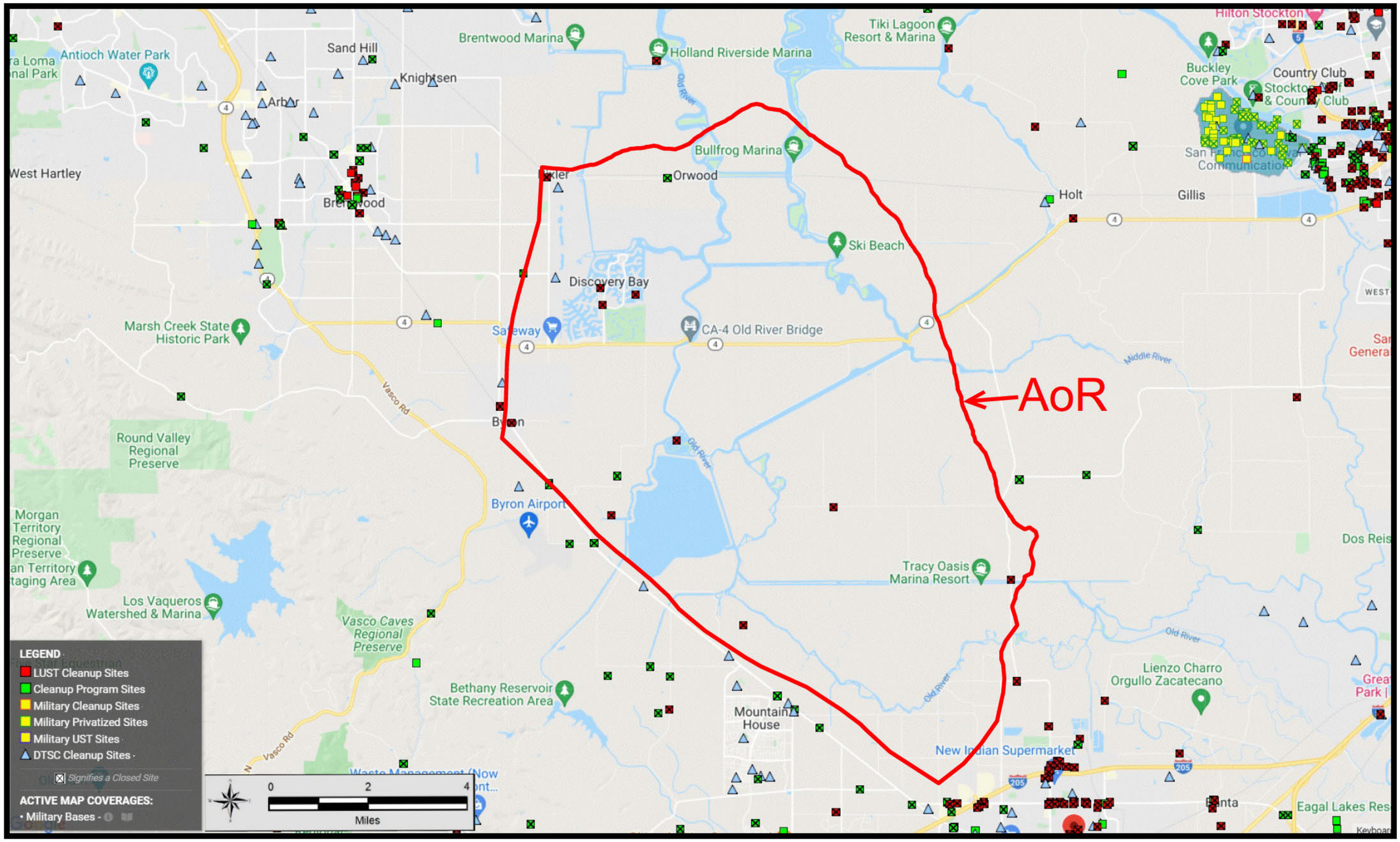

Figure 2.2-8 State and EPA approved Cleanup Sites

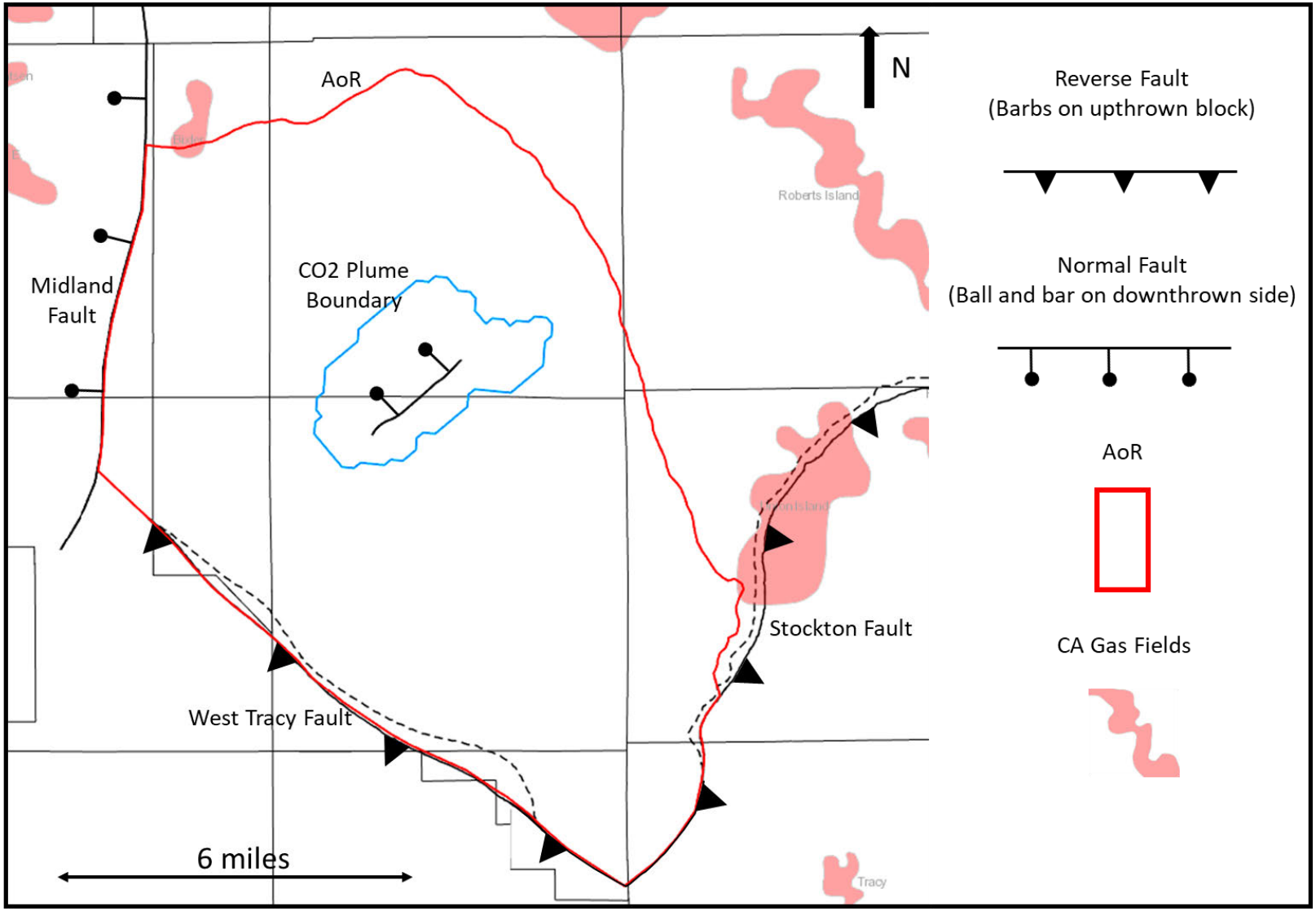

Figure 2.3-1. Faults interpreted from seismic, well, and published data that intersect the AoR.

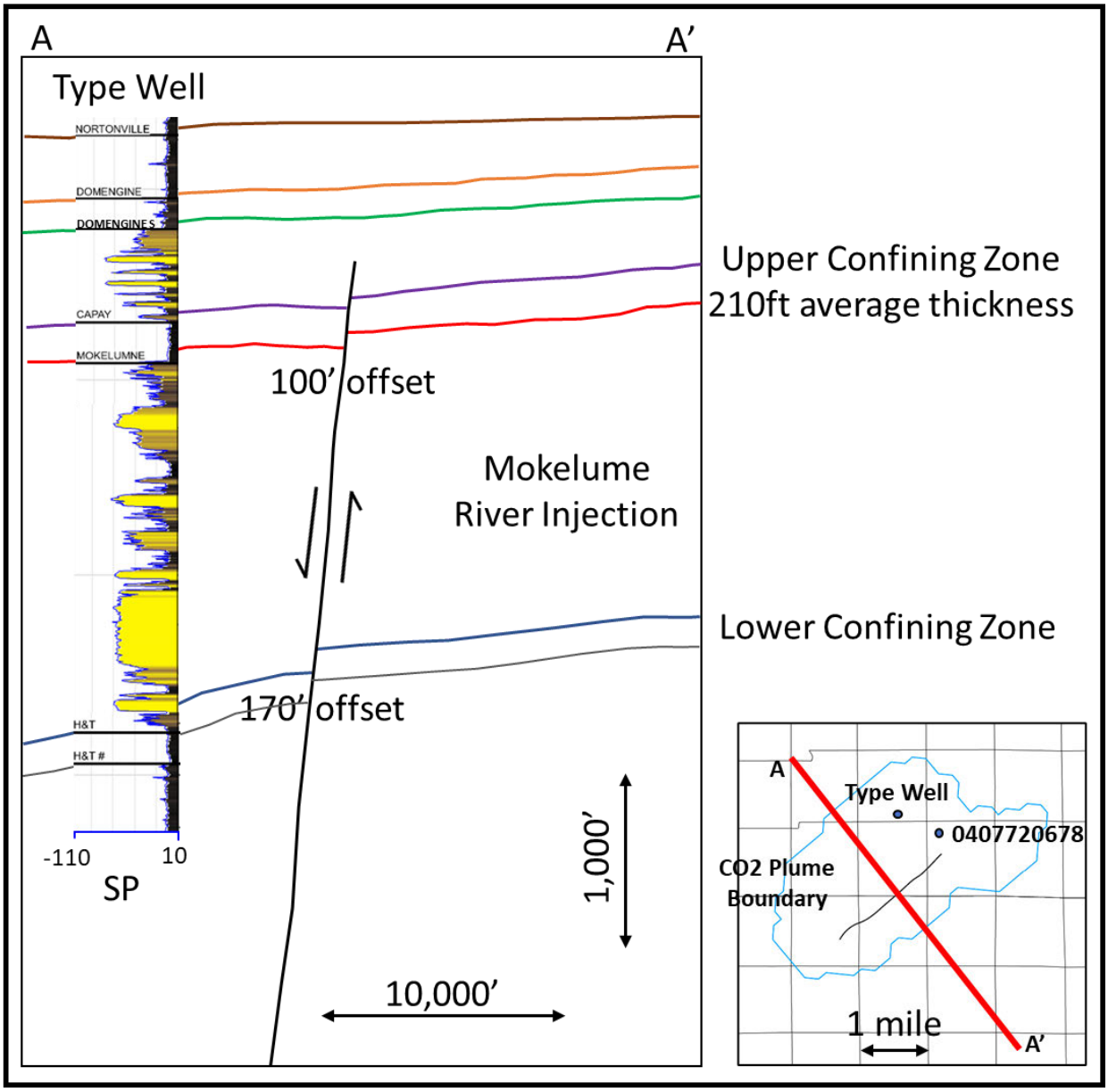

Figure 2.3-2. Schematic cross-section across the normal fault within the CO_2 plume boundary. Properties of the Capay Shale will be confirmed in pre-operational testing and this fault will be monitored during injection in the Domengine sands above.

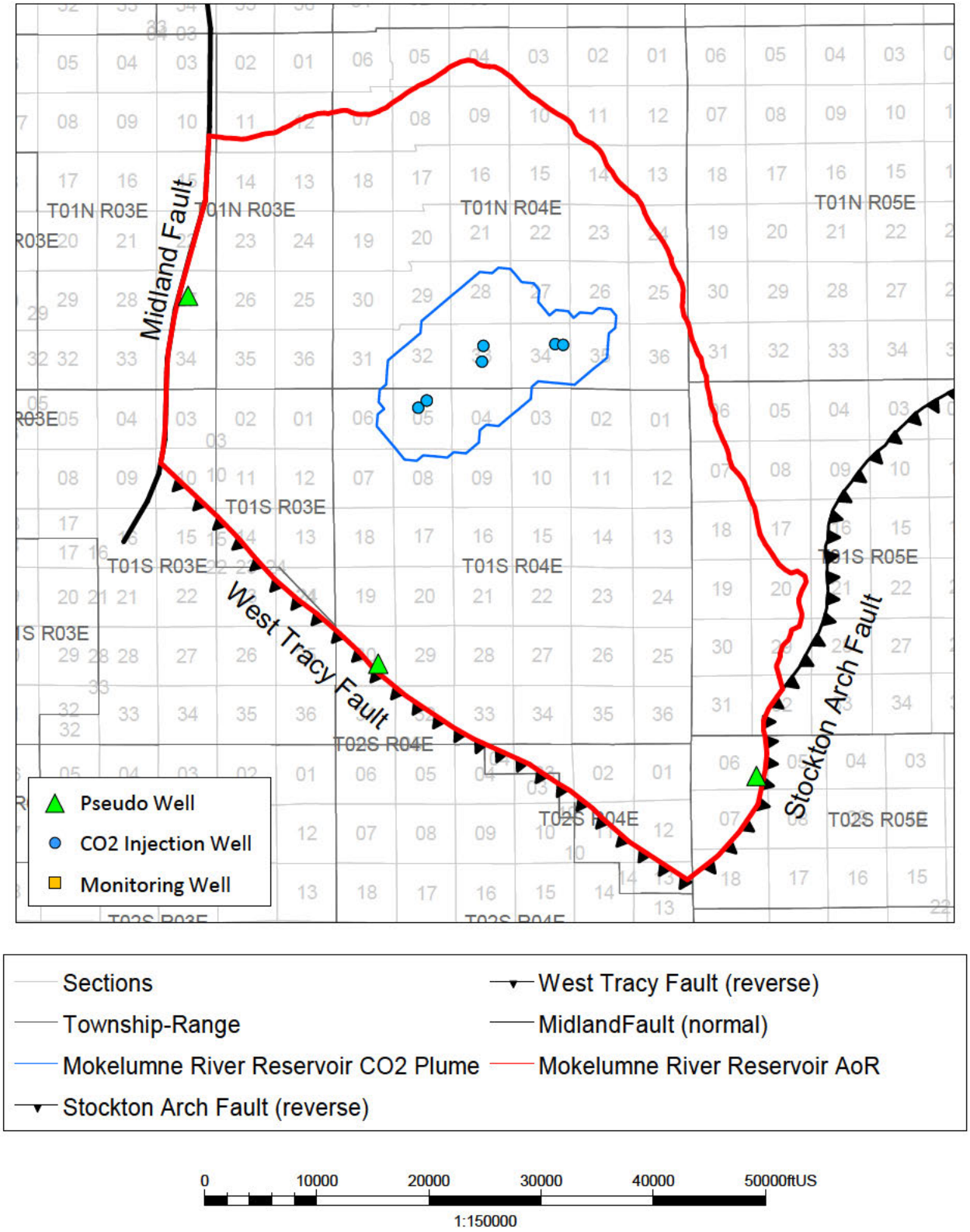

Figure 2.3-3. Green triangles show pseudo well locations at central areas along the three bounding faults relative to the AoR. Pressure data was extracted from the plume model to capture the expected pressure values at each location. Average of these results are presented in Table 2.3-1.

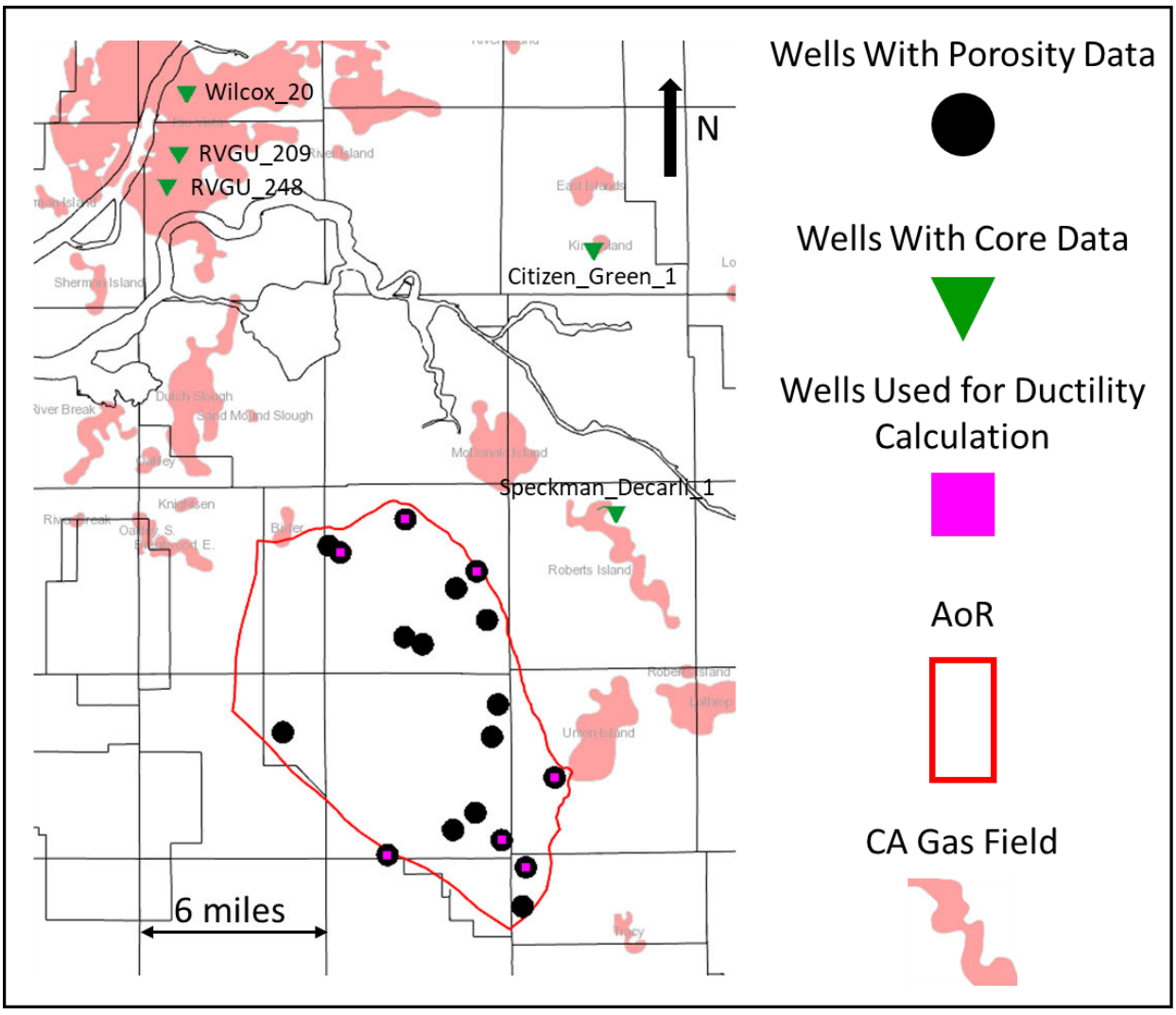

Figure 2.4-1. Map showing location of wells with mineralogy data relative to the AoR.

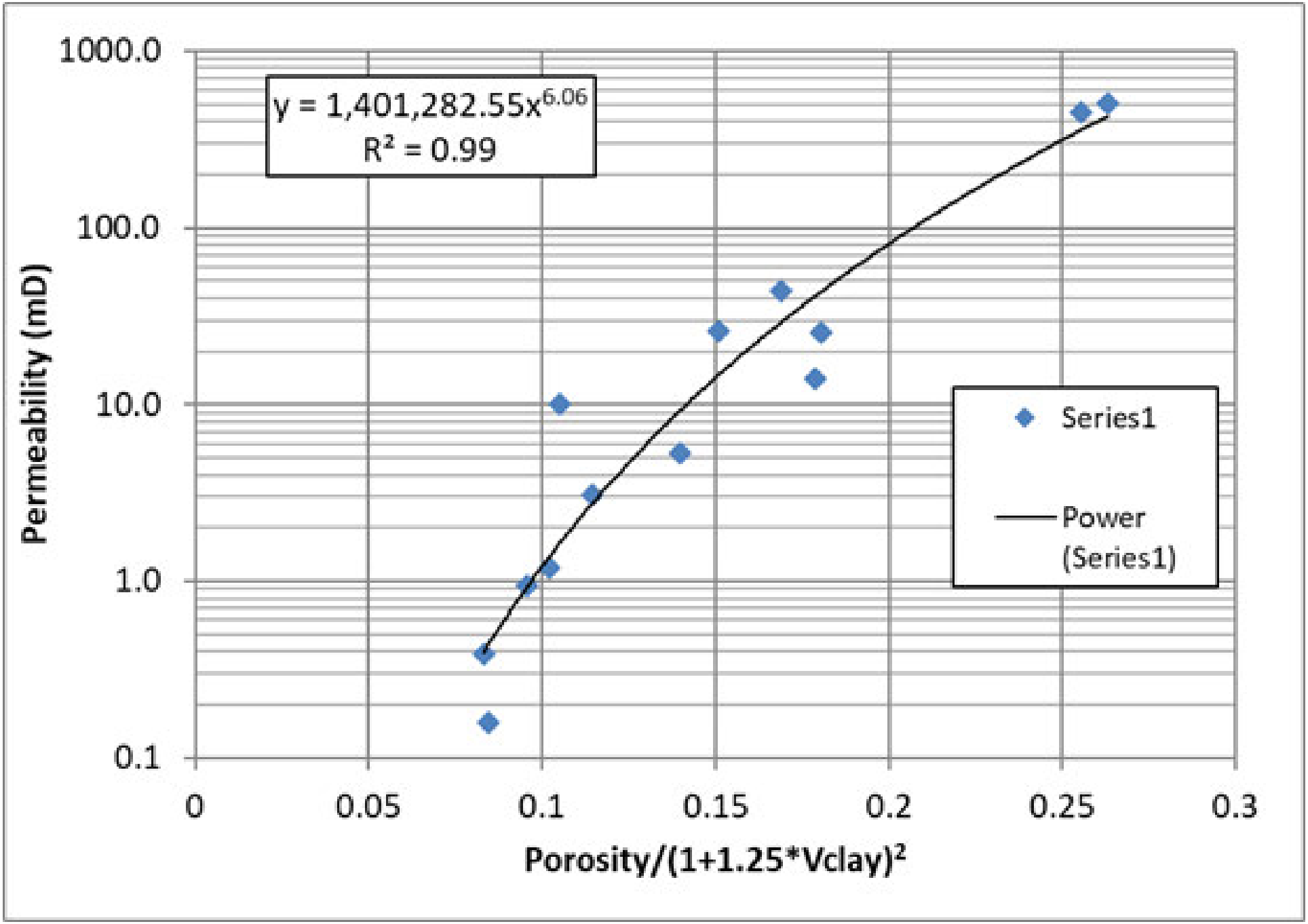

Figure 2.4-2. Permeability transform for Sacramento basin zones.

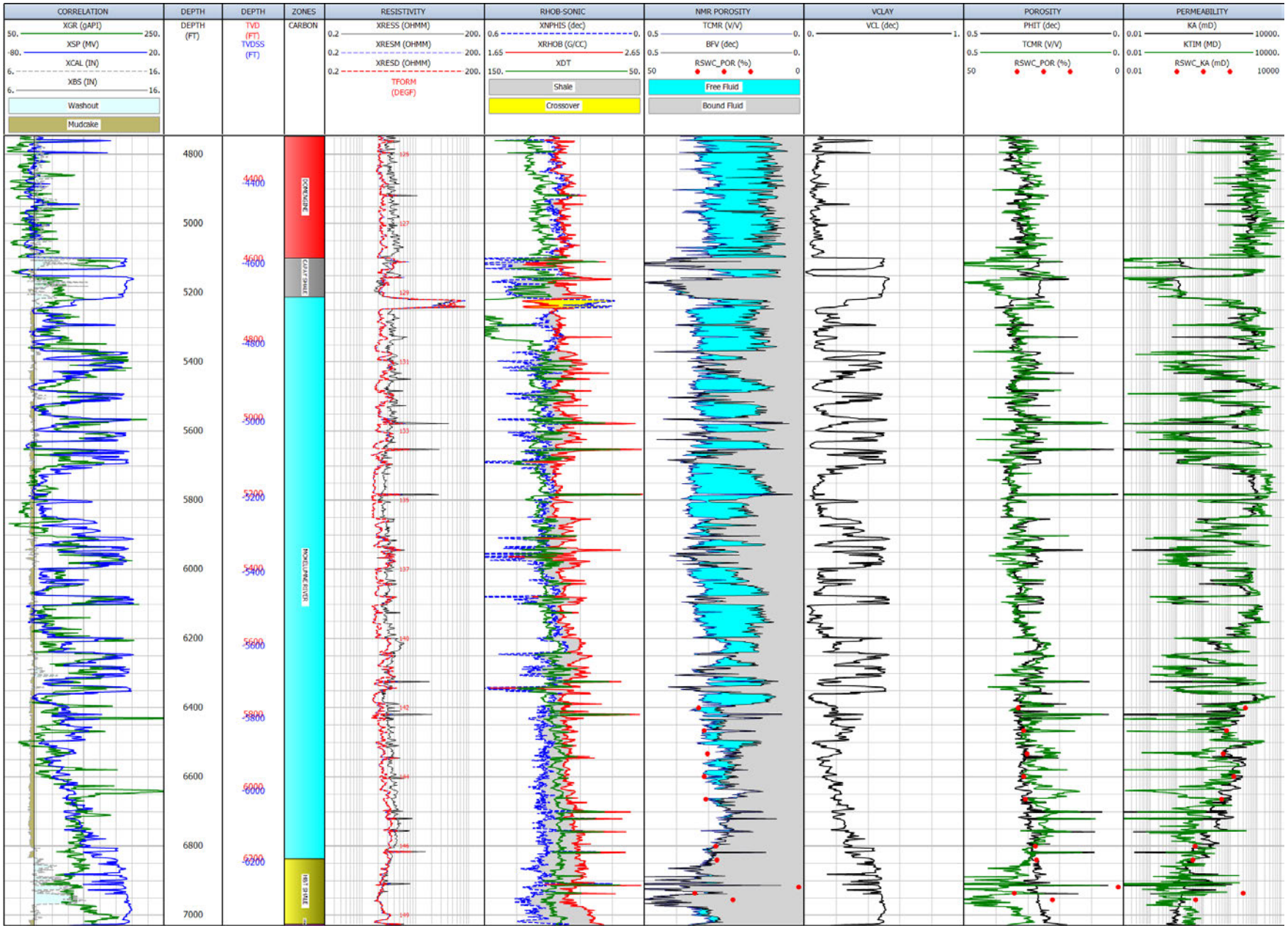

Figure 2.4-3. Example log from the Citizen_Green_1 well in King Island Gas Field. The last track shows a comparison of the permeability calculated from the transform (black) shown in **Figure 2.4-2** to permeability calculated from an NMR log (green) and rotary sidewall core permeability (red dots). Track 1: Correlation and caliper logs. Track 2: Measured depth. Track 3: Vertical depth and vertical subsea depth. Track 4: Zones. Track 5: Resistivity. Track 6: Compressional sonic, density, and neutron logs. Track 7: NMR total porosity and bound fluid. Track 8: Volume of clay. Track 9: Porosity calculated from density (black) and NMR total porosity (green). Track 10: Permeability calculated using permeability transform (black) and NMR Timur-Coates permeability (green).

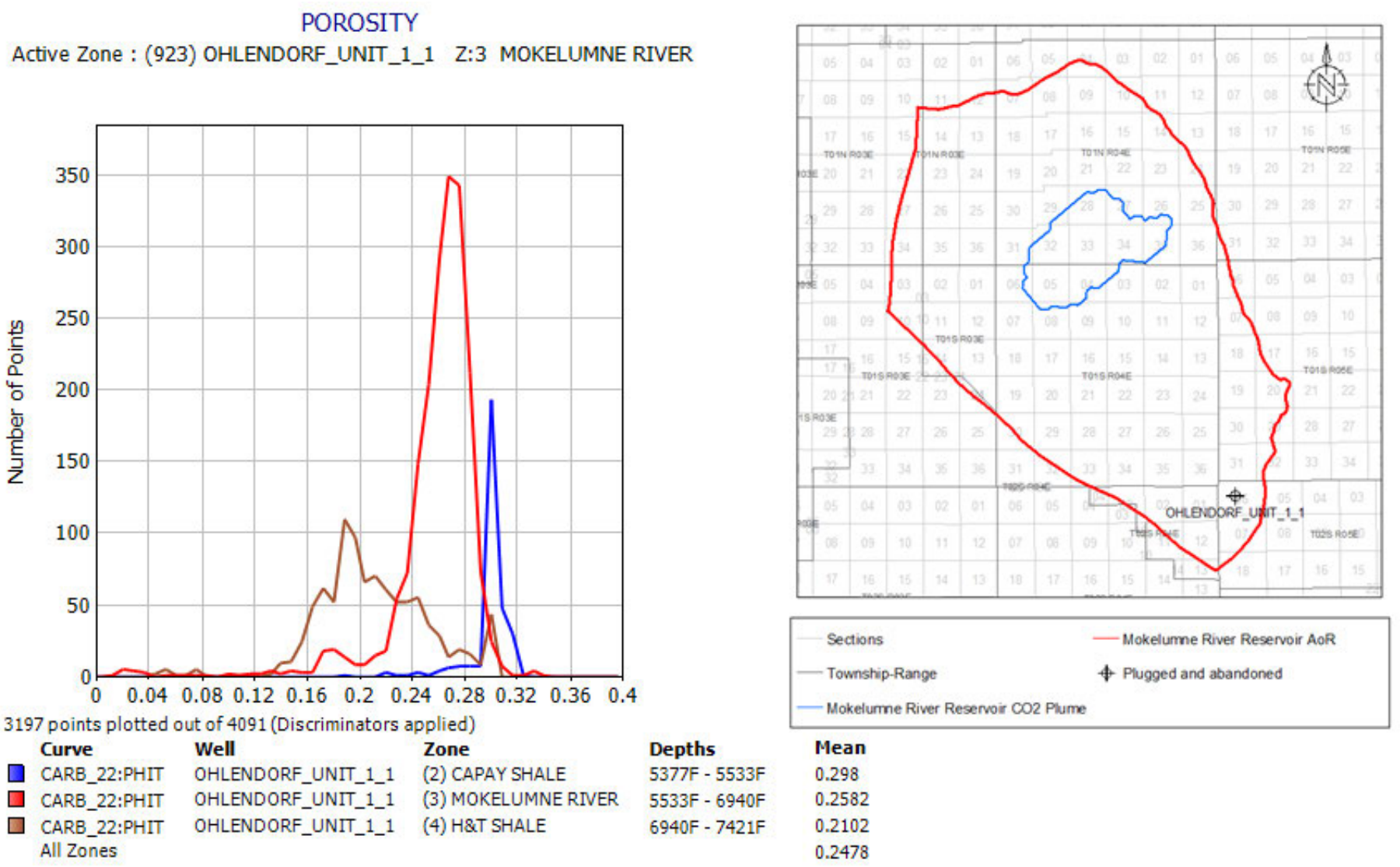

Figure 2.4-4. Porosity histogram for well Ohlendorf_Unit_1_1. In the histogram, blue represents the Capay Shale, red the Mokelumne River Formation, and brown the H&T Shale. For the two shale intervals, only data with VCL>0.25 is shown, and for the Mokelumne River only data with VCL<=0.25 is shown.

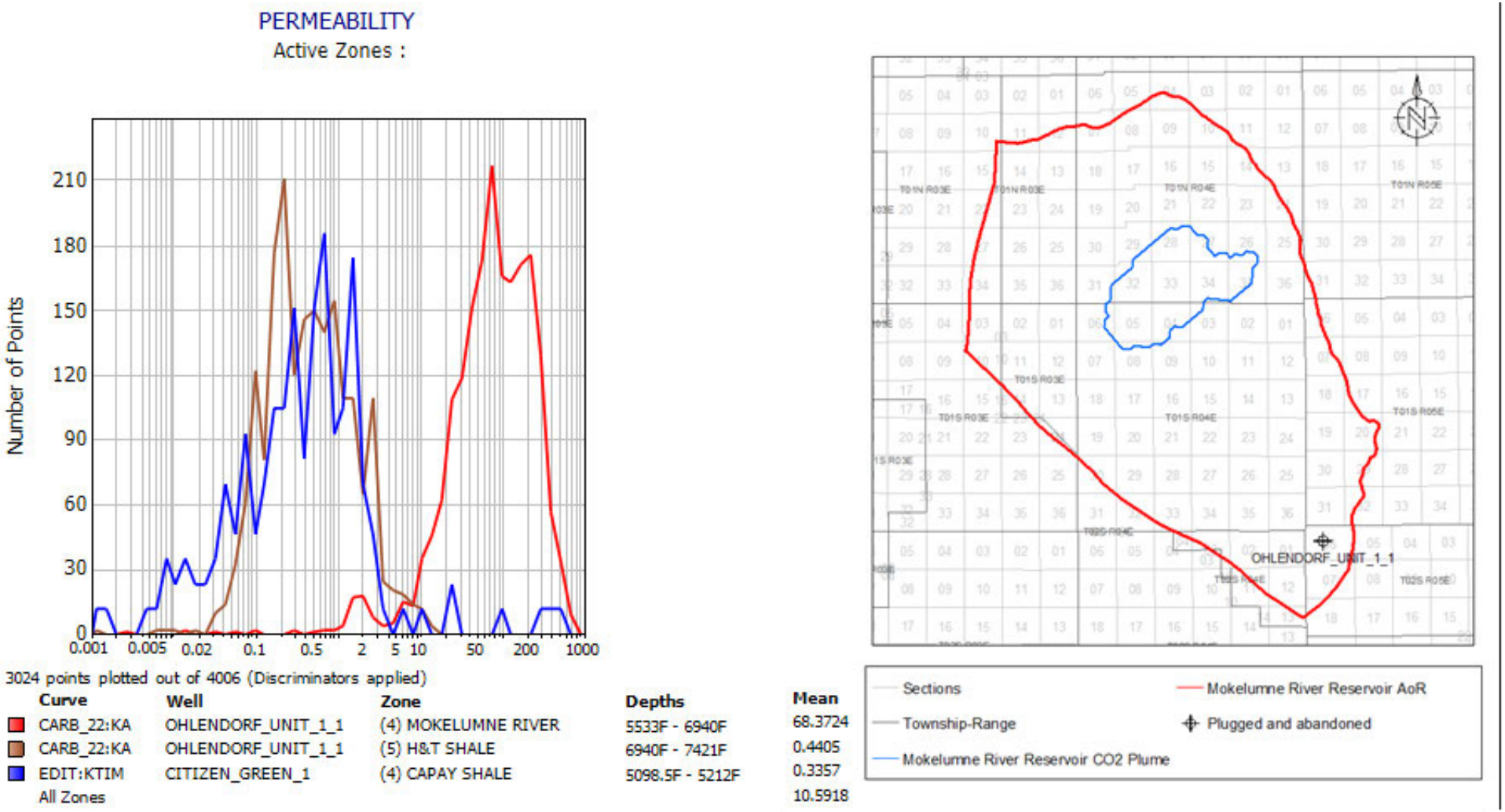

Figure 2.4-5. Permeability histogram for wells Ohlendorf_Unit_1_1 and Citizen_Green_1. In the histogram, blue represents the Capay Shale, red the Mokelumne River Formation, and brown the H&T Shale. For the two shale intervals, only data with VCL>0.25 is shown, and for the Mokelumne River Formation only data with VCL<=0.25 is shown.

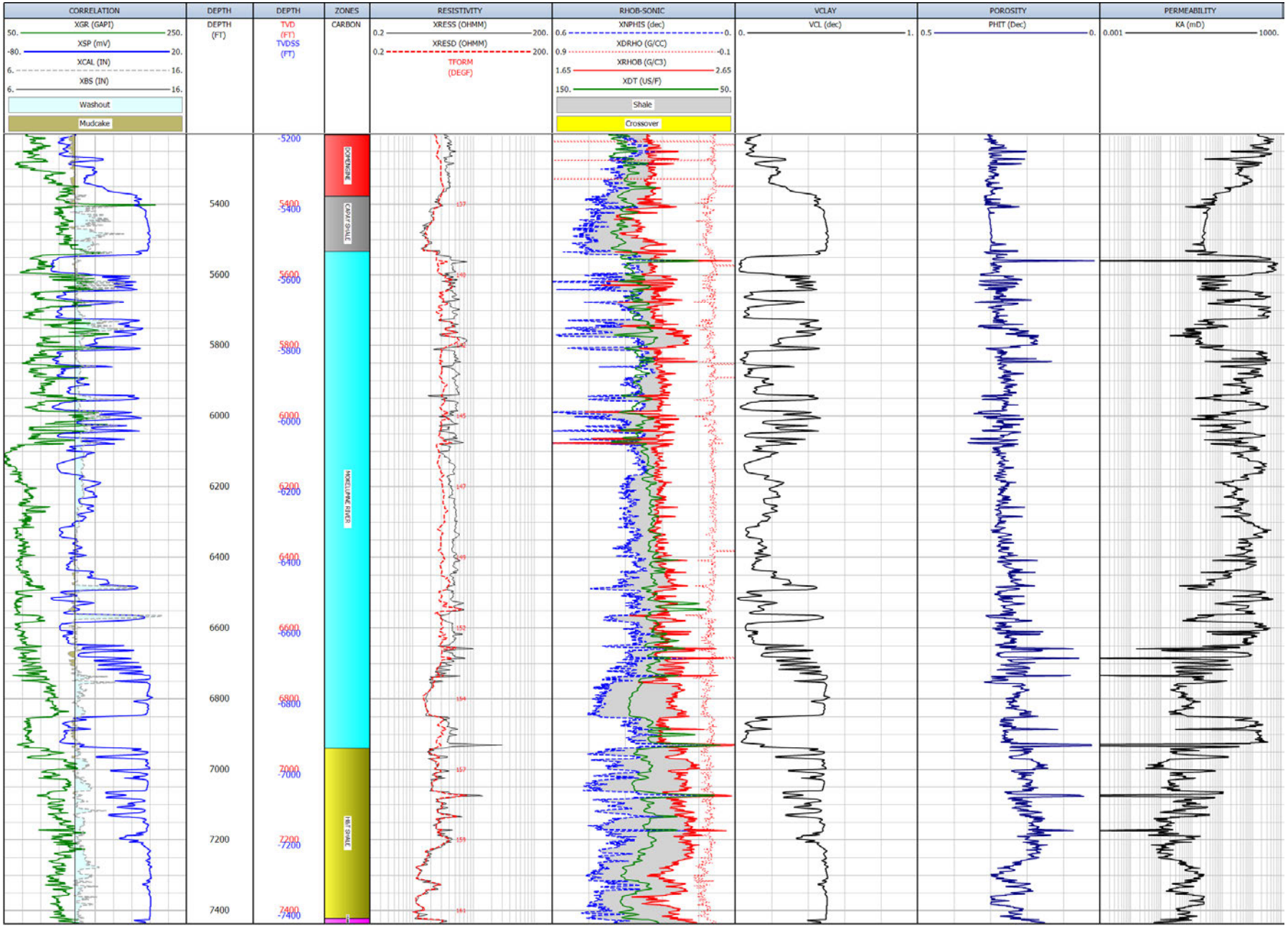

Figure 2.4-6. Log plot for well Ohlendorf_Unit_1_1, showing the log curves used as inputs into calculations of clay volume, porosity and permeability, and their outputs. Track 1: Correlation and caliper logs. Track 2: Measured depth. Track 3: Vertical depth and vertical subsea depth. Track 4: Zones. Track 5: Resistivity. Track 6: Compressional sonic, neutron, and density logs. Track 7: Volume of clay. Track 8: Porosity calculated from log curves. Track 9: Permeability calculated using transform. See **Figure 2.4-4** for well location.

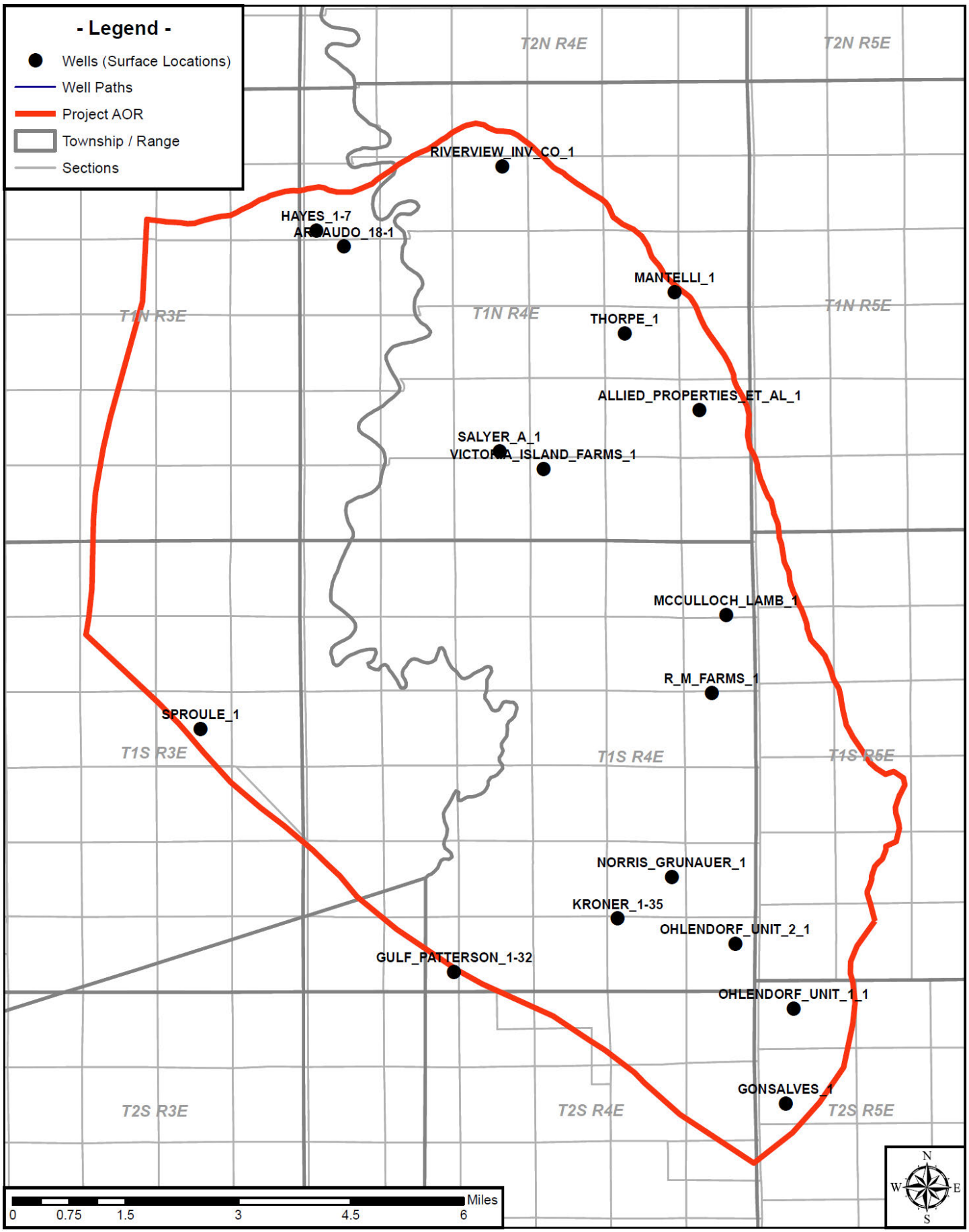

Figure 2.4-7. Map of wells with porosity and permeability data.

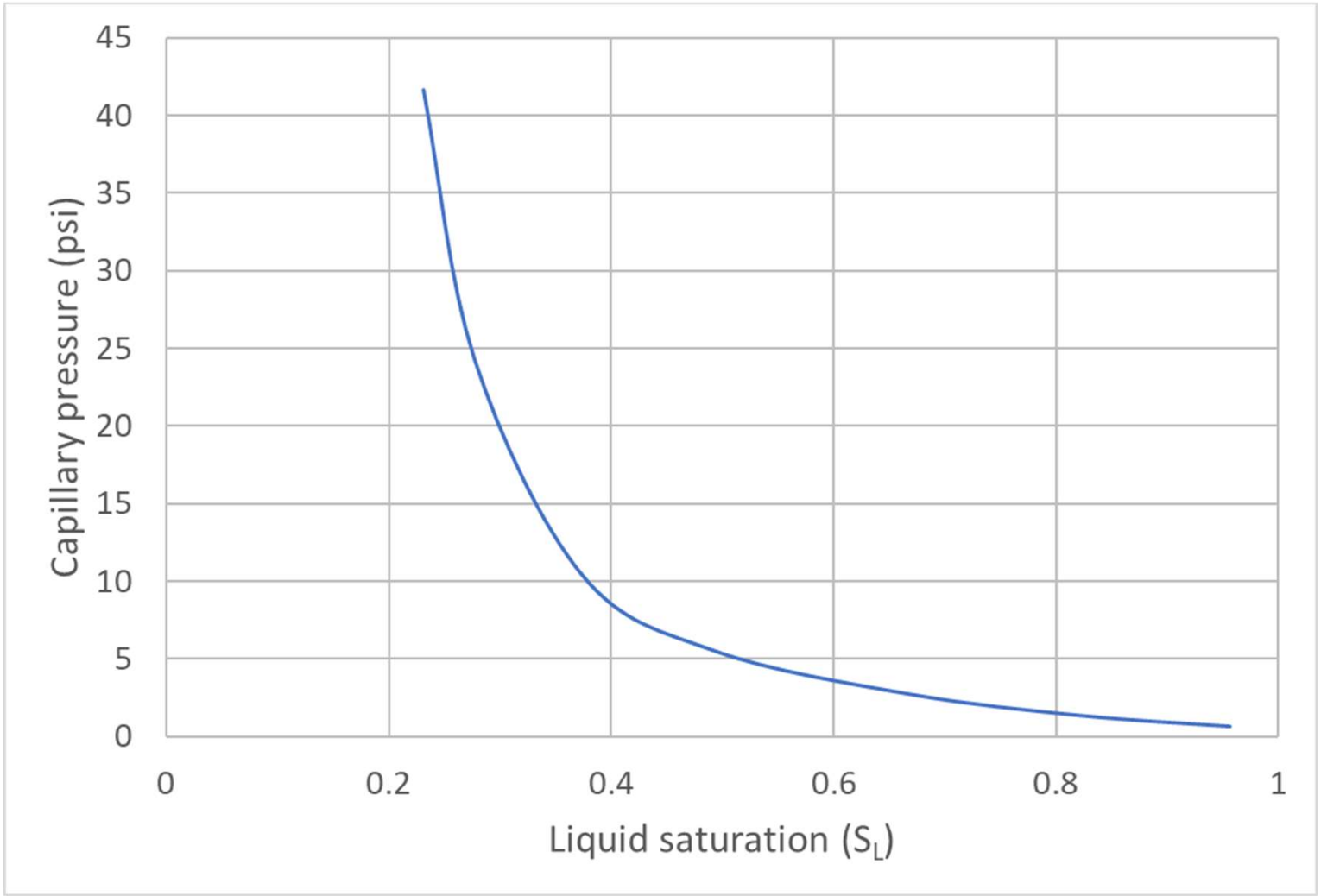

Figure 2.4-8: Injection zone capillary pressure used for Computational Modeling

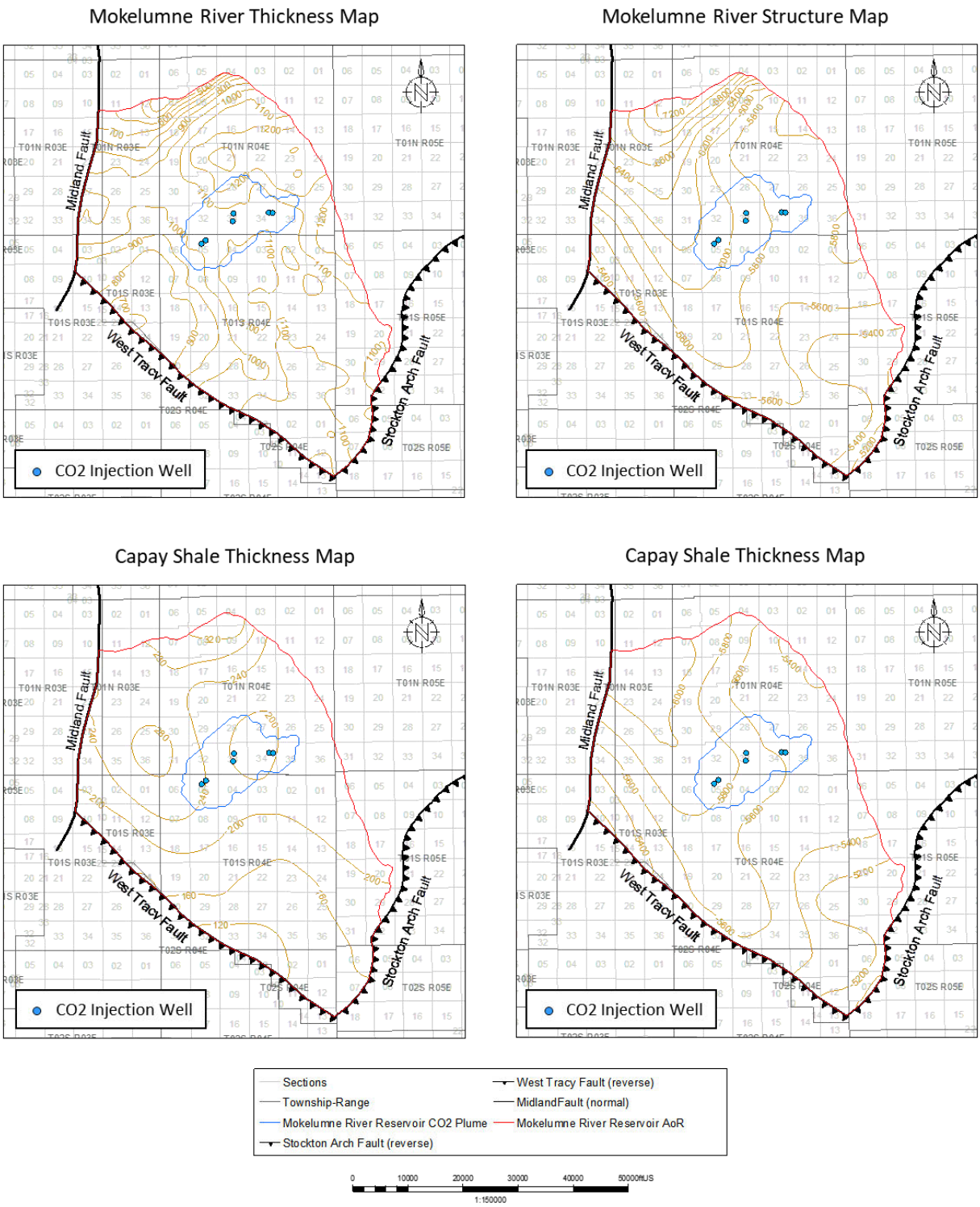

Figure 2.4-9. Thickness and structure maps for the Mokelumne River and Capay Shale Formations within the AoR.

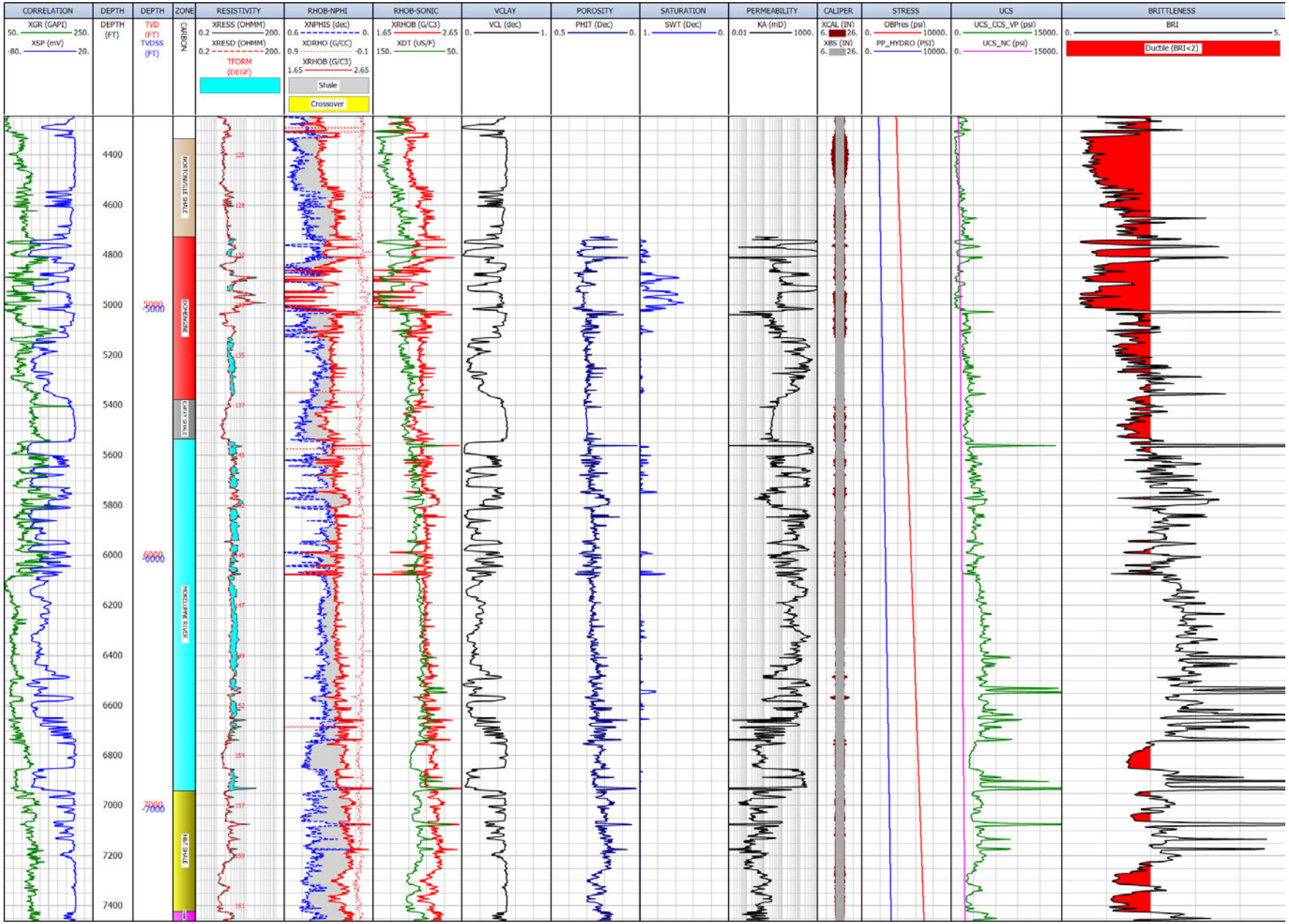

Figure 2.5-1. Unconfined compressive strength and ductility calculations for well Ohlendorf_Unit_1_1. The Capay Shale ductility is less than two, as is the shallower Nortonville Shale. Track 1: Correlation logs. Track 2: Measured depth. Track 3: Vertical depth and vertical subsea depth. Track 4: Zones. Track 5: Resistivity. Track 6: Density and neutron logs. Track 7: Density and compressional sonic logs. Track 8: Volume of clay. Track 9: Porosity calculated from sonic and density. Track 10: Water saturation. Track 11: Permeability. Track 12: Caliper. Track 13: Overburden pressure and hydrostatic pore pressure. Track 14: UCS and UCS_NC. Track 15: Brittleness. See **Figure 2.4-4** for well location.

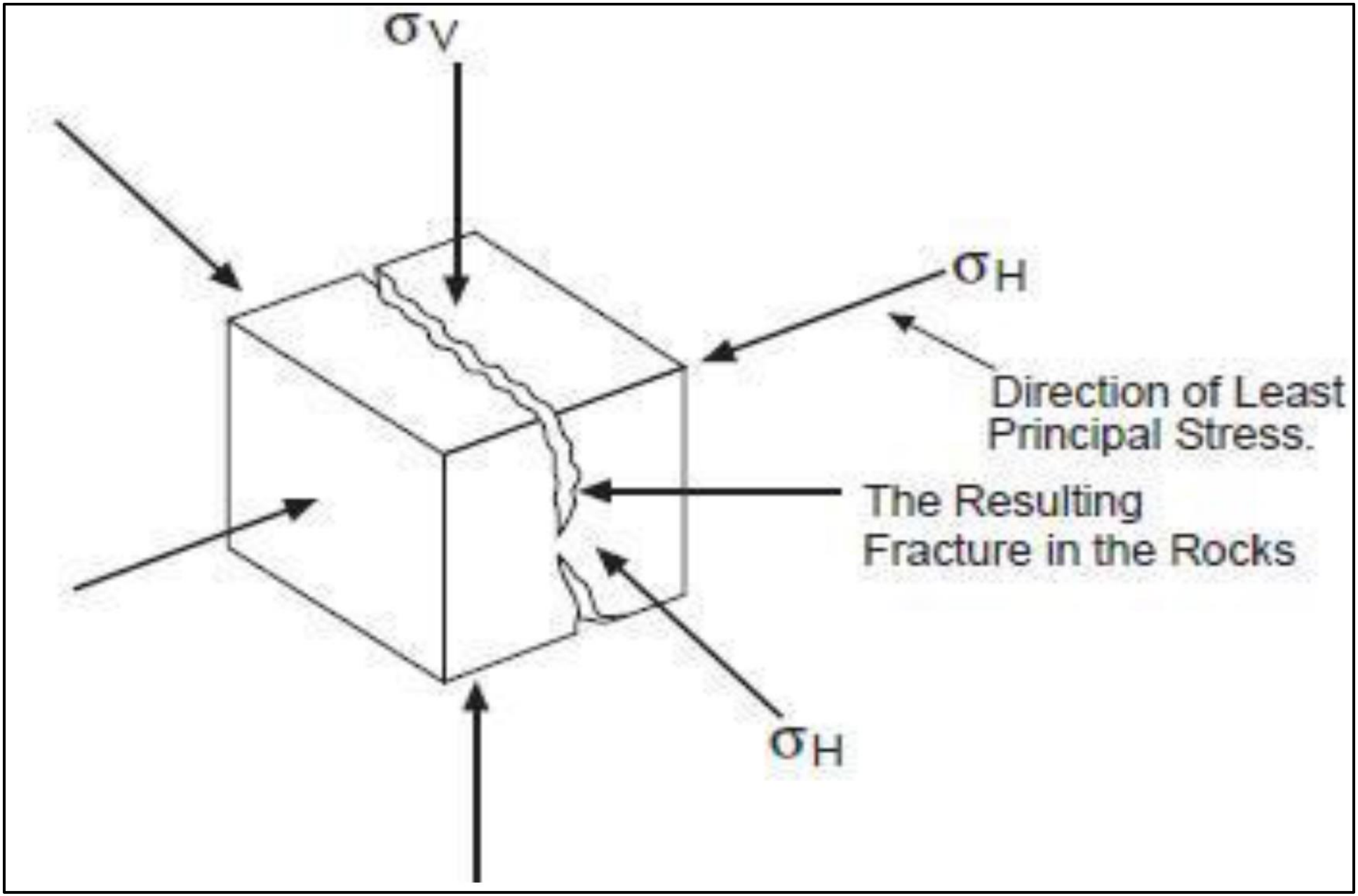

Figure 2.5-2: Stress diagram showing the three principal stresses and the fracturing that will occur perpendicular to the minimum principal stress.

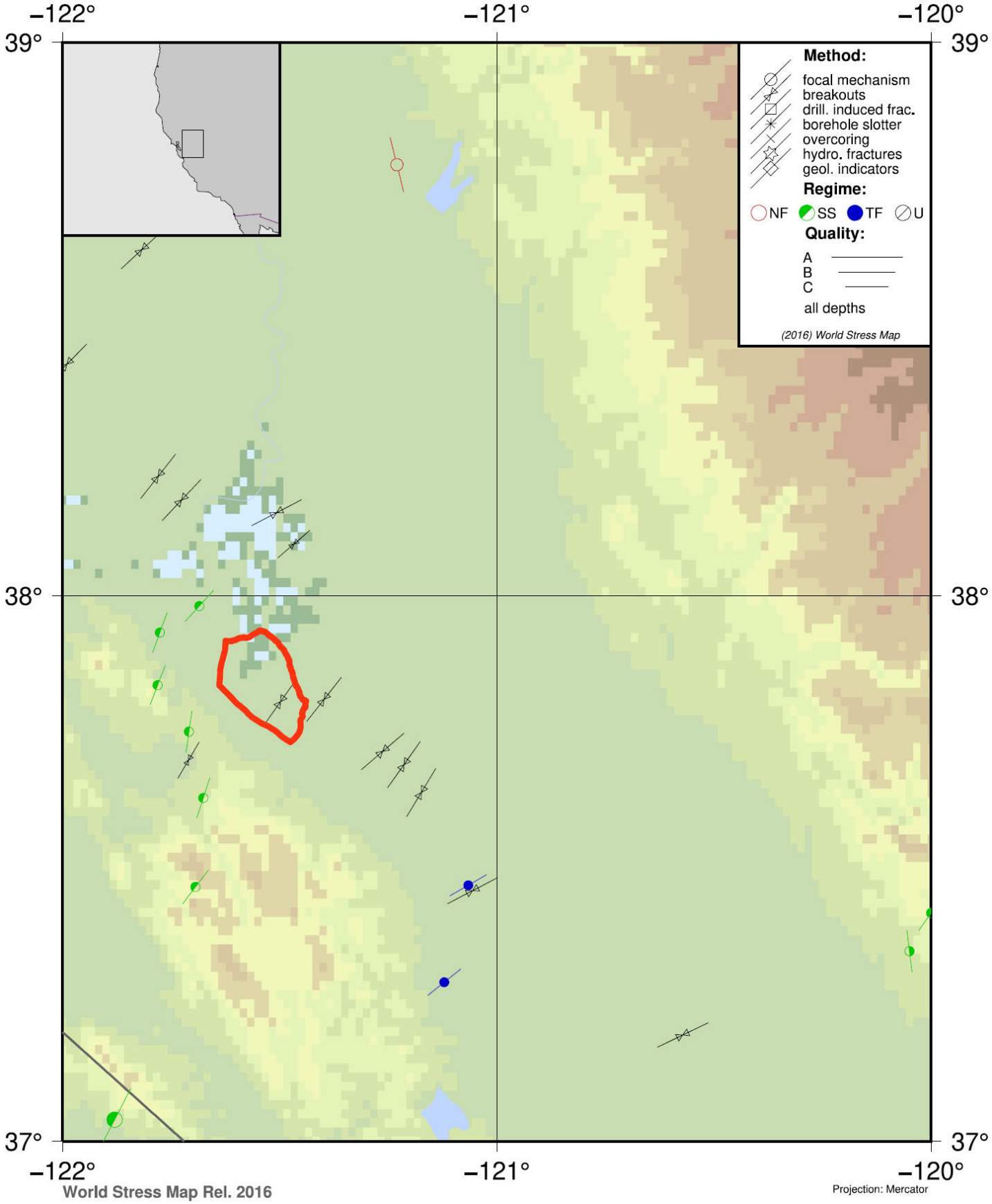

Figure 2.5-3: World Stress Map output showing S_{Hmax} azimuth indicators and earthquake faulting styles in the Sacramento Basin (Heidbach et al., 2016). In red is the outline of the Mokelumne River Reservoir AoR. The background coloring represents topography.

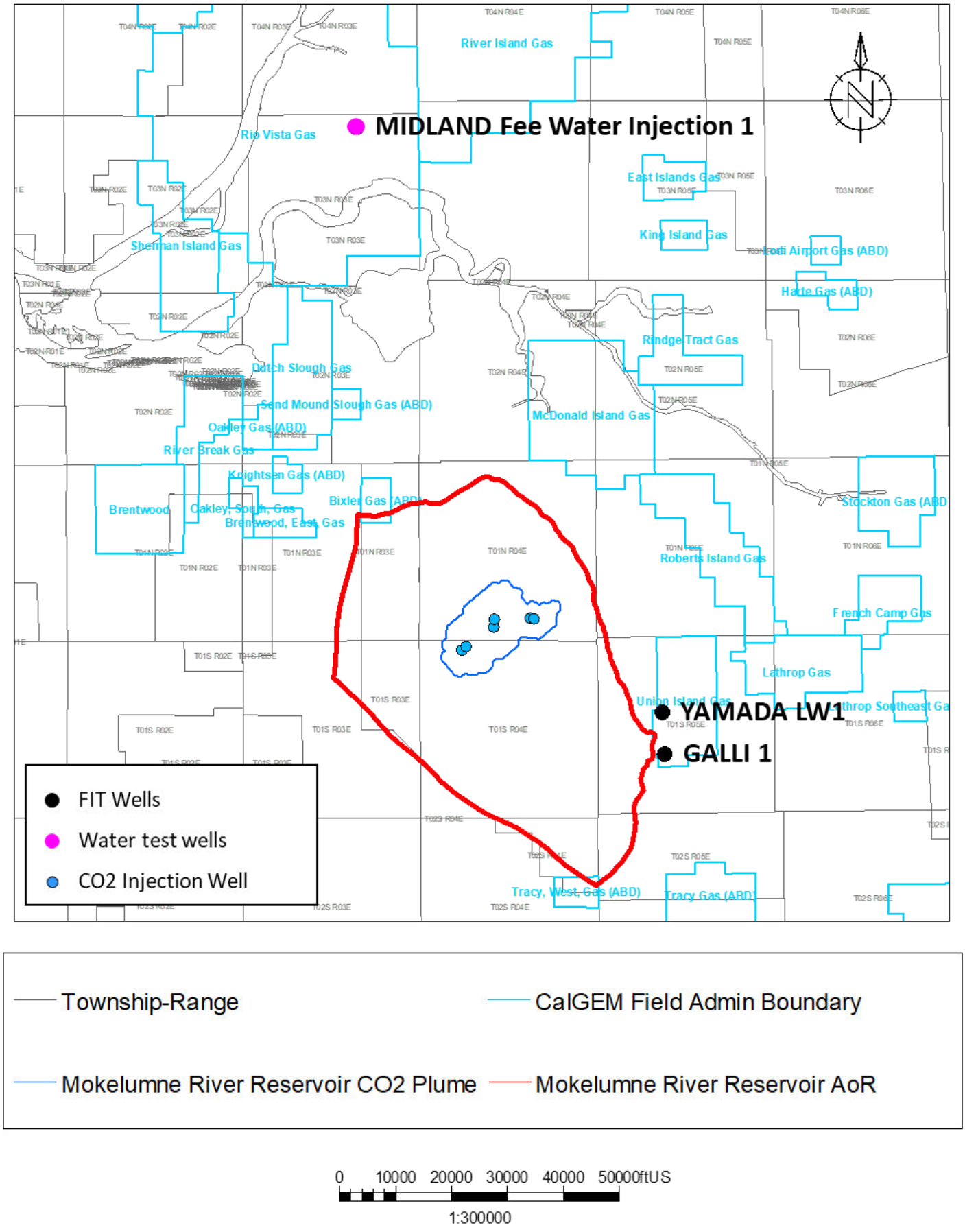

Figure 2.5-4: Map showing the location of wells with formation integrity tests (FIT).

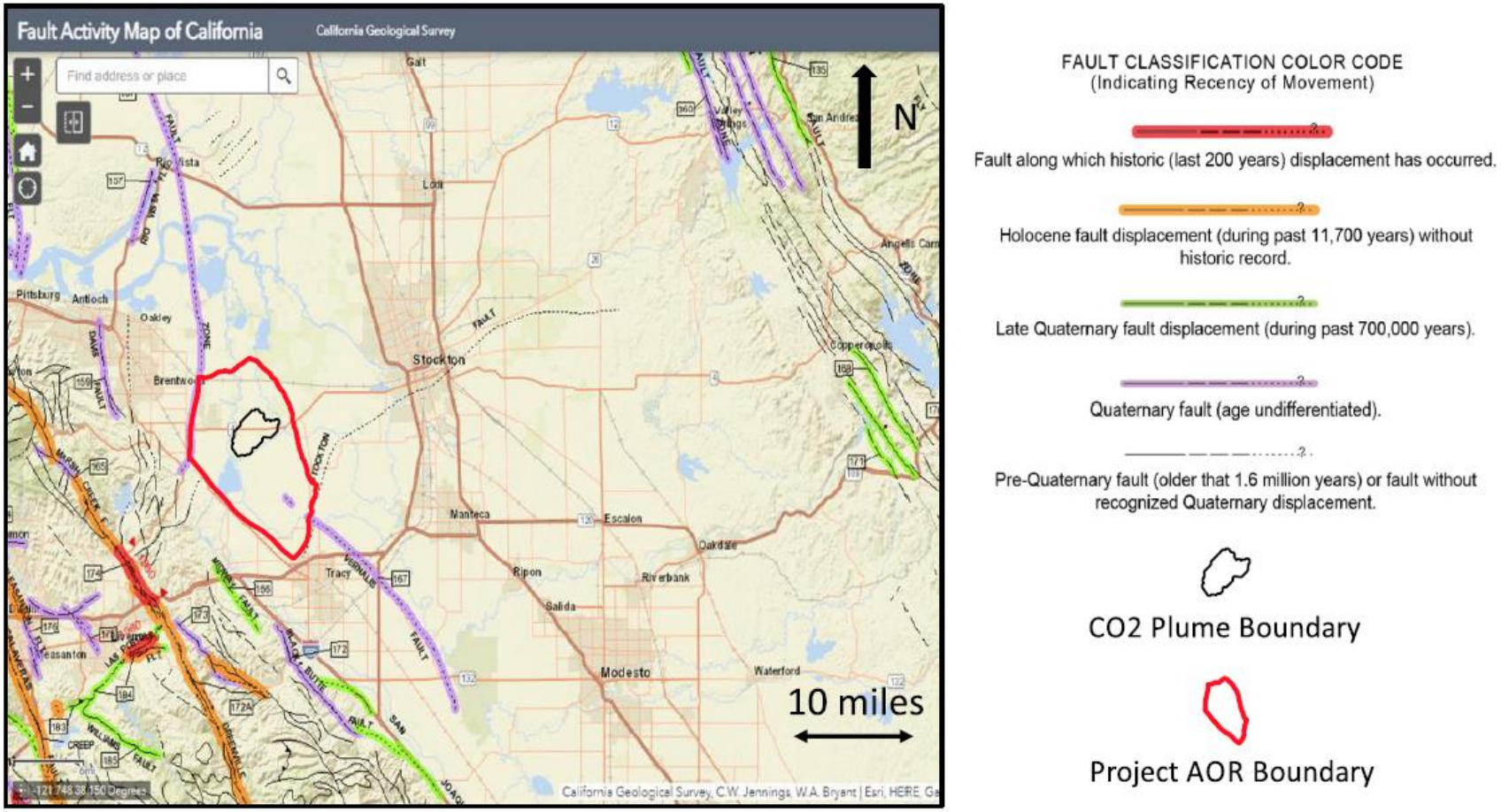

Figure 2.6-1. Fault Activity Map from the California Geologic Survey. Fault traces shown agree with the interpretation of CRC/CTV. The Stockton Arch Fault is considered Pre-Quaternary associated with Post-Eocene/Pre-Miocene movement. The Midland Fault was active in the late Cretaceous-Eocene time, however the southern end of the Midland fault has been interpreted as reactivated as a reverse fault in the late Cenozoic transpressional tectonic setting.

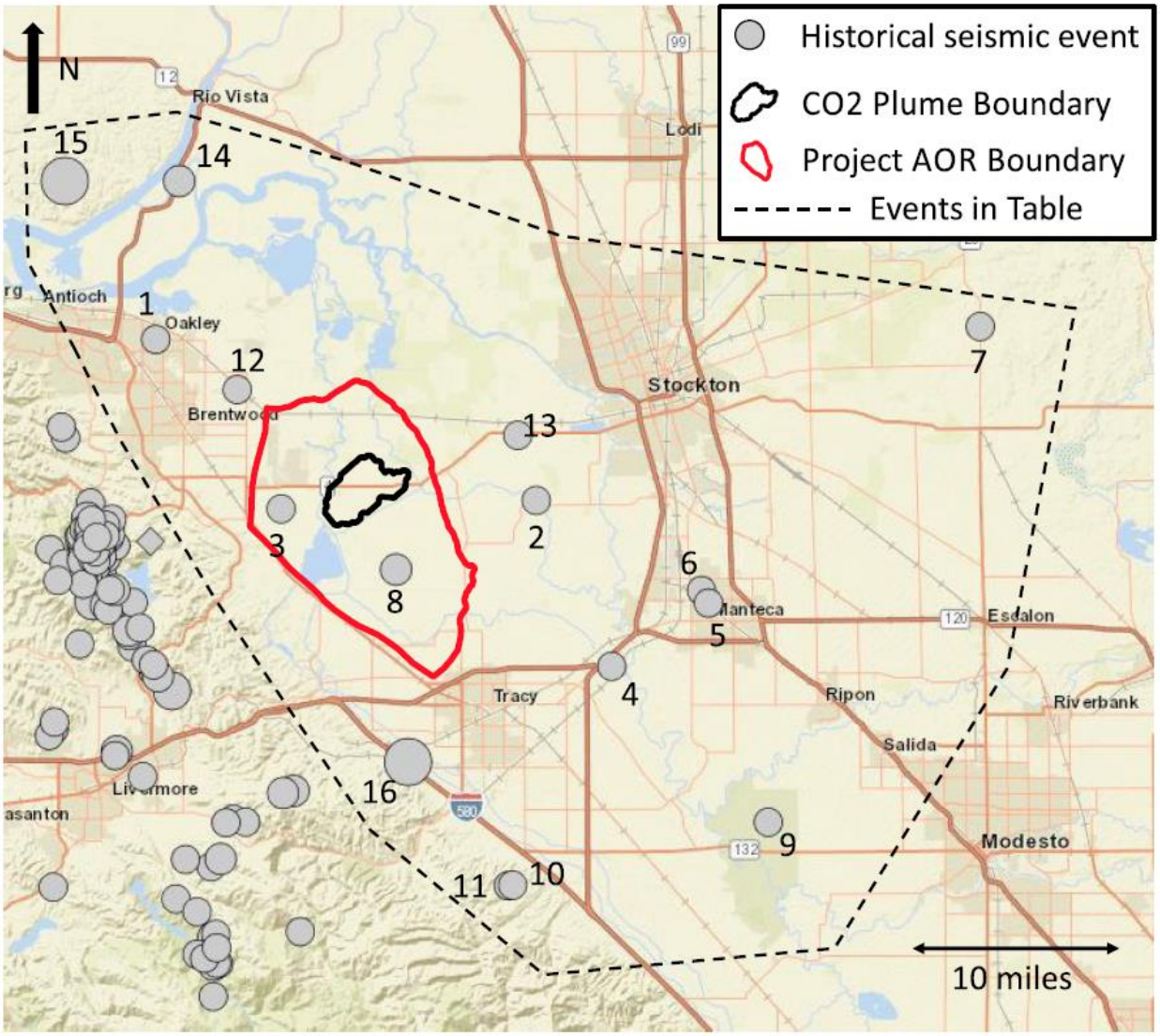

Figure 2.6-2. Historical earthquakes from the USGS catalog tool for the greater area. Data from these events are compiled in **Table 2.6-1** in chronological order associated with events 1 through 16 on the map. Events are sized by magnitude and those to the west are removed due to their association with a different fault trend.

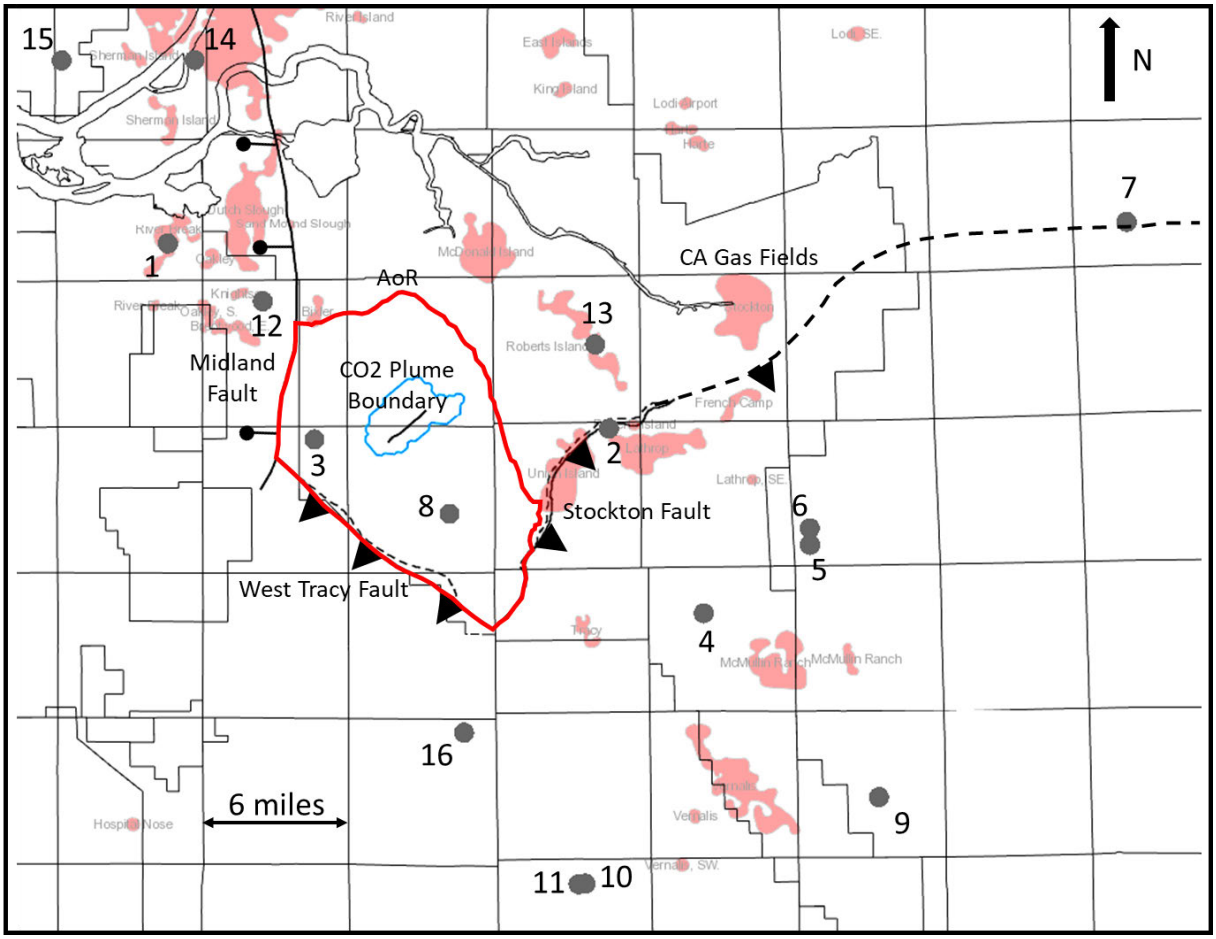

Figure 2.6-3. Summary map of event locations from the USGS catalog relative to the mapped faults in the AoR of CTV III. California Gas Fields are also shown for reference.

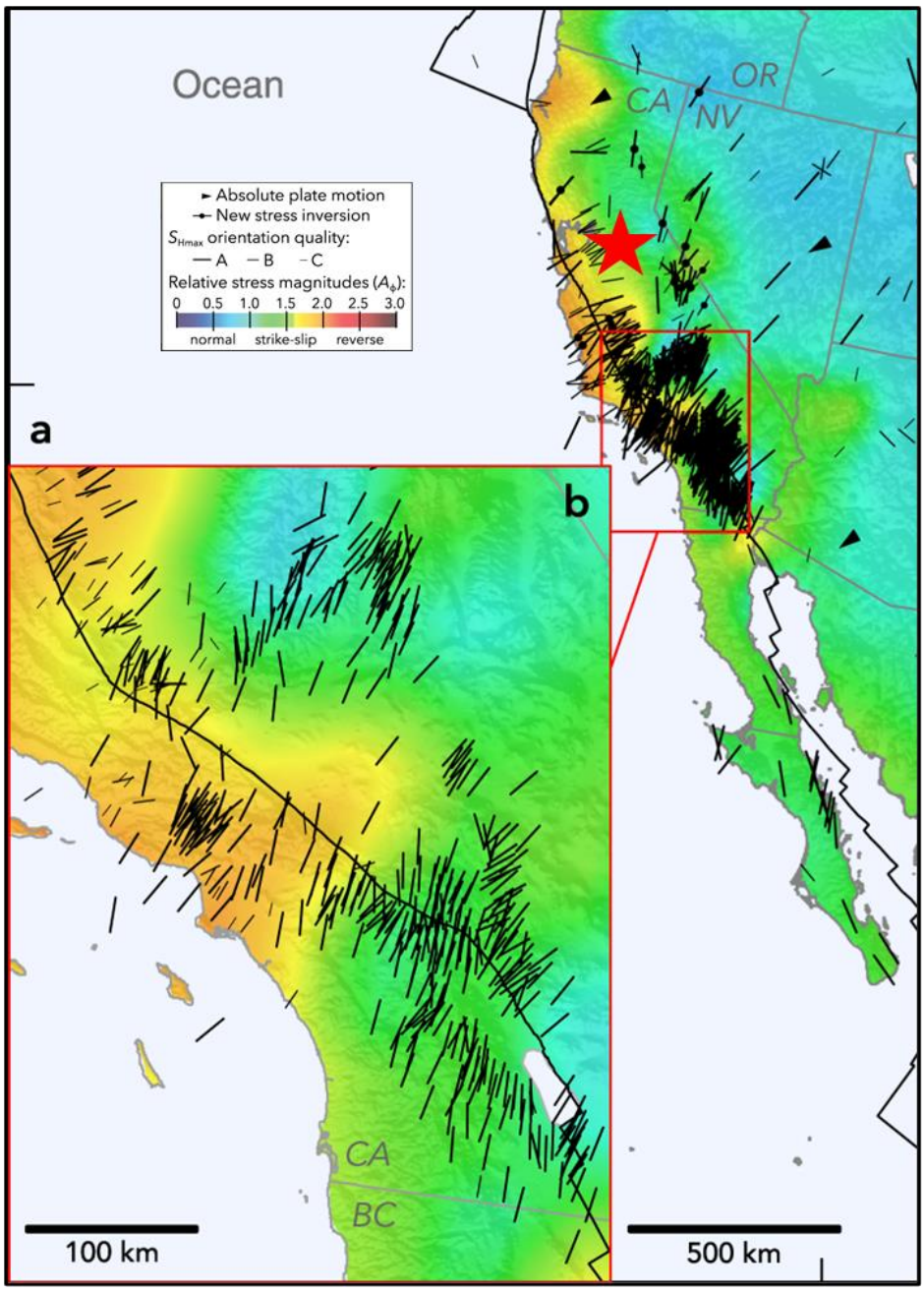

Figure 2.6-4. Image modified from Lund-Snee and Zoback (2020) showing relative stress magnitudes across California. Red star indicates the CTV III site area.

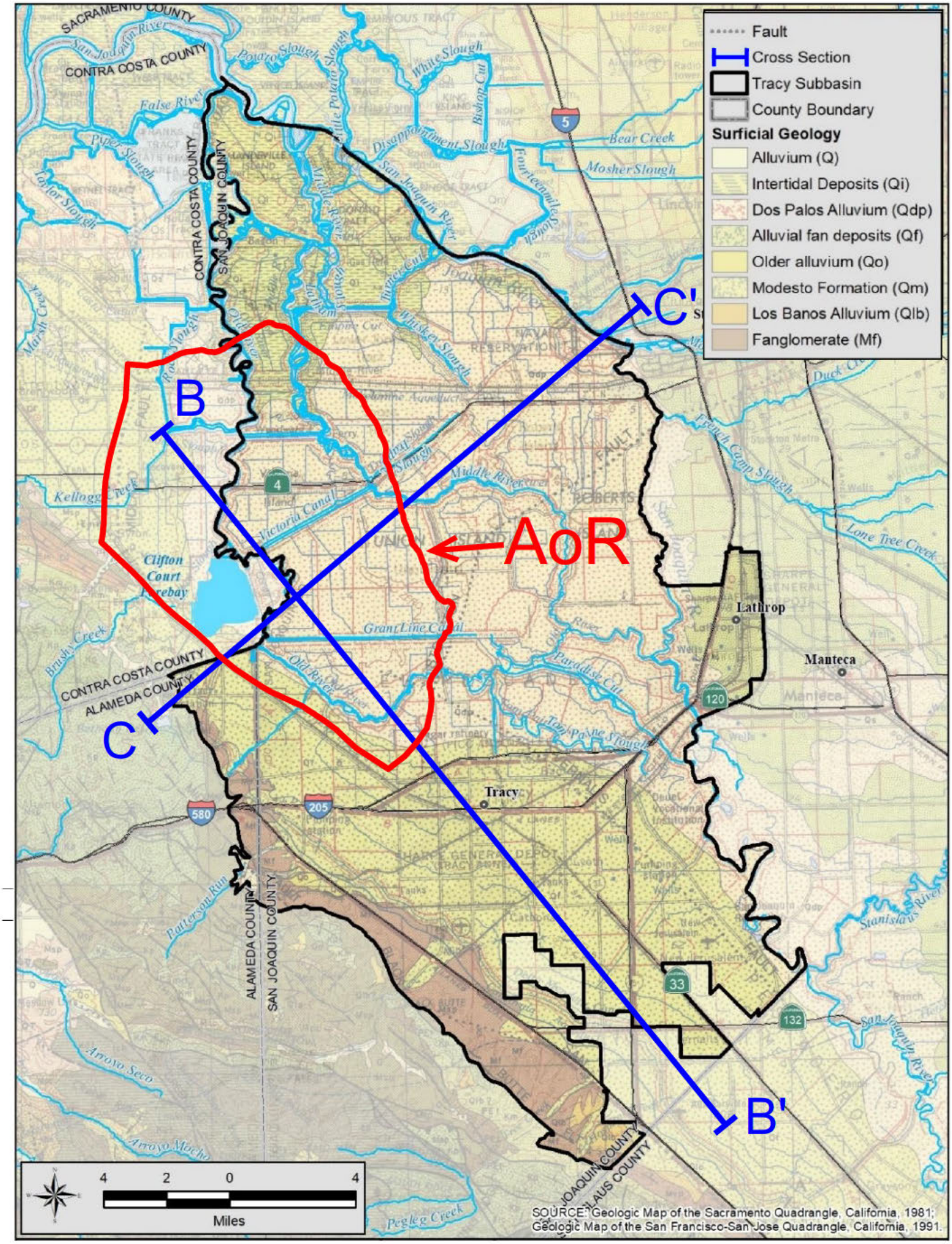

Modified from: GEI Consultants, Inc.; Tracy Subbasin Groundwater Sustainability Plan. November 1, 2021.

Figure 2.7-1 Tracy Subbasin, Surface Geology, and Cross Section Index Map

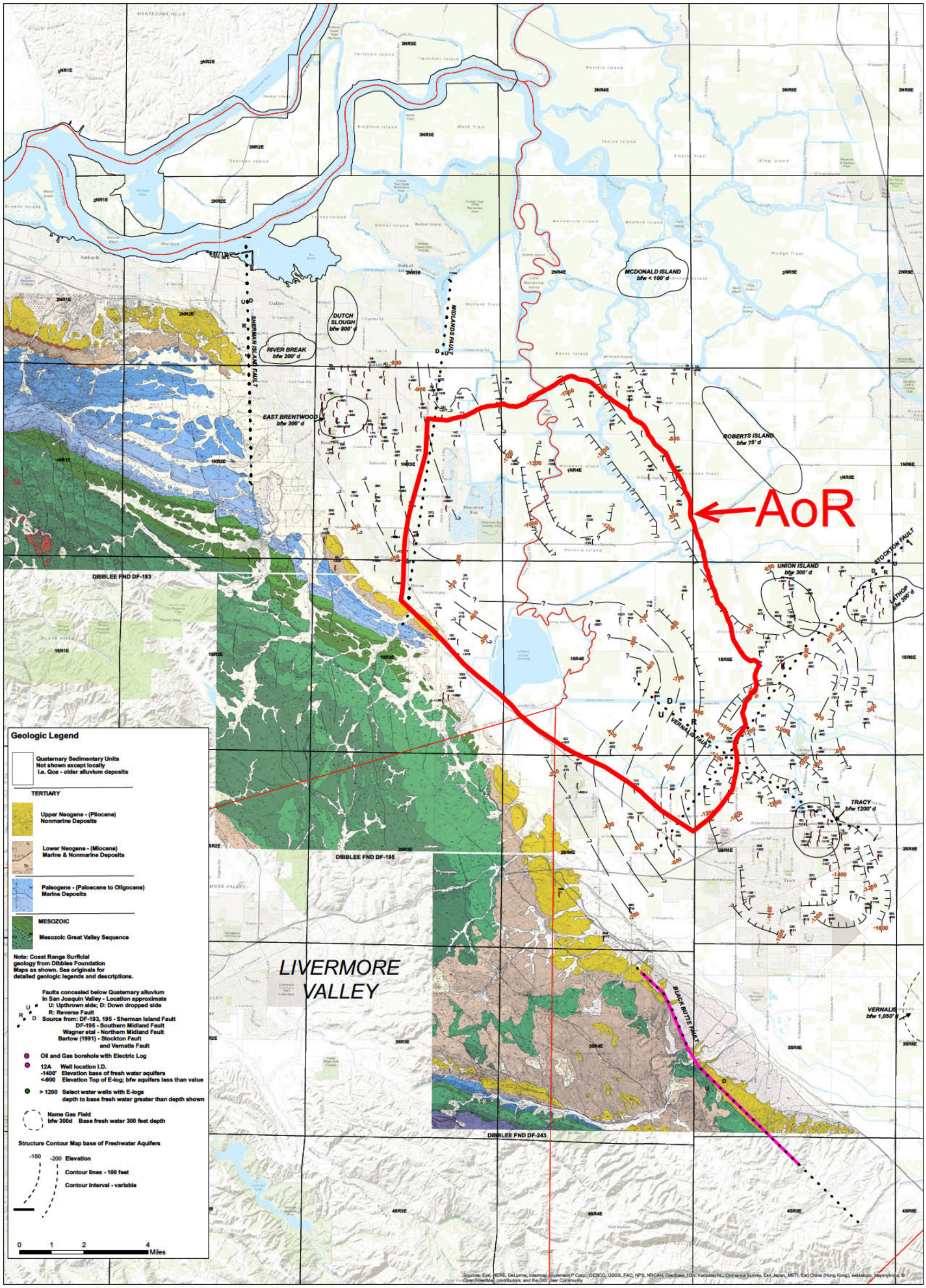

Modified from: Luhdorff & Scalmanini, Consulting Engineers, Inc., An Evaluation of Geologic Conditions, East Contra Costa County, March 29, 2016

Figure 2.7-2 Geologic Map and Base of Fresh Water

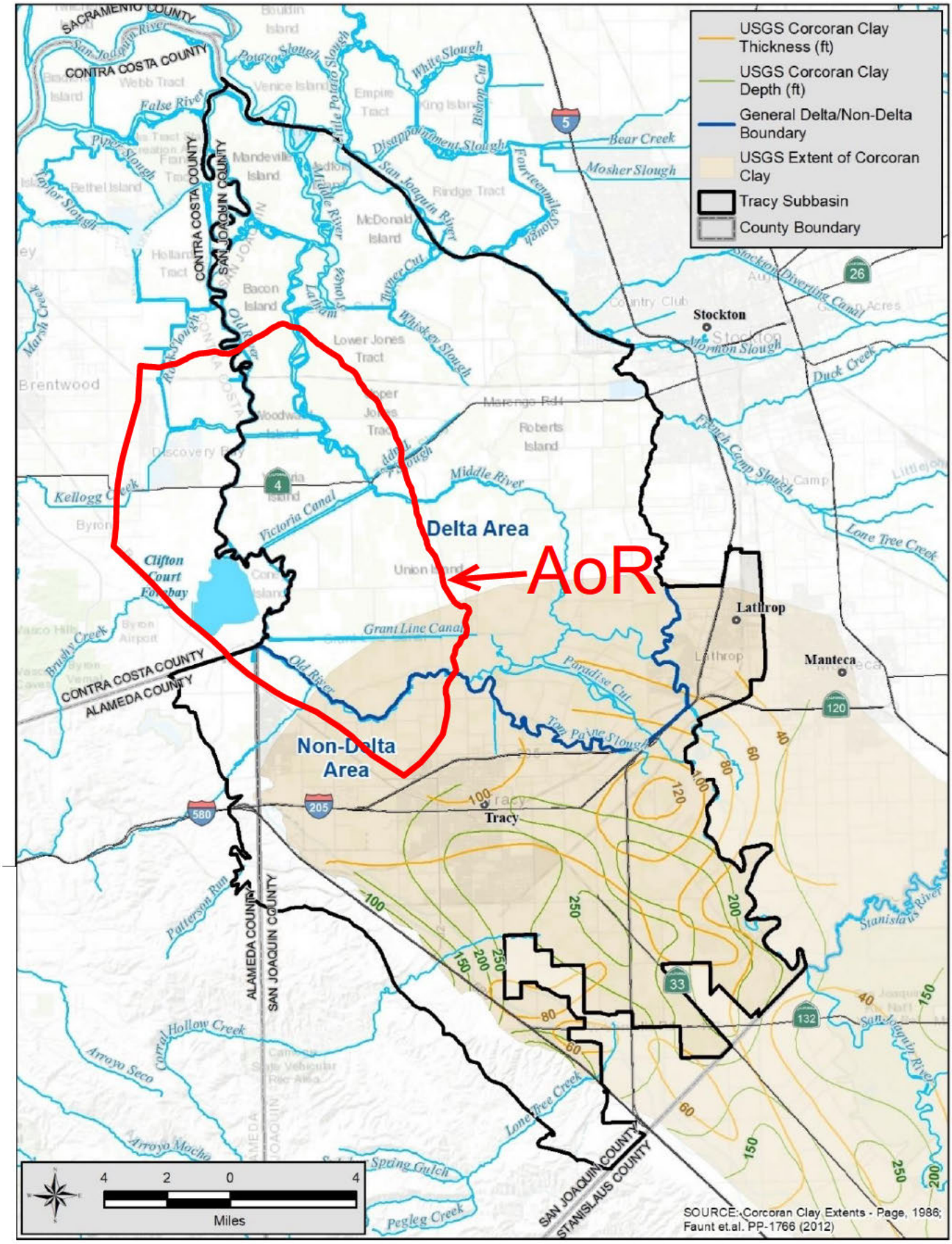

Modified from: GEI Consultants, Inc.; Tracy Subbasin Groundwater Sustainability Plan. November 1, 2021.

Figure 2.7-3 Estimated Corcoran Clay Thickness and Extent

Legend

Well used for geology, hydrogeology interpretation, and water quality and levels where available

Wells used for water quality and water level data

Geologic Contact Line (dashed where inferred)

Gravel
Sands
Silt/Clay
Corcoran Clay

Qdp = Dos Palos Alluvium
Qf = Alluvial Fan Deposits
Qm = Modesto Formation
QTt = Tulare Fm
SJ = San Joaquin Clays

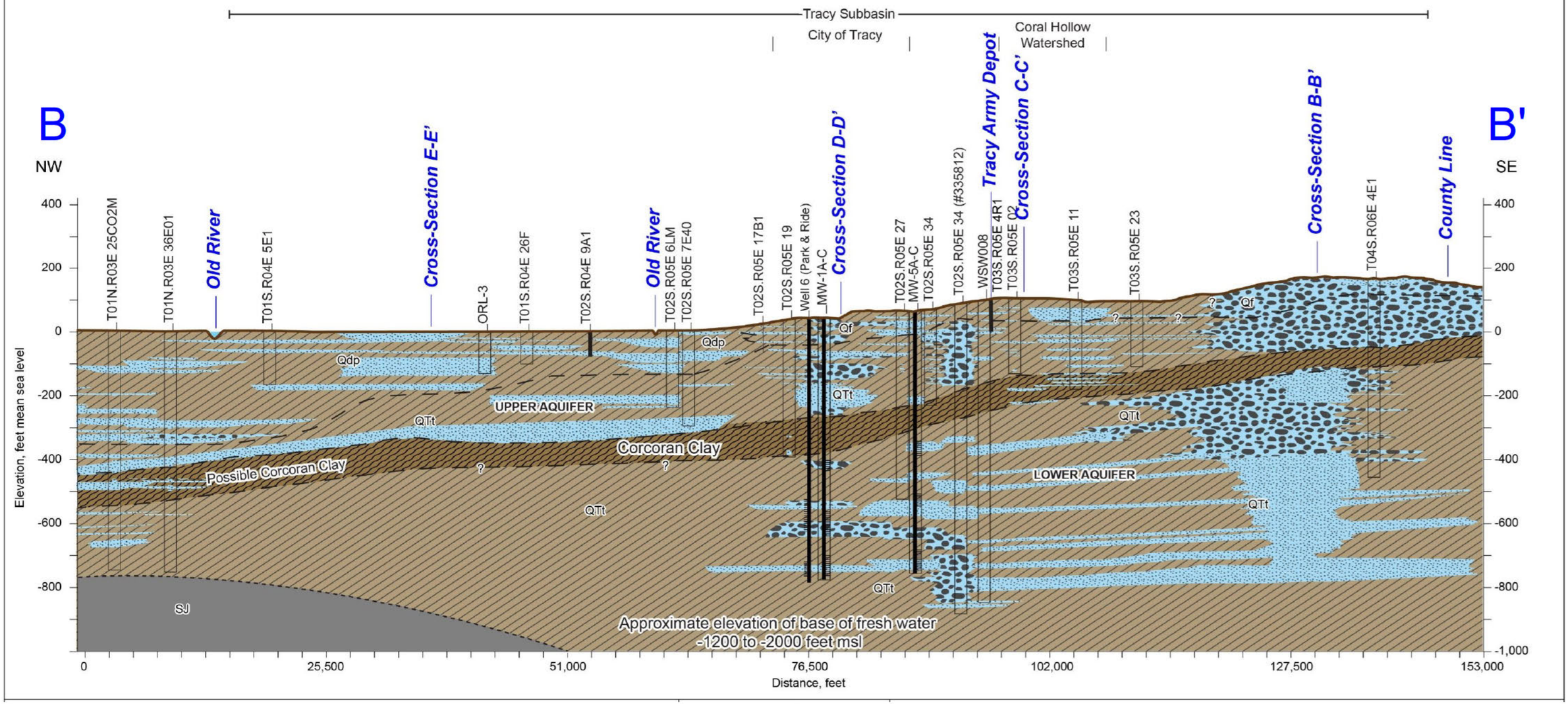

Modified from: GEI Consultants, Inc.; Tracy Subbasin Groundwater Sustainability Plan. November 1, 2021.

Figure 2.7-4 Geologic Cross Section B-B'

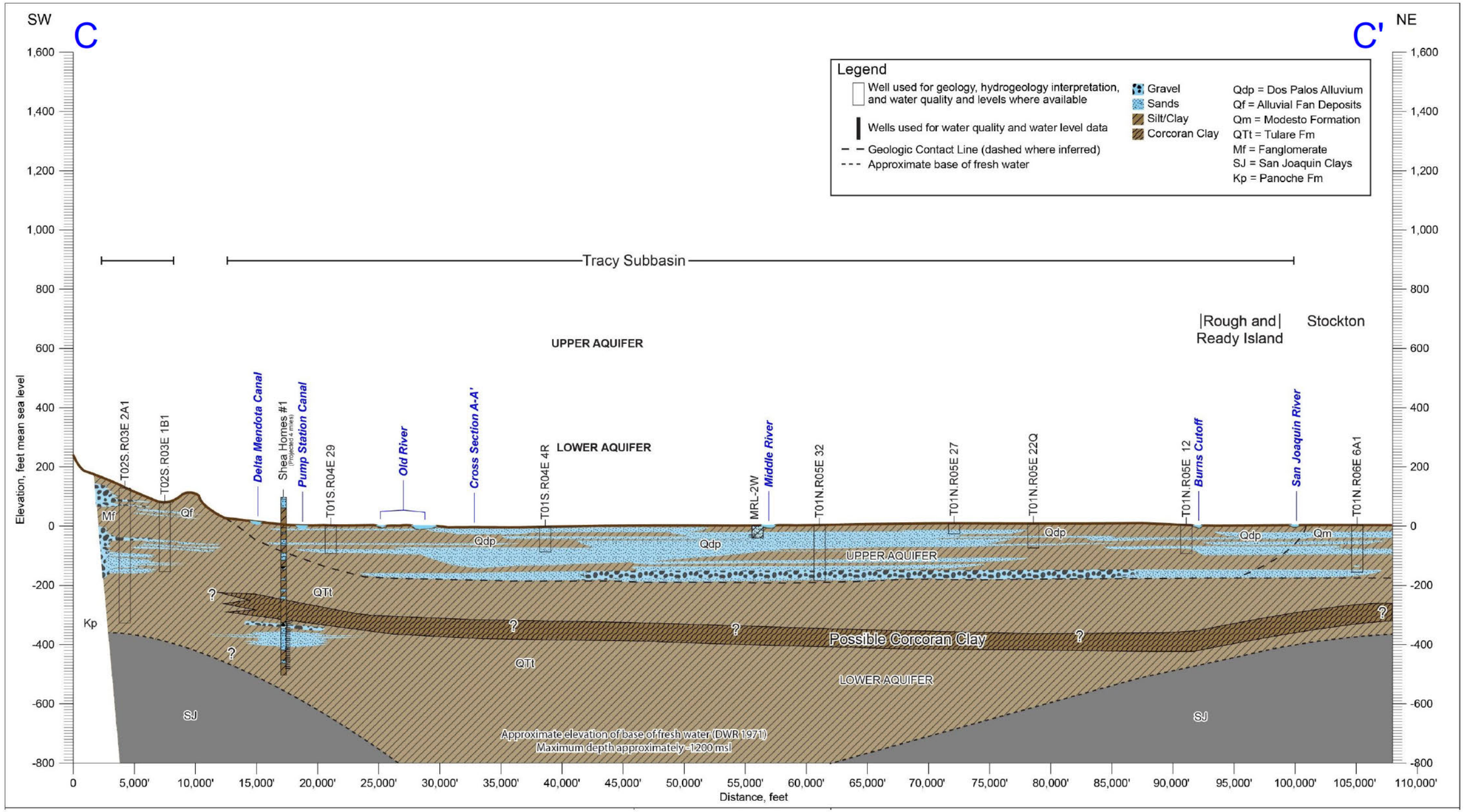

Modified from: GEI Consultants, Inc.; Tracy Subbasin Groundwater Sustainability Plan. November 1, 2021.

Figure 2.7-5 Geologic Cross Section C- C'

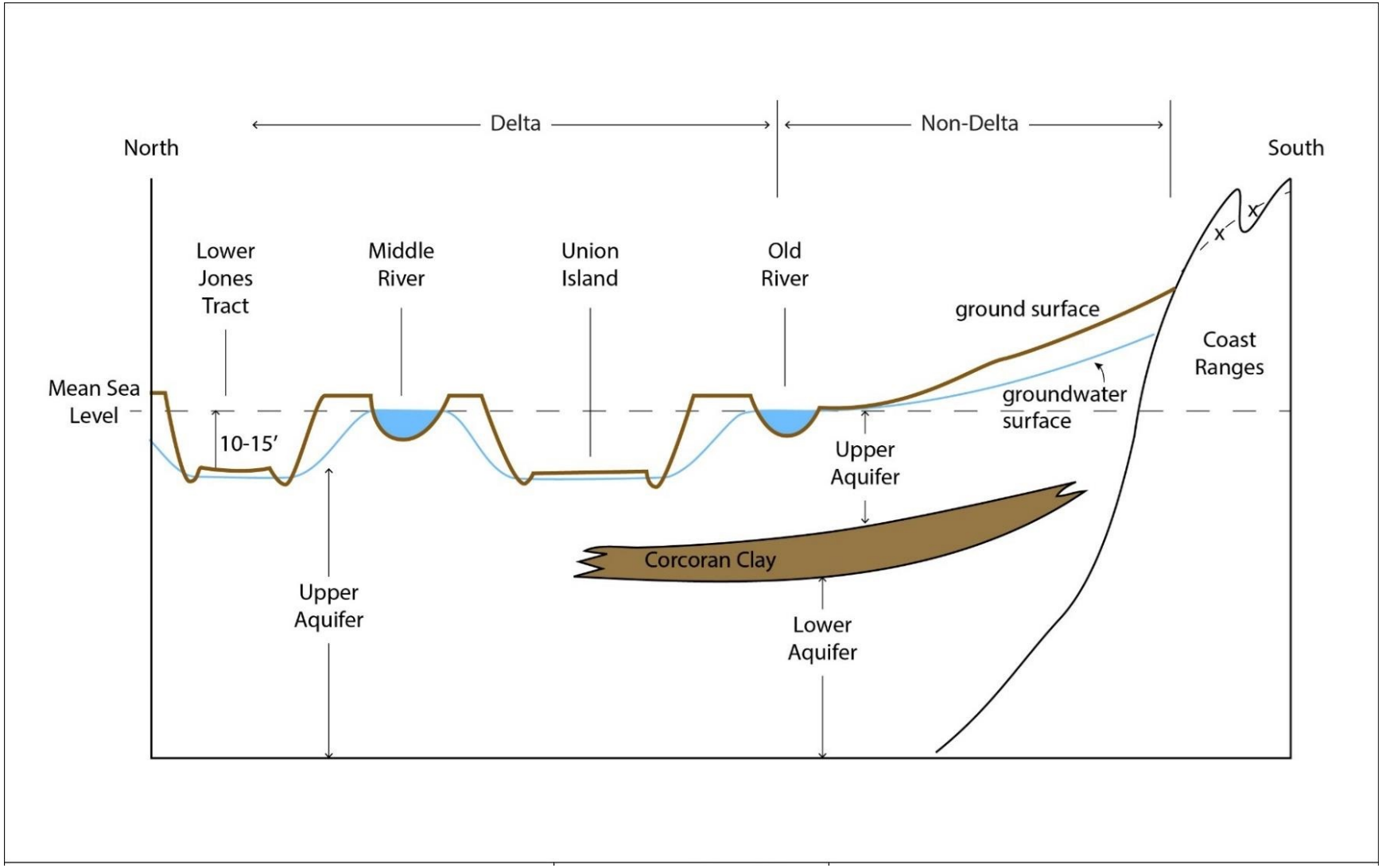

Modified from: GEI Consultants, Inc.; Tracy Subbasin Groundwater Sustainability Plan. November 1, 2021.

Figure 2.7-6 Principal Aquifer Schematic Profile

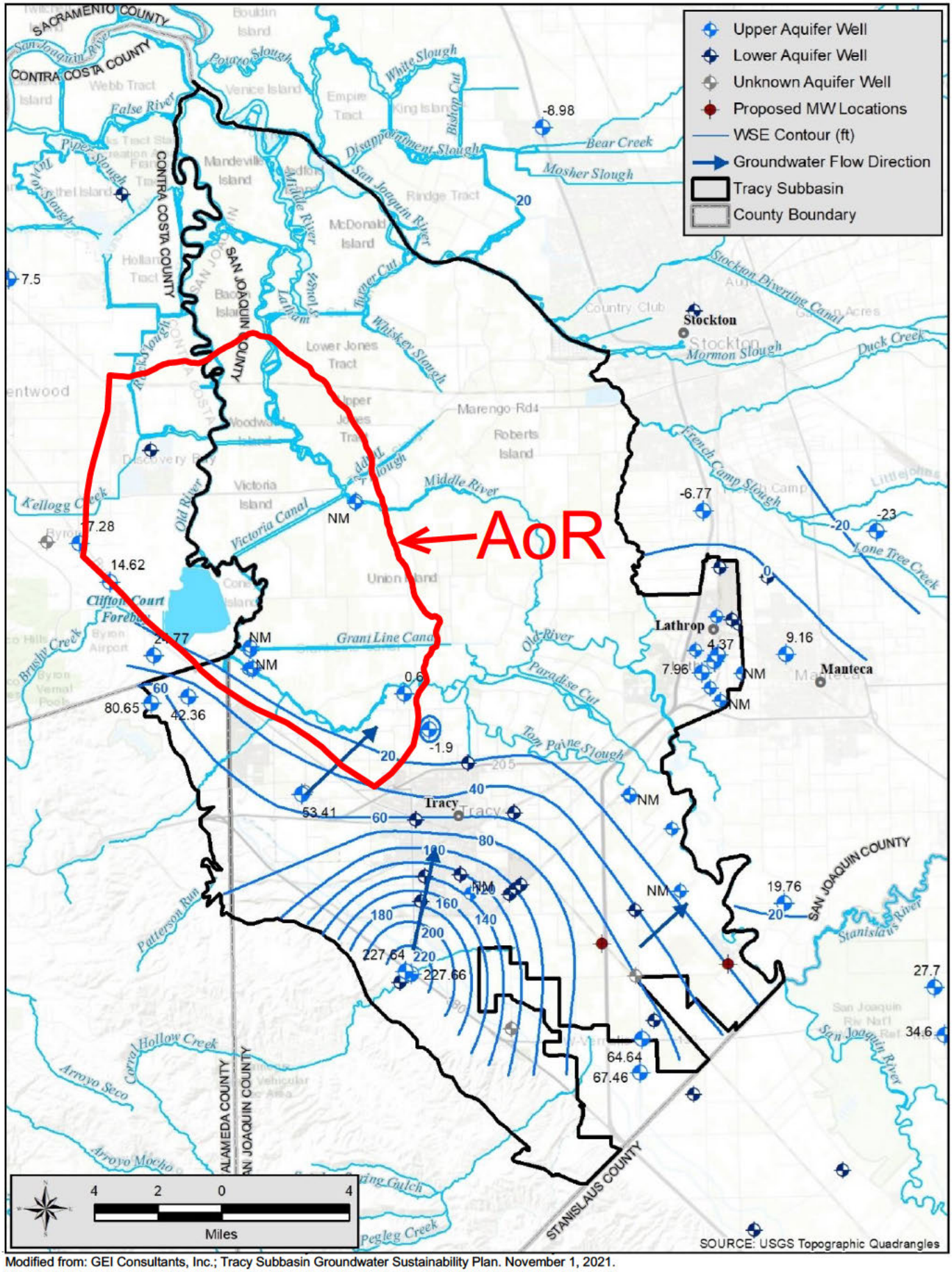

Modified from: GEI Consultants, Inc.; Tracy Subbasin Groundwater Sustainability Plan. November 1, 2021.

Figure 2.7-7 Upper Aquifer Groundwater Elevation- Fall 2019

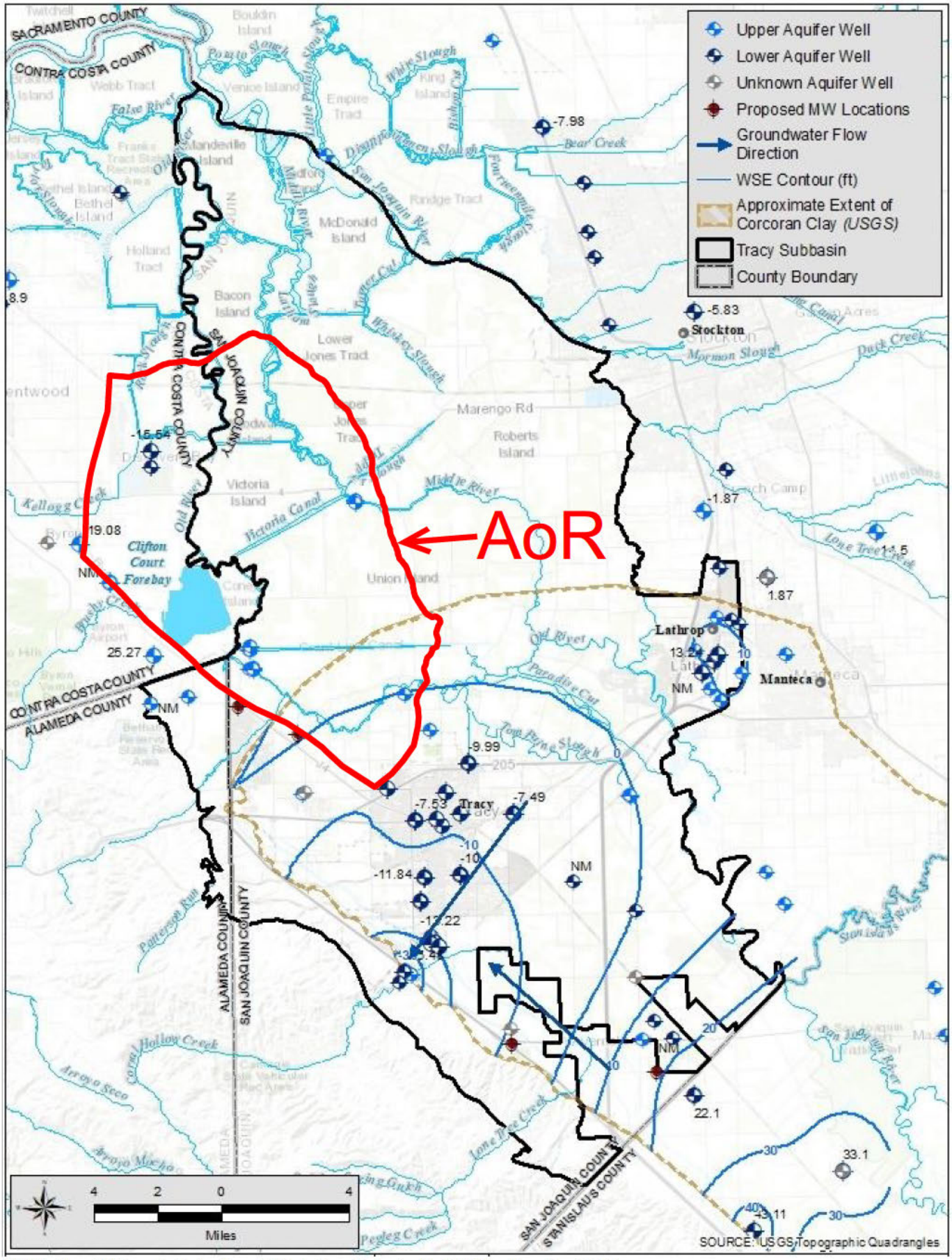

Modified from: GEI Consultants, Inc.; Tracy Subbasin Groundwater Sustainability Plan. November 1, 2021.

Figure 2.7-8 Lower Aquifer Groundwater Elevation- Spring 2019

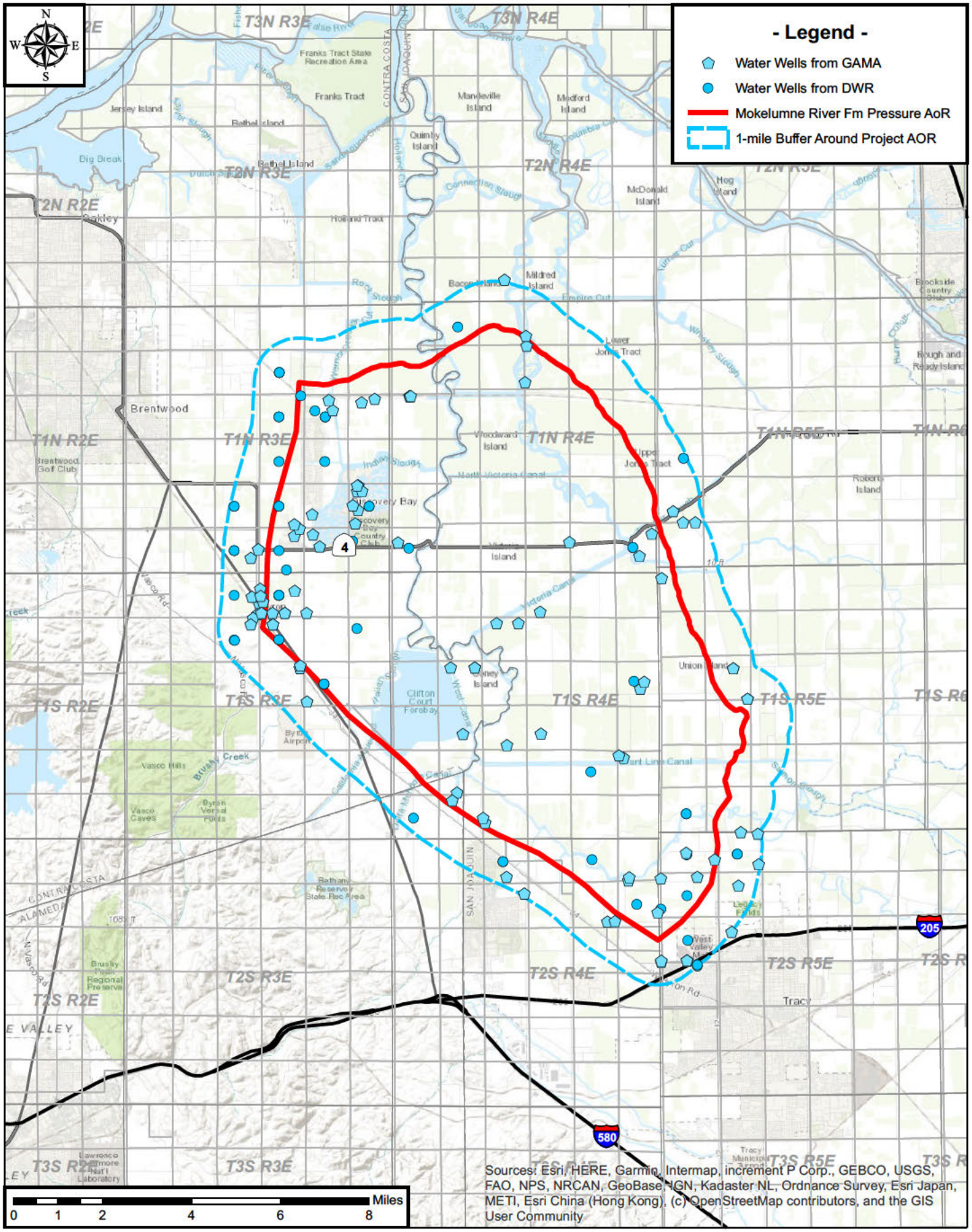

Figure 2.7-9 Water Well Location Map

GEOCHEMICAL ANALYSIS OF WATER Pro-391

DATE OF REPORT	June 4, 1980	WELL NO.	Midland Fee WI-1, Sec. 3
DATE OF SAMPLING	No date	COMPANY	Chevron USA
SAMPLED BY	Operator	FIELD	Rio Vista, 3N/3E
LABORATORY NO.	32-8N-48	ZONE	
ANALYST	Yamada	SAMPLE SOURCE	

RADICALS		PARTS PER MILLION MILLIGRAMS PER LITER	REACTING VALUE EQUIVALENTS PER MILLION	REACTING VALUE PERCENT
SODIUM	Na	5053.6	219.82	48.73
CALCIUM	Ca	61.5	3.07	0.68
MAGNESIUM	Mg	8.9	0.73	0.16
BARIUM	Ba			
STRONTIUM	Sr			
POTASSIUM	K	75	1.92	0.43
SULPHATE	SO_4	294.9	6.14	1.36
CHLORIDE	Cl	6867.2	193.70	42.94
CARBONATE	CO_3	58.8	1.96	0.44
BICARBONATE	HCO_3	1448.5	23.74	5.26
HYDROXIDE	OH			
IODIDE	I			
SILICA	SiO_2	12.8		
IRON, ALUMINA	R_2O_3	8.2		
TOTAL		13889.4	451.08	100.00

GROUP	CHEMICAL CHARACTER	MISCELLANEOUS		
ALKALIS	PRIMARY SALINITY	BORON	77.2	PPM
EARTHS	SECONDARY SALINITY	HYDROGEN SULFIDE	Absent	
STRONG ACIDS	PRIMARY ALKALINITY	EQUIVALENT SALT	12000	PPM
WEAK ACIDS	SECONDARY ALKALINITY	RESISTIVITY @ 77°F	0.470	O.M.
Ca/EARTHS		CHLORINITY	11320	PPM
CHLORIDE SALINITY		SPECIFIC GRAVITY	1.0100	
SULPHATE SALINITY	CARBONATE/CHLORIDE	pH	8.32	

REMARKS

D. F. Moran
G. C. Cates
1-C Laboratory

TICKELL GRAPH
%REACTING VALUE

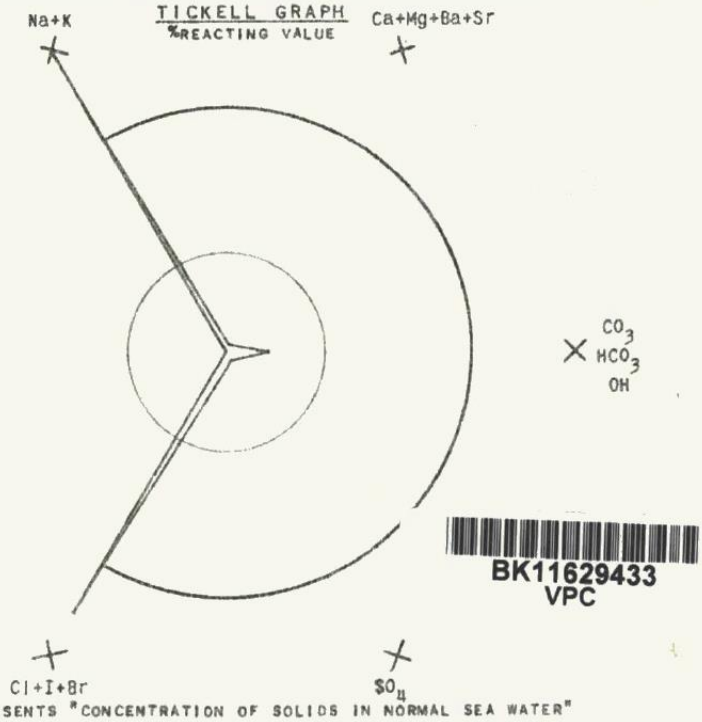

ARC REPRESENTS "CONCENTRATION OF SOLIDS IN NORMAL SEA WATER"

PRO-391 (REV. 7-71)
PRINTED IN U.S.A.

SIGNED: R. M. Yamada

Figure 2.8-1: Water geochemistry for the Midland_Fee_Water_Injection_1 well.

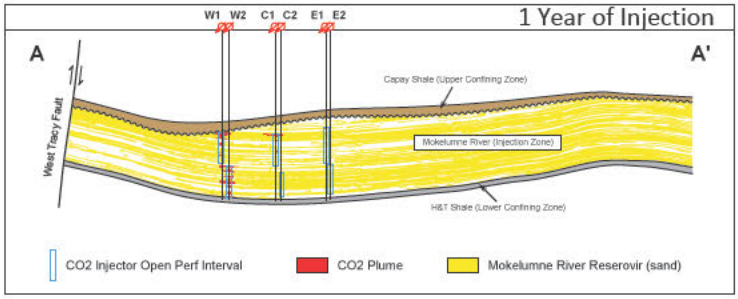

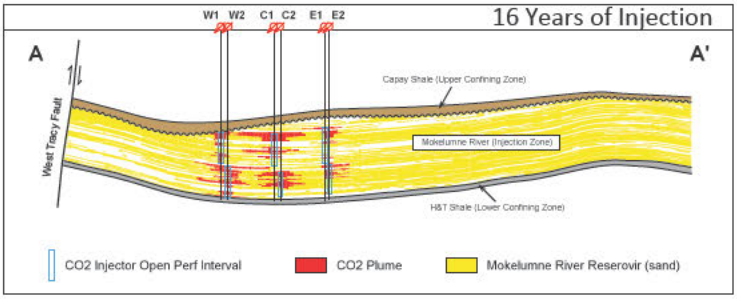

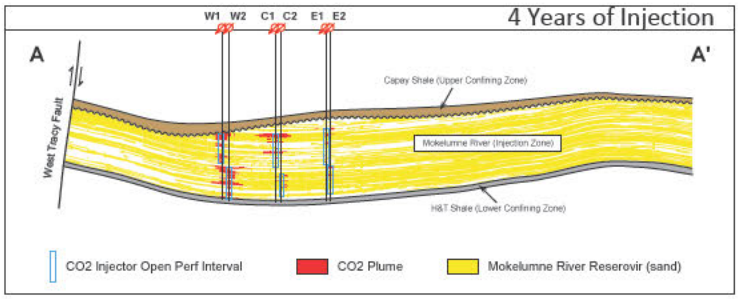

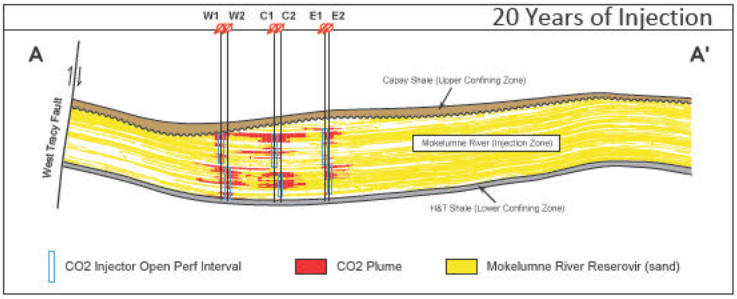

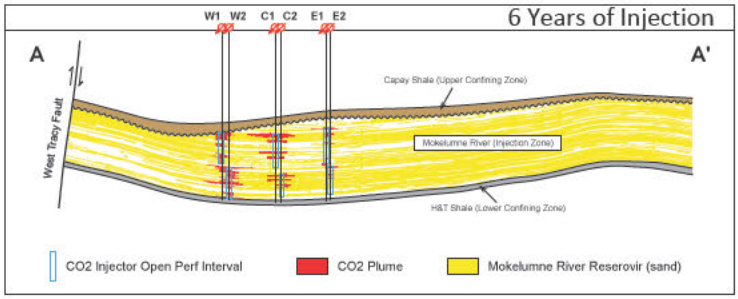

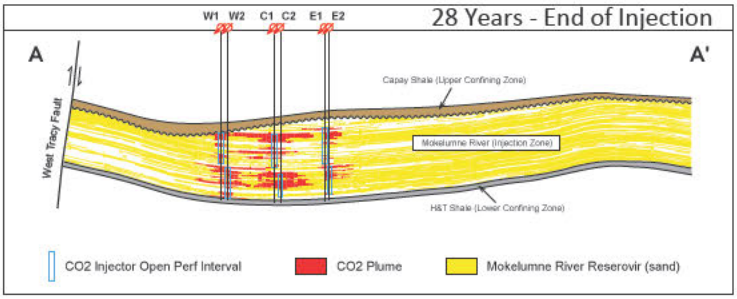

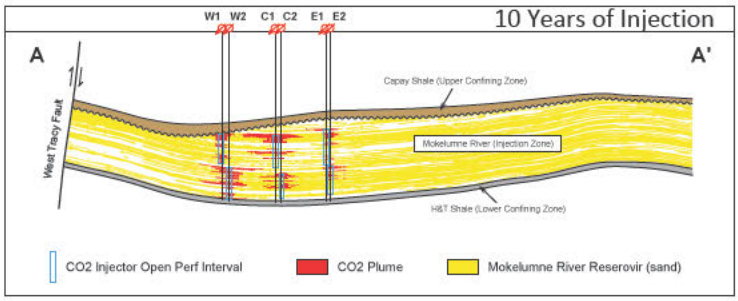

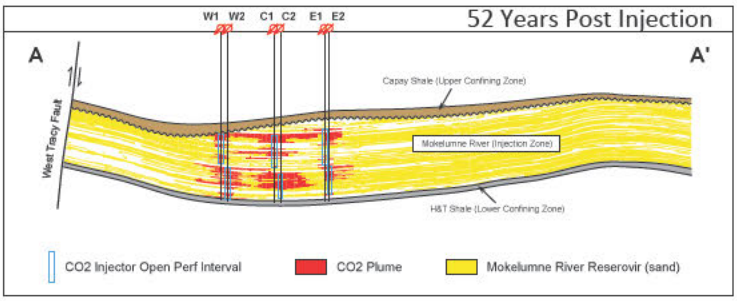

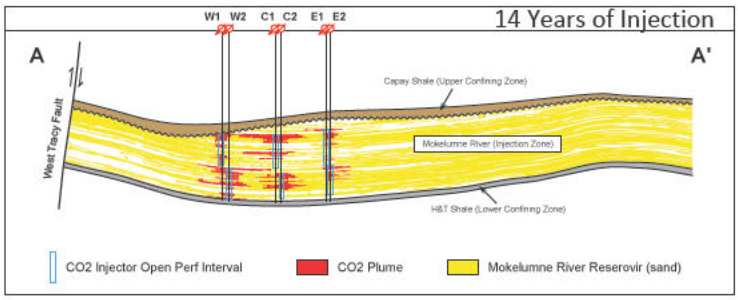

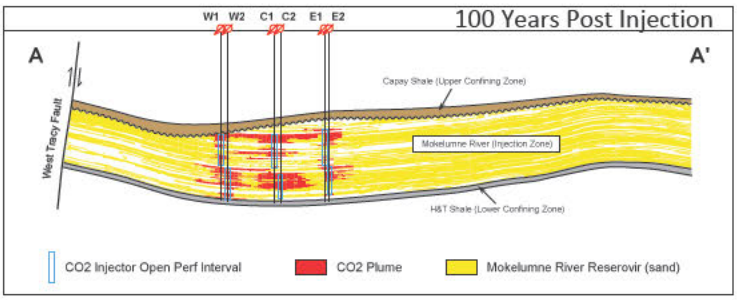

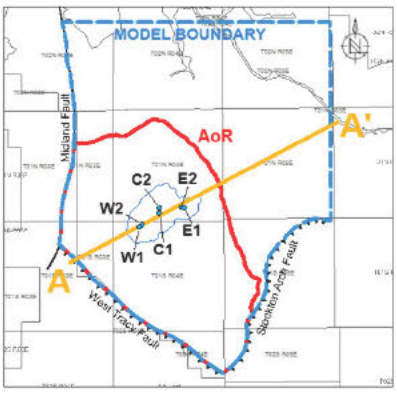

Figure 2.10-1. Proximity of CO2 to the West Tracy Fault, lateral dispersion of CO2 throughout time and confinement under the overlying Capay Shale through time.

NARRATIVE REPORT - TABLES

Table 2.3-1. Summary of results of pressures extracted from modeling at the pseudo well locations shown in **Figure 2.3-3**. Maximum pressure is 14 years after initial injection starts. Pressure averages shown in both absolute and gradient formats for the Mokelumne River Formation.

Well Location	Depth Range (TVD)	Initial Pressure Average	Max Pressure Average	100 years Post Inj Pressure Average	Delta Average
Midland Fault	6299'-7899'	2915 PSI / 0.415 psi/ft	3120 PSI / 0.444 psi/ft	2916 PSI / 0.415 psi/ft	205 PSI
West Tracy Fault	5729'-7019'	2637 PSI / 0.413 psi/ft	2822 PSI / 0.442 psi/ft	2637 PSI / 0.413 psi/ft	185 PSI
Stockton Arch Fault	5351'-6831'	2498 PSI / 0.412 psi/ft	2653 PSI / 0.438 psi/ft	2498 PSI / 0.412 psi/ft	155 PSI

Table 2.4-1: Formation mineralogy from x-ray diffraction and Fourier transform infrared spectroscopy (FTIR) in four wells.

Well	Zone	Depth (ft)	Quartz	Plagioclase	K-Feldspar	Calcite	Dolomite	Glauconite	Pyrite	Kaolinite	Chlorite	Illite & Mica	Smectite	MXL I/S	Total Clay
Wilcox_20	Capay	4622.0	42.2	18.7	10.7	0.0	0.0		0.6	9.4	3.4	4.5		10.5	27.8
Wilcox_20	Capay	4905.0	34.9	20.7	10.2	0.7	0.0		1.1	15.2	5.8	5.8		5.5	32.3
RVGU_209	Capay	4442.5	26.0	25.0	17.0	1.0	0.0			5.0	3.0			23.0	31.0
RVGU_209	Capay	4480.5	26.0	23.0	20.0	0.0	0.0			0.0	6.0			25.0	31.0
RVGU_209	Capay	4476.5	30.0	23.0	18.0	0.0	0.0			5.0	9.0			15.0	29.0
RVGU_209	Capay	4454.5	30.0	29.0	15.0	0.0	0.0			2.0	6.0			18.0	26.0
RVGU_209	Capay	4498.5	34.0	26.0	19.0	0.0	0.0			1.0	2.0			18.0	21.0
RVGU_209	Capay	4500.5	28.0	19.0	19.0	0.0	0.0			0.0	12.0			22.0	34.0
RVGU_248	Capay	4425.5	35.0	25.0	15.0					5.0	5.0	5.0	10.0		25.0
Speckman_Decarli_1	Mokelumne	6987.0	35.0	18.0	17.0	0.0	0.0	3.0	0.0	10.0	4.0			13.0	27.0
Speckman_Decarli_1	Mokelumne	6989.0	26.0	21.0	15.0	0.0	0.0	0.0	0.0	12.0	8.0			18.0	38.0
Speckman_Decarli_1	Mokelumne	6991.0	39.0	25.0	19.0	0.0	0.0	1.0	0.0	3.0	2.0			11.0	16.0
Speckman_Decarli_1	Mokelumne	7000.0	28.0	26.0	17.0	0.0	0.0	2.0	0.0	10.0	4.0			13.0	27.0
Speckman_Decarli_1	Mokelumne	7002.0	20.0	17.0	14.0	0.0	0.0	0.0	0.0	19.0	8.0			22.0	49.0
Speckman_Decarli_1	Mokelumne	7006.0	28.0	30.0	15.0	0.0	0.0	2.0	0.0	8.0	6.0			11.0	25.0
Speckman_Decarli_1	H&T Shale	8828.0	23.0	21.0	9.0	3.0	0.0	0.0	1.0	12.0	5.0			26.0	43.0
Speckman_Decarli_1	H&T Shale	8830.0	30.0	17.0	11.0	0.0	0.0	0.0	4.0	3.4	14.4	6.1	14.1		38.0
Speckman_Decarli_1	H&T Shale	8909.0	20.0	20.0	13.0	0.0	0.0	2.0	2.0	5.0	3.0			35.0	43.0
Speckman_Decarli_1	H&T Shale	8937.0	20.0	12.0	8.0	0.0	0.0	0.0	2.0	14.0	6.0			38.0	58.0
Speckman_Decarli_1	H&T Shale	8939.0	24.0	18.0	11.0	1.0	0.0	0.0	3.0	3.0	15.5	7.7	16.8		43.0
Speckman_Decarli_1	H&T Shale	8940.0	23.0	29.0	12.0	0.0	0.0	0.0	0.0	4.0	5.0			27.0	36.0
Speckman_Decarli_1	H&T Shale	8942.0	23.0	15.0	10.0	0.0	0.0	0.0	2.0	12.0	5.0			33.0	50.0
Speckman_Decarli_1	H&T Shale	9439.0	20.0	14.0	9.0	0.0	0.0	0.0	1.0	0.0	5.0			51.0	56.0
Speckman_Decarli_1	H&T Shale	9441.0	21.0	19.0	12.0	2.0	0.0	0.0	3.0	0.0	0.0			43.0	43.0

Table 2.4-2: Capay Shale and Mokelumne River Formation gross thickness and depth within the AoR.

Zone	Property	Low	High	Mean
Upper Confining Zone Capay Shale	Thickness (feet)	100	360	207
	Depth (feet TVD)	4954	6164	5582
Reservoir Mokelumne River Formation	Thickness (feet)	316	1336	1024
	Depth (feet TVD)	5044	10281	7395

Table 2.6-1. Data from USGS earthquake catalog for faults in the region of CTV III.

Number	Date	Latitude	Longitude	Depth (km)	Magnitude	Last Updated	Location
1	6/22/2018	37.99	-121.72	10.4	3.2	7/9/2021	1km SW of Oakley, CA
2	10/15/2010	37.88	-121.39	14.6	3.1	1/23/2017	9 km WSW of Taft Mosswood, California
3	9/29/2002	37.87	-121.61	4.3	3.4	2/12/2020	2 km ENE of Byron, California
4	2/10/1992	37.77	-121.32	14.6	3.1	2/9/2016	8km SSW of Lathrop, California
5	2/4/1991	37.81	-121.24	7.7	3.1	12/18/2016	2 km NW of Manteca, California
6	2/3/1991	37.82	-121.24	9.4	3.1	12/18/2016	2 km E of Lathrop, California
7	1/27/1980	38.00	-121.00	6.0	3.3	4/2/2016	8km ESE of Linden, CA
8	8/6/1979	37.83	-121.51	6.0	4.3	4/1/2016	6km NNE of Mountain House, CA
9	2/2/1979	37.66	-121.19	18.0	3.5	4/1/2016	10km WSW of Salida, CA
10	10/6/1976	37.61	-121.41	2.9	3.3	12/15/2016	13 km S of Tracy, California
11	9/5/1976	37.61	-121.41	6.5	3.5	12/15/2016	13 km S of Tracy, California
12	6/9/1975	37.96	-121.65	15.0	3.1	12/15/2016	2 km SE of Knightsen, California
13	2/2/1944	37.93	-121.40	6.0	3.8	1/28/2016	7km SW of Country Club, CA
14	2/14/1909	38.10	-121.70		4.5	6/4/2018	7 km S of Rio Vista, California
15	05/19/1889	38.10	-121.80		6.0	2/16/2021	North of Antioch, California
16	07/15/1866	37.70	-121.50		6.0	1/30/2021	Southwest of Stockton, California

Table 2.7-1- Water Supply Well Information

Data Source	WCR Number	Wells from GAMA	Legacy Log Number	Planned Use or Former Use	LAT (DWR)	LONG (DWR)	LAT & LONG Accuracy (DWR)	LAT (GAMA)	LONG (GAMA)	T	R	S	APN	Date Work Ended	Total Completed Depth	Top of Perforated Interval	Bottom of Perforated Interval	Static Water Level
DWR	WCR0045932	NA	E027683	NA	37.84561	-121.61393	Centroid of Section	NA	NA	01S	03E	14	NA	NA	NA	NA	NA	NA
DWR	WCR0086914	NA	E068053A	NA	37.88968	-121.48668	Centroid of Section	NA	NA	01N	04E	36	NA	NA	NA	NA	NA	NA
DWR	WCR0139689	NA	E013489	NA	37.90359	-121.59496	Centroid of Section	NA	NA	01N	03E	25	NA	NA	NA	NA	NA	NA
DWR	WCR0187739	NA	NA	NA	37.91861	-121.46563	Centroid of Section	NA	NA	01N	05E	19	NA	NA	NA	NA	NA	NA
DWR	WCR0225444	NA	E068052	NA	37.88968	-121.48668	Centroid of Section	NA	NA	01N	04E	36	NA	NA	NA	NA	NA	NA
DWR	WCR0210369	NA	65480	Water Supply Domestic	37.90376	-121.6505	Centroid of Section	NA	NA	01N	03E	28	NA	8/18/1987	240	220	240	65
DWR	WCR0283695	NA	E027681	NA	37.84561	-121.61393	Centroid of Section	NA	NA	01S	03E	14	NA	NA	NA	NA	NA	NA
DWR	WCR1980-0008(	NA	148888	Water Supply Domestic	37.90376	-121.6505	Centroid of Section	NA	NA	01N	03E	28	NA	4/15/1980	175	NA	NA	NA
DWR	WCR1951-0004:	NA	39-465	Water Supply Domestic	37.78785	-121.5041	Centroid of Section	NA	NA	02S	04E	2	NA	11/14/1951	80	64	76	NA
DWR	WCR1980-0032	NA	81516	Water Supply Domestic	37.94732	-121.63181	Centroid of Section	NA	NA	01N	03E	10	NA	9/7/1980	222	NA	NA	NA
DWR	WCR1974-0008:	NA	87178	Water Supply Domestic	37.80269	-121.4653	Centroid of Section	NA	NA	01S	05E	31	NA	2/14/1974	120	90	100	NA
DWR	WCR1984-0011	NA	154244	Water Supply Domestic	37.78745	-121.54066	Centroid of Section	NA	NA	02S	04E	4	NA	10/21/1984	170	NA	NA	NA
DWR	WCR1990-0005	NA	01-462Q	Monitoring	37.80177	-121.57738	Centroid of Section	NA	NA	01S	04E	31	NA	8/31/1990	50	NA	NA	NA
DWR	WCR1991-0062	NA	374968	Water Supply Domestic	37.96181	-121.55819	Centroid of Section	NA	NA	01N	04E	5	58-90-44	4/11/1991	375	35	50	NA
DWR	WCR1995-0041	NA	547412	Water Supply Irrigation - A	37.8601	-121.63239	Centroid of Section	NA	NA	01S	03E	10	2-130-8	8/11/1995	160	80	154	23
DWR	WCR1995-0062	NA	567878	Water Supply Domestic	37.8601	-121.63239	Centroid of Section	NA	NA	01S	03E	10	2-150-20	1/17/1995	120	66	86	5
DWR	WCR2004-0050	NA	756733e	Other Geothermal Heat E	37.9182	-121.61316	Centroid of Section	NA	NA	01N	03E	23	255-340-1	8/26/2004	265	NA	NA	NA
DWR	WCR2000-0025	NA	725228	Water Supply Domestic	37.87465	-121.63233	Centroid of Section	NA	NA	01S	03E	3	2-40-54	2/3/2000	390	330	340	30
DWR	WCR2000-0026	NA	725236	Water Supply Domestic	37.87465	-121.63233	Centroid of Section	NA	NA	01S	03E	3	2-270-1	3/27/2000	200	130	155	25
DWR	WCR2000-0026	NA	725239	Water Supply Domestic	37.88919	-121.65061	Centroid of Section	NA	NA	01N	03E	33	11/6/1932	4/6/2000	280	70	90	30
DWR	WCR2020-0095	NA	NA	Water Supply Domestic	37.88286055	-121.62915	NA	NA	NA	01N	03E	34	11200049	6/16/2020	280	240	280	NA
DWR	WCR2016-0093	NA	E0332983	Unknown	37.939666	-121.622947	Unknown	NA	NA	01N	03E	15	NA	12/19/2016	NA	NA	NA	NA
DWR	WCR2013-0065	NA	e0186183	Other Unused	37.8922222	-121.6019444	NA	NA	NA	01N	03E	36	8-230-37	7/8/2013	NA	NA	NA	NA
DWR	WCR0004144	NA	NA	NA	37.81654	-121.50441	Centroid of Section	NA	NA	01S	04E	26	NA	NA	NA	NA	NA	NA
DWR	WCR0073374	NA	105875	Water Supply Domestic	37.86008	-121.65068	Centroid of Section	NA	NA	01S	03E	9	NA	4/6/1978	136	75	135	NA
DWR	WCR0098744	NA	146834	Water Supply Domestic	37.94732	-121.63181	Centroid of Section	NA	NA	01N	03E	10	NA	NA	62	52	62	NA
DWR	WCR0045658	NA	NA	NA	37.78745	-121.54066	Centroid of Section	NA	NA	02S	04E	4	NA	NA	NA	NA	NA	NA
DWR	WCR0103521	NA	E013488	NA	37.90359	-121.59496	Centroid of Section	NA	NA	01N	03E	25	NA	NA	NA	NA	NA	NA
DWR	WCR1988-0034	NA	253474	Water Supply Domestic	37.87462	-121.65064	Centroid of Section	NA	NA	01S	03E	4	NA	3/15/1988	180	NA	NA	NA
DWR	WCR1987-0084	NA	65481	Water Supply Domestic	37.84561	-121.61393	Centroid of Section	NA	NA	01S	03E	14	NA	8/19/1987	62	NA	NA	NA
DWR	WCR1987-0052	NA	252851	Water Supply Domestic	37.77597	-121.46509	Centroid of Section	NA	NA	02S	05E	7	NA	11/1/1987	200	NA	NA	NA
DWR	WCR1998-0017	NA	520808	Water Supply Domestic	37.88917	-121.63225	Centroid of Section	NA	NA	01N	03E	34	NA	8/18/1998	340	245	265	55
DWR	WCR1994-0012	NA	416840	Water Supply Domestic	37.93281	-121.6319	Centroid of Section	NA	NA	01N	03E	15	15-150-2	1/6/1994	220	71	91	25
DWR	WCR1997-0020	NA	520729	Water Supply Domestic	37.94732	-121.63181	Centroid of Section	NA	NA	01N	03E	10	15-110-1	2/19/1997	157	125	150	15
DWR	WCR1997-0071	NA	e068445	Monitoring	37.88978	-121.57877	Centroid of Section	NA	NA	01N	04E	31	NA	8/7/1997	20	10	20	NA
DWR	WCR2000-0026	NA	725242	Other Unused	37.87465	-121.63233	Centroid of Section	NA	NA	01S	03E	3	2-270-3	5/4/2000	NA	NA	NA	NA
DWR	WCR2003-0016	NA	749495	Water Supply Domestic	37.90369	-121.63214	Centroid of Section	NA	NA	01N	03E	27	11-180-54	3/4/2003	320	278	298	55
DWR	WCR2008-0010	NA	946804	Monitoring	37.76146	-121.46495	Centroid of Section	NA	NA	02S	05E	18	212-50-60	8/14/2008	17	7	17	NA
DWR	WCR2008-0019	NA	e0078476	Monitoring	37.8636111	-121.6002778	NA	NA	NA	01S	03E	12	2-250-3	8/26/2008	600	NA	NA	NA
DWR	WCR2012-0048	NA	e0152708	Other Unused	37.7530556	-121.4611111	NA	NA	NA	02S	05E	19	238-600-25	5/15/2012	NA	NA	NA	NA
DWR	WCR2012-0048	NA	e0152713	Other Unused	37.7533333	-121.4611111	NA	NA	NA	02S	05E	19	238-600-23	5/15/2012	NA	NA	NA	NA
DWR	WCR2018-0089	NA	NA	Water Supply Domestic	37.9346837	-121.6171459	NA	NA	NA	01N	03E	14	015-170-032	8/8/2018	206	186	206	48
DWR	WCR0007675	NA	E0106583	NA	37.93272	-121.61299	Centroid of Section	NA	NA	01N	03E	14	NA	NA	NA	NA	NA	NA
DWR	WCR2013-0055	NA	e0169248	Water Supply Domestic	37.7716667	-121.4758333	NA	NA	NA	02S	05E	7	212-30-8	1/18/2013	385	230	270	10
DWR	WCR0296962	NA	87190	NA	37.77322	-121.4858	Centroid of Section	NA	NA	02S	04E	12	NA	NA	NA	NA	NA	NA
DWR	WCR0316437	NA	111903	NA	37.78943	-121.46519	Centroid of Section	NA	NA	02S	05E	6	NA	NA	NA	NA	NA	NA
DWR	WCR1952-0002	NA	39-1172	Water Supply Domestic	37.84609	-121.48636	Centroid of Section	NA	NA	01S	04E	13	NA	4/29/1952	89	66	74	NA
DWR	WCR1982-0010	NA	233803	Water Supply Domestic	37.91825	-121.63201	Centroid of Section	NA	NA	01N	03E	22	NA	3/1/1982	160	NA	NA	NA
DWR	WCR1988-0040	NA	250523	Water Supply Domestic	37.78951	-121.44446	Centroid of Section	NA	NA	02S	05E	5	NA	7/13/1988	232	NA	NA	NA
DWR	WCR1986-0021	NA	180386	NA	37.93272	-121.61299	Centroid of Section	NA	NA	01N	03E	14	NA	6/4/1986	320	NA	NA	NA
DWR	WCR1989-0038	NA	291597	Water Supply Domestic	37.86	-121.6505556	NA	NA	NA	01S	03E	9	NA	7/31/1989	95	NA	NA	NA
DWR	WCR1989-0043	NA	287278	Water Supply Domestic	37.78943	-121.46519	Centroid of Section	NA	NA	02S	05E	6	NA	3/21/1989	210	NA	NA	NA
DWR	WCR1989-0053	NA	303990	Water Supply Domestic	37.90369	-121.63214	Centroid of Section	NA	NA	01N	03E	27	NA	4/22/1989	280	NA	NA	NA
DWR	WCR1998-0049	NA	703030	Cathodic Protection	37.93281	-121.6319	Centroid of Section	NA	NA	01N	03E	15	15-240-4	11/17/1998	300	198	300	NA
DWR	WCR2004-0005	NA	915644	Water Supply Domestic	37.87465	-121.63233	Centroid of Section	NA	NA	01S	03E	3	2-40-41	NA	400	245	285	56
DWR	WCR1997-0068	NA	576785	Other Unused	37.78951	-121.44446	Centroid of Section	NA	NA	02S	05E	5	NA	1/14/1997	NA	NA	NA	NA
DWR	WCR2007-0042	NA	e059689	Water Supply Domestic	37.88919	-121.65061	Centroid of Section	NA	NA	01N	03E	33	11-100-29	8/8/2007	240	170	230	57
DWR	WCR2009-0004	NA	944758	Water Supply Domestic	37.80269	-121.4653	Centroid of Section	NA	NA	01S	05E	31	189-50-28	5/10/2009	100	80	100	11
DWR	WCR2009-0055	NA	e0098479	Water Supply Domestic	37.78943	-121.46519	Centroid of Section	NA	NA	02S	05E	6	212-20-2	9/2/2009	250	130	200	20
DWR	WCR2009-0070	NA	e0106578	Monitoring	37.93272	-121.61299	Centroid of Section	NA	NA	01N	03E	14	15-240-3	8/30/2009	22	7	22	11
DDW	NA	0706049-001	NA	NA	NA	NA	NA	37.889643	-121.64089	01N	03E	33	NA	NA	NA	NA	NA	NA
DDW	NA	0706027-003	NA	NA	NA	NA	NA	37.872023	-121.64059	01S	03E	4	NA	NA	NA	NA	NA	NA
DDW	NA	0710009-004	NA	NA	NA	NA	NA	37.891667	-121.58333	01N	04E	31	NA	NA	NA	NA	NA	NA

Data Source	WCR Number	Wells from GAMA	Legacy Log Number	Planned Use or Former Use	LAT (DWR)	LONG (DWR)	LAT & LONG Accuracy (DWR)	LAT (GAMA)	LONG (GAMA)	T	R	S	APN	Date Work Ended	Total Completed Depth	Top of Perforated Interval	Bottom of Perforated Interval	Static Water Level
DDW	NA	3900713-001	NA	NA	NA	NA	NA	37.84	-121.44	01S	05E	17	NA	NA	NA	NA	NA	NA
DWR	NA	01S03E03M001M	NA	NA	NA	NA	NA	37.8741	-121.64	01S	03E	3	NA	NA	NA	NA	NA	NA
DWR	NA	01N03E34A001M	NA	NA	NA	NA	NA	37.894	-121.626	01N	03E	34	NA	NA	NA	NA	NA	NA
DWR	NA	01S03E15A001M	NA	NA	NA	NA	NA	37.8508	-121.624	01S	03E	15	NA	NA	NA	NA	NA	NA
DWR	NA	01N04E03N001M	NA	NA	NA	NA	NA	37.9555	-121.53	01N	04E	3	NA	NA	NA	NA	NA	NA
WB_CLEANUP	NA	T10000003258-MW	NA	NA	NA	NA	NA	37.9394031	-121.57828	01N	04E	18	NA	NA	NA	NA	NA	NA
USGS_NWIS	NA	USGS-3745001212	NA	NA	NA	NA	NA	37.7548611	-121.46547	02S	05E	18	NA	NA	NA	NA	NA	NA
USGS_NWIS	NA	USGS-3746451212	NA	NA	NA	NA	NA	37.7790949	-121.44411	02S	05E	8	NA	NA	NA	NA	NA	NA
USGS_NWIS	NA	USGS-3747461212	NA	NA	NA	NA	NA	37.7960389	-121.43606	02S	05E	5	NA	NA	NA	NA	NA	NA
DDW	NA	0707580-001	NA	NA	NA	NA	NA	37.868416	-121.64122	01S	03E	4	NA	NA	NA	NA	NA	NA
DDW	NA	0710009-006	NA	NA	NA	NA	NA	37.890398	-121.61556	01N	03E	35	NA	NA	NA	NA	NA	NA
DDW	NA	0710009-001	NA	NA	NA	NA	NA	37.908333	-121.6	01N	03E	25	NA	NA	NA	NA	NA	NA
DDW	NA	0710009-008	NA	NA	NA	NA	NA	37.910276	-121.59949	01N	03E	25	NA	NA	NA	NA	NA	NA
DDW	NA	0105002-001	NA	NA	NA	NA	NA	37.809915	-121.5596	01S	04E	29	NA	NA	NA	NA	NA	NA
DWR	NA	01S03E03P001M	NA	NA	NA	NA	NA	37.8688	-121.635	01S	03E	3	NA	NA	NA	NA	NA	NA
DWR	NA	01S03E03H001M	NA	NA	NA	NA	NA	37.876	-121.626	01S	03E	3	NA	NA	NA	NA	NA	NA
USGS_NWIS	NA	USGS-3752021213	NA	NA	NA	NA	NA	37.8671477	-121.64301	01S	03E	9	NA	NA	NA	NA	NA	NA
USGS_NWIS	NA	USGS-3745161212	NA	NA	NA	NA	NA	37.7543735	-121.47606	02S	05E	7	NA	NA	NA	NA	NA	NA
DDW	NA	0707545-001	NA	NA	NA	NA	NA	37.934872	-121.60995	01N	03E	14	NA	NA	NA	NA	NA	NA
DDW	NA	3901484-001	NA	NA	NA	NA	NA	37.943625	-121.53076	01N	04E	10	NA	NA	NA	NA	NA	NA
DDW	NA	3900583-001	NA	NA	NA	NA	NA	37.84	-121.44	01S	05E	17	NA	NA	NA	NA	NA	NA
DWR	NA	01N03E33J001M	NA	NA	NA	NA	NA	37.8868	-121.644	01N	03E	33	NA	NA	NA	NA	NA	NA
DWR	NA	01S03E03Q001M	NA	NA	NA	NA	NA	37.8688	-121.63	01S	03E	3	NA	NA	NA	NA	NA	NA
DWR	NA	01S05E32R001M	NA	NA	NA	NA	NA	37.7965	-121.443	01S	05E	32	NA	NA	NA	NA	NA	NA
USGS_NWIS	NA	USGS-3746371213	NA	NA	NA	NA	NA	37.7768728	-121.53217	02S	04E	9	NA	NA	NA	NA	NA	NA
USGS_NWIS	NA	USGS-3746521212	NA	NA	NA	NA	NA	37.7810395	-121.48939	02S	04E	1	NA	NA	NA	NA	NA	NA
DDW	NA	0707545-002	NA	NA	NA	NA	NA	37.938171	-121.61158	01N	03E	14	NA	NA	NA	NA	NA	NA
DDW	NA	0710009-016	NA	NA	NA	NA	NA	37.902313	-121.59978	01N	03E	25	NA	NA	NA	NA	NA	NA
DDW	NA	3910011-032	NA	NA	NA	NA	NA	37.754682	-121.46525	02S	05E	18	NA	NA	NA	NA	NA	NA
DWR	NA	01S04E33M001M	NA	NA	NA	NA	NA	37.8001	-121.548	01S	04E	33	NA	NA	NA	NA	NA	NA
DWR	NA	01S04E09C001M	NA	NA	NA	NA	NA	37.8651	-121.543	01S	04E	9	NA	NA	NA	NA	NA	NA
DWR	NA	01S04E13K003M	NA	NA	NA	NA	NA	37.8435	-121.484	01S	04E	13	NA	NA	NA	NA	NA	NA
DWR	NA	02S05E18N001M	NA	NA	NA	NA	NA	37.7547	-121.476	02S	05E	18	NA	NA	NA	NA	NA	NA
WB_CLEANUP	NA	T10000003258-MW	NA	NA	NA	NA	NA	37.9391663	-121.57819	01N	04E	18	NA	NA	NA	NA	NA	NA
USGS_NWIS	NA	USGS-3756191213	NA	NA	NA	NA	NA	37.9385349	-121.59273	01N	03E	13	NA	NA	NA	NA	NA	NA
DDW	NA	0707598-001	NA	NA	NA	NA	NA	37.874137	-121.64348	01S	03E	4	NA	NA	NA	NA	NA	NA
DDW	NA	0706029-001	NA	NA	NA	NA	NA	37.876694	-121.64011	01S	03E	3	NA	NA	NA	NA	NA	NA
DDW	NA	0710009-003	NA	NA	NA	NA	NA	37.897833	-121.60092	01N	03E	25	NA	NA	NA	NA	NA	NA
DDW	NA	3901449-001	NA	NA	NA	NA	NA	37.891449	-121.51277	01N	04E	34	NA	NA	NA	NA	NA	NA
DWR	NA	01S03E10C001M	NA	NA	NA	NA	NA	37.8651	-121.635	01S	03E	10	NA	NA	NA	NA	NA	NA
DWR	NA	01S03E14N001M	NA	NA	NA	NA	NA	37.8399	-121.621	01S	03E	14	NA	NA	NA	NA	NA	NA
DWR	NA	01S04E21Q001M	NA	NA	NA	NA	NA	37.8254	-121.539	01S	04E	21	NA	NA	NA	NA	NA	NA
DWR	NA	01S04E09A001M	NA	NA	NA	NA	NA	37.8651	-121.534	01S	04E	9	NA	NA	NA	NA	NA	NA
DWR	NA	02S04E01P001M	NA	NA	NA	NA	NA	37.7821	-121.489	02S	04E	1	NA	NA	NA	NA	NA	NA
DWR	NA	01N04E36A001M	NA	NA	NA	NA	NA	37.894	-121.479	01N	04E	36	NA	NA	NA	NA	NA	NA
DWR	NA	01N05E30R002M	NA	NA	NA	NA	NA	37.8977	-121.461	01N	05E	30	NA	NA	NA	NA	NA	NA
USGS_NWIS	NA	USGS-3751061213	NA	NA	NA	NA	NA	37.8515927	-121.62384	01S	03E	15	NA	NA	NA	NA	NA	NA
USGS_NWIS	NA	USGS-3748271213	NA	NA	NA	NA	NA	37.8074274	-121.56162	01S	04E	32	NA	NA	NA	NA	NA	NA
USGS_NWIS	NA	USGS-3748061213	NA	NA	NA	NA	NA	37.8015943	-121.54884	01S	04E	32	NA	NA	NA	NA	NA	NA
USGS_NWIS	NA	USGS-3757321213	NA	NA	NA	NA	NA	37.9588124	-121.53023	01N	04E	3	NA	NA	NA	NA	NA	NA
USGS_NWIS	NA	USGS-3749161212	NA	NA	NA	NA	NA	37.8210384	-121.49106	01S	04E	25	NA	NA	NA	NA	NA	NA
USGS_NWIS	NA	USGS-3746141212	NA	NA	NA	NA	NA	37.7704842	-121.47745	02S	04E	12	NA	NA	NA	NA	NA	NA
USGS_NWIS	NA	USGS-3750001212	NA	NA	NA	NA	NA	37.8499722	-121.44578	01S	05E	17	NA	NA	NA	NA	NA	NA
USGS_NWIS	NA	USGS-3747101212	NA	NA	NA	NA	NA	37.7860392	-121.43578	02S	05E	5	NA	NA	NA	NA	NA	NA
DDW	NA	0710009-002	NA	NA	NA	NA	NA	37.903779	-121.60186	01N	03E	25	NA	NA	NA	NA	NA	NA
DWR	NA	01S03E03M002M	NA	NA	NA	NA	NA	37.8724	-121.639	01S	03E	3	NA	NA	NA	NA	NA	NA
DWR	NA	01N03E25C001M	NA	NA	NA	NA	NA	37.9085	-121.598	01N	03E	25	NA	NA	NA	NA	NA	NA
DWR	NA	01S04E17C001M	NA	NA	NA	NA	NA	37.8507	-121.562	01S	04E	17	NA	NA	NA	NA	NA	NA
DWR	NA	01S04E25D001M	NA	NA	NA	NA	NA	37.8218	-121.493	01S	04E	25	NA	NA	NA	NA	NA	NA
DWR	NA	01N04E36K003M	NA	NA	NA	NA	NA	37.8868	-121.484	01N	04E	36	NA	NA	NA	NA	NA	NA
DWR	NA	01S05E06D001M	NA	NA	NA	NA	NA	37.8796	-121.475	01S	05E	6	NA	NA	NA	NA	NA	NA
DWR	NA	01N05E30L001M	NA	NA	NA	NA	NA	37.9013	-121.47	01N	05E	30	NA	NA	NA	NA	NA	NA
DWR	NA	02S05E17B001M	NA	NA	NA	NA	NA	37.764	-121.447	02S	05E	17	NA	NA	NA	NA	NA	NA
GAMA_USGS	NA	TRCYFP-03	NA	NA	NA	NA	NA	37.7548611	-121.46547	02S	05E	18	NA	NA	NA	NA	NA	NA
USGS_NWIS	NA	USGS-3753471213	NA	NA	NA	NA	NA	37.8963137	-121.62384	01N	03E	34	NA	NA	NA	NA	NA	NA

Data Source	WCR Number	Wells from GAMA	Legacy Log Number	Planned Use or Former Use	LAT (DWR)	LONG (DWR)	LAT & LONG Accuracy (DWR)	LAT (GAMA)	LONG (GAMA)	T	R	S	APN	Date Work Ended	Total Completed Depth	Top of Perforated Interval	Bottom of Perforated Interval	Static Water Level
USGS_NWIS	NA	USGS-375437121351	NA	NA	NA	NA	NA	37.9102023	-121.59995	01N	03E	25	NA	NA	NA	NA	NA	NA
USGS_NWIS	NA	USGS-374657121321	NA	NA	NA	NA	NA	37.7824282	-121.53939	02S	04E	4	NA	NA	NA	NA	NA	NA
USGS_NWIS	NA	USGS-374654121281	NA	NA	NA	NA	NA	37.781595	-121.47606	02S	04E	13	NA	NA	NA	NA	NA	NA
USGS_NWIS	NA	USGS-374724121271	NA	NA	NA	NA	NA	37.7899281	-121.4655	02S	05E	6	NA	NA	NA	NA	NA	NA
DDW	NA	0710009-007	NA	NA	NA	NA	NA	37.90095	-121.61862	01N	03E	26	NA	NA	NA	NA	NA	NA
DWR	NA	01S03E09A001M	NA	NA	NA	NA	NA	37.8651	-121.644	01S	03E	9	NA	NA	NA	NA	NA	NA
DWR	NA	01S03E10C002M	NA	NA	NA	NA	NA	37.8651	-121.635	01S	03E	10	NA	NA	NA	NA	NA	NA
DWR	NA	01S03E03Q002M	NA	NA	NA	NA	NA	37.8688	-121.63	01S	03E	3	NA	NA	NA	NA	NA	NA
DWR	NA	01N03E13C001M	NA	NA	NA	NA	NA	37.9374	-121.598	01N	03E	13	NA	NA	NA	NA	NA	NA
DWR	NA	01S04E20K001M	NA	NA	NA	NA	NA	37.829	-121.557	01S	04E	20	NA	NA	NA	NA	NA	NA
DWR	NA	01S04E17A001M	NA	NA	NA	NA	NA	37.8507	-121.552	01S	04E	17	NA	NA	NA	NA	NA	NA
DWR	NA	02S05E06R001M	NA	NA	NA	NA	NA	37.7821	-121.461	02S	05E	6	NA	NA	NA	NA	NA	NA
GAMA_USGS	NA	TRCY-07	NA	NA	NA	NA	NA	37.8499722	-121.44578	01S	05E	17	NA	NA	NA	NA	NA	NA
USGS_NWIS	NA	USGS-375228121381	NA	NA	NA	NA	NA	37.8743698	-121.63995	01S	03E	3	NA	NA	NA	NA	NA	NA
DDW	NA	0900112-001	NA	NA	NA	NA	NA	37.868889	-121.63964	01S	03E	3	NA	NA	NA	NA	NA	NA
DDW	NA	0710009-017	NA	NA	NA	NA	NA	37.894299	-121.6184	01N	03E	35	NA	NA	NA	NA	NA	NA
DWR	NA	01N03E27R001M	NA	NA	NA	NA	NA	37.8977	-121.626	01N	03E	27	NA	NA	NA	NA	NA	NA
DWR	NA	01S03E02N001M	NA	NA	NA	NA	NA	37.8688	-121.621	01S	03E	2	NA	NA	NA	NA	NA	NA
DWR	NA	01S04E17A002M	NA	NA	NA	NA	NA	37.8507	-121.552	01S	04E	17	NA	NA	NA	NA	NA	NA
DWR	NA	01S04E22L001M	NA	NA	NA	NA	NA	37.829	-121.525	01S	04E	22	NA	NA	NA	NA	NA	NA
DWR	NA	01S04E03P002M	NA	NA	NA	NA	NA	37.8688	-121.525	01S	04E	3	NA	NA	NA	NA	NA	NA
DWR	NA	02S04E11R001M	NA	NA	NA	NA	NA	37.7676	-121.498	02S	04E	11	NA	NA	NA	NA	NA	NA
DWR	NA	01N05E30Q003M	NA	NA	NA	NA	NA	37.8977	-121.466	01N	05E	30	NA	NA	NA	NA	NA	NA
WB_CLEANUP	NA	T10000003258-MW	NA	NA	NA	NA	NA	37.939404	-121.57787	01N	04E	18	NA	NA	NA	NA	NA	NA
USGS_NWIS	NA	USGS-374604121251	NA	NA	NA	NA	NA	37.7677065	-121.49495	02S	04E	11	NA	NA	NA	NA	NA	NA
USGS_NWIS	NA	USGS-375045121281	NA	NA	NA	NA	NA	37.84576	-121.48245	01S	04E	13	NA	NA	NA	NA	NA	NA
USGS_NWIS	NA	USGS-374716121271	NA	NA	NA	NA	NA	37.7877059	-121.45384	02S	05E	6	NA	NA	NA	NA	NA	NA

Notes:
1= All depths are based on feet below ground surface
WCR= Department of Water Resources Well Completion Report
LAT= Latitide
LONG= Longitude
T= Township
R= Range
S= Section
APN= Assessor Parcel Number
NA= Data is not available or not applicable
GAMA= State Water Board's GAMA website

Table 2.8-1: Injection zone formation fluid properties at reservoir conditions

Formation Fluid Property	Estimated Value/Range
Density, g/cm3	1.01
Viscosity, cp	1.26
TDS, ppm	~14,000-16,000

Table 7.1 : Injectate compositions

Component	Injectate 1	Injectate 2
	Mass%	**Mass%**
CO2	99.213%	99.884%
H2	0.051%	0.006%
N2	0.643%	0.001%
H2O	0.021%	0.000%
CO	0.029%	0.001%
Ar	0.031%	0.000%
O2	0.004%	0.000%
SO2+SO3	0.003%	0.000%
H2S	0.001%	0.014%
CH4	0.004%	0.039%
NOx	0.002%	0.000%
NH3	0.000%	0.000%
C2H6	0.000%	0.053%
Ethylene	0.000%	0.002%
Total	**100.00%**	**100.00%**

Table 7.2: Simplified 4 component composition for Injectate 1 and Injectate 2

Injectate 1	
Component	**mass%**
CO2	99.213%
N2	0.643%
SO2+SO3	0.003%
H2S	0.001%

Injectate 2	
Component	**mass%**
CO2	99.884%
CH4	0.039%
C2H6	0.053%
H2S	0.014%

Table 7.3. Injectate properties range over project life at downhole conditions for Injectate 1 and Injectate 2

Injectate property at downhole conditions	Injectate 1	Injectate 2
Viscosity, cp	0.054	0.056
Density, lb/ft^3	41.39	42.56
Compressibility factor, Z	0.464	0.453